2019-07-26

Billfish Behavior and Habitat Use in the Presence of Environmental Forcing and Commercial Exploitation

Bruce Gibbs Pohlot
University of Miami, bruce.pohlot@gmail.com

UNIVERSITY OF MIAMI

BILLFISH BEHAVIOR AND HABITAT USE IN THE PRESENCE OF ENVIRONMENTAL FORCING AND COMMERCIAL EXPLOITATION

By

Bruce Gibbs Pohlot

A DISSERTATION

Submitted to the Faculty
of the University of Miami
in partial fulfillment of the requirements for
the degree of Doctor of Philosophy

Coral Gables, Florida

August 2019

UNIVERSITY OF MIAMI

A dissertation submitted in partial fulfillment of
the requirements for the degree of
Doctor of Philosophy

BILLFISH BEHAVIOR AND HABITAT USE IN THE PRESENCE OF ENVIRONMENTAL FORCING AND COMMERCIAL EXPLOITATION

Bruce Gibbs Pohlot

Approved:

_____ Nelson Ehrhardt, Ph.D. Professor Emeritus Marine Ecosystems and Society	_____ Andrew Bakun, Ph.D. Professor Emeritus Marine Biology and Ecology
_____ David Die, Ph.D. Research Associate Professor Marine Ecosystems and Society	_____ Arthur Mariano, Ph.D. Professor Ocean Sciences
_____ Michael Domeier, Ph.D. Director Marine Conservation Science Institute	_____ Guillermo Prado, Ph.D. Dean of the Graduate School

POHLOT, BRUCE GIBBS (Ph.D., Marine Biology and Fisheries)

Billfish Behavior and Habitat Use in the Presence of Environmental Forcing and Commercial Exploitation (August 2019)

Abstract of a dissertation at the University of Miami.

Dissertation supervised by Professor Nelson Ehrhardt.
No. of pages in text. (276)

The Pacific Sailfish (*Istiophorus platypterus)* and Blue Marlin (*Makaira nigricans)* are vital resources to Central American economies along the eastern tropical Pacific Ocean through recreational catch-and-release sport fisheries and as retainable bycatch mostly in commercial longline tuna and mahi fisheries. Incidental billfish mortality resulting from bycatch reduces population abundance and negatively impacts catch rates in economically important recreational fisheries. Recreational and artisanal billfish fisheries management in the region is left to individual countries which rarely have fishery statistical systems or the means to independently assess such fisheries, resulting in a lack of fishery dependent catch data especially for less commercially valued species such as the billfish. Because of observed stock declines and a lack of a formal stock assessment research, there exists an immediate need to understand Pacific Sailfish and Blue Marlin population dynamic characteristics to understand exploitation and design fishery regulations to protect the species and fisheries. Therefore, the goal of this dissertation was to understand the Pacific Sailfish and Blue Marlin behavior and dynamic habitat use in the Eastern Pacific Ocean (EPO) in support of billfish conservation programs based on a species ecosystem analysis framework. This dissertation utilized

newly developed methods to assess intra-daily sailfish behavior and sensory strategies using advanced technologies and data collection in accelerometry never before applied to non-captive animals. Sailfish activity data revealed a strong photokinetic response to light intensity confirming the visual system of billfish and the available light within their habitat to be driving factors in intra-daily feeding behavior. A behavioral modelling technique applied for the first time to billfish was incorporated into long term migratory analysis revealing differentiated behavioral characteristics between sailfish and blue marlin relative to migratory speed and distances as well as spatial foraging versus searching behavioral patterns. Behavioral modelling parameter values and daily activity levels were used to infer post-satellite tag release behavior indicating that recovery periods exist in both sailfish and blue marlin following recreational catch and release. These behavioral parameters along with geo-referenced sailfish and blue marlin purse seine catch statistics were analyzed via generalized additive models (GAM) using divergence, vorticity, sea surface temperature, and chlorophyll-a as explanatory variables. GAM models revealed a lack of association between sailfish and the explanatory variables, but a stronger relationship existed between blue marlin behavior and the explanatory variables. These differences were associated to significant differences in spatial migratory patterns between the two species. Tuna purse seine catch rates were determined not to indicate distribution or relative abundance for either sailfish or blue marlin due to the bycatch nature of these species within the fishery and their very low incidental catch. Finally, an analysis of dispersal range of sailfish and blue marlin revealed the extent and residency of sailfish and blue marlin migratory ranges within exclusive economic zones indicating a need for management to be applied over large

transnational spatial scales. It was found that sailfish and blue marlin have local hotspots within the EPO with sailfish showing preference for the outer edges of the Costa Rica Dome and blue marlin having a clear association with the Coco's Island Ridge region characterized by an abundance of fish aggregating devices.

Dedication

I would like to dedicate this work to my parents, Helen and Bruce Pohlot, for their constant love, support, and encouragement throughout my life.

Thank you

Acknowledgments

The work completed as part of this dissertation would not have been possible without the help of my advisor, Dr. Nelson Ehrhardt, who provided an atmosphere of discovery from the moment I stepped foot in his office as a Master's degree student. Dr. Ehrhardt's guidance and friendship was unwavering and our research discussions are always fruitful. I have learned a tremendous amount about scientific and research processes from Dr. Ehrhardt and I truly thank him for his commitment to my success as a graduate student and marine biologist.

I would also like to thank my committee for their support, patience, and encouragement: Dr. Andrew Bakun, Dr. David Die, Dr. Michael Domeier, and Dr. Arthur Mariano.

Many thanks to my funding sources from the Central American Billfish Association and the Billfish Research Program at University of Miami. Along the way, our research was assisted by a wide variety of stakeholders in Central America from recreational fishermen to fishing lodges and private citizens. I would like to specifically thank Tim Choate, Paul Jones, and Carlos Pellas for their commitment and contribution to our research in satellite tagging. I would like to also thank the crew of the Typhoon II, Donald McGuinness and Jose Moya, George Beckwith and the crew of the Dragin Fly, Casa Vieja Lodge, Crocodile Bay Lodge, Pacific Fins Lodge, and all those who allowed us to join their fishing trips in support of our science.

Finally, I would like to thank all my friends along the way especially my girlfriend Caroline who is the most supportive and caring person I have ever met. Thanks to my labmates and close friends Dr. Vallierre Deleveaux, Julie Brown, and Dr. Mark

Fitchett who were always helpful and enjoyable to spend time and travel alongside. The crew of the second floor of CIMAS including Molly Stevens and Holly Perryman always provided entertaining discussion and adventures. To all those professors, friends, and colleagues at RSMAS who supported me in one way or another I genuinely thank you.

TABLE OF CONTENTS

Page

LIST OF FIGURES ix

LIST OF TABLES xxiv

Chapter

1 **Introduction** 1
Overview 1
Oceanographic Processes Relevant to Marine Resource Distribution in the EPO 2
Identification of Research opportunity 10
Goal…. 11
Objectives 11

2 **An analysis of sailfish daily activity in the Eastern Pacific Ocean using satellite tagging and recreational fisheries data** 13
Overview 13
Materials and Methods 15
Results 22
Discussion 28

3 **Exploring Sailfish and Blue Marlin Migratory Characteristics through Satellite Tagging and Behavioral Modeling** 37
Overview 37
Materials and Methods 40
PSAT Deployment Methodology 40
PSAT Location Data Collection and Processing 45
Acceleration and Depth Analysis from SeaTag-MOD PSATs 47
Behavioral Change Point Methodology 48
Results 52
PSAT Migratory Characteristics 52
Behavioral Change Point Analysis 54
Individual Behavior Analysis: Sailfish 57
Individual Behavior Analysis: Blue Marlin 94
Distribution of Change Points 111
Comparison of BCPA Parameters Among Species 111
Sailfish 111
Blue Marlin 114
Using BCPA and Acceleration to Explore Post Release Mortality 116
Discussion 119
Satellite Tagging Program Implementation 119

Using PSAT Data in BCPA to Examine Behavioral Modes 123
The Potential Influence of Fish Aggregating Devices (FADs) 126
Post-release Behavior and Recovery 128

4 **An Analysis of Environmental Signals effecting Billfish Behavior** 131
Overview 131
Materials and Methods 134
PSAT and Catch Data 135
Environmental Data Organization and Preference Analysis 136
Vertical Habitat Use Information 139
Generalized Additive Modelling 139
Results 142
PSAT Environmental Preference 142
Sailfish 143
Blue Marlin 146
Vertical Habitat Use of Sailfish from Short term Deployment 148
Sailfish GAM Results 151
BCPA Parameter GAM Model Selection 151
BCPA Parameter GAM Analysis 156
Mu.hat (Speed) 156
S.hat (Variability) 160
Rho.hat (Autocorrelation) 164
IATTC Purse Seine GAM Model Selection 169
IATTC Purse Seine GAM Analysis 172
Blue Marlin GAM Results 176
BCPA Parameter GAM Model Selection 176
BCPA Parameter GAM Analysis 180
Mu.hat (Speed) 180
S.hat (Variability) 184
Rho.hat (Autocorrelation) 188
IATTC Purse Seine GAM Model Selection 193
IATTC Purse Seine GAM Analysis 197
Discussion 202
Environmental Preference 202
Generalized Additive Modelling 206

5 **Assessing the extent of sailfish and blue marlin migratory range relative to management boundaries and protected areas** 210
Overview 210
Materials and Methods 217
Distributional Mean Center Analysis 219
Kernel Density Dispersal Range Analysis 221
Kernel Density Overlap of Sailfish and Yellowfin Tuna 224
Exclusive Economic Zones and Closed Area Residence 225
Catch Analysis of YFT in Costa Rica Closed Area 226
Results 226

Distributional Mean Center Estimation 226
Kernel Density Dispersal Range Analysis and EEZ Residence 230
Sailfish 230
Blue Marlin 233
Kernel Density Overlap of Sailfish and YFT 236
Costa Rica Closed Area Residence 237
YFT Purse Seine Catch Relative to Area Closure 241
Discussion 244
Distributional Population Mean Centers 244
Dispersal Range Analysis 248
Exclusive Economic Zone Billfish Residence 253
Purse Seine Catch Relative to Area Closure 253
Concluding Remarks on Sailfish and Blue Marlin Habitat Range 258

6 **Conclusion** 261

WORKS CITED…… 265

List of Figures

Figure 1.1 Mean wind pattern vectors are shown on top for the winter month of February and summer month of August with shading representing position of wind divergence indicative of the position of the ITCZ. On bottom the surface current pattern vectors are shown with major current systems labeled (From Fielder 2002)) 4

Figure 1.2 Surface current pattern in the EPO shown by mean surface drifter circulation vectors (From Kessler 2006) 6

Figure 1.3 Images of two diagrams illustrating the potential vorticity contours on three isopycnal surfaces for an anticyclonic eddy (A) and a cyclonic eddy (B) (From: Zhang et al. 2014) 7

Figure 1.4 Map depicting the annual mean depth of the thermocline and location of the Costa Rica Dome. (From Fiedler 2002) 8

Figure 1.5 Image from AQUA Modis showing monthly average of chlorophyll concentration from February 2014 during the deployment period of satellite tagged Sailfish and Blue Marlin. Image shows presence of CRD and locally increased productivity. 9

Figure 2.1 The study area of the Eastern Pacific Ocean shown by the circle off Puerto Quetzal, Guatemala..... 16

Figure 2.2 Image showing 3-axis orientation of the accelerometer in the SeaTag-MOD. X and Y axes are perpendicular to the length of the tag while the Z axis runs the length of the tag. Additional tag battery not shown attached. 18

Figure 2.3 Validation of light data from 2005 Costa Rica/Panama PSAT (Gray Line) using floating PSAT light information from Guatemala in 2013 (Black Line). Standardizing data removed effect of light intensity differences focusing only on relationship between timings at two locations and times..... 21

Figure 2.4 Image of SeaTag-MOD attached to Pacific sailfish from the 2012 study. Photo of sailfish tagged for this acceleration study provided by Marc Montocchio of 36North 23

Figure 2.5 Plot showing the close intra-daily relationship between light level from a PSAT tagged sailfish on primary axis and standardized sailfish activity (acceleration) on the secondary axis. Sailfish are shown to be active between 06:00 and 18:00 when the sun is above the horizon but are not active when light is not available at night. PSAT tagged sailfish showed increased activity during the fully illuminated moon after 19:00 with a peak coinciding with the peak of moonlight intensity between 21:00 and 22:00 hours..... 24

Figure 2.6 Average depth (m) by hour (primary axis) and average light by hour (secondary axis) from an IGFA PSAT tagged sailfish from 21 September to 21 October 2005 is shown in the plot. On average, sailfish diving behaviors only occurred when the sun was above the horizon with little to no diving activity when light was unavailable 25

Figure 2.7 The hourly relationship between three data types: sailfish raises (sailfish seen by crew around vessel) in the Guatemala charter fleet (Black Dashed Line), sailfish catch in a Nicaragua fishing tournament (Grey Dashed Line), and sailfish activity (accelerations) hourly averages with standard deviation bars (Solid Black Line). The highest number of encounters in the fishery occurs between 09:00 and 14:00 hours but are relatively low prior and after this time range whereas sailfish activity is highest between 11:00 and 16:00 hours with sustained high activity until 17:00 hours..... 26

Figure 2.8 Plots of model results from a non-linear least squares hazard model fit to sailfish activity (a), sailfish catch in a Nicaragua fishing tournament (b), and sailfish raises from the Guatemala charter fleet (c). Observed data is shown with Black Markers with model fits shown with Black Dashed Lines. Model fits and parameter values are shown in Table 1. 27

Figure 2.9 Sailfish activity (acceleration) results showing the range of acceleration data values (a) with observed values represented by open black circles and the range of values indicated by the gray shaded region. Figure (b) shows this same gray shaded region representing the range of activity values with the modeled line fits for sailfish catch and raises from Figures 8b and 8c. The range of high activity persists longer into the afternoon and evening than fishery encounters suggest sailfish are actively feeding..... 31

Figure 2.10 Histogram of depth residency of 7 tagged sailfish off Guatemala separating daytime hours, 6am-6pm, (dark gray bars) and nighttime hours, 6am-6pm, (light gray bars). The x-axis is the percent (%) residency within the specified 6.4m depth bin (y-axis). Error bars represent the standard error of the estimate..... 33

Figure 2.11 One month depth profile of PSAT tagged sailfish off Costa Rica/Panama from 2005. Black line with open triangles represents the daily average depth while the black line with black squares represents the daily maximum depth. The gray shaded bar shows the World Ocean Atlas fall season depth range of the 1ml/l dissolved oxygen in the region where the tagged sailfish was present. The level of oxygen can be considered a barrier to most organisms not specifically adated to low oxygen..... 34

Figure 3.1 Top: SeaTag-GEO satellite tag used for long term deployments. Bottom: SeaTag-MOD satellite tag with attached battery section used for short term deployments and high-resolution data capture 40

Figure 3.2 The SeaTag attachment tethers. Top to bottom: Medium (Sailfish only) Domeier umbrella dart, Large (Blue Marlin only Domeier umbrella dart, Stainless Floy dart (Short Deployments, Seatag-MOD) 43

Figure 3.3 Enhanced view of Domeier dart with attached Dacron and applied heat shrink material over monofilament tether..... 45

Figure 3.4 Four plots showing the output of the BCPA modeling procedure for sailfish 134260. Top left shows the migratory path where a green triangle marks the PSAT deployment location and a red square the endpoint or PSAT pop-off point. Color of the line represents the autocorrelation parameter. The top right is a phase plot representing relationship between the 3 parameters estimated from the BCPA with the autocorrelation parameter shown in color and size coded circles. The bottom left plot shows the change points where the pink lines represent the time of the changepoint within the trial and the thickness of the line representing the number of days used for the selection of the change point. The black open circles represent the mean of the BCPA analysis with the red lines indicating the standard deviation. Finally, the bottom right set of diagnostic plots includes a QQ-norm plot, histogram and autocorrelation function of the standardized data from the model..... 60

Figure 3.5 Four plots showing the output of the BCPA modeling procedure for sailfish 134268. Top left shows the migratory path where a green triangle marks the PSAT deployment location and a red square the endpoint or PSAT pop-off point . Color of the line represents the autocorrelation parameter. The top right is a phase plot representing relationship between the 3 parameters estimated from the BCPA with the autocorrelation parameter shown in color and size coded circles. The bottom left plot shows the change points where the pink lines represent the time of the changepoint within the trial and the thickness of the line representing the number of days used for the selection of the change point. The black open circles represent the mean of the BCPA analysis with the red lines indicating the standard deviation. Finally, the bottom right set of diagnostic plots includes a QQ-norm plot, histogram and autocorrelation function of the standardized data from the model..... 62

Figure 3.6 Four plots showing the output of the BCPA modeling procedure for sailfish 134276. Top left shows the migratory path where a green triangle marks the PSAT deployment location and a red square the endpoint or PSAT pop-off point. Color of the line represents the autocorrelation parameter. The top right is a phase plot representing relationship between the 3 parameters estimated from the BCPA with the autocorrelation parameter shown in color and size coded circles. The bottom left plot shows the change points where the pink lines represent the time of the changepoint within the trial and the thickness of the line representing the number of days used for the selection of the change point. The black open circles represent the mean of the BCPA analysis with the red lines indicating the standard deviation. Finally, the bottom right set of diagnostic plots includes a QQ-norm plot, histogram and autocorrelation function of the standardized data from the model..... 64

Figure 3.7 Four plots showing the output of the BCPA modeling procedure for sailfish 134288. Top left shows the migratory path where a green triangle marks the PSAT deployment location and a red square the endpoint or PSAT pop-off point. Color of the line represents the autocorrelation parameter. The top right is a phase plot representing relationship between the 3 parameters estimated from the BCPA with the autocorrelation parameter shown in color and size coded circles. The bottom left plot shows the change points where the pink lines represent the time of the changepoint within the trial and the thickness of the line representing the number of days used for the selection of the change point. The black open circles represent the mean of the BCPA analysis with the red lines indicating the standard deviation. Finally, the bottom right set of diagnostic plots includes a QQ-norm plot, histogram and autocorrelation function of the standardized data from the model..... 66

Figure 3.8 Four plots showing the output of the BCPA modeling procedure for sailfish 134267. Top left shows the migratory path where a green triangle marks the PSAT deployment location and a red square the endpoint or PSAT pop-off point. Color of the line represents the autocorrelation parameter. The top right is a phase plot representing relationship between the 3 parameters estimated from the BCPA with the autocorrelation parameter shown in color and size coded circles. The bottom left plot shows the change points where the pink lines represent the time of the changepoint within the trial and the thickness of the line representing the number of days used for the selection of the change point. The black open circles represent the mean of the BCPA analysis with the red lines indicating the standard deviation. Finally, the bottom right set of diagnostic plots includes a QQ-norm plot, histogram and autocorrelation function of the standardized data from the model..... 68

Figure 3.9 Four plots showing the output of the BCPA modeling procedure for sailfish 134272. Top left shows the migratory path where a green triangle marks the PSAT deployment location and a red square the endpoint or PSAT pop-off point. Color of the line represents the autocorrelation parameter. The top right is a phase plot representing relationship between the 3 parameters estimated from the BCPA with the autocorrelation parameter shown in color and size coded circles. The bottom left plot shows the change points where the pink lines represent the time of the changepoint within the trial and the thickness of the line representing the number of days used for the selection of the change point. The black open circles represent the mean of the BCPA analysis with the red lines indicating the standard deviation. Finally, the bottom right set of diagnostic plots includes a QQ-norm plot, histogram and autocorrelation function of the standardized data from the model..... 70

Figure 3.10 Four plots showing the output of the BCPA modeling procedure for sailfish 134273. Top left shows the migratory path where a green triangle marks the PSAT deployment location and a red square the endpoint or PSAT pop-off point. Color of the line represents the autocorrelation parameter. The top right is a phase plot representing relationship between the 3 parameters estimated from the BCPA with the autocorrelation parameter shown in color and size coded circles. The bottom left plot shows the change points where the pink lines represent the time of the changepoint within the trial and the

thickness of the line representing the number of days used for the selection of the change point. The black open circles represent the mean of the BCPA analysis with the red lines indicating the standard deviation. Finally, the bottom right set of diagnostic plots includes a QQ-norm plot, histogram and autocorrelation function of the standardized data from the model..... 73

Figure 3.11 Four plots showing the output of the BCPA modeling procedure for sailfish 134275. Top left shows the migratory path where a green triangle marks the PSAT deployment location and a red square the endpoint or PSAT pop-off point. Color of the line represents the autocorrelation parameter. The top right is a phase plot representing relationship between the 3 parameters estimated from the BCPA with the autocorrelation parameter shown in color and size coded circles. The bottom left plot shows the change points where the pink lines represent the time of the changepoint within the trial and the thickness of the line representing the number of days used for the selection of the change point. The black open circles represent the mean of the BCPA analysis with the red lines indicating the standard deviation. Finally, the bottom right set of diagnostic plots includes a QQ-norm plot, histogram and autocorrelation function of the standardized data from the model..... 75

Figure 3.12 Four plots showing the output of the BCPA modeling procedure for sailfish 1342780. Top left shows the migratory path where a green triangle marks the PSAT deployment location and a red square the endpoint or PSAT pop-off point. Color of the line represents the autocorrelation parameter. The top right is a phase plot representing relationship between the 3 parameters estimated from the BCPA with the autocorrelation parameter shown in color and size coded circles. The bottom left plot shows the change points where the pink lines represent the time of the changepoint within the trial and the thickness of the line representing the number of days used for the selection of the change point. The black open circles represent the mean of the BCPA analysis with the red lines indicating the standard deviation. Finally, the bottom right set of diagnostic plots includes a QQ-norm plot, histogram and autocorrelation function of the standardized data from the model..... 78

Figure 3.13 Four plots showing the output of the BCPA modeling procedure for sailfish 134285. Top left shows the migratory path where a green triangle marks the PSAT deployment location and a red square the endpoint or PSAT pop-off point. Color of the line represents the autocorrelation parameter. The top right is a phase plot representing relationship between the 3 parameters estimated from the BCPA with the autocorrelation parameter shown in color and size coded circles. The bottom left plot shows the change points where the pink lines represent the time of the changepoint within the trial and the thickness of the line representing the number of days used for the selection of the change point. The black open circles represent the mean of the BCPA analysis with the red lines indicating the standard deviation. Finally, the bottom right set of diagnostic plots includes a QQ-norm plot, histogram and autocorrelation function of the standardized data from the model..... 81

Figure 3.14 Four plots showing the output of the BCPA modeling procedure for sailfish 134258. Top left shows the migratory path where a green triangle marks the PSAT deployment location and a red square the endpoint or PSAT pop-off point. Color of the line represents the autocorrelation parameter. The top right is a phase plot representing relationship between the 3 parameters estimated from the BCPA with the autocorrelation parameter shown in color and size coded circles. The bottom left plot shows the change points where the pink lines represent the time of the changepoint within the trial and the thickness of the line representing the number of days used for the selection of the change point. The black open circles represent the mean of the BCPA analysis with the red lines indicating the standard deviation. Finally, the bottom right set of diagnostic plots includes a QQ-norm plot, histogram and autocorrelation function of the standardized data from the model..... 84

Figure 3.15 Four plots showing the output of the BCPA modeling procedure for sailfish 134241. Top left shows the migratory path where a green triangle marks the PSAT deployment location and a red square the endpoint or PSAT pop-off point. Color of the line represents the autocorrelation parameter. The top right is a phase plot representing relationship between the 3 parameters estimated from the BCPA with the autocorrelation parameter shown in color and size coded circles. The bottom left plot shows the change points where the pink lines represent the time of the changepoint within the trial and the thickness of the line representing the number of days used for the selection of the change point. The black open circles represent the mean of the BCPA analysis with the red lines indicating the standard deviation. Finally, the bottom right set of diagnostic plots includes a QQ-norm plot, histogram and autocorrelation function of the standardized data from the model..... 86

Figure 3.16 Four plots showing the output of the BCPA modeling procedure for sailfish 134252. Top left shows the migratory path where a green triangle marks the PSAT deployment location and a red square the endpoint or PSAT pop-off point. Color of the line represents the autocorrelation parameter. The top right is a phase plot representing relationship between the 3 parameters estimated from the BCPA with the autocorrelation parameter shown in color and size coded circles. The bottom left plot shows the change points where the pink lines represent the time of the changepoint within the trial and the thickness of the line representing the number of days used for the selection of the change point. The black open circles represent the mean of the BCPA analysis with the red lines indicating the standard deviation. Finally, the bottom right set of diagnostic plots includes a QQ-norm plot, histogram and autocorrelation function of the standardized data from the model..... 89

Figure 3.17 Four plots showing the output of the BCPA modeling procedure for sailfish 134263. Top left shows the migratory path where a green triangle marks the PSAT deployment location and a red square the endpoint or PSAT pop-off point. Color of the line represents the autocorrelation parameter. The top right is a phase plot representing relationship between the 3 parameters estimated from the BCPA with the autocorrelation parameter shown in color and size coded circles. The bottom left plot shows the change points where the pink lines represent the time of the changepoint within the trial and the

thickness of the line representing the number of days used for the selection of the change point. The black open circles represent the mean of the BCPA analysis with the red lines indicating the standard deviation. Finally, the bottom right set of diagnostic plots includes a QQ-norm plot, histogram and autocorrelation function of the standardized data from the model..... 91

Figure 3.18 Four plots showing the output of the BCPA modeling procedure for sailfish 134266. Top left shows the migratory path where a green triangle marks the PSAT deployment location and a red square the endpoint or PSAT pop-off point. Color of the line represents the autocorrelation parameter. The top right is a phase plot representing relationship between the 3 parameters estimated from the BCPA with the autocorrelation parameter shown in color and size coded circles. The bottom left plot shows the change points where the pink lines represent the time of the changepoint within the trial and the thickness of the line representing the number of days used for the selection of the change point. The black open circles represent the mean of the BCPA analysis with the red lines indicating the standard deviation. Finally, the bottom right set of diagnostic plots includes a QQ-norm plot, histogram and autocorrelation function of the standardized data from the model..... 93

Figure 3.19 Four plots showing the output of the BCPA modeling procedure for blue marlin 134283. Top left shows the migratory path where a green triangle marks the PSAT deployment location and a red square the endpoint or PSAT pop-off point. Color of the line represents the autocorrelation parameter. The top right is a phase plot representing relationship between the 3 parameters estimated from the BCPA with the autocorrelation parameter shown in color and size coded circles. The bottom left plot shows the change points where the pink lines represent the time of the changepoint within the trial and the thickness of the line representing the number of days used for the selection of the change point. The black open circles represent the mean of the BCPA analysis with the red lines indicating the standard deviation. Finally, the bottom right set of diagnostic plots includes a QQ-norm plot, histogram and autocorrelation function of the standardized data from the model..... 95

Figure 3.20 Four plots showing the output of the BCPA modeling procedure for blue marlin 134277. Top left shows the migratory path where a green triangle marks the PSAT deployment location and a red square the endpoint or PSAT pop-off point. Color of the line represents the autocorrelation parameter. The top right is a phase plot representing relationship between the 3 parameters estimated from the BCPA with the autocorrelation parameter shown in color and size coded circles. The bottom left plot shows the change points where the pink lines represent the time of the changepoint within the trial and the thickness of the line representing the number of days used for the selection of the change point. The black open circles represent the mean of the BCPA analysis with the red lines indicating the standard deviation. Finally, the bottom right set of diagnostic plots includes a QQ-norm plot, histogram and autocorrelation function of the standardized data from the model..... 98

Figure 3.21 Four plots showing the output of the BCPA modeling procedure for blue marlin 134254. Top left shows the migratory path where a green triangle marks the PSAT deployment location and a red square the endpoint or PSAT pop-off point. Color of the line represents the autocorrelation parameter. The top right is a phase plot representing relationship between the 3 parameters estimated from the BCPA with the autocorrelation parameter shown in color and size coded circles. The bottom left plot shows the change points where the pink lines represent the time of the changepoint within the trial and the thickness of the line representing the number of days used for the selection of the change point. The black open circles represent the mean of the BCPA analysis with the red lines indicating the standard deviation. Finally, the bottom right set of diagnostic plots includes a QQ-norm plot, histogram and autocorrelation function of the standardized data from the model..... 100

Figure 3.22 Four plots showing the output of the BCPA modeling procedure for blue marlin 134251. Top left shows the migratory path where a green triangle marks the PSAT deployment location and a red square the endpoint or PSAT pop-off point. Color of the line represents the autocorrelation parameter. The top right is a phase plot representing relationship between the 3 parameters estimated from the BCPA with the autocorrelation parameter shown in color and size coded circles. The bottom left plot shows the change points where the pink lines represent the time of the changepoint within the trial and the thickness of the line representing the number of days used for the selection of the change point. The black open circles represent the mean of the BCPA analysis with the red lines indicating the standard deviation. Finally, the bottom right set of diagnostic plots includes a QQ-norm plot, histogram and autocorrelation function of the standardized data from the model..... 102

Figure 3.23 Four plots showing the output of the BCPA modeling procedure for blue marlin 134248. Top left shows the migratory path where a green triangle marks the PSAT deployment location and a red square the endpoint or PSAT pop-off point. Color of the line represents the autocorrelation parameter. The top right is a phase plot representing relationship between the 3 parameters estimated from the BCPA with the autocorrelation parameter shown in color and size coded circles. The bottom left plot shows the change points where the pink lines represent the time of the changepoint within the trial and the thickness of the line representing the number of days used for the selection of the change point. The black open circles represent the mean of the BCPA analysis with the red lines indicating the standard deviation. Finally, the bottom right set of diagnostic plots includes a QQ-norm plot, histogram and autocorrelation function of the standardized data from the model..... 104

Figure 3.24 Four plots showing the output of the BCPA modeling procedure for blue marlin 134244. Top left shows the migratory path where a green triangle marks the PSAT deployment location and a red square the endpoint or PSAT pop-off point. Color of the line represents the autocorrelation parameter. The top right is a phase plot representing relationship between the 3 parameters estimated from the BCPA with the autocorrelation parameter shown in color and size coded circles. The bottom left plot shows the change points where the pink lines represent the time of the changepoint within the trial and the

thickness of the line representing the number of days used for the selection of the change point. The black open circles represent the mean of the BCPA analysis with the red lines indicating the standard deviation. Finally, the bottom right set of diagnostic plots includes a QQ-norm plot, histogram and autocorrelation function of the standardized data from the model..... 106
Figure 3.25 Four plots showing the output of the BCPA modeling procedure for blue marlin 134240. Top left shows the migratory path where a green triangle marks the PSAT deployment location and a red square the endpoint or PSAT pop-off point. Color of the line represents the autocorrelation parameter. The top right is a phase plot representing relationship between the 3 parameters estimated from the BCPA with the autocorrelation parameter shown in color and size coded circles. The bottom left plot shows the change points where the pink lines represent the time of the changepoint within the trial and the thickness of the line representing the number of days used for the selection of the change point. The black open circles represent the mean of the BCPA analysis with the red lines indicating the standard deviation. Finally, the bottom right set of diagnostic plots includes a QQ-norm plot, histogram and autocorrelation function of the standardized data from the model..... 108

Figure 3.26 Four plots showing the output of the BCPA modeling procedure for blue marlin 134255. Top left shows the migratory path where a green triangle marks the PSAT deployment location and a red square the endpoint or PSAT pop-off point. Color of the line represents the autocorrelation parameter. The top right is a phase plot representing relationship between the 3 parameters estimated from the BCPA with the autocorrelation parameter shown in color and size coded circles. The bottom left plot shows the change points where the pink lines represent the time of the changepoint within the trial and the thickness of the line representing the number of days used for the selection of the change point. The black open circles represent the mean of the BCPA analysis with the red lines indicating the standard deviation. Finally, the bottom right set of diagnostic plots includes a QQ-norm plot, histogram and autocorrelation function of the standardized data from the model..... 110

Figure 3.27 Map showing behavioral change point location for both sailfish (Green Circles) and blue marlin (Blue Circles) 112

Figure 3.28 Plots showing parameter estimated for all modeled sailfish. Top: Plot of mu.hat equivalent to speed; Middle: Plot of s.hat equivalent to variability of movement; Bottom: Plot of rho.hat equivalent to “movement inertia” or autocorrelation 113

Figure 3.29 Plots showing parameter estimated for all modeled blue marlin. Top: Plot of mu.hat equivalent to speed; Middle: Plot of s.hat equivalent to variability of movement; Bottom: Plot of rho.hat equivalent to “movement inertia” or autocorrelation 115

Figure 3.30 Plot of sailfish depth residency for 7 tagged sailfish off the Guatemalan coast during April 2012..... 116

Figure 3.31 Plot of average acceleration activity for 7 PSAT tagged sailfish of the Guatemalan coast during April 2012 117

Figure 3.32 Plot of all tagged sailfish and their resulting BCPA results showing the number of days before the first behavioral change point occurred. This indicates a behavioral shift hypothesized as the postrelease recovery period before the sailfish returns to typical behavior 118

Figure 3.33 Plot of all tagged sailfish and their resulting BCPA results showing the number of days before the first behavioral change point occurred. This indicates a behavioral shift hypothesized as the postrelease recovery period before the sailfish returns to typical behavior 119

Figure 4.1 Two adaptations of histograms with a red polygon of the density of values of divergence throughout the tropical EPO, and a blue line of the density of divergence values actually visited by PSAT tagged sailfish 143

Figure 4.2 Two adaptations of histograms with a red polygon of the density of values of vorticity throughout the tropical EPO, and a blue line of the density of vorticity values actually visited by PSAT tagged sailfish 144

Figure 4.3 Two adaptations of histograms with a red polygon of the density of values of SST throughout the tropical EPO, and a blue line of the density of SST values actually visited by PSAT tagged sailfish 145

Figure 4.4 Two adaptations of histograms with a red polygon of the density of values of divergence throughout the tropical EPO, and a blue line of the density of divergence values actually visited by PSAT tagged blue marlin. 146

Figure 4.5 Two adaptations of histograms with a red polygon of the density of values of vorticity throughout the tropical EPO, and a blue line of the density of vorticity values actually visited by PSAT tagged blue marlin 147

Figure 4.6 Two adaptations of histograms with a red polygon of the density of values of SST throughout the tropical EPO, and a blue line of the density of SST values actually visited by PSAT tagged blue marlin 148

Figure 4.7 Plot of the depth residency of sailfish tagged off Guatemala in 2012 (white bars) overlaid on DO data at latitude 13N obtained from World Ocean Atlas 149

Figure 4.8 Plot of the depth residency of sailfish tagged off Costa Rica in 2013 (white bars) overlaid on DO data at latitude 8N obtained from World Ocean Atlas 149

Figure 4.9 Plot of the depth residency of sailfish tagged off Guatemala in 2012 (white bars) overlaid on SST data at latitude 13N obtained from NOAA OISST 150

Figure 4.10 Plot of the depth residency of sailfish tagged off Costa Rica in 2013 (white bars) overlaid on SST data at latitude 8N obtained from NOAA OISST 151

Figure 4.11 Histogram density plots for each of the response variables: speed or mu.hat (top), movement variability or s.hat (middle), and autocorrrelation of movement or rho.hat (bottom) 152

Figure 4.12 Histogram density plots for each of the explanatory variables: vorticity (top left), divergence (top right), SST (middle left), Time or # of days postrelease (middle right), Latitude (bottom left), and longitude (bottom right) 153

Figure 4.13 Model result for sailfish speed parameter BCPA GAM..... 157

Figure 4.14 Sailfish speed parameter GAM model diagnostics including QQ-norm plot (top left), residuals versus linear predictor (trop right), histogram of model residuals (bottom left), and response variable against model fitted values (bottom right) 159

Figure 4.15 Sailfish speed parameter GAM model diagnostics including plot of model residuals against the speed variable (top left), squared residuals against speed variable (top right), and standardized residuals against model fitted values 159

Figure 4.16 Sailfish speed parameter GAM model smoother diagnostics..... 160

Figure 4.17 Model result for movement variability or s.hat BCPA GAM 161

Figure 4.18 Sailfish variability parameter GAM model diagnostics including QQ-norm plot (top left), residuals versus linear predictor (trop right), histogram of model residuals (bottom left), and response variable against model fitted values (bottom right) 163

Figure 4.19 Sailfish variability parameter GAM model diagnostics including plot of model residuals against the variability variable (top left), squared residuals against variability variable (top right), and standardized residuals against model fitted values 163

Figure 4.20 Sailfish variability parameter GAM model smoother diagnostics 164

Figure 4.21 Model result for autocorrelation or rho.hat BCPA GAM..... 165

Figure 4.22 Sailfish autocorrelation parameter GAM model diagnostics including QQ-norm plot (top left), residuals versus linear predictor (top right), histogram of model residuals (bottom left), and response variable against model fitted values (bottom right) 167

Figure 4.23 Sailfish autocorrelation parameter GAM model diagnostics including plot of model residuals against the autocorrelation variable (top left), squared residuals against

autocorrelation variable (top right), and standardized residuals against model fitted values 168

Figure 4.24 Sailfish autocorrelation parameter GAM model smoother diagnostics. .. 168

Figure 4.25 Histogram density plots for the response variable sailfish CPUE in original non-transformed state (top) and log-transformed (bottom) 169

Figure 4.26 Histogram density plots for each of the explanatory variables: vorticity (top left), divergence (top right), Chlorophyll-a (middle left), SST (middle right), Latitude (bottom left), and longitude (bottom right) 170

Figure 4.27 Results of sailfish catch data GAM 173

Figure 4.28 Sailfish catch data GAM model diagnostics including QQ-norm plot (top left), residuals versus linear predictor (trop right), histogram of model residuals (bottom left), and response variable against model fitted values (bottom right) 175

Figure 4.29 Sailfish catch data GAM model diagnostics including plot of model residuals against sailfish CPUE (top left), squared residuals against sailfish CPUE (top right), and standardized residuals against model fitted values 175

Figure 4.30 Diagnostic of smoother applied to latitude in sailfish catch data GAM... 176

Figure 4.31 Histogram density plots for each of the response variables: speed or mu.hat (top), movement variability or s.hat (middle), and autocorrrelation of movement or rho.hat (bottom) 177

Figure 4.32 Histogram density plots for each of the explanatory variables: vorticity (top left), divergence (top right), SST (middle left), Time or # of days postrelease (middle right), Latitude (bottom left), and longitude (bottom right) 178

Figure 4.33 Model result for blue marlin speed parameter BCPA GAM 181

Figure 4.34 Blue marlin speed parameter GAM model diagnostics including QQ-norm plot (top left), residuals versus linear predictor (trop right), histogram of model residuals (bottom left), and response variable against model fitted values (bottom right) 183

Figure 4.35 Blue marlin speed parameter GAM model diagnostics including plot of model residuals against the speed variable (top left), squared residuals against speed variable (top right), and standardized residuals against model fitted values 183

Figure 4.36 Blue marlin speed parameter GAM model smoother diagnostics..... 184

Figure 4.37 Model result for blue marlin movement variability or s.hat BCPA GAM 185

Figure 4.38 Blue marlin variability parameter GAM model diagnostics including QQ-norm plot (top left), residuals versus linear predictor (trop right), histogram of model residuals (bottom left), and response variable against model fitted values (bottom right) 187

Figure 4.39 Blue marlin variability parameter GAM model diagnostics including plot of model residuals against the variability variable (top left), squared residuals against variability variable (top right), and standardized residuals against model fitted values. 187

Figure 4.40 Blue Marlin variability parameter GAM model smoother diagnostics 188

Figure 4.41 Model result for blue marlin autocorrelation or rho.hat BCPA GAM 189

Figure 4.42 Blue marlin autocorrelation parameter GAM model diagnostics including QQ-norm plot (top left), residuals versus linear predictor (trop right), histogram of model residuals (bottom left), and response variable against model fitted values (bottom right) 191

Figure 4.43 Blue marlin autocorrelation parameter GAM model diagnostics including plot of model residuals against the autocorrelation variable (top left), squared residuals against autocorrelation variable (top right), and standardized residuals against model fitted values 192

Figure 4.44 Blue marlin autocorrelation parameter GAM model smoother diagnostics..... 192

Figure 4.45 Histogram density plots for the response variable blue marlin CPUE in original non-transformed state (top) and log-transformed (bottom) 194

Figure 4.46 Histogram density plots for each of the explanatory variables: vorticity (top left), divergence (top right), Chlorophyll-a (middle left), SST (middle right), Latitude (bottom left), and longitude (bottom right) 195

Figure 4.47 Results of blue marlin catch data GAM 198

Figure 4.48 Blue marlin catch data GAM model diagnostics including QQ-norm plot (top left), residuals versus linear predictor (trop right), histogram of model residuals (bottom left), and response variable against model fitted values (bottom right) 200

Figure 4.49 Blue marlin catch data GAM model diagnostics including plot of model residuals against blue marlin CPUE (top left), squared residuals against blue marlin CPUE (top right), and standardized residuals against model fitted values..... 201

Figure 4.50 Diagnostic of smoothers applied to explanatory variables in blue marlin catch data GAM..... 201

Figure 4.51: Satellite tag tracks from the March 2013 PSAT deployment period showing the distribution of sailfish around the Costa Rica Dome during the spring of 2013. The tracks are overlaid on the average location of the CRD adapted from Fiedler 2002... 204

Figure 5.1 Map showing the study area of the Eastern Pacific Ocean and exclusive economic zones associated with each nation indicated by black lines 211

Figure 5.2 Top: Distribution and amount of bycatch in the purse seine fishery from 1993 to 2012 showing relatively low levels of billfish bycatch in the fishery compared to longline fishing. Bottom: Longline bycatch amount and distribution from 1993 to 2012 indicating the large level of billfish bycatch especially in the early years presented 212

Figure 5.3 Map of the fishing zones designated by the Presidential Decree in Costa Rica in 2014 216

Figure 5.4 Map showing the distribution of set types in the EPO purse seine fishery with red shades indicating free school/unassociated sets, blue shades indicating dolphin associated sets, and green shades indicating object oriented/fish aggregating device sets..... 218

Figure 5.5 Map of sailfish satellite tagging locations (red dots), total sailfish catch in the purse seine (green circles), and mean centers of population distribution for each of these data types (green asterisk refers to purse seine catch mean center and red asterisk to satellite tag location mean center..... 228

Figure 5.6 Map of blue marlin satellite tagging locations (yellow dots), total blue marlin catch in the purse seine (blue circles), and mean centers of population distribution for each of these data types (blue asterisk refers to purse seine catch mean center and yellow asterisk to satellite tag location mean center..... 228

Figure 5.7 Map of mean centers of distribution for sailfish (light blue square=purse seine catch mean center, light blue square with dot=sailfish satellite tag location mean center) and blue marlin (blue circle=purse seine catch mean center, blue circle with dot=blue marlin satellite tag mean center) and yellowfin tuna(YFT)(yellow triangle=purse seine catch mean center from 2010-2015, yellow triangle with dot=purse seine catch mean center from 2000-2010) 229

Figure 5.8 Map showing the extent of the estimated sailfish dispersal range from satellite tagging locations. The shades of blue range from 25% to 100% darkest to lightest. The darkest blue indicates the highest density of satellite tag locations corresponding to the 25% dispersal range where 75% of tagging locations fall. The next darkest shade of blue indicates the 50% dispersal range referring to 50% of tagging locations etc 231

Figure 5.9: Map showing the extent of the estimated blue marlin dispersal range from satellite tagging locations. The shades of blue range from 25% to 100% darkest to lightest. The darkest blue indicates the highest density of satellite tag locations corresponding to the 25% dispersal range where 75% of tagging locations fall. The next darkest shade of blue indicates the 50% dispersal range referring to 50% of tagging locations etc 235

Figure 5.10: Sailfish and YFT purse seine catch overlap between 2000 and 2012 where higher values of correlation indicated higher numbers of sailfish caught with YFT in purse seine sets..... 237

Figure 5.11: Map of the kernel density of sailfish satellite tagging locations within the Costa Rica Exclusive Economic Zone that was split into fishing zones in 2014 239

Figure 5.12: Map of the kernel density of blue marlin satellite tagging locations within the Costa Rica Exclusive Economic Zone that was split into fishing zones in 2014 239

Figure 5.13 Map showing the distribution of purse seine YFT catch in the region off Costa Rica from 2014 prior to the implementation of the Presidential decree taking place at the end of that year splitting the Costa Rica EEZ into fishing zones. Purse seine fgishing was allowed in zones C and D in this year and represented a large potion of purse seine YFT catch within the Costa Rican EEZ..... 243

Figure 5.14 Map showing the distribution of purse seine YFT catch in the region off Costa Rica from 2015 following the implementation of the Presidential decree splitting the Costa Rica EEZ into fishing zones. Purse seine fgishing was not allowed in zones C and D in this year and this is made evident by the redistribution of YFT catch following the decree 244

Figure 5.15 Blue marlin catch per unit effort by 1 degree (latxlon) squares for years 2000-2015..... 247

Figure 5.16 Figure showing spatial distribution of purse seine sets from 2010 to 2015..... 248

Figure 5.17 Thermocline depth isolines captured from Fiedler 2002 overlaid on winter SST from February 2013 and sailfish satellite tag tracks 251

Figure 5.18 An index of longline fishing intensity (number of sets/time) is indicated in yellow to red scale with red referring to highest fishing intensity. Satellite tag tracks from sailfish are overlaid on the longline intensity indicating regions of possible vulnerability of sailfish to longline fishing practices especially off Guatemala and Costa Rica..... 259

List of Tables

Table 2.1: Modeling results from a non-linear least squares hazard model fit to three data types: Sailfish Activity, sailfish catch from a Nicaragua fishing tournament, and sailfish raises in the Guatemala charter fleet. Parameter values (α, β, γ) are provided for each type of data as well each model fit (R2) 27

Table 3.1 Sailfish PSAT deployment statistics..... 53

Table 3.2 Blue Marlin PSAT deployment statistics..... 53

Table 3.3: List of all estimated behavioral change points for PSAT tagged sailfish coupled with location and date of occurrence..... 56

Table 3.4: List of all estimated behavioral change points for PSAT tagged blue marlin coupled with location and date of occurrence..... 57

Table 4.1: Environmental data used in regression analyses and sources..... 134

Table 4.2 Correlation matrix showing explanatory variables used for sailfish BCPA GAM analysis. 155

Table 4.3 List of sailfish BCPA GAM models created by the step.GAM function in R program. Steps are listed in order for each response variable with descending values of AIC..... 156

Table 4.4 Correlation matrix for explanatory variables in sailfish catch data GAM... 171

Table 4.5 List of sailfish catch data GAM models produced by the step.GAM function in R software in order of decreasing AIC 172

Table 4.6 Correlation matrix showing explanatory variables used for blue marlin BCPA GAM analysis 179

Table 4.7 List of blue marlin BCPA GAM models created by the step.GAM function in R program. Steps are listed in order for each response variable with descending values of AIC..... 180

Table 4.8 Correlation matrix for explanatory variables in blue marlin catch data GAM 196

Table 4.9 List of blue marlin catch data GAM models produced by the step.GAM function in R software in order of decreasing AIC..... 197

Table 5.1 Table indicating the percent (%) residency of 21 tagged sailfish in the Exclusive Economic Zones of countries where tag tracks occurred..... 232

Table 5.2 Table indicating the percent (%) residency of 10 tagged blue marlin in the Exclusive Economic Zones of countries where tag tracks occurred..... 235

Table 5.3 Residence (% time) of satellite tagged sailfish within Costa Rica's Exclusive Economic Zone 240

Table 5.4: Residence (% time) of satellite tagged blue marlin within Costa Rica's Exclusive Economic Zone 240

Table 5.5 Catch of Yellowfin tuna between the geographical boundaries of 80-93W and 1-12N for years 2009-2015 including effort in number of sets, total catch and catch per unit effort 242

Chapter 1: Introduction

Overview

Billfish species are top predators in tropical and subtropical marine ecosystems with significant biological and ecological roles that contribute to marine biodiversity and healthy trophic systems. These billfish species are caught incidentally in tuna and tuna-like fisheries throughout the world oceans, while supporting economically and socially important recreational billfish fisheries in many coastal communities. Because they are part of the bycatch in major multinational multi-gear fisheries, billfish harvests are not always regulated and enforcement of regulations appears hard to comply with when the resources are subjected to multinational ocean governance regimes. Under these exploitation conditions billfish are often over exploited and some populations are critically depleted as claimed by Myers and Worm (2003).

Historically, in the Eastern Pacific Ocean (EPO) off the coast of Central America billfish support spectacular recreational fisheries where the world's highest catch rates and many of the world's trophy records for billfish have been obtained (Ehrhardt and Fitchett 2006). Billfish availability is linked to high density of prey resources mostly found closer to the ocean surface due to habitat compression; therefore, billfish catchability and availability to commercial fishing gear is further enhanced by oceanographic characteristics. Comparatively little is known about the ecosystem dynamics that are important to the population dynamics of large pelagic predators such as billfish, tuna, mahi-mahi, and sharks. Ecosystem dynamics are more complex in this region due to seasonal biophysical processes that cause conspicuous coastal upwelling that parcel the available habitat of the pelagic food chain. Oceanographic processes

are the result of a combination of wind, current, and geostrophic forces that enhance ocean productivity through upwelling and concentration of nutrients in specific locations that prompt the lower trophic level species such as plankton and small pelagic resources to flourish and aggregate. Oceanographic processes create a seasonally localized or stratified food chain, and predatory species find available prey and ideal habitat for their offspring: food and retention mechanisms for their eggs and larvae.

In this Dissertation, I identify the most salient, albeit most likely, biophysical mechanisms that may be associated with habitat use by billfish species, more specifically the Pacific Sailfish, *Istiophorus platypterus* (Shaw, 1792), and Blue Marlin, *Makaira nigricans* (Lacepède, 1802). As such, the Dissertation offers to assess critical aspects of billfish behavior relative to light and ocean conditions and how such behavior elicits optimal habitat use. Remote sensing technologies to measure fish behavior and ocean conditions are used as tools in support of modelling billfish population dynamics. The Dissertation progresses from intra-daily analysis of sailfish behavior in Chapter 2, to behavioral modeling of long term migratory tracks in Chapter 3, followed by statistical analysis of environmental influence on behavioral traits and billfish catch in Chapter 4, and eventually an analysis of billfish spatial distribution relative to international management boundaries and commercial catch in the region in Chapter 5.

Oceanographic Processes Relevant to Marine Resource Distribution in the EPO

In the EPO, upwelling regimes are dynamic and have dramatic effects on the levels of available dissolved oxygen at depth due to the shallowing of the mixed layer as deeper, nutrient rich but oxygen poor water is brought to the surface. Typical of eastern

boundary upwelling systems such as those off Africa and Central America, an Oxygen Minimum Zone (OMZ) is present and is more intense in the Pacific compared to the Atlantic due to a lack of oxygen injecting currents (Brandt et al. 2015). The reduction of available oxygen at depth (~100-900 meters) occurs in the EPO seasonally along with a shallowing of the thermocline and mixed layer (Stramma et al. 2010). The occurrence of OMZs and the associated vertical structure of the distribution of oxygen is shaped by the balance of oceanographic ventilation, circulation, mixing, and biological production/consumption of oxygen by organisms (Brandt et al. 2015, Karstensen et al. 2008). Off Central America, much of the OMZ is suboxic meaning the concentration of oxygen is below 5 μmol kg^{-1} with the northern core of this OMZ centered at 12-15^{o} N (Stramma et al. 2010). This suboxic level of oxygen is intolerable to most organisms including billfish and the pelagic fish that represent a majority of billfish prey thus acting as a vertical barrier, limiting migration to only the waters with suitable oxygen levels (typically shallower than 100m). The minimum oxygen layer where the limit of animal habitat occurs is ever-changing with wind and upwelling patterns which may also affect the horizontal movement of billfish due to preference for prey resources that are found in higher dissolved oxygen levels.

The seasonal environment in the EPO drives the wind and current patterns, which, in turn, drive the level of upwelling and distribution of dissolved oxygen thus the OMZ. The seasonally shifting Intertropical Convergence Zone (ITCZ), the equatorial belt where trade winds converge (Figure 1.1, top)(Fiedler 2002) and dramatically differing wind regimes occur during winter compared to the summer when it migrates as far north as over Costa Rica. In winter, the ITCZ is further south producing northeasterly trade winds

thus intensifying the wind jet features of Mexico's isthmus of Tehauntepec and Costa Rica's Gulf of Papagayo and producing increased numbers of eddy formations compared to summer when the ITCZ is over Costa Rica and the southeasterly trade winds dominate the surface wind regime (Figure 1.1).

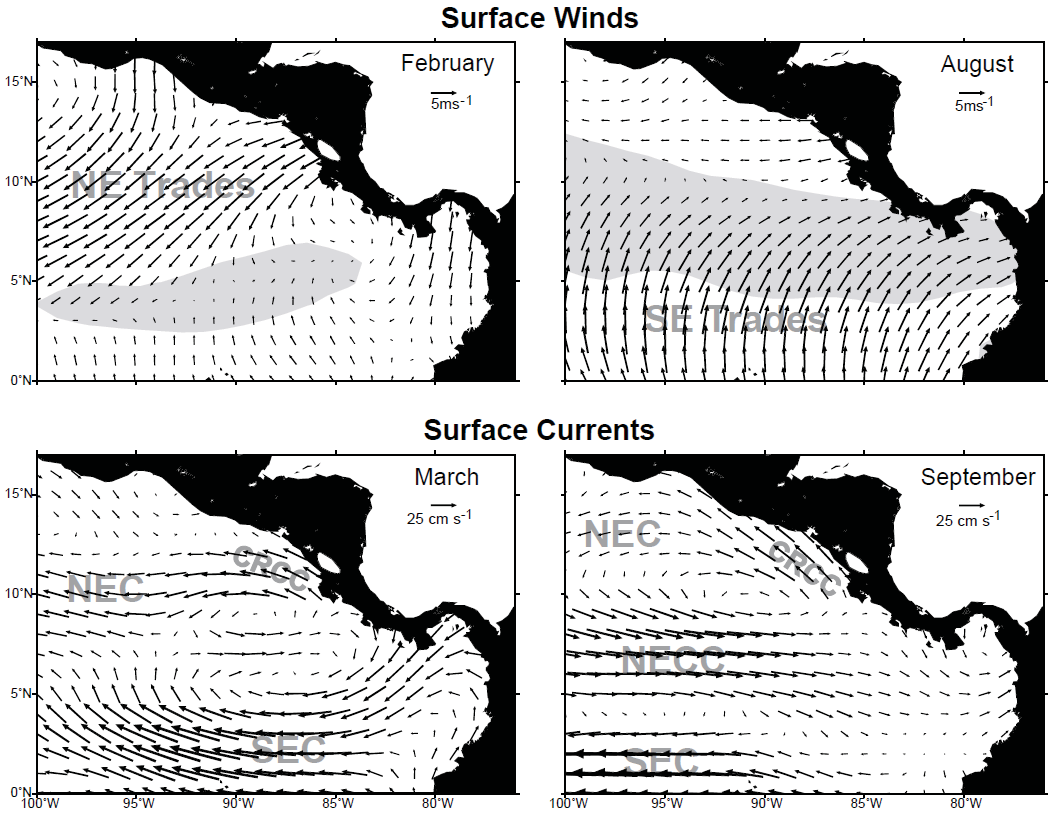

Figure 1.1 Mean wind pattern vectors are shown on top for the winter month of February and summer month of August with shading representing position of wind divergence indicative of the position of the ITCZ. On bottom the surface current pattern vectors are shown with major current systems labeled (From Fiedler 2002)

EPO currents such as the Costa Rican Coastal Current (CRCC), the North Equatorial Current (NEC), and the North Equatorial Counter Current (NECC) create a subtropical gyre known as the EPO warm pool (Figure 1.1, bottom)(Fiedler 2002). In winter and spring the circulation is well defined due to intensified wind jets; however, in

summer and fall the CRCC turns more poleward slightly weakening the gyre circulation. Through visualization of surface drifters, the overall current regime shows the slower moving EPO warm pool between the Tehuantepec and Papagayo wind jets (Figure 1.2)(Kessler 2006). In the region off Central America, currents converge and interact with the surrounding waters and wind jets producing eddy and meander features, which affect the localized upwelling. Eddy features off Central America are predominantly anticyclonic, which downwell water in the core and upwell along the outer edge, and although cyclonic eddy formations do occur, they are relatively uncommon and not as well understood (Willett et al. 2006). Based on the dynamics of upwelling and the known association with organisms and convergent fronts (Bakun 2006) one would expect animals to be found in outer edge of cyclonic eddy features where water and nutrients upwelled at the core converge and conversely, or in the core of anticyclonic eddies where convergence occurs (Figure 1.3)(Zhang et al. 2014). Research performed on Pacific seaturtles has found an association between seaturtles presence and the edges of eddy features regardless of rotation (Polovina et al 2006). Why seaturtles or any predatory animal chooses to remain in the outer edge of an eddy where shear forces dominate is of interest due to the lack of information of the feeding dynamics of predators within these large scale eddy regimes and the possibility that billfish may exhibit similar behavioral patterns in the EPO.

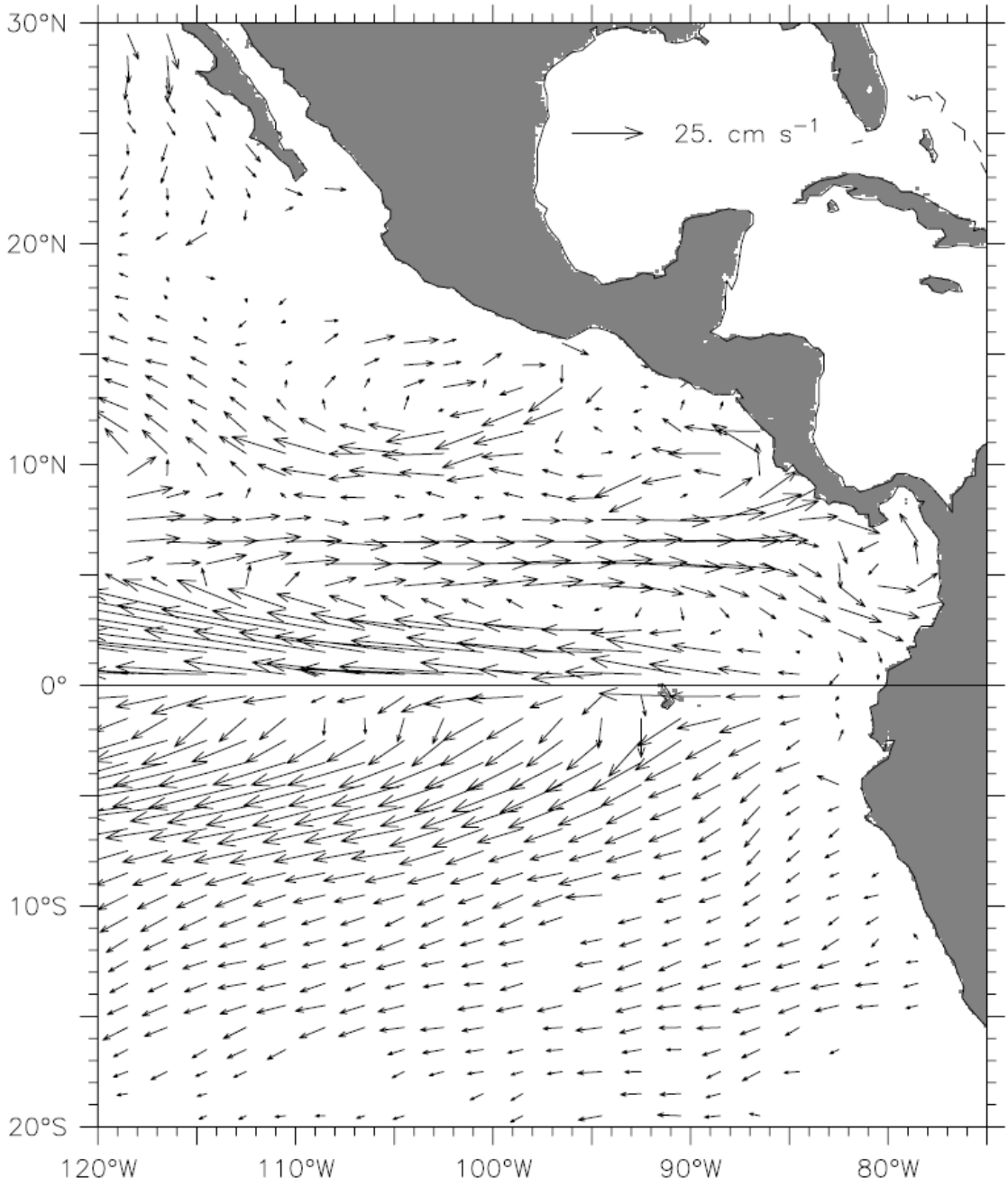

Figure 1.2: Surface current pattern in the EPO shown by mean surface drifter circulation vectors (From Kessler 2006)

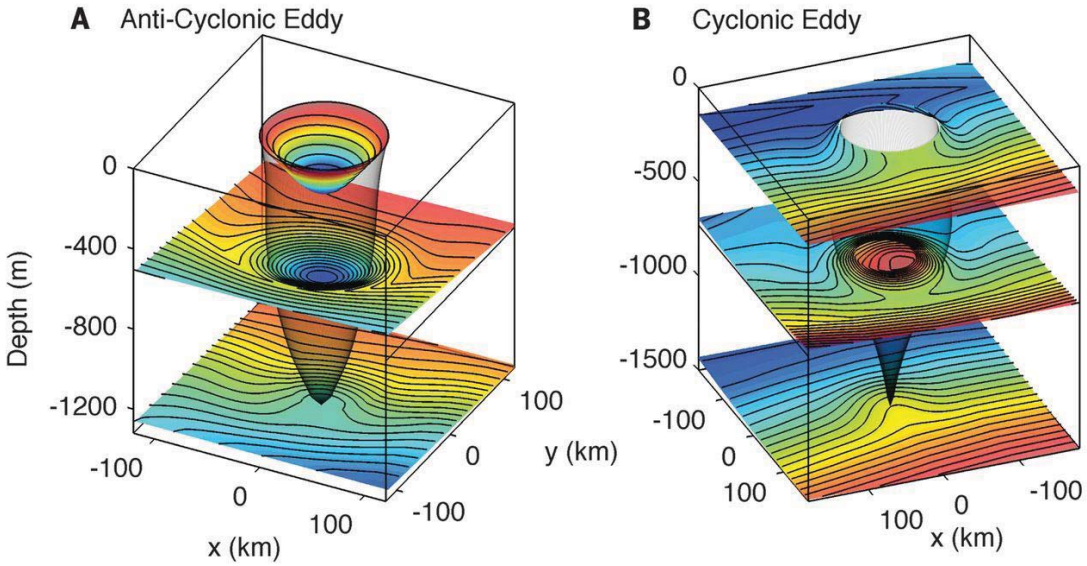

Figure 1.3 Images of two diagrams illustrating the potential vorticity contours on three isopycnal surfaces for an anticyclonic eddy (A) and a cyclonic eddy (B) (From: Zhang et al. 2014)

One of the most prominent ocean features exemplifying the dynamic processes previously described is the presence of the Costa Rica Dome (CRD) (Figure 1.4) which is formed by the conjunction of the CRCC, the complex of equatorial currents, the Papagayo wind jet, and relative instability in current regimes (Willett et al. 2006). The CRD has a surrounding cyclonic circulation caused by the CRCC which produces upwelling and a shallowing of the thermocline within the dome feature (Fiedler 2002). Although seasonally weakening and strengthening, the CRD feature is evident year-round and is known for its biological productivity due to the upwelling of nutrient rich water (Figure 1.5). This water is low in available oxygen with a minimum oxygen layer much shallower than surrounding waters thus limiting vertical migration above the CRD. Spotted Dolphin (*Stenella attenuata*) sightings suggest the species is typically associated with predatory pelagic fish, like Yellowfin Tuna (YFT) (*Thunnus Albacares),* which are

not found in large numbers directly on the CRD compared to the regions surrounding it. Fiedler (2002) hypothesized that such condition is due to the shallow thermocline, therefore, it can be assumed that in areas where prey species are abundant for large schools of YFT and Spotted Dolphin it would be an equally productive feeding place for billfish.

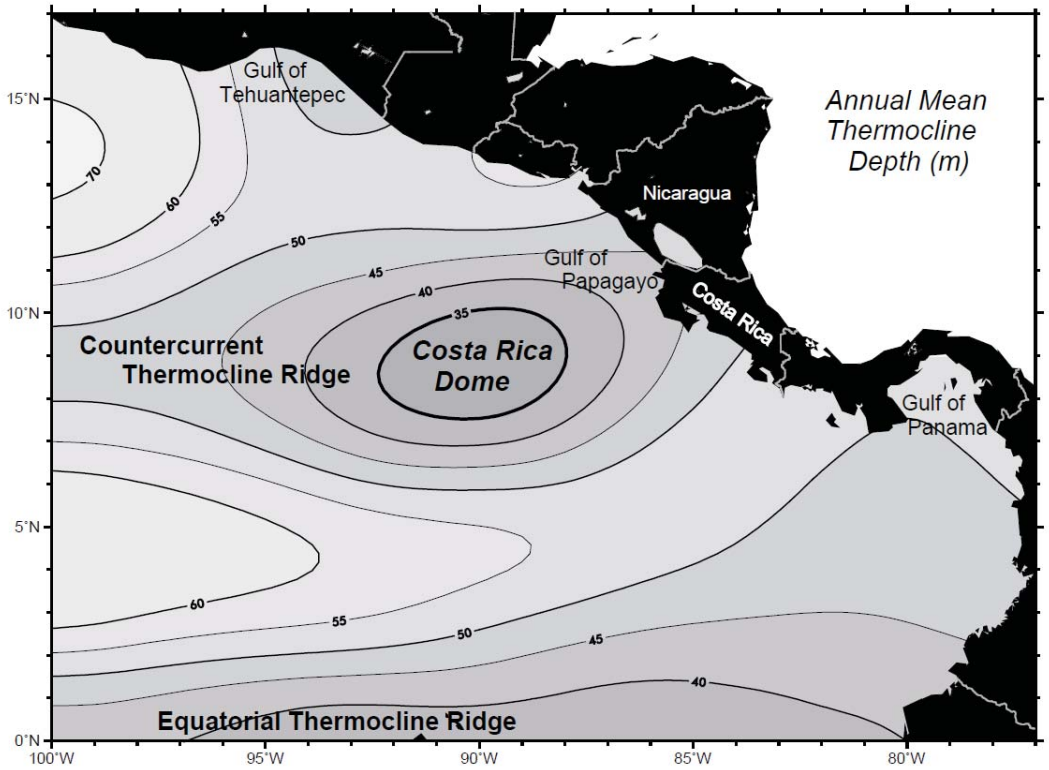

Figure 1.4 Map depicting the annual mean depth of the thermocline and location of the Costa Rica Dome. (From Fiedler 2002)

Characteristics of the EPO's pelagic ecosystem provide a niche for top predators such as billfish to exist in high densities due to the accumulation of prey in surface waters and a reduction of available vertical habitat due to oxygen constraints at depth (Ehrhardt and Fitchett 2006, Fernández-Álamo, and Färber-Lorda 2006). The EPO's complex biophysical processes effect the characterization of billfish population dynamics through prey species aggregations in an oxygen-constrained environment.

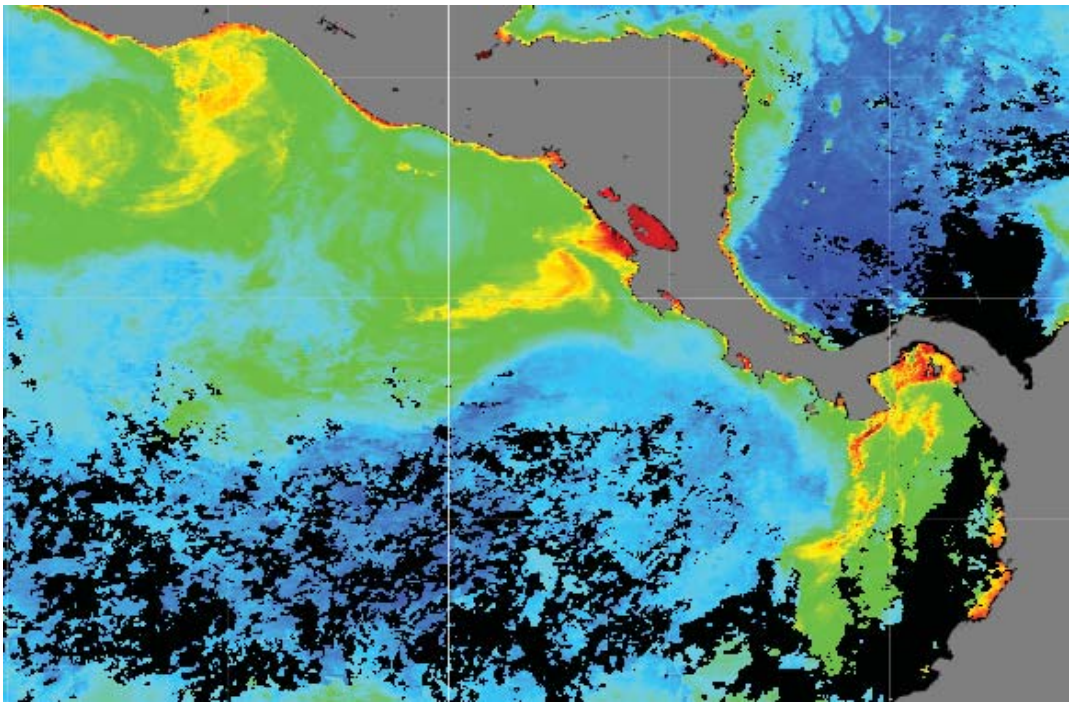

Figure 1.5 Image from AQUA Modis showing monthly average of chlorophyll concentration from February 2014 during the deployment period of satellite tagged Sailfish and Blue Marlin. Image shows presence of CRD and locally increased productivity.

In the frame of an ecosystem-based research design, the proposed dissertation research seeks to elucidate the behavioral mechanisms of habitat resource use by sailfish and blue marlin as well as analyze competing factors affecting exploitation of these billfish as bycatch in the tuna, mahi-mahi, and shark fisheries off Central America. With such knowledge, conservation and management regimes can be improved, especially in developing countries along the Pacific coast of Central America where enforcement of national and international rules is insufficient or lacking.

Identification of Research Opportunity

Distinct oceanographic formations resulting from seasonally changing winds and ocean currents are characteristic in the EPO. These could be aggregating or disaggregating biomass of plankton, juvenile stages of predatory fish, and small pelagic prey species. This conglomerate is low on the trophic chain and does not perform large scale migrations, mostly showing dispersal or aggregation as a function of the sequences and duration of biophysical events generated by seasonal upwelling regimes and eddy/meander formation. The processes governing population success of plankton and small pelagics are linked directly to energy source allocation to top predators. Such aggregation of prey provides more bio-energetically efficient feeding opportunities for adult billfish and other top predators but also to larvae and juveniles of these species cohabitating with small pelagics and associated with the plankton.

It is postulated here that these seasonal patterns in eddy/meander formation and associated upwelling regimes are important factors relative to feeding and spawning characteristics of billfish species. A fundamental hypothesis of this dissertation is that the regional eddy/meander dynamics in the EPO may frame the behavioral population characteristics of adult billfish. Such conditions are observed by extraordinary seasonal availabilities of billfish at the time of peak seasonal wind jets in winter which spin off eddy/meander formations in the regions off Guatemala and Costa Rica. Consequently, it is of significant scientific interest to elucidate the consistent billfish preference for habitat based on seasonal changes in the ecosystem.

Data or information coming from new technologies in satellite tagging and satellite oceanography generates the opportunity to integrate billfish habitat preferences

through analysis of spatial-temporal ecosystem-based factors effecting the behavior and distribution of sailfish and blue marlin. The intent of this Dissertation is to define, model, and assess behavior as well as habitat range and dimensionality available to billfish in the EPO.

Goal

To understand the Pacific Sailfish and Blue Marlin behavior and dynamic habitat use in the EPO in support of billfish conservation programs based on species ecosystem analysis framework.

Objectives

1. To assess the intra-daily behavior and habitat use of Sailfish in the EPO. (Chapter 2)

2. To determine the extent and characteristics of Sailfish and Blue Marlin migrations in the eastern Pacific Ocean off Central America (Chapter 3)

3. To quantitatively explore and model migratory characteristics of Sailfish and Blue Marlin relative to spatial/temporal oceanographic variables and the purse seine fleet targeting yellowfin tuna. (Chapter 4)

4. To explore the effectiveness of fishery management of the Yellowfin Tuna purse seine fleet relative to billfish vulnerability in Costa Rica under current (Post-2014) management strategies. (Chapter 5)

Chapter 2: An analysis of sailfish daily activity in the Eastern Pacific Ocean using satellite tagging and recreational fisheries data[1]

Overview

The Eastern Pacific Ocean (EPO) off Central America and Panama is widely considered to be one of the world's best fishing locations, where high recreational catch rates of billfish species, especially sailfish, are observed. Concomitantly, recreational fishing industries have significantly developed in the last 20 years in places such as Guatemala, Costa Rica, and Panama, contributing significantly to local economies. Such fishing tourism relies heavily on maintaining high catch rates in fishing operations under a catch-and-release modality in conventional and fly fishing. Such operations are dependent on knowledge of intra-daily, daily, and seasonal behavior of billfish species and this chapter focuses on the examination of these daily and intra-daily behavioral traits.

Despite the conspicuous appearance of sailfish in the EPO, little is understood of the population dynamics which are critical for management and conservation of the species. Similarly, the behavioral aspects that are important to successful catch-and-release recreational fisheries are also poorly understood. Attempts at formal stock assessments for sailfish in the region were not successful due to a lack of historical catch information (Hinton and Maunder, IATTC 2013); however, fishing mortality may be well above estimates of natural mortality for sailfish (Fitchett 2015), which is an indication

[1] **The data, analyses, and interpretation contained in this chapter substantially embody a work published (Pohlot, B., Ehrhardt, N., (2017) An analysis of sailfish daily activity in the Eastern Pacific Ocean using satellite tagging and recreational fisheries data. ICES J. Mar Sci). Although the co-author(s) of this manuscript are appropriately attributed, the data and analyses represent my original research.**

that the stock may be subjected to significant exploitation. Additionally, habitat characteristics affecting fish behavior and habitat based methods of catchability estimation, which should be included in modern stock assessment methods, are currently missing from formal Pacific sailfish assessment attempts (Hinton and Nakano 1996, Freon and Misund 1999, Bigelow et al. 2002, Bigelow and Maunder 2007). Sailfish are the most coastal of the billfish species in the EPO, inhabiting complex regional upwelling systems that have been hypothesized to be affected by low dissolved oxygen at shallow depths, conspicuous seasonal oceanic fronts and temperature limitations, as well as the aggregation of prey above the shallow mixed layer (Bakun 2006, Ehrhardt and Fitchett 2006, Prince and Goodyear 2006, Friederichs 2009). Because of difficulties in fine-scale temporal and spatial data collection, little information is available about the intra-daily physical activity of billfish in general, let alone, sailfish.

The coupling of the highly dynamic sailfish behavior to environmental conditions can provide important insights into patterns of animal behavior that may help to improve use and conservation of the resource in the regional recreational fisheries. Pop-off satellite tags (PSAT) represent the only viable means of effectively collecting data relevant to individual sailfish behavioral characteristics due to the highly migratory nature of the species and the relative isolation of the EPO tag deployment region making recovery difficult. In this region, sailfish have been tagged using PSATs with relative success; examining migratory, temperature and depth patterns of tagged animals (Braun et al. 2015, Domeier et al. 2003, Prince et al. 2006). Since the undertaking of those tagging endeavors, satellite tag technologies that record acceleration present an opportunity to confirm previous findings and uncover new billfish behavioral

characteristics previously not possible to examine. Such investigation is possible by recording time referenced accelerometry at high-rate sampling. This study aims to take advantage of modern advancements in satellite and hardware capability to examine the hourly behavior of sailfish in the EPO related to the amount of available sunlight in the environment. These results are then compared with hourly fishing success in billfish tournaments and in for-hire recreational fishing trips carried out in the Pacific Central American region with the purpose of dimensioning fishing strategies relative to fish behavior.

Methods and Materials

The recent incorporation of a solar panel and accelerometer in the Sea Tag-MOD PSAT developed by Desert Star Systems LLC (Marina, CA) provided the opportunity to collect relatively high-resolution sailfish swimming behavior data and the ability to maintain power for data transmission with a small battery attachment. The SeaTag-MOD's used in this study collect 3-axis magnetometer and accelerometer data, each collected at the user-specified resolution. Seven of these SeaTag-MOD PSATs were deployed on Pacific sailfish in an area off Puerto Quetzal, Guatemala (Figure 2.1) on 4 April 2012 on recreational fishing vessel *Captain Hook*. All Sailfish were caught using recreational methods of trolling artificial lures (teasers) and dead ballyhoo baited on circle hooks. Tag placement and sailfish handling techniques followed the billfish tagging protocol developed by Prince et al. (2002a) with the addition of Oxytetracylcin and Neosporin© antibiotics to the Hallprint floy dart head used to attached the PSAT to fish. To maximize animal and tag survival, PSATs were only attached to healthy (non-

bleeding, non-damaged, not gut hooked) sailfish and each sailfish was positioned boatside with water flowing over its gills, until researchers were satisfied the animal had been revived. Mortality and injury were minimized using non-offset circle hooks and by never removing sailfish from the water (Prince et al. 2002b, Schlenker et al. 2016).

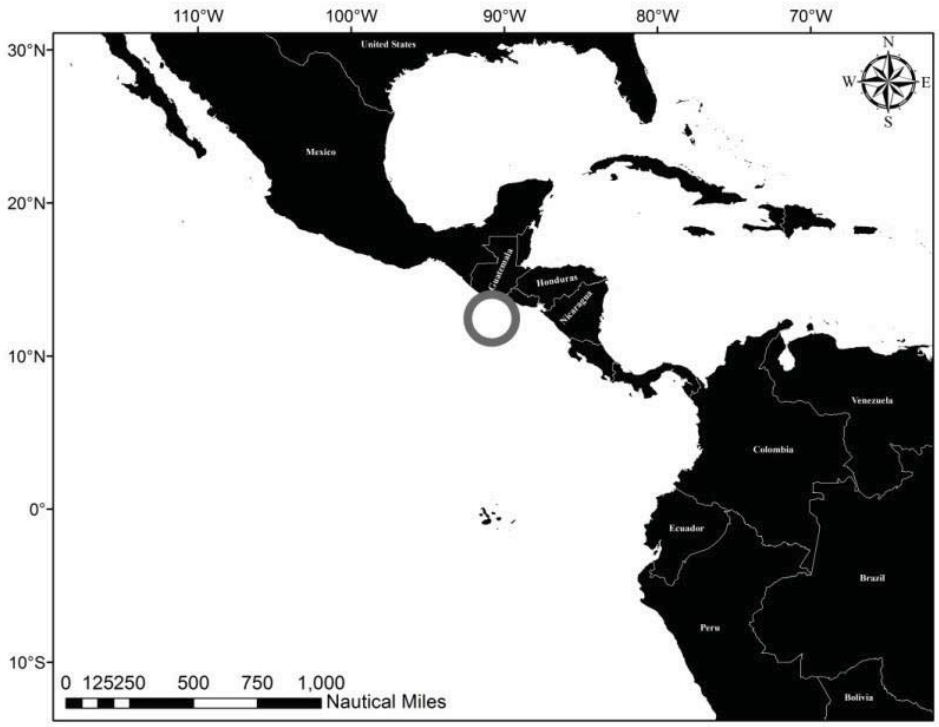

Figure 2.1: The study area of the Eastern Pacific Ocean shown by the circle off Puerto Quetzal, Guatemala

A sticker on each tag in English, Spanish, and Japanese, explains that there is a $300 reward for the return on the tag to encourage commercial longliners and recreational fishermen to return tags where the fish was caught or tag was found separately. Due to the distrust of many local longliners to management and the prevalence of illegal fishing by outside countries, the expectation of tag returns is low. A system of physical recovery other than a rewarded return was in place at the time of the tagging studies. The system uses radio direction finding to locate the transmitting tag.

The system required the tag to be within range of vessels available for hire along the coast of Central America.

Acceleration data is measured in *G*'s which are defined as the acceleration caused by Earth's gravity, where 1 *G* is equivalent to 9.8 m/s^2. These accelerations can occur in any direction in three-dimensional space; however, on Earth the constant downward 1 *G* is always present due to gravity, both on land and in water. Laboratory "mini-missions" consisting of hourly and daily PSAT data collection were conducted using a floating PSAT in a container prior to the initial deployment to determine an acceleration sampling rate that could be compressed and relayed through the ARGOS system of satellites. ARGOS satellites receive and distribute sensor data from transmitting devices such as PSATs and represent a data choke point in terms of transmitting large datasets such as high-rate accelerometry from a floating device in the ocean. Based on the experience gained during the "mini-missions", the SeaTag-MOD PSAT's accelerometer was configured to collect *G*'s in three axes (*x, y, z*) (Figure 2.2) every 0.64 seconds; however, such a transmission rate is not feasible for long term studies due to PSAT power and data storage limitations in the available technology as of 2012 (M. Flagg, Pers. Comm.). For this purpose, the total *G* is calculated every 0.64 seconds by incorporating the single axis *G* measurements and applying to the equation:

$$Total\ G = \sqrt{x^2 + y^2 + z^2}$$

Onboard the PSAT, the standard deviation of the total *G* over 3-minute periods was calculated and transmitted to ARGOS, providing deviation values where a larger *G* standard deviation indicates a wider range of accelerations during the 3-minute sampling period duration, and therefore, a wider range of fish activity, indicating a behavior other

than cruising (i.e. not accelerating). Although the PSAT used is capable of relatively high-resolution data capture through firmware manipulation, this study sought to find the best compromise of battery life to satellite data transmission capability while providing useful analysis of sailfish behavior. Because of this compromise, study duration was limited to 10 days for this first deployment.

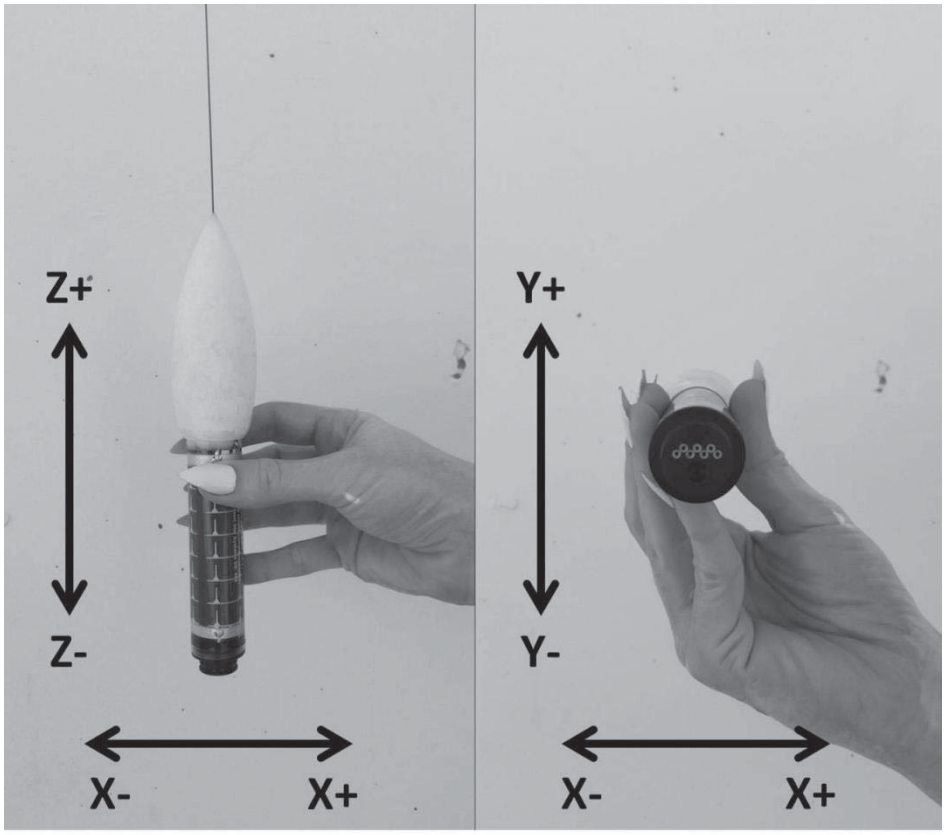

Figure 2.2: Image showing 3-axis orientation of the accelerometer in the SeaTag-MOD. X and Y axes are perpendicular to the length of the tag while the Z axis runs the length of the tag. Additional tag battery not shown attached.

The deployment period of PSATs took place during the full moon which occurred on 6 April 2012. SeaTag-MOD PSATs use the solar panel to measure light for geolocation; however, this solar panel is not sensitive to lower moon light levels and recorded activity due to such low night lighting conditions could not be matched. Therefore, light data containing moon light levels was explored from all satellite tagging

databases containing such information and available to these researchers from Eastern Pacific PSAT tagged billfish or floating PSATs.

In the absence of sea surface moon light level data from Guatemala, data gathering from tagging databases followed the restrictions that the animal needed to remain in the upper surface layer and to have been active during a time of similar moon phase and altitude. This was accomplished using data retrieved from the International Game Fish Association (IGFA) tag database from 2005 where a Pacific sailfish was tagged with a Wildlife Computers Inc. mk10 satellite tag capable of recording low light levels and deployed during the full moon on 17-18 September 2005 off the Costa Rica/Panama coast. This PSAT remained at an average depth of 7.24 meters during the full day period with average depth for nighttime (full moon) hours at 2.98 meters. This sailfish PSAT was physically recovered, providing data stored every 15 seconds, and included a light sensor sensitive enough to measure moon light levels (Wildlife Computers Support, Pers. Comm).

To examine the validity of using light levels from the 2005 IGFA study as a proxy for the current study, historical moonrise and moonset times were obtained from the US Naval Observatory Astronomical Applications Department to compare the two time/location points. The 2005 moonrise times were reported within the same hour as the 2012 Guatemala times (between 18:30 and 19:30 for both). Likewise, the moonsets were also approximately the same. Additionally, moon altitude reached its maximum at or near 23:30 in both locations, and the altitude, or angle from the horizon, was within 12 degrees. This analysis shows that although the region of tag residence from the 2005 IGFA study off Costa Rica and Panama is latitudinally distant from the study area in

Guatemala, the effect on the pattern of light availability remains the same only with a difference in intensity of light, which is removed through data standardization making light hourly signals compatible in a unit-less scale.

The September 2005 light data was seasonally compensatory with the data obtained during the April 2012 deployment on either side of winter. Due to differing locations and dates between data types, additional validation was performed to ensure light data used from the 2005 IGFA study was congruent with the actual seasonal light environment seen by the April 2012 PSAT tagged sailfish in Guatemala. This was accomplished by obtaining data from a floating Wildlife Computers Inc. miniPAT PSAT placed by IGFA in 2013 in the same Guatemala location as our 2012 study. The nearest available seasonal light data was extracted from this miniPAT, specifically from the month of May, and compared to the sunlight data reported from the 2005 tag. The investigation revealed the light pattern found in the PSAT placed in 2005 off Costa Rica and Panama to be nearly identical to the PSAT light patterns obtained in Guatemala in 2013 (Figure 2.3), further validating the use of light patterns from the 2005 tag for this study, despite being from latitudinally different locations. Variability witnessed in the PSAT light data from Costa Rica/Panama is due to the estimation of light while on the sailfish at a shallow depth. Conversely, the 2013 Guatemala was not attached to a fish, and this floating tag was consistently at the surface, producing a smooth curve. This confirmation permitted the use of daytime hourly light data from 2005 off Costa Rica/Panama for the present study, which, unlike the other PSAT data discussed, is conveniently available in full time series for sun and moon light levels.

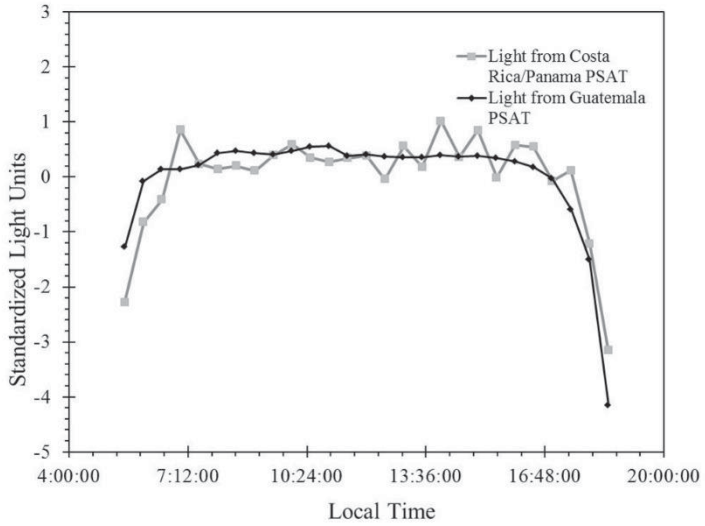

Figure 2.3: Validation of light data from 2005 Costa Rica/Panama PSAT (Gray Line) using floating PSAT light information from Guatemala in 2013 (Black Line). Standardizing data removed effect of light intensity differences focusing only on relationship between timings at two locations and times.

Sailfish hourly activity was measured as the average standard deviation of acceleration within 3 minute periods on daily cycles and was further analyzed relative to an index of fish abundance expressed by raised sailfish (i.e. fish seen by captain and crew around vessel) statistics in the Guatemalan for-hire recreational fishery. Mean statistics on number of fish raised in the recreational fishery are well correlated with catch-and-release statistics where only 43% of the fish raised are actually caught (Ehrhardt and Fitchett 2006); therefore, rates of raised fish should be a better quantitative indicator of sailfish presence compared to catch alone. This is further emphasized because often catch rates are zero even when fish were raised to the boats. Hourly sailfish raise and resulting fish catch statistics were collected using a satellite logbook system specifically implemented on six recreational charter vessels that operated in the Guatemala fishery. For this purpose a smartphone was used to log and automatically geolocate the raises, hookups, and caught billfish and other pelagic species entered by captains while actively

fishing. Data used from the satellite logbook system was from the 2012 fishing season (November 2011 to April 2012). Logbook data was filtered to remove the effect of vessel traveling to and from the fishing grounds with only full hours spent on the fishing grounds cruising at trolling speed remaining to ensure analysis of active fishing only. A similar analysis was also performed using tournament catch data available in hourly catch and release format from the Flor de Caña billfish tournament which took place on 14-16 August 2014, off the nearby country of Nicaragua. Only data from the 2014 tournament was available at the time of this study.

To quantitatively compare trends in sailfish behavior during mid-morning hours through sunset; sailfish acceleration, tournament hourly catch per vessel, and recreational fish raise data were each fit using a non-linear least squares hazard model with three parameters in a double exponential format as follows

$$(1 - e^{-\alpha t^{(\beta-1)}})\gamma,$$

where γ is a scaling parameter, t is time, and α and β are parameters to express shape and steepness of the fitted distribution, respectively.

Results

The seven deployed SeaTag-MODs collected data from the time of deployment until the programmed release date followed immediately by ARGOS satellite transmission. Data was relayed through ARGOS opportunistically resulting in intermittent groups of data, not necessarily in sequence of being retrieved from the tag. To ensure maximum data retrieval, transmitting tags were allowed to transmit until all data was retrieved or the PSAT stopped transmitting. Three tags transmitted full acceleration data (100%) for the 10-day period with minimal data transmission gaps while one tag transmitted seven of the 10 days (70%) of acceleration data and a fifth tag

transmitting three full days (30%). Two tags only transmitted depth and location. No fish mortality occurred during this study and none of the PSATs were physically recovered. PSATs not reaching full duration were due to tag shedding caused by force from the large size of the tag and battery (145 grams and 230mm in length) combined with the fast swimming nature of sailfish (Figure 2.4).

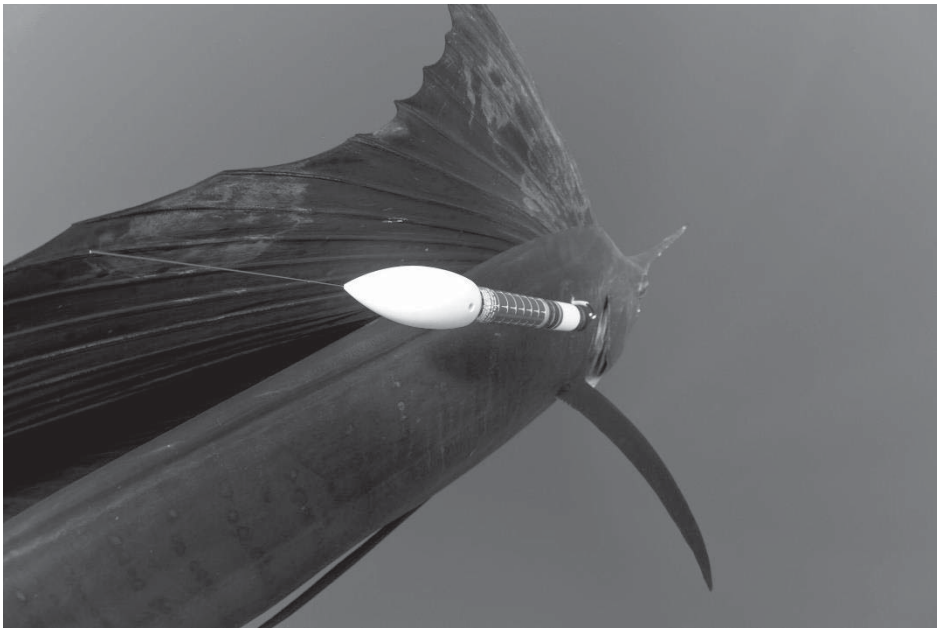

Figure 2.4: Image of SeaTag-MOD attached to Pacific sailfish from the 2012 study. Photo of sailfish tagged for this acceleration study provided by Marc Montocchio of 36North.

Sailfish acceleration data was standardized to the nighttime average after the moon had set, where the animal appeared inactive providing a dataset including a total 40 sailfish data days which could then be compared to the available light from a full moon deployed satellite tag (Figure 2.5). Complete data from five tagged sailfish showed a pattern of increased activity concomitant with an increase in acceleration variance during daylight hours with no sustained activity occurring during dark periods of night (Figure 2.5). As the sun rose in the early morning just before 06:00 hours, sailfish activity begins to increase but at a slower rate than the increase in light intensity. The peak of activity

was found between 11:00 and 17:00 hours local time when light is at a maximum. Following this peak there is a sharp decline in sailfish activity directly coinciding with the decline in light intensity as the sun sets over the horizon at 18:00 hours.

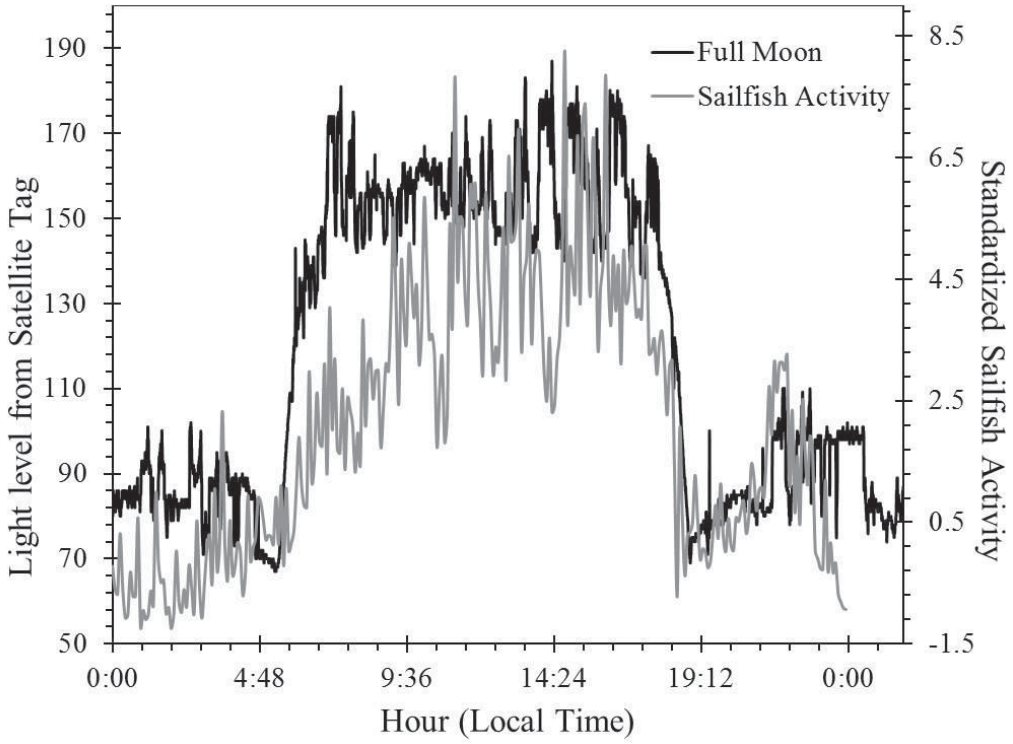

Figure 2.5: Plot showing the close intra-daily relationship between light level from a PSAT tagged sailfish on primary axis and standardized sailfish activity (acceleration) on the secondary axis. Sailfish are shown to be active between 06:00 and 18:00 when the sun is above the horizon but are not active when light is not available at night. PSAT tagged sailfish showed increased activity during the fully illuminated moon after 19:00 with a peak coinciding with the peak of moonlight intensity between 21:00 and 22:00 hours.

Following the setting of the sun, accelerometer tagged sailfish showing an increase in activity beginning around 19:00 hours local time which coincided with the rise of the fully illuminated moon, occurring 2 days into the tag deployment, indicating activity in response to light of the moon. During the full moon, sailfish reached a maximum nighttime activity between 21:00 and 22:00 hours relating to the highest

illumination of the moon during the time of the trial. This activity immediately declined following the peak of moonlight intensity (Figure 2.5).

Available light and depth data from the 2005 IGFA PSAT reveals an extremely close relationship with light and diving behavior (Figure 2.6). Using a monthly average for light and depth, it is evident the sailfish only undertook deep dives during the daytime hours (06:00-18:00) with little to no diving behavior at night.

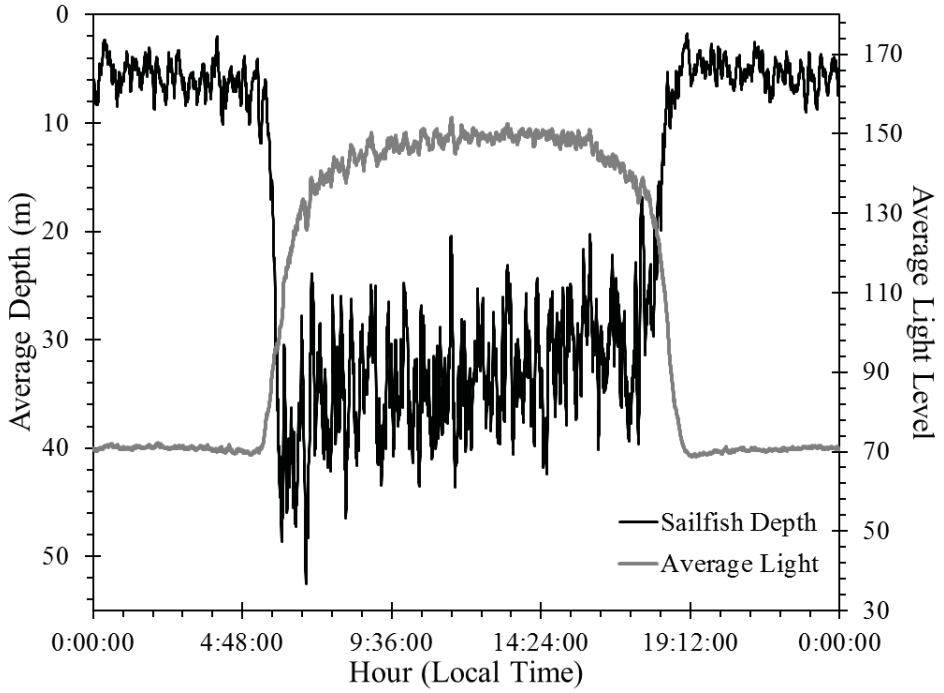

Figure 2.6: Average depth (m) by hour (primary axis) and average light by hour (secondary axis) from an IGFA PSAT tagged sailfish from 21 September to 21 October 2005 is shown in the plot. On average, sailfish diving behaviors only occurred when the sun was above the horizon with little to no diving activity when light was unavailable.

The analysis of sailfish activity through daily dynamics of catch and raise statistics reveals the highest number of sailfish-bait encounters occurs between 09:00 and 14:00 hours local time in both sailfish raises in Guatemala and sailfish catch in the Nicaragua fishing tournament (Figure 2.7). In both the catch data as well as the reported raises, there is an increase in encounters during the morning period followed by a peak

plateau from 09:00 to 14:00 hours which drops off steadily after 14:00 hours. Tournament data suggest a slight decrease in catch rates at noon which was not observed by Guatemalan fishers. Both catch data and raise data suggest similar patterns in amount of sailfish encountered during each hour.

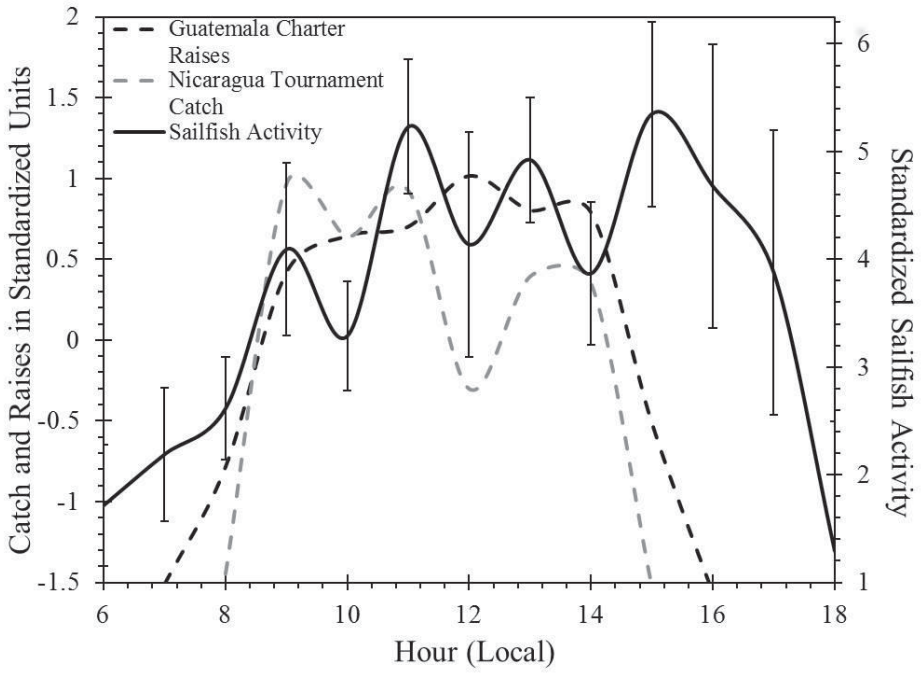

Figure 2.7: The hourly relationship between three data types: sailfish raises (sailfish seen by crew around vessel) in the Guatemala charter fleet (Black Dashed Line), sailfish catch in a Nicaragua fishing tournament (Grey Dashed Line), and sailfish activity (accelerations) hourly averages with standard deviation bars (Solid Black Line). The highest number of encounters in the fishery occurs between 09:00 and 14:00 hours but are relatively low prior and after this time range whereas sailfish activity is highest between 11:00 and 16:00 hours with sustained high activity until 17:00 hours.

Model fitting to acceleration, catches, and raises resulted in R^2 values of 0.627, 0.559, and 0.826 respectively (Table 2.1). In comparing the fitted estimations, the declining trend is evident beginning around 14:00 hours local time for catch and raise data and around 17:00 hours for acceleration (Figure 8a-c). Acceleration about the

estimated line is real variability in sailfish activity level and cannot be considered error about a regression, an important distinction in the visual analysis of Figure 2.8a.

Table 2.1: Modeling results from a non-linear least squares hazard model fit to three data types: Sailfish Activity, sailfish catch from a Nicaragua fishing tournament, and sailfish raises in the Guatemala charter fleet. Parameter values (α, β, γ) are provided for each type of data as well each model fit (R^2).

Data Type	R^2 Value of Fit	Parameter	Parameter Value
Sailfish Activity	0.627	α	9.787e36
		β	30.570
		γ	4.905
Nicaragua Tournament Catch	0.559	α	3.517e7
		β	7.440
		γ	100
Guatemala Charter Raises	0.826	α	3.878e21

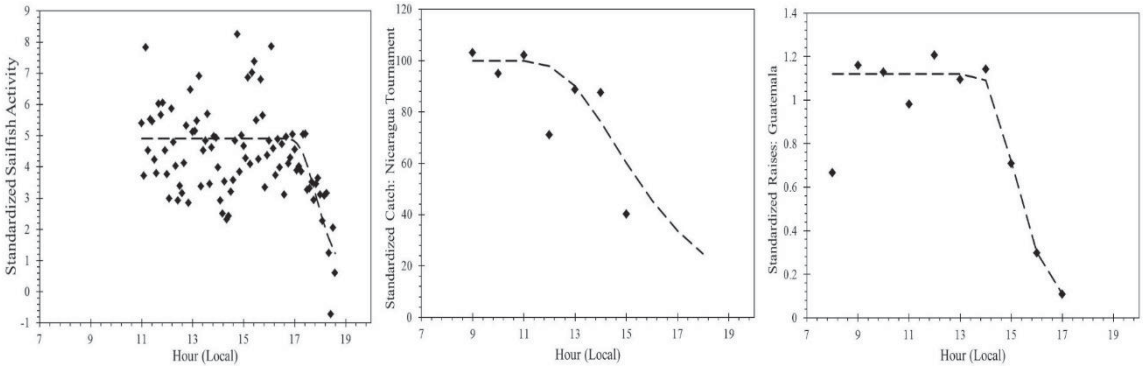

Figure 2.8: Plots of model results from a non-linear least squares hazard model fit to sailfish activity (a), sailfish catch in a Nicaragua fishing tournament (b), and sailfish raises from the Guatemala charter fleet (c). Observed data is shown with Black Markers with model fits shown with Black Dashed Lines. Model fits and parameter values are shown in Table 1.

Discussion

In all oceans the capability of predator fish to survive and grow relies on their ability to catch prey species and successfully reproduce. In the EPO, the pelagic environment provides little to no opportunity for physical cover or refuge and is vertically limiting by dissolved oxygen (Bakun 2006, Ehrhardt and Fitchett 2006, Prince and Goodyear 2006). For the purpose of feeding in this unique environment, the billfish has evolved complex physiological strategies especially in their visual capability, with billfish having some of the highest optical sensitivities of any teleost (Fritches et al. 2003b). Laboratory studies of the billfish brain and eye have revealed vision to be the dominant sense, supported by the well-developed optic tectum brain structure, which is involved in visual signal integration (Fritches et al. 2003a, Fritches et al. 2003b, Lisney and Collin 2006, Southwood et al. 2008). Billfish retinal analyses have been historically limited by technologies available at the time (Tamura and Wisby 1963, McFarland and Munz 1975, Kawamura et al. 1981); however, more recent evidence suggests billfish species to possess the eye structure and visual pigments necessary to discriminate colors and that the retina is quite well adapted to maximize visual acuity in the open ocean environment, where the interface of bright and dim light occurs (Fritches et al. 2000, Fritches and Warrant 2001, Fritches and Warrant 2004, Kröger et al. 2009). In the open ocean, light decreases logarithmically with depth where at 300m, only 0.003% of the surface light is available (Fritches et al. 2003b). Prey items are best visualized if the background light wavelength at a given depth matches the visual pigments in the retina of the predator. This is true for the billfish retina in the open ocean where only the violet,

blue, and green shades (430-550nm) are available at depth deeper than around 150-200m (Fritches et al. 2003a, Bone and Moore 2008).

Knowing vision is the dominant sense reveals the importance of the amount of available light, especially at depth. The level of information that can be attained from an image is a function of the number of photons, or amount of light, used to create said image (Lythgoe 1979). The amount of light available to a billfish directly affects the ability to feed, being that visual spatial and temporal resolution are linked to the brightness of the habitat (Southwood et al. 2008). With the domination of vision as the sensory strategy of billfish feeding, it is no surprise that PSAT tagged sailfish exhibited higher activity and bait encounters during the daytime hours when light is fully available and, similarly, that the increase in light of the full moon caused an increase in sailfish activity. The positive activity response to the moon as well as the timing of sailfish bait encounters implies the circadian rule applies to billfish in that a positive relationship between activity and light is witnessed (Godin 1981). This concept is further supported by the overall lack of sailfish acceleration variance during the nighttime hours when the moon was not present. Based on these findings, we can suggest that Pacific sailfish are exhibiting an exclusive pattern of diurnal activity, not feeding nocturnally absent a full moon, and that their response to the light is likely an evolved response to optimize feeding efficiency.

Billfish occupy the same pelagic habitat as two top predator species, the yellowfin tuna (YFT) and spotted dolphin, which are known to form a mutual association (Scott et al. 2012) that has been widely used by tuna purse seiners to locate and catch schooling yellowfin associated with spotted dolphin aggregations. Spotted dolphin have very

different sensory strategies compared to billfish or yellowfin tuna due to their ability to echolocate. An analysis of gut contents of spotted dolphin and YFT was performed by Scott and Cattanach (1998), revealing spotted dolphin to be overnight and early morning feeders with a majority of their sampled stomachs containing undigested food between 07:00 and 11:00 hours but few stomachs had any trace of food after 13:00 hours (Scott and Cattanach 1998 Figure 14). Yellowfin tuna, which have a more similar visual system to billfish, were found to contain full stomachs further into the daytime hours than spotted dolphins (Scott and Cattanach 1998 Figure 14), a YFT behavioral pattern that appears much more similar to sailfish (Figures 2.5, 2.6, 2.7, and 2.8).

Results from recreational bait encounters of raises and tournament catch presented here suggest sailfish activities related to feeding behavior that decreases steadily in the afternoon between 12:00 and 14:00 hours until 17:00 hours when recreational data is no longer available. This finding in the recreational fleet coincides with the timing of lesser full stomachs in the late afternoon in YFT analyses reported by Scott and Cattanach (1998 Figure 14); however, sailfish acceleration data suggests these tagged animals remained active longer into the early evening hours than encounter data implies (Figure 2.9). The reasoning for this mismatch of timing can only be hypothesized but could be related to a social behavior following feeding and eventual food satiation. An important note here is the prevalence of free jumping sailfish witnessed by Costa Rican captains in the late afternoon which could be related to this social behavior (D. McGuinness, Pers. Comm.).

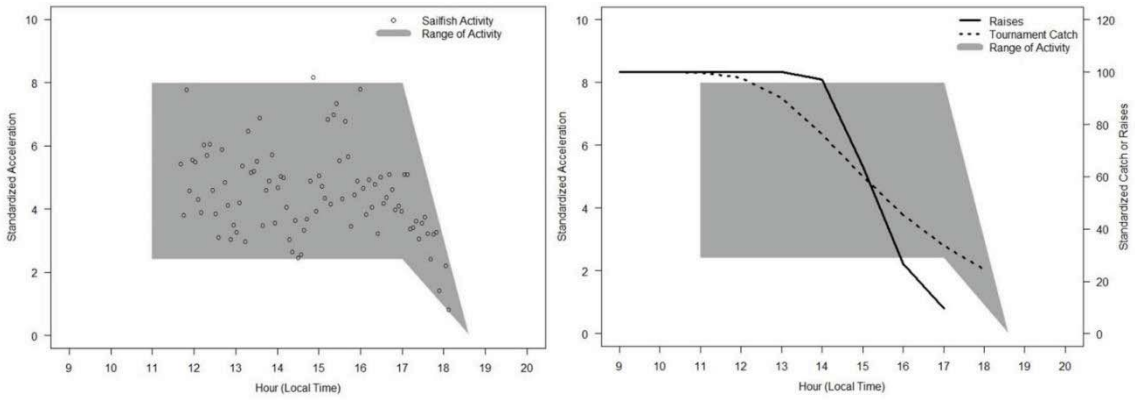

Figure 2.9: Sailfish activity (acceleration) results showing the range of acceleration data values (a) with observed values represented by open black circles and the range of values indicated by the gray shaded region. Figure (b) shows this same gray shaded region representing the range of activity values with the modeled line fits for sailfish catch and raises from Figures 8b and 8c. The range of high activity persists longer into the afternoon and evening than fishery encounters suggest sailfish are actively feeding.

The stomach content analyses reported by Scott and Cattanach (1998), along with the results of hourly activity in this study, suggest that top predators in the EPO are making use of their sensory advantages by timing their feeding behavior to best fit their sensory strategy. Spotted dolphin, using echolocation, are feeding at night when the sailfish and YFT are at a visual disadvantage based on their eye morphology and inability to echolocate. Sailfish and YFT feed during the daytime hours when the sun provides enough light for their vision to function at depth. These relationships among predators can be considered evolutionarily advantageous especially if daily timings of feeding facilitates a higher diversity of predators in the EPO ecosystem by decreasing the amount of predator-predator interactions.

Depth of diving and the timing of billfish diving is related directly to the activity level of billfish as well as their availability to the surface oriented recreational fishery. As mentioned previously, available light and the wavelengths outside of the blue-green-

violet shades decrease rapidly with depth. This acts to limit billfish vertically to the epipelagic zone where enough light is present during daylight hours. Of the fine scale (hourly) billfish depth data that is available, studies have found sailfish and marlin species to remain in the upper surface mixed layer sometimes as shallow as 10m a vast majority of the time, while only undergoing deeper excursions for short periods and almost always during the daytime (Holland et al. 1990, Block et al. 1992, Brill et al. 1993, Graves et al. 2002, Gunn et al. 2003, Kraus and Rooker 2007, Sippel et al. 2007, Chiang et al. 2011). Although a depth analysis was not the primary focus of this research project, 12-hour depth histograms were available from 7 Guatemala PSAT tagged sailfish revealing differences between daytime (6AM-6PM) and nighttime (6PM- 6AM) hours with fish being shallower on average at night and doing shallower dives (Figure 2.10). Undergoing dives only during daylight hours confirms the necessity of light for billfish activity knowing their vision is least acute when no light is present. This paper contends that the primary reason for sailfish to remain in the upper water column in all oceans is the advantage provided by increased light, or photon, availability in their ability to visualize prey. Few deep dives by billfish are witnessed in the EPO but their visual system suggests they have the ability to undertake feeding excursions to depths much deeper based on data from the Costa Rica/Panama deployed IGFA PSAT used for light analysis in this study. This PSAT tagged sailfish, on average, exhibited diving behavior consistent with the hypotheses provided by this study in that the sailfish only dove deeper only during hours when light was available, i.e. during the day with little to no diving related behaviors witnessed at night(Figure 2.6). Due to the satellite transmitted data being organized as histograms averaged over 12 hour periods, the slight increase in

diving behavior expected with the increased illumination of the full moon could not be analyzed.

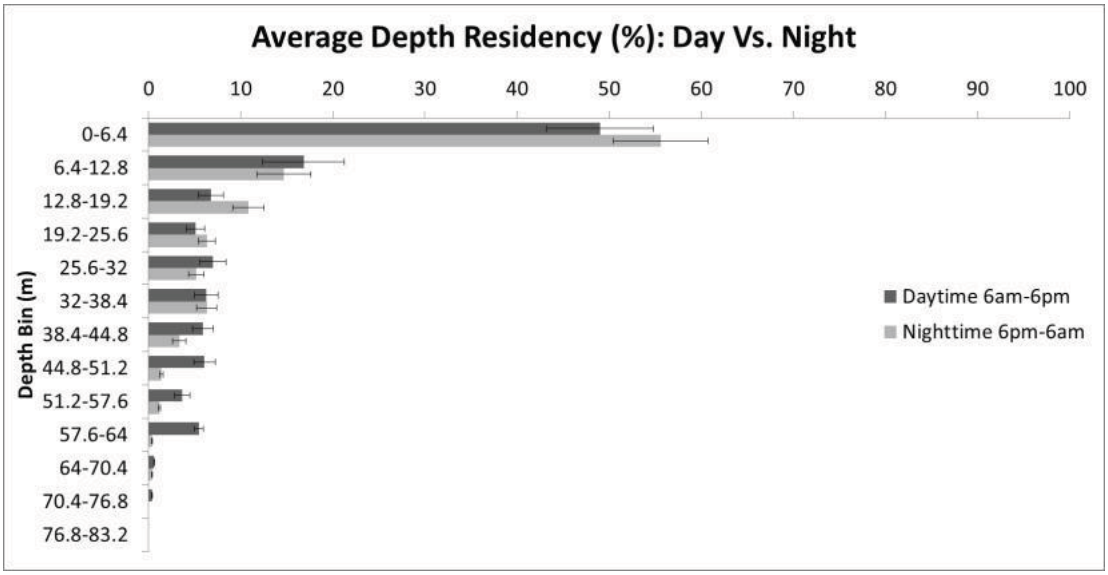

Figure 2.10: Histogram of depth residency of 7 tagged sailfish off Guatemala separating daytime hours, 6am-6pm, (dark gray bars) and nighttime hours, 6am-6pm, (light gray bars). The x-axis is the percent (%) residency within the specified 6.4m depth bin (y-axis). Error bars represent the standard error of the estimate.

The presence of an oxygen minimum zone (OMZ) characterizes the EPO ecosystem limiting the amount of available oxygen to both predator and prey (Ehrhardt and Fitchett 2006). On average, the OMZ in the EPO off Central America is typically shallower (<100-150m) than the maximum depth of available light a sailfish is capable of occupying (>200m). In fact, preliminary results from the single recuperated IGFA PSAT tagged sailfish off Costa Rica/Panama, where the EPO OMZ is deepest, suggests maximum diving behavior is coincident with the depth of the average OMZ (130m-180m) although the average depth is much shallower (Figure 2.11). In short, the OMZ could be acting as a physical barrier and could be negatively affecting the evolutionary advantage of hunting at the interface of bright and dim light due to the prey and predator inability to occupy depths where light wavelengths are ideal for billfish hunting. On the

other hand, habitat compression facilitates the concentration of billfish prey in shallower regions of the water column where light conditions are optimal for the billfish to successfully pursue prey.

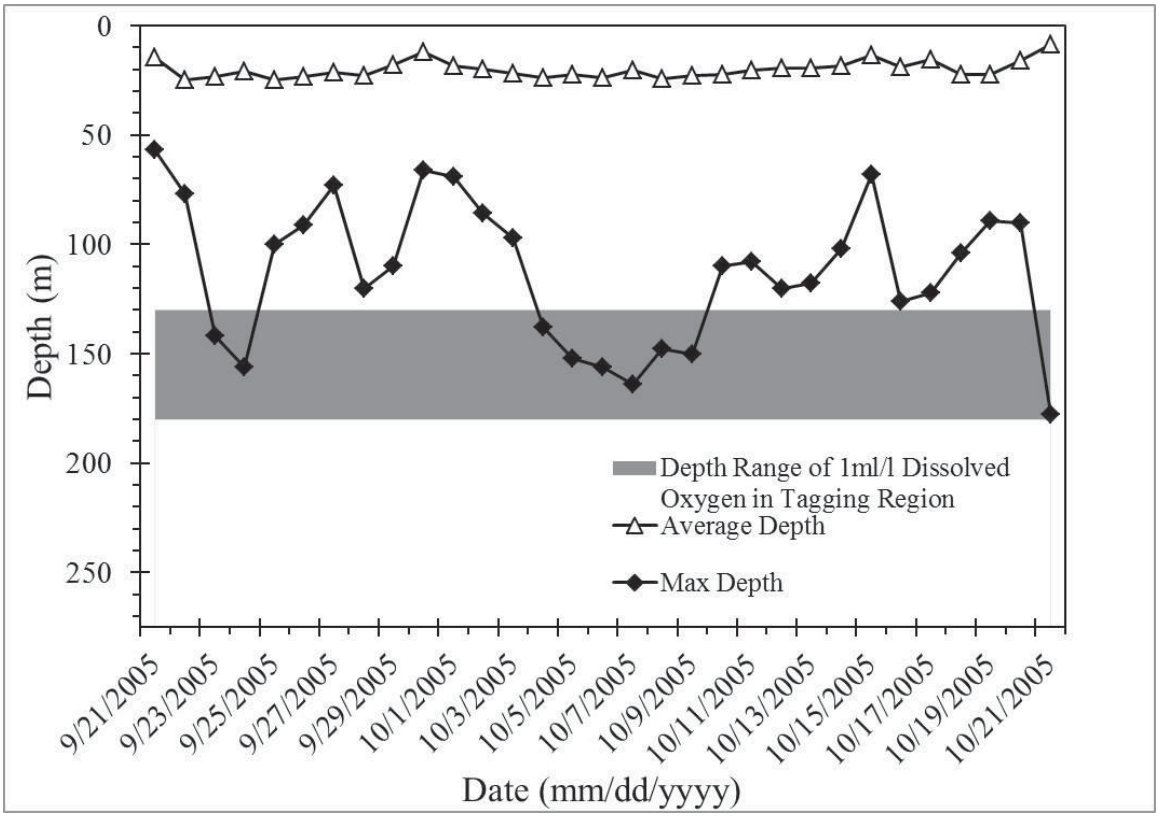

Figure 2.11: One month depth profile of PSAT tagged sailfish off Costa Rica/Panama from 2005. Black line with open triangles represents the daily average depth while the black line with black squares represents the daily maximum depth. The gray shaded bar shows the World Ocean Atlas fall season depth range of the 1ml/l dissolved oxygen in the region where the tagged sailfish was present. The level of oxygen can be considered a barrier to most organisms not specifically adated to low oxygen.

Given the widely accepted hypothesis that sailfish are vertically limited in the EPO due to OMZ, the results of this study necessitate a review of such behavior in other sailfish stocks. Although sailfish preference for the upper water column has been found in many studies in multiple oceans, the max depths witnessed by researchers vary widely,

possibly due to OMZ presence. Compared to the EPO where sailfish remain at the surface and rarely undergo deep dives, in the Atlantic off Brazil where no OMZ is present, PSAT tagged sailfish were found to dive as deep as 376m and 560m (Mourato et al. 2014). Another notable sailfish stock exists off Taiwan also where there is no OMZ present and sailfish here dive as deep as 214m (Chiang et al. 2011). Hoolihan et al. 2011 looked at diving behavior in two locations with OMZs (EPO and eastern tropical Atlantic) and one without (western North Atlantic) finding deeper diving trends where the OMZ was not present with a sailfish off Florida reaching 340m. Reiterating the max depth found in the EPO in this study is 76.8m and 180m from IGFA's tagged sailfish in the region of the EPO where the OMZ is deepest thus these EPO sailfish are remaining much shallower than that their counterparts from other oceans. This is most likely attributed to the direct relationship hypothesized between depth of the OMZ and max diving depth of sailfish.

Knowing billfish are limited to the upper water column in the EPO due to light and available oxygen, we hypothesize that the high catch rates seen in the recreational fishery off Central America may be due to increased density of sailfish at the surface, not necessarily coupled with high abundance. The results of billfish hourly activity levels presented here suggest patterns in billfish behavior which could lead to mechanisms for success by recreational fishing vessels practicing non-extractive billfishing. Such unique habitat characteristics for the prey and the predator also raise caution regarding the higher catchability that extends to the intensive extractive tuna and mahi-mahi fisheries in the region where billfish are incidentally caught. In the absence of regional billfish fishery

management, the likelihood of overexploiting billfish species that are limited to only the upper epipelagic is very high.

Billfish have evolved complex physical adaptations to thrive in the pelagic environment. This is more conspicuously so in the dissolved oxygen deprived, habitat compressed eastern tropical Pacific Ocean off Central America. Such evolutionary adaptations are most evidenced by their visual ability in the dimly lit ocean where light is scarce. Results presented in this paper suggest Pacific sailfish optimize their ability to obtain food by maximizing the efficiency of their hunting times to only when enough light is available for their vision to function effectively.

As presented, the examination of sailfish behavior provides a first look at using satellite transmitted acceleration as an index of fish activity and recreational fishery statistics as a means to analyze a highly migratory species' hourly behavior. Existing knowledge of the physiology of the billfish eye and brain reveals the complex evolutionary adaptation of billfish vision to their habitat in the epipelagic open ocean. This study provides insight into the potential pattern of billfish availability to catch and release recreational fisheries in the EPO which support a beneficial multi-million dollar tourism industry to Central American economies. The potential pattern of exploitation and the vulnerability of sailfish due to their increased density dependent catchability, as well as other billfish, to surface oriented extractive fishing is of concern based on the findings presented in this study. The potential for overexploitation due to available habitat compression should be a driving frame at the time that billfish fisheries management regimes are established for this species in the study region.

Chapter 3: Exploring Sailfish and Blue Marlin Migratory Characteristics through Satellite Tagging and Behavioral Modeling

Overview

The Billfish Research Program at RSMAS developed and implemented a pop-off billfish satellite tagging program in two of the main billfish recreational fishing destinations in the Eastern Pacific Ocean (EPO), Guatemala and Costa Rica, since April 2012. This extensive tagging program was developed and implemented to generate data pertinent to the goal and objectives of this Dissertation to examine the behavior and habitat use of billfish in the EPO. Deployment of Desert Star Systems SeaTag-MOD and SeaTag-GEO satellite tags were planned for Pacific Sailfish and Blue Marlin during recreational fishing seasons (November-June). An experimental design was implemented using both short term and long-term satellite tag deployment periods, thus providing the ability to examine individual fish behavioral information on differing temporal and spatial scales. This chapter uses the described satellite tagging data to analyze individual fish behaviors using a modeling procedure to distinguish behavioral modes.

Collaboration with the tag manufacturer Desert Star Systems (DSS) led to a specialized version of their premanufactured software, permitting the collection of high resolution short term data and, eventually, a smaller long term satellite tag capable of collecting over a year worth of migration pattern information. SeaTag-MOD tags (Figure 3.1 bottom), some of the results from which were discussed in Chapter 2 of this dissertation, were implemented for short-term deployment (10-20 days) studies and employ accelerometers as well as traditional sensors for temperature and depth to obtain a high-resolution view of billfish behavior in the

three-dimensional environment of the ocean. SeaTag-GEO tags (Figure 3.1 top) are used for long term deployments (180+ days) and employ a smaller, less technologically complex satellite tag that can be deployed for over 365 days to collect location (geomagnetic field strength and day length estimates) and temperature information.

These long-term studies are the first in the EPO using improved geolocation and provide the ability to examine sailfish and blue marlin habitat use. Desert Star Systems has improved geolocation in both SeaTag models by including a sensor to measure the strength of Earth's geomagnetic field which improves location accuracy from over 60 miles with traditional light-based algortihms to 35 miles with Desert Star's SeaTrack software and, in some cases, errors below 20 miles (Desert Star Systems Documentation) Geomagnetic fields are not uniform across the globe making geomagnetic geolocation only viable where isolines are onsistently latitudinal; however, geomagnetic field isolines off the Central American Pacific coast line up in a manner ideal for maximum geolocation precision. Traditional satellite tag geolocation has some major drawbacks due to uncertainty in estimating latitude from light especially during spring and autumn equinoxes where light based geolocation is impossible (Klimley et al. 2017). Further complicating light based geolocation is the likelihood for outside factors to effect location estimation such to clouds, position on the animal, water clarity, or mountain ranges that can effect the amount of light at sunrise and sunset. Traditional methods seek to find the most probable track which may include significant error in daily estimates due to these issues which are, in some cases, impossible to account. The application of

environmental factors to further filter and limit error such as the inclusion of bathymetry or sea surface temperature algortihms much improve tradtional light-based methods (Domeier et al. 2006); however, these require extensive sea surface temperature datasets and vertical coverage of such parameters to link to animal depth and location. The inclusion of geomagnetic geolocation provides critically important accuracy and precision compared to light based geolocation especially in analyses such as those done in this chapter that require knowledge of fish location for comparative analyses using environmental data. In traditional PSATs an error of 60 miles and having nearly one month of unusable data each spring and fall would dramatically limit the credibility of local environmental analyses where the improved location quality of the SeaTags and lack of an equinox effect make daily anlysis of environmental characteristics more viable.

Also improving location algorithm accuracy and precision in the SeaTag line of tags is the presence of the tag's onboard solar panel which wraps around the tag to collect light from all angles and also acts as a sole means of power or can act as additional power for transmission when batteries are included. Tag configuration software was developed by our research group and Desert Star Systems, for the specific purpose of billfish behavior analysis through long term and three-dimensional data collection using an efficient means of acquiring data while maintaining tag power and transmission capability (Desert Star Systems Document, 2013).

Figure 3.1: Top: SeaTag-GEO satellite tag used for long term deployments. Bottom: SeaTag-MOD satellite tag with attached battery section used for short term deployments and high-resolution data capture.

The capabilities and resulting data from the SeaTag line of PSATs permits more complex analyses of behavioral characteristics related to the persistence velocity and turning angles estimated from PSAT tracks. Furthermore, modeling of tag tracks and associated parameter values provide the opportunity to examine behavioral characteristics derived from PSAT data related to spatial and temporal habitat use and post-release recovery estimation.

Methods and Materials

PSAT Deployment Methodology

Seven SeaTag-MOD tags were placed on April 4th, 2012 off Guatemala for the purpose of analyzing acceleration activity of sailfish over a 10-day study. SeaTag-GEO tags were placed between 2013 and 2015 off Costa Rica's coast from Quepos

and the southern portion of the Osa Peninsula. The SeaTag-GEO deployments were as follows based of date released: 20 PSATs placed on sailfish off Quepos, Costa Rica between March 17th, 2013 and March 19, 2013, 4 PSATs placed on blue marlin and 3 PSATs placed on sailfish between December 10, 2013 and December 12, 2013, 2 PSATs placed on sailfish on March 9, 2014, 8 PSATs placed on blue marlin and 4 PSATS placed on sailfish between May 2, 2014 and May 3, 2014, 6 PSATs placed on sailfish on February 25, 2015, and 3 PSATs placed on blue marlin on July 14, 2015 In total, 57 satellite tags (50 GEO tags and 7 MOD tags) have been deployed on sailfish and blue marlin. Of the 50 GEO tags placed, 35 were on sailfish and 15 on blue marlin.

Sensor data is collected by the SeaTag-GEOs based on the sampling specifications programmed in the tag prior to deployment. SeaDock, the program provided by Desert Star Systems to program each SeaTag uses different docking mechanisms for the SeaTag-MOD and SeaTag-GEO but the same programming steps. The process of programming the SeaTag-MOD was described in Chapter 2 of this dissertation. The programming of the SeaTag-GEO is similar but with fewer steps due to the fact that this tag only collects daily locations and temperature.

Tags are programmed to do onboard organization and calculations of observations collected by sensors to compress the data into transmittable form. Depth was collected throughout the trial but observations were summarized into residency by depth bin for 12 hour periods(day/night). Transmitted data was therefore percent of time the fish spent in each depth bin for the purpose of examining diel behavior patterns. Tags were set to transmit one location per day for the SeaTag-GEO and time

of collection was synchronized for all tags. Unique to this study is the complement of acceleration through the SeaTag-MOD's equipped 3-axis accelerometer from which results were presented in Chapter 2 and are used for post-release analyses in this Chapter.

Because of the sensitivity of the accelerometer and the time length of the long term studies, an appropriate anchoring mechanism was created such that tag shedding was minimized. It was necessary to minimize the unsteady side to side movement of the tag caused by the hydrodynamic characteristics of the tag shape. To minimize unnecessary movement, both SeaTag models required a ball bearing swivel at the base of the tag. This was provided by the manufacturer in the SeaTag-MODs and added by the researchers in the SeaTag-MODs using monofilament and a crimp to match the materials of the swivels provided on the SeaTag-MOD knowing the manufacturer had performed corrosion resistance testing. Materials used in the attachments must be biocompatible to eliminate risk of infection/mortality and limit the rejection response of the animal to the inserted monofilament and anchor. Only surgical quality non-metal materials can be inserted into the animal and all materials, whether inside the animal or not, require extreme resistance to corrosion due to the saltwater environment and the likelihood for many metals to effectively melt away under such conditions. Fishermen and other researchers success was consulted, and effectiveness and lasting ability was discussed relative to the best brands of crimps, monofilament, and swivels (Personal Communication, Echave 2016). Initial deployments used manufacturer provided attachment mechanisms made from coated stainless steel wire and a Hallprint floy dart head for the short term SeaTag-MOD 10

day deployment in 2012 off Guatemala (Figure 3.2). These anchoring mechanisms were deemed unsuitable for long term deployments using the SeaTag-MOD shape of PSAT.

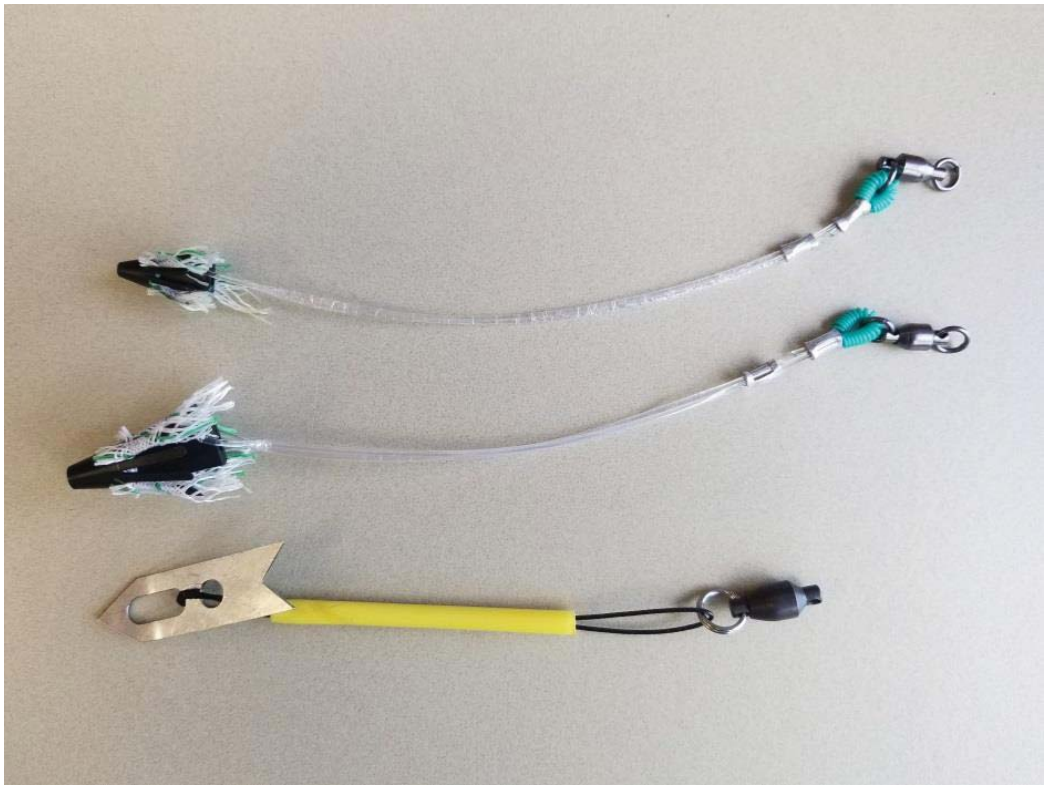

Figure 3.2: The SeaTag attachment tethers. Top to bottom: Medium (Sailfish only) Domeier umbrella dart, Large (Blue Marlin only Domeier umbrella dart, Stainless Floy dart (Short Deployments, Seatag-MOD)

Following the 2012 short term SeaTag-MOD deployment a new PSAT anchoring mechanism was developed for future long term studies. These long term studies employed the much smaller SeaTag-GEO but this still has the same hydrodynamic issue seen by the SeaTag-MOD thus required significant effort to maximize PSAT trial duration before shedding. In 2013, the dart head was changed from the Hallprint floy to the Domeier dart (https://www.marinecsi.org/2010/05/21/umbrella-darts/) with attached dacron

webbing to promote tissue growth around the umbrella shaped head. The medium sized Domeier dart was used for sailfish applications while the large size was used for blue marlin. This Domeier dart head is flexible and was thought to create less injury as the wound heals while the fish is swimming with PSAT attached.

Based on unanimous opinions among commercial fishermen, Jinkai brand monofilament and crimps were used exclusively to anchor the dart head to the PSAT base due to their reputation for corrosion resistance in the salt environment and their availablilty from mainstream fishing retail outlets. To minimize hydrodynamic resistance, a shrinkwrap is commonly used over the monofilament between the PSAT base and the dart head (Prince et al. 2002, Musyl et al. 2011, Domeier et al. 2006). Knowing this would be inserted into the fish it was determined the shrinkwrap material was required to be biocompatible. An exhaustive search to find such a material resulted in the incorporation of Vention Medical shrinkwrap designed for human surgical applications. This was applied to secure the monofilament loop created by attaching the Domeier dart without the need to include a metal crimp near the insertion region of the PSAT anchor (Figure 3.3). The resulting PSAT anchor system was fully biocompatible and was further designed to reduce infection and injury by coating each anchor in Oxytetracyclin antibiotic powder and hydrophobic Neosporin antibiotic oitment immediately prior to deployment.

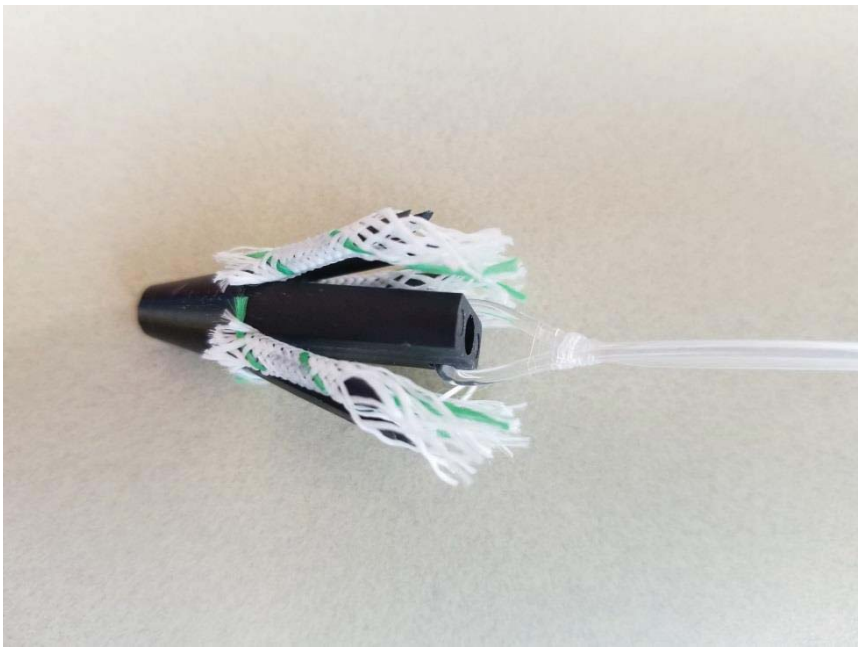

Figure 3.3: Enhanced view of Domeier dart with attached Dacron and applied heat shrink material over monofilament tether.

PSAT Location Data Collection and Processing

Desert Star Systems provides a suite of software for analysis of their PSAT data. The first program is SeaWatch which is used to connect and download data from the ARGOS system. The program is required to decode incoming ARGOS transmissions into a format useable by researchers. SeaWatch runs in the background of a computer and connects once per hour to download data from the ARGOS system. The result of SeaWatch running is a .CSV Microsoft Excel file for each PSAT including all the information necessary to estimate location as well as other data such as temperature, depth, and acceleration depending on how the tag was configured. The non-location data can be extracted from the .CSV file and analyzed where the location remains in this format for processing in the next of the series of programs called SeaTrack. SeaWatch is allowed to run until the PSAT disappears/stops

transmitting or all data is recovered upon which the tag ID is turned off through ARGOS to prevent charges on that PSAT ID.

SeaTrack is the location processing software provided by Desert Star Systems to create a PSAT location and track file from the data organized by SeaWatch. The program uses the 3-axis magnetometer values for each day and an estimated noon time to determine latitude and longitude of the PSAT on the given day. The first step is estimating the magnetic offset correction value by calculating the Earth's magnetic field strength at the tag deployment location on the date of deployment and looking at the difference between what the NOAA magnetic field calculator for that date and location provides versus what the PSAT actually recorded on that day. This value is then input into SeaTrack for location estimation. Within the SeaTrack processing algorithm, this offset is applied to all geoposition estimates as it is inherent to the satellite tag. The correction is validated once the tag pops off the fish to ensure correction was consistent throughout the deployment trial.

Further processing includes optional filtering of data to smooth the tracks and remove excessive inter-daily error. Although this day filtering was performed initially, for the purpose of behavioral modeling, filtering over more than one day was not undertaken due to the potential for unrealistic smoothing of tracks that may not represent actual behavioral differences in migration. Distance filtering was performed by creating a box around the entire region in the SeaTrack program using the provided map. The box limits the estimation of geolocations to only the area within the bounding box. The box was drawn to encompass the entire EPO from California to the north, Peru to the south, and out west to Hawaii. Further distance filtering

allows the input of a maximum distance a fish could travel within a given day. This value limits the migratory distance to only the maximum value inputted. It was important to ensure the maximum daily distance inputted was a larger value than what was physically possible for the sailfish or blue marlin so a value of 200 miles per day was chosen.

Once validated, processed tag tracks are saved and loaded into Google Earth and ArcGIS for visual analysis. Geolocation data can be exported as .csv files into R Programming software for statistical and behavioral analysis as well.

Acceleration and Depth Analysis from SeaTag-MOD PSATs

As mentioned in Chapter 2 of this dissertation, a total G-acceleration value is calculated onboard the PSAT using the equation $Total\ G = \sqrt{x^2 + y^2 + z^2}$ which removes "wobble" accelerations on the x and y axes caused by the tag being pulled in the z-axis direction from the base by the fish. The tag then calcuates the standard deviation of those total G values every 3 minutes and transmits those 3 minute standard deviations to the ARGOS satellite. Mean values of 1G were assumed prior to data collection configuration and confirmed through experimental testing and transmitted animal data from the first April 2012 deployment. Analyses of accelerometer data provides insight into behavioral preference related to diel activity level post-release which may temporarily effect migratory patterns due to a known post-release recovery period by the fish.

Depth histogram data is set to collect in 12 hour increments (6AM-6PM and 6PM-6AM Local time) for the purpose of diel analysis of depth behavior. Histogram

data are in the form of percent residency by depth bin. Depth bin ranges are determined by max depth of animal tagged with smaller bin ranges for shallower max depth in multiples of 3.2m. Depth data transmitted through ARGOS and compiled in SeaWatch was plotted and averaged using Microsoft Excel. Depth bins were normalized to largest bin transmitted. Statistical analyses consisting of simple t-tests were performed on depth residency data using R statistical software to determine significance of depth bin residency in the first half of the trial versus the second half to determine significant diving differences over time.

Depth data transmitted through ARGOS and compiled in the program SeaWatch are plotted and averaged using Microsoft Excel and R. Depth bins are normalized to largest bin set transmitted (6.4m or 12.8m bins). Regression analyses are performed on depth residency data using a program written in the statistical programming R language to determine significance of diving behavior for individual fish and depth bins as well as among tagged fish. Depth histograms are then compared to oceanographic variables of dissolved oxygen level at depth, temperature at depth, and salinity at depth in both Guatemala and Costa Rica.

Behavioral Change Point Methodology

Mathematical modeling of animal movement data is a complex process with a variety of avenues of analysis of the diffusive properties such as: random walks, fractal dimension analyses, state space modeling, and Markov process modeling, as well as advanced behavioral models (Schick et al. 2008). The movement data available from satellite tagging is not independent spatially or temporally and has thus

required the use of these more advanced models to deal with statistical issues such as autocorrelation and introduced observation error due to satellite tracking technology. Due to these complications and with the aid of new developments in technology available for telemetry studies, recently much research has focused on modeling the migratory patterns of satellite tracked animals using applied ecological models. Modeling efforts typically measure segments of migratory track lengths in between directional changes, building up a distribution of track lengths that can be statistically analyzed (Turchin 1998). Characterization of move track length distributions are a much discussed topic in migration analyses (e.g. Milner-Gulland et al. 2011). In many cases, movement is analyzed using some version of a correlated random walk (CRW) routine; however, the presence of data gaps in satellite recuperated data poses a major problem to CRW analysis (Gurarie 2008). With the presence of gaps in movement data it becomes difficult to estimate velocities and turning angles at regular consistent intervals without interpolation which may not reflect the actual animal behavior. Due to added complications caused by "gappiness" or irregular time series information in movement data, Gurarie (2008) presents a modeling method taking account for data gaps called the Behavioral Change Point Analysis (BCPA). This is accomplished by describing a persistence movement component, examining the likelihood of an animal persisting or taking a perpendicular turn then developing behavioral mode definitions based on breakpoints in the movement. Satellite tag location estimates are used to estimate track step lengths and turning angles to calculate velocities(V) and turning angles (Ψ) which are transformed into two

geometrically orthogonal variables, persistence velocity $V_P(t)$ and turning velocity $V_t(t)$ through the following calculations:

$$V_P(t) = V(T_i)\cos\big(\Psi(T_i)\big)$$
$$V_t(t) = V(T_i)\sin\big(\Psi(T_i)\big)$$

These two velocity variable transformations result in the ability to model each with stationary Gaussian models and can be approximated by mixed normal distributions, a convenient feature of the transformation. An important aspect of the BCPA is the fact that the orthogonal velocity components are characterized by three parameters, a mean (μ), a variance (σ^2), and an autocorrelation (ρ). The mean and standard deviation is estimated with the data but the autocorrelation parameter (ρ) must be estimated based on the data and a likelihood framework employing probability density estimation to a conditional distribution (W(t)) at time interval τ_i from which velocity components are assumed to be a sample. Conditional likelihood of ρ given all W observations is given by

$$L(\rho|\boldsymbol{W},\boldsymbol{T},\hat{\mu},\hat{\sigma}) = \prod_{i=1}^{n} f(W_i|W_{i-1},\tau_i,\rho,\hat{\mu},\hat{\sigma})$$

where each observation W_i is estimated based on the previous observation by

$$W_i = \mu + \rho^{\tau_i}(W_{i-1} - \mu) + \varepsilon_i$$

where ρ^{τ_i} represents the autocorrelation based on the time gap τ_i and an error term ε_i. Finally, the estimate for $\hat{\rho}$ is calculated from the likelihood function as follows

$$\hat{\rho} = \underset{\rho}{\operatorname{argmax}}\, L(\rho|\boldsymbol{W},\boldsymbol{T},\hat{\mu},\hat{\sigma})$$

All three parameters can be estimated jointly, producing maximum likelihood estimates; however, Gurarie et al. (2009) recommends direct calculation of μ and σ to

reduce computational intensity. The authors describe the resulting autocorrelation coefficient estimate as “movement inertia” which can be measured as a property of movement.

By examining the parameter changes that occur during the course of a migration, behavioral change points can be identified because changes in parameter values can be assumed to represent differing behavioral patterns. To put the variables in terms of biological movement, persistence velocity parameter changes reveal the following information: μ refers to the speed and directness of the movement, σ refers to variability in movement (direction shifts), and ρ refers to the direction and correlation of the movement. Estimation of change points requires the use of multiple models where each model allows none, one, two or all parameter values to change at the “Most Likely Change Point (MLCP)” and models are evaluated using Akaike’s and Bayesian Information Criterion tests. The best model result is used as the expected change point but one animal is likely to experience many change points over the course of the migration. For this purpose, data is organized separately for analysis. Most likely change points are estimated and recorded based on the BCPA package provided by R software based on information criteria test results which choose the best model automatically. Further analysis allows estimation of parameters and these were stored separately for analysis of individual parameters in Chapter 4 of this dissertation.

To identify multiple change points in the data, Gurarie et al. (2009) developed a novel process that is robust to gaps in data. The process employs the single change point process described previously but within a user-specified time window. The

window size is a required input and is determined at the discretion of the user with a size of 20 recommended as the minimum for viable analyses. Once a change point is identified, the window is moved to the next time step to continue identification of other change points. Each time the window is moved, the parameters are estimated again, improving the robustness of the model for the identification of shifts in behavioral modes.

Results

PSAT Migratory Characteristics

Of the sailfish and blue marlin tagged, and to secure meaningful spatial-temporal descriptions of the tracks, only tags collecting more than 35 days at large were incorporated for analysis using the BCPA methodology. For this reason, a total of 21 sailfish tags and 10 blue marlin tags were employed for this analysis from a total of 35 sailfish PSATs and 15 blue marlin PSATs deployed.

For sailfish, the average deployment duration was 70.29 days with a range of 35-179 days. Blue marlin deployments averaged 71.90 days and ranged from 38-200 days. The average distance traveled by sailfish during this study was 3638.62nm with a range of 1019-13462nm. For blue marlin, the average distance traveled was 2163.3nm with a range of 350-8537nm. Average distance traveled per day was 50.77nm with a range of 26.50-90.61nm for sailfish and an average of 25.61nm with a range of 9.21-43.47nm per day for blue marlin. The average speed for all sailfish was found to be 2.12 knots which converts to 1.09 m/s while the blue marlin average speed was calculated as 1.07 knots or 0.55 m/s. (Tables 3.1 & 3.2)

Table 3.1 List of satellite tagged sailfish including: Days at Large, Distance Traveled, and Distance per Day

Sailfish ID	Days at Large	Distance Traveled	Nautical Miles/Day
134241	58	1542	26.59
134242	41	1878	45.80
134250	47	1394	29.66
134252	104	4937	47.47
134257	35	1730	49.43
134258	179	13462	75.21
134260	91	4511	49.57
134263	82	6796	82.88
134266	89	5643	63.40
134267	48	3065	63.85
134268	61	4541	74.44
134270	36	1019	28.31
134272	63	2189	34.75
134273	57	1649	28.93
134275	46	4168	90.61
134276	54	3880	71.85
134279	42	1958	46.62
134280	93	3147	33.84
134281	40	2059	51.48
134285	149	4202	28.20
134288	61	2641	43.30
Average	70.29	3638.62	50.77
		Average Knots	2.12
		Average m/s	1.09

Table 3.2 List of satellite tagged sailh including: Days at Large, Distance Traveled, and Distance per Day

Blue Marlin ID	Days at Large	Distance Traveled	Nautical Miles/Day
134240	58	856	14.76
134244	45	777	17.27
134245	66	852	12.91

134248	38	350	9.21
134251	46	1240	26.96
134254	68	1863	27.40
134255	43	1663	38.67
134277	200	8537	42.69
134283	95	4130	43.47
134284	60	1365	22.75
Average	71.9	2163.3	25.61
		Average Knots	1.07
		Average m/s	0.55

Behavioral Change Point Analysis

The Behavioral Change Point Analysis (BCPA) was performed on sailfish and blue marlin using an observational time window of 20 days. A window step of 0.5 days was chosen to ensure maximum BCPA analyses within each individual billfish dataset .The minimum recommended window size and step length was necessary due to the average deployment times of tagged sailfish (70.29 days) and blue marlin (71.9 days) being relatively short compared to higher resolution GPS datasets for which the BCPA was originally designed. . This window stepping procedure was used for each PSAT deployment over 35 days in duration. Parameter changes within a given window included: speed travelled ($\hat{\mu}$) , the standard deviation of the BCPA which equates to the variability of movement ($\hat{\sigma}$) encompassing directionality changes, and the autocorrelation coefficient ($\hat{\rho}$), or movement inertia. Once the 3 parameters are estimated for the BCPA, behavioral change points are estimated based on a cluster width input which indicates the minimum number of days within which parameter changes can be considered to be from the same behavioral shift. High values (>3 days) for cluster width require parameter shifts over longer periods resulting in fewer behavioral change points estimated, while lower

values (1-2 days) result in many change points as it includes many smaller scale parameter changes over the shorter included range. The assumption made by using a 3-day cluster width is that a sailfish or blue marlin changes behavioral modes (searching, foraging/meandering) based on the natural environment experienced by the animal and the expanse of the EPO requires longer time scales for interaction by the tagged animal. Although daily behavioral shifts are theoretically possible and likely, variation in the parameters of this dataset is not suitable for single day cluster widths given the once-a-day reporting of the SeaTag-GEO tags thus may not represent a biologically relevant analysis without more temporally resolute PSAT data. A cluster width of 3 days was chosen for this analysis such that a behavioral change in either a sailfish or a blue marlin will require at least three days of a consistent parameter shift to be accepted as a change point.

The BCPA produced behavioral change points for 15 of the 21 sailfish and 8 of the 10-blue marlin tagged with PSATs. Six sailfish and two blue marlin were not found to incur any significant behavioral shifts indicating no differentiable behavior over the course of the migratory track and are thus not included in this and future analysis of behavioral change points in this dissertation. Although not included for the purpose of this dissertation, a lack of behavioral changes is, in itself, significant, indicating an overall lack of variability in movement and speed throughout the entirety of the migration witnessed between deployment and pop-off. In total, the analysis identified 96 behavioral changes consisting of 3 to 15 change points for individual sailfish (Table 3.3). A total of 34 behavioral changes were identified for blue marlin and ranged from 1-13 change points for individual fish (Table 3.4)

Table 3.3: List of all estimated behavioral change points for PSAT tagged sailfish coupled with location and date of occurrence

Date	Latitude	Longitude	Sailfish ID		Date	Latitude	Longitude	Sailfish ID
4/9/2014	12.83	-88.23	134260		6/16/2014	12.75	-91.77	134285
4/14/2014	13.35	-89.39	134260		7/1/2014	12.77	-91.89	134285
4/19/2014	12.16	-94.61	134260		7/29/2014	12.03	-89.20	134285
5/2/2014	14.23	-95.24	134260		8/6/2014	11.72	-88.93	134285
5/7/2014	12.72	-94.78	134260		8/15/2014	11.42	-91.19	134285
5/20/2014	9.59	-90.80	134260		8/22/2014	11.09	-90.86	134285
3/21/2014	6.09	-84.71	134268		8/29/2014	11.26	-90.78	134285
3/29/2014	5.56	-85.26	134268		3/28/2014	11.01	-92.63	134258
4/7/2014	5.80	-83.15	134268		4/4/2014	7.06	-88.21	134258
4/12/2014	6.27	-79.71	134268		4/10/2014	6.96	-84.77	134258
4/18/2014	6.57	-79.43	134268		4/15/2014	8.22	-83.09	134258
3/27/2014	9.88	-88.36	134276		4/25/2014	13.06	-93.40	134258
4/10/2014	10.91	-91.42	134276		4/29/2014	15.86	-98.30	134258
4/18/2014	9.42	-92.14	134276		5/10/2014	13.26	-95.40	134258
4/27/2014	9.45	-91.39	134276		5/21/2014	6.88	-90.56	134258
4/5/2014	8.91	-85.34	134288		5/25/2014	5.63	-89.75	134258
4/11/2014	9.32	-87.24	134288		6/1/2014	5.68	-91.76	134258
4/15/2014	9.32	-85.85	134288		6/8/2014	6.96	-86.97	134258
5/1/2014	12.67	-93.95	134288		6/18/2014	9.50	-89.24	134258
4/1/2014	11.79	-88.94	134267		6/22/2014	9.85	-85.85	134258
4/12/2014	12.68	-89.13	134267		6/28/2014	7.47	-88.30	134258
4/15/2014	12.48	-89.11	134267		7/4/2014	8.51	-87.25	134258
5/18/2014	6.34	-86.76	134272		12/30/2013	7.47	-86.66	134241
6/4/2014	8.25	-88.54	134272		1/3/2014	5.39	-87.51	134241
6/19/2014	10.98	-89.19	134272		1/19/2014	7.95	-84.43	134241
4/4/2014	11.93	-88.60	134273		1/24/2014	5.85	-81.59	134241
4/29/2014	12.36	-89.23	134273		1/29/2014	6.17	-82.11	134241
5/4/2014	11.37	-91.60	134273		3/7/2015	9.70	-89.73	134252
5/13/2014	12.29	-90.55	134273		3/10/2015	10.89	-89.19	134252
4/1/2014	9.86	-87.15	134275		3/14/2015	12.37	-93.05	134252
4/4/2014	10.96	-88.12	134275		3/23/2015	12.85	-93.21	134252
4/9/2014	12.83	-90.62	134275		4/9/2015	12.50	-93.38	134252
4/18/2014	12.32	-90.02	134275		4/20/2015	10.71	-91.64	134252
5/15/2014	5.00	-87.29	134280		5/3/2015	8.51	-96.98	134252
5/26/2014	4.77	-86.69	134280		3/3/2015	6.33	-84.44	134263
5/29/2014	4.77	-86.91	134280		3/6/2015	5.38	-85.63	134263
6/6/2014	3.87	-86.08	134280		3/15/2015	7.00	-86.25	134263
6/28/2014	1.51	-80.54	134280		3/27/2015	6.11	-87.66	134263
7/7/2014	0.99	-81.91	134280		4/2/2015	9.06	-88.52	134263
7/25/2014	5.94	-78.61	134280		4/11/2015	8.85	-87.42	134263
3/31/2014	10.27	-87.74	134285		4/26/2015	11.18	-87.65	134263
4/10/2014	11.88	-87.10	134285		3/5/2015	9.67	-85.45	134266
4/16/2014	12.06	-90.25	134285		3/19/2015	9.40	-91.55	134266
4/27/2014	13.20	-90.76	134285		3/25/2015	9.53	-85.60	134266
5/1/2014	13.32	-92.26	134285		4/6/2015	10.56	-86.98	134266
5/16/2014	11.58	-95.28	134285		4/12/2015	13.34	-90.13	134266
6/4/2014	11.54	-91.55	134285		5/4/2015	11.75	-96.31	134266
6/9/2014	12.03	-89.02	134285		5/14/2015	6.77	-93.88	134266

Table 3.4: List of all estimated behavioral change points for PSAT tagged blue marlin coupled with location and date of occurrence

Date	Latitude	Longitude	Blue Marlin ID		Date	Latitude	Longitude	Blue Marlin ID
8/26/2014	7.95	-82.68	134283		12/19/2013	7.45	-83.81	134254
9/9/2014	6.97	-85.48	134283		12/29/2013	6.67	-85.57	134254
9/14/2014	6.15	-84.84	134283		1/5/2014	6.16	-86.97	134254
9/18/2014	6.78	-84.14	134283		1/14/2014	5.73	-86.19	134254
7/29/2014	4.19	-81.29	134277		2/6/2014	8.09	-84.26	134254
8/9/2014	3.43	-81.25	134277		12/27/2013	6.29	-86.04	134251
8/17/2014	2.56	-79.75	134277		12/30/2013	7.04	-85.89	134251
8/29/2014	3.68	-78.91	134277		1/15/2014	11.43	-89.08	134251
9/6/2014	7.26	-78.75	134277		5/28/2014	7.55	-82.29	134248
9/12/2014	8.77	-79.25	134277		5/30/2014	5.48	-86.52	134244
9/17/2014	7.89	-79.96	134277		5/15/2014	7.07	-84.10	134240
9/29/2014	6.79	-78.79	134277		5/30/2014	7.12	-84.16	134240
10/10/2014	6.78	-79.56	134277		6/5/2014	6.96	-84.46	134240
10/26/2014	5.71	-78.29	134277		6/17/2014	8.29	-85.67	134240
11/3/2014	6.29	-79.13	134277		6/20/2014	8.95	-85.52	134240
11/10/2014	4.69	-80.92	134277		1/3/2014	3.96	-85.23	134255
11/19/2014	6.03	-81.25	134277		1/9/2014	3.50	-82.41	134255

Individual Behavior Analysis: Sailfish

The BCPA resulting plots for Sailfish 134260 are shown in Figure 3.4, which began its migration with relatively direct movement resulting in high "movement inertia" autocorrelation coefficient ($\hat{\rho}$) values during the initial westward migratory path (yellow portion of trackline) (Figure 3.4 Top Left). "Movement inertia" should be envisioned as the forward momentum or propensity to continue the same path for the PSAT equipped animal. Autocorrelation results (color of the track line) in the "path plot" (Figure 3.4 Top Left) indicate the directness or persistence of the PSAT track path with the highest values occurring where PSAT tracks travel in straight lines over numerous days with minimal turning steps or meandering. Sailfish 134260 then begins to exhibit a more meandering behavioral pattern when autocorrelation decreases due to lack of sustained directive

movement indicated in the plot by a color change of the trackline from yellow to green to blue as the sailfish travelled to the northwest portion of the plot. Meandering behavioral patterns consist of sequential turning steps over the given region indicative of a searching behavioral mode or lack of "momentum" compared to a traveling behavioral mode where "momentum" is maintained. Autocorrelation increases following the period of meandering in the northwestern portion of the migration as the sailfish travels in a looping path toward the southeast before entering another period of meandering or searching prior to PSAT release from the fish. Overall, this sailfish undertook smooth transitions between periods of more directed movements indicating traveling mode with high autocorrelation and periods of searching or foraging with less "momentum", more complexity of the migratory track, and decreased autocorrelation values. Trackline thickness indicates proportional differences in the mean estimated BCPA along the track. In this sailfish the line thickness indicates a relative lack of difference within the mean BCPA on scales large enough to be visualized in the trackplot.

The phase plot (Figure 3.4 Top Right) shows the relationship between the speed travelled ($\hat{\mu}$), the standard deviation of the BCPA which equates to the variability of movement of ($\hat{\sigma}$) encompassing directionality changes, and finally the autocorrelation coefficient ($\hat{\rho}$). Sailfish 134260 travels at relative moderate speed with low variability during the initial highly autocorrelated phase of the migration before becoming highly variable and speed slowing with increased meandering behavior. The transition back to highly autocorrelated behavior as the sailfish loops to the southeast an increase in speed is observed followed by an abrupt decrease in speed and an overall decreasing movement variability level ($\hat{\sigma}$) until the end of the PSAT deployment period.

Sailfish 134260 generated 6 change points on days 24, 29, 34, 46, 51, and 54 (Figure 3.4 Bottom Left). These change points represent significant behavioral shifts in the 3 parameter values of the BCPA and are estimated based on the number of days incorporated into the behavioral change indicated by the thickness of the pink change point line on the plot. Behavioral change points incorporating a longer time period of parameter shift are indicated by a thicker pink line in the figure where the thickness of such line is proportional to the number of days incorporated into the specific change point. If a shift occurs over 10 days with differing behavior on either side of the 10-day period, a thick pink line will be present where a 3-day parameter shift is indicated by a very thin or nearly invisible pink line. Moving forward, thick pink lines indicating longer timescales of behavioral change will be referred to as strong change points where shorter behavioral changes will be referred to as weak change point. Both strong and weak change points are significant and represent legitimate behavioral changes with the only difference applied being the number of days at which the PSAT undertook said specific behaviors. Of the 6 change points estimated for Sailfish 134260 only the first behavioral change on day 24 is a weak change point but clearly coincides with the change in behavior from more directed and persistent traveling to a meandering searching pattern. Each change point can be clearly associated with a migrational change indicated in the path and phase plot previously especially the strongest behavioral changes on days 29 and 51.

According to Gurarie et al. (2009) the most important statistical assumptions of the BCPA, are a Gaussian error structure of the movement data and an exponential decay of the autocorrelation. The diagnostic plots include a QQ-Norm plot and histogram of

residuals to ensure the normally distributed standardized residuals and an Autocorrelation Function (ACF) plot to ensure the exponential decay. These plots are given in figure 3.4 (Bottom Right) and indicate the assumptions of the standardized residuals have been met for Sailfish 134260.

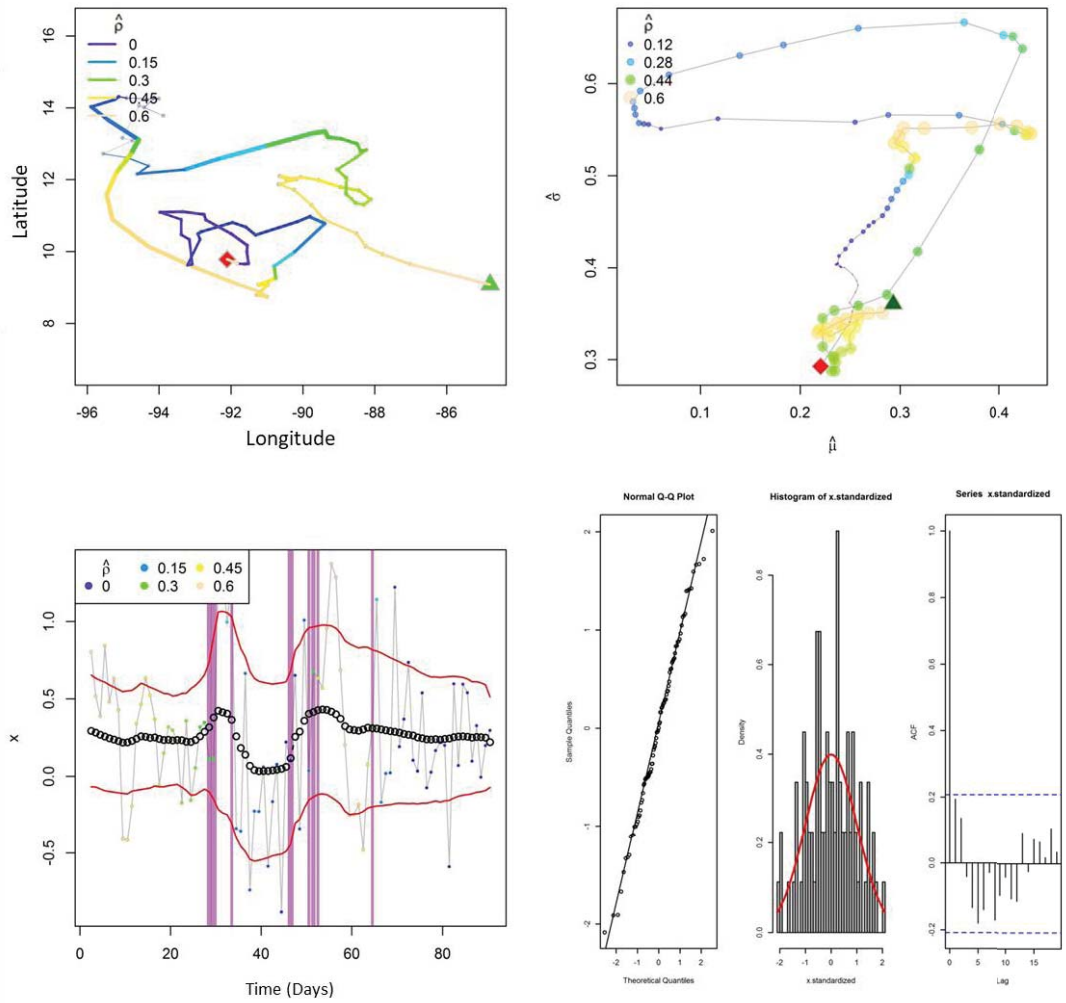

Figure 3.4: Four plots showing the output of the BCPA modeling procedure for sailfish 134260. Top left shows the migratory path where a green triangle marks the PSAT deployment location and a red square the endpoint or PSAT pop-off point. Color of the line represents the autocorrelation parameter. The top right is a phase plot representing relationship between the 3 parameters estimated from the BCPA with the autocorrelation parameter shown in color and size coded circles. The bottom left plot shows the change points where the pink lines represent the time of the changepoint within the trial and the thickness of the line representing the number of days used for the selection of the change point. The black open circles

represent the mean of the BCPA analysis with the red lines indicating the standard deviation. Finally, the bottom right set of diagnostic plots includes a QQ-norm plot, histogram and autocorrelation function of the standardized data from the model.

Figure 3.5 shows BCPA results for Sailfish 134268 which begins the migratory path with a moderately tortuous meandering pattern indicating foraging for the initial leg of the migration southward then westward. This period is followed by eastward movement and a shift to more directed travelling behavior indicated by higher values of the autocorrelation coefficient ($\hat{\rho}$) (Figure 3.5 Top Left). Following this eastward travelling movement, Sailfish 134268 exhibits its highest autocorrelated behavior as it travels northward. Comparatively to other PSAT tagged sailfish, Sailfish 134268 was one of the slowest migrating fish witnessed in the study and a minority among sailfish in that in travelled eastward where the majority travelled in an overall westward trajectory. Trackline thickness for this sailfish indicates a relative lack of proportional difference within the mean BCPA enough to be visualized on the small scale of the plot.

The phase plot shows the relatively low speed ($\hat{\mu}$) but high variability ($\hat{\sigma}$)of the initial southward and westward meandering movement. As the sailfish began traveling eastward and eventually northward, a decrease in variability and overall increase in speed was witnessed. The shift from eastward to northward toward the end of the trial can be seen in the phase plot through the change in variability but is not as evident in the change in speed which was remained relatively constant following the eastward turn.

Sailfish 134268 exhibited 5 total change points with the first occurring 12 days into the trial followed by change points on days 20 (two lines represent one change point in plot), 29, 34, and 40 (Figure 3.5 Bottom Left). Of these 5 change points, 3 are considered strong and are shown in the plot while 2 are weak change points. These weak change points can be attributed to differing behaviors that cause strong outliers such as

the behavioral pattern in the mean of the BCPA on day 12 where outliers to the mean exist on days 11 and 12 leading to the designation of a weak change point. The same occurs for the weak change on day 29 where three outliers follow in the 3 days after. The strong change points can be attributed to the major behavioral shifts such as the change to eastward directed movement beginning on day 20 for example.

The diagnostic plots (Figure 3.5 Bottom Right) indicate the assumption of normality of the standardized residuals has been met for Sailfish 134268 although a tail exists in the QQ-norm plot indicating a slight deviation from normality due to some behavioral characteristic of the migratory track. The histogram and autocorrelation function; however, appear to satisfy the requirement of normality in this analysis.

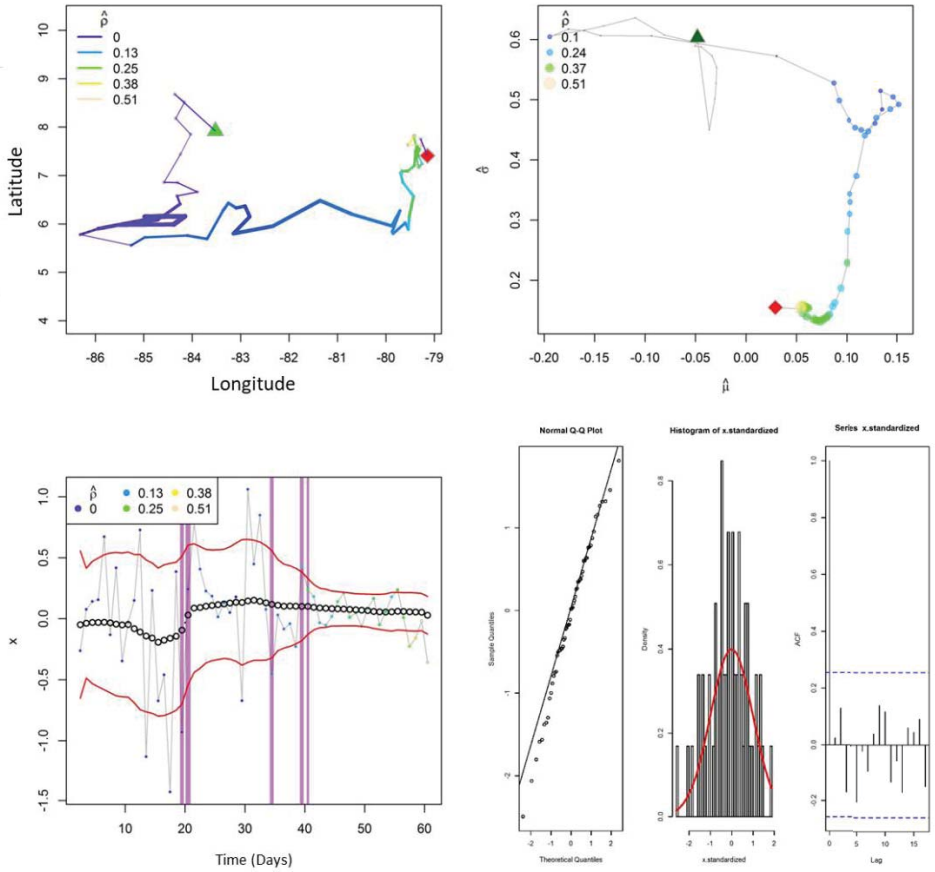

Figure 3.5 Four plots showing the output of the BCPA modeling procedure for sailfish 134268. Top left shows the migratory path where a green triangle marks the PSAT deployment location and a red square the endpoint or PSAT pop-off point . Color of the line represents the autocorrelation parameter. The top right is a phase plot representing relationship between the 3 parameters estimated from the BCPA with the autocorrelation parameter shown in color and size coded circles. The bottom left plot shows the change points where the pink lines represent the time of the changepoint within the trial and the thickness of the line representing the number of days used for the selection of the change point. The black open circles represent the mean of the BCPA analysis with the red lines indicating the standard deviation. Finally, the bottom right set of diagnostic plots includes a QQ-norm plot, histogram and autocorrelation function of the standardized data from the model.

Figure 3.6 shows BCPA results for Sailfish 134276 which begins the migratory path with highly directed southwestward movement. This is followed by a northern directional change while remaining directed in a traveling/searching mode. During the northward movement, the sailfish begins to exhibit more meandering/foraging as the track becomes more tortuous and changes direction eastward the westward. As the sailfish tracks west it continues this foraging mode until the sailfish abruptly changes behavior and continues traveling west but in a much more directed travelling pattern. The sailfish then loops to the southeast then back to the northwest while increasing the autocorrelation or directness of the track until the PSAT pops off at the most westward location of the track (Figure 3.6 Top Left). Trackline thickness for this sailfish indicates a relative lack of difference within the mean BCPA enough to be visualized on the small scale of the plot.

The phase plot shows a wide range of speed ($\hat{\mu}$) in this sailfish with highest overall velocity occurring during the periods of highest autocorrelation at the beginning and end of the migratory path. During the initial directed path following deployment, Sailfish 134276 exhibits very low variability ($\hat{\sigma}$) but increased dramatically until the

period of more meandering where the sailfish began to forage. This is followed by a leveling out in variability during this foraging and finally a return to a period of low variability when the sailfish changed back to ta traveling or searching pattern before release.

Sailfish 134276 was estimated to have undergone 4 major strong behavioral changes on days 11, 25, 33, and 42 although plotting reveals potential small-scale behavioral changes surrounding days 11, 25, and 33 which may not be included in the overall model due to a 3-day cluster width as a model parameter input (Figure 3.6 Bottom Left). The day 42 change point is not visualized on the plot which indicates a relatively small parameter value change prior and after this day.

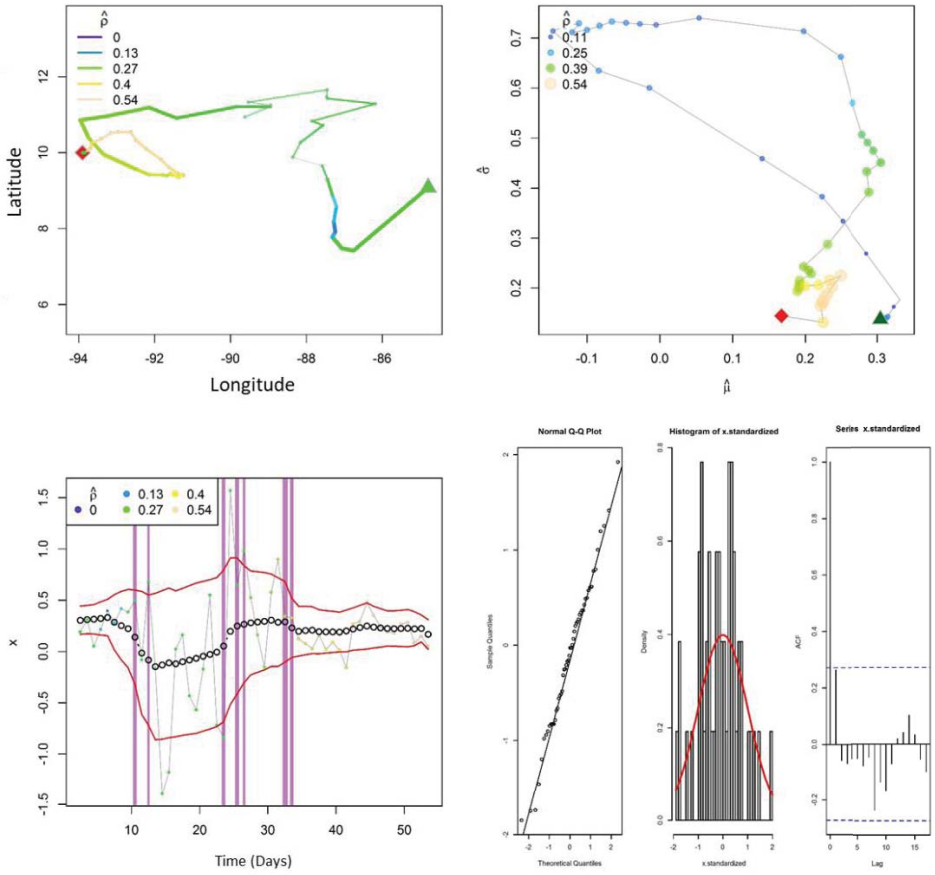

Figure 3.6: Four plots showing the output of the BCPA modeling procedure for sailfish 134276. Top left shows the migratory path where a green triangle marks the PSAT deployment location and a red square the endpoint or PSAT pop-off point. Color of the line represents the autocorrelation parameter. The top right is a phase plot representing relationship between the 3 parameters estimated from the BCPA with the autocorrelation parameter shown in color and size coded circles. The bottom left plot shows the change points where the pink lines represent the time of the changepoint within the trial and the thickness of the line representing the number of days used for the selection of the change point. The black open circles represent the mean of the BCPA analysis with the red lines indicating the standard deviation. Finally, the bottom right set of diagnostic plots includes a QQ-norm plot, histogram and autocorrelation function of the standardized data from the model.

The diagnostic plots (Figure 3.6 Bottom Right) indicate the assumption of normality of the standardized residuals has been met for Sailfish 134276. All three of the diagnostics indicate good fit with only a small tail on the left side of the histogram showing very slight irregular fitting.

Figure 3.7 shows BCPA results for Sailfish 134288 and shows an initial highly tortuous foraging pattern immediately following deployment as the sailfish travelled toward the northwest. As the migratory path continued, the track becomes more directed but continues on the overall northwestward direction. This sailfish showed very low autocorrelation ($\hat{\rho}$) during the initial foraging phase followed by an increase throughout the trial duration with highest autocorrelation values occurring during final portion of the track (Figure 3.7 Top Left). Trackline thickness for this sailfish indicates a relative difference in the foraging phase of the sailfish track with the thinnest section of trackline compared to the more directed traveling behavior.

The initial movements occur at a very low speed ($\hat{\mu}$) with very low variability ($\hat{\sigma}$) during the first foraging portion of the migration. When the behavioral pattern changes from foraging to more directed, the variability increases dramatically and levels off during the first half of the migration followed by a decrease in variability when

autocorrerelation peaks toward the endpoint of the track. Speed remains low at the start but begins increasing dramatically as the sailfish becomes more directed and continues to increase overall until the end of the trial (Figure 3.7 Top Right).

Sailfish 134288 had 4 behavioral changes on days 20, 26, 30, and 46 (Figure 3.7 Bottom Left). Change point on day 20 appears strongest, including the most days of a behavioral trend compared to the 3 other change points. Change points on days 30 and 46 do not appear on the plot but the large deviation in the BCPA can be seen on those days where values are strong outliers creating behavioral change points with few days included thus very thin lines not visible in the plot.

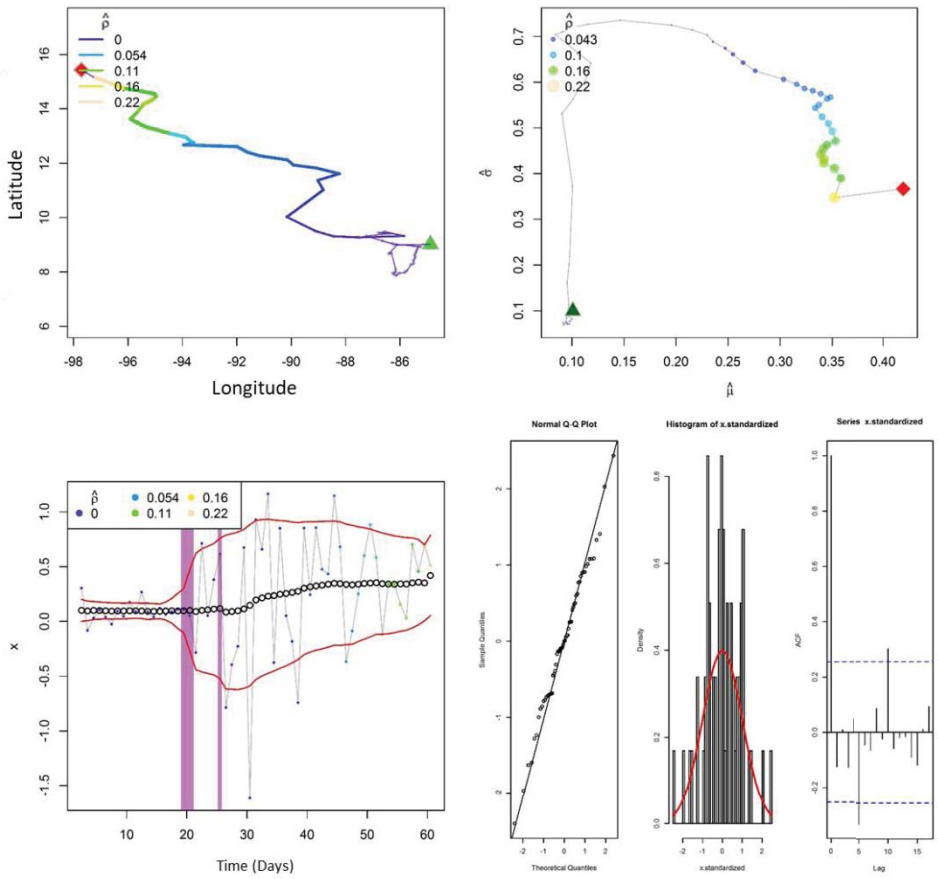

Figure 3.7: Four plots showing the output of the BCPA modeling procedure for sailfish 134288. Top left shows the migratory path where a green triangle marks the PSAT deployment location and a red square the endpoint or PSAT pop-off point.

Color of the line represents the autocorrelation parameter. The top right is a phase plot representing relationship between the 3 parameters estimated from the BCPA with the autocorrelation parameter shown in color and size coded circles. The bottom left plot shows the change points where the pink lines represent the time of the changepoint within the trial and the thickness of the line representing the number of days used for the selection of the change point. The black open circles represent the mean of the BCPA analysis with the red lines indicating the standard deviation. Finally, the bottom right set of diagnostic plots includes a QQ-norm plot, histogram and autocorrelation function of the standardized data from the model.

The diagnostic plots (Figure 3.7 Bottom Right) indicate the assumption of normality of the standardized residuals has been met for Sailfish 134288 in all three of the diagnostics with only the QQ-Norm plot showing slight deviation from normal on the tail but within acceptable range.

Figure 3.8 shows BCPA results for Sailfish 134267 and begins with moderate autocorrelation ($\hat{\rho}$) and exhibits an overall lack of tortuosity with a majority of the migratory path indicating traveling behavior as opposed to searching/meandering. An overall northwest trajectory is taken with increasing autocorrelation throughout, showing highest autocorrelation and persistence of movement in the final quarter of the track when movement occurs in a straight line (Figure 3.8 Top Left). Trackline thickness for this sailfish indicates a relative lack of difference within the mean BCPA enough to be visualized on the small scale of the plot.

The trial begins with the highest variability ($\hat{\sigma}$) witnessed in this sailfish although values are relatively low and decrease throughout the trial as the track become more directed and less tortous. Speed ($\hat{\mu}$) decreases at the onset of the trial before increasing as the track becomes more directed (Figure 3.8 Top Right).

Sailfish 134267 had 3 behavioral changes on days 15, 25, and 29 (Figure 3.8 Bottom Left). Change points on days 15 and 29 appear on the plot where a weaker

change point is found associated with an outlier on day 25 thus does not appear on the plot.

The diagnostic plots (Figure 3.8 Bottom Right) indicate the assumption of normality of the standardized residuals has been met for Sailfish 134267 in all three of the diagnostics. The histogram of residuals has a wider range in the tails than is expected but overall is acceptable.

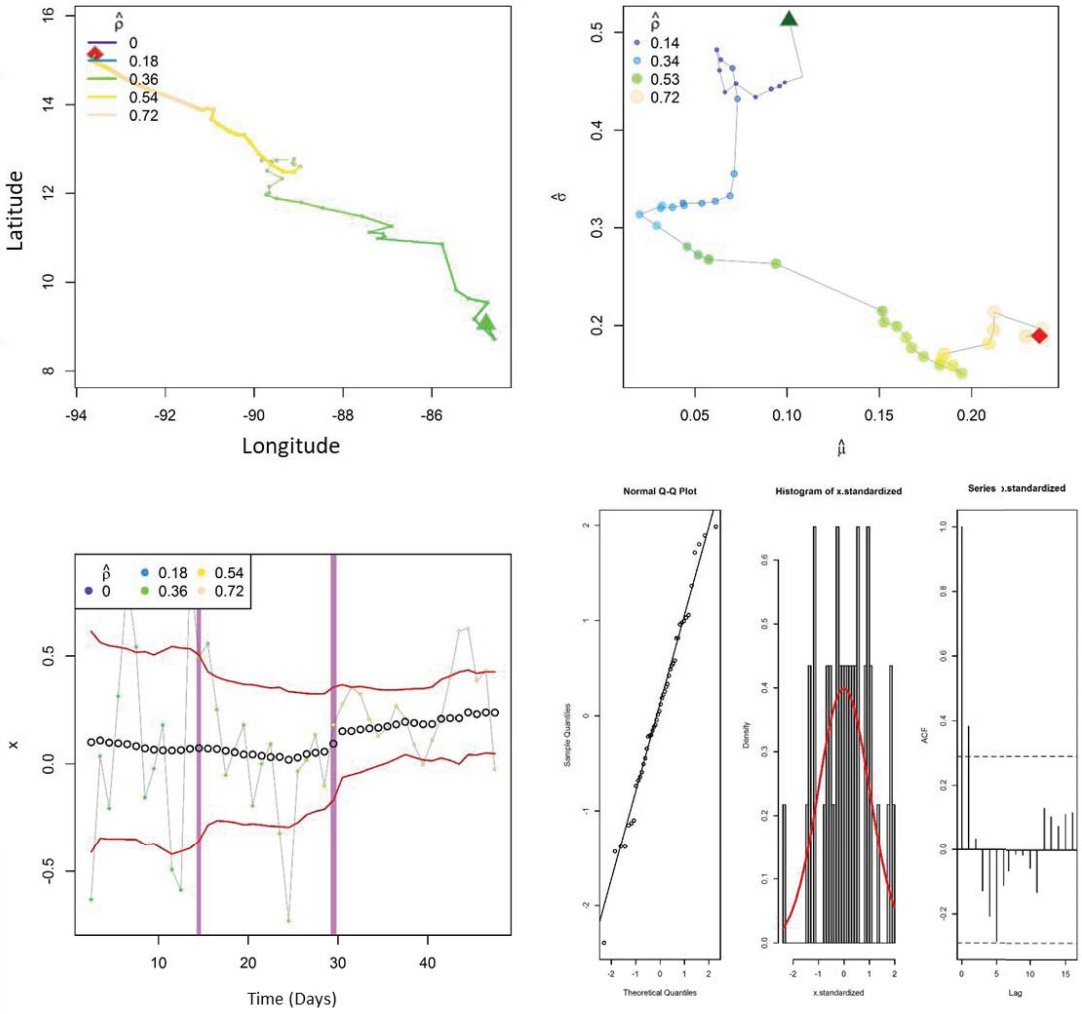

Figure 3.8: Four plots showing the output of the BCPA modeling procedure for sailfish 134267. Top left shows the migratory path where a green triangle marks the PSAT deployment location and a red square the endpoint or PSAT pop-off point. Color of the line represents the autocorrelation parameter. The top right is a phase

plot representing relationship between the 3 parameters estimated from the BCPA with the autocorrelation parameter shown in color and size coded circles. The bottom left plot shows the change points where the pink lines represent the time of the changepoint within the trial and the thickness of the line representing the number of days used for the selection of the change point. The black open circles represent the mean of the BCPA analysis with the red lines indicating the standard deviation. Finally, the bottom right set of diagnostic plots includes a QQ-norm plot, histogram and autocorrelation function of the standardized data from the model.

Figure 3.9 shows BCPA results for Sailfish 134272 which exhibited low autocorrelation ($\hat{\rho}$) throughout the trial, never increasing above 0.38 of the maximum of 1.0 fully correlated movement (Figure 3.9 Top Left). To reiterate, the colors of the plot indicate relative autocorrelation values within this sailfish thus high values seen in yellow are relative only to this fish which exhibits only low levels of autocorrelation. This sailfish travels westward immediately following deployment in a relatively straight line during the first few days of the trial but dramatically shifts behavior to a southward then northward tortuous and meandering foraging pattern. Unique to this fish is a zig-zag pattern with many straight line opposing directional changes but lacking the meandering curvature seen in many other sailfish. This could indicate foraging behavior specific to this particular location and time. This foraging behavior continues before becoming more directed but less autocorrelated just prior to trial end (Figure 3.9 Top Left). Trackline thickness for this sailfish indicates a relative change in the mean BCPA values throughout the trial as the line becomes thicker as the track progresses in time and space.

The phase plot clearly shows where the highly tortuous movements in the early stages of the track show high variability ($\hat{\sigma}$) and relatively low speed ($\hat{\mu}$) while the sailfish undergoes the small directional shifts referred to as the zig-zag pattern. As the migration progresses, speed increases and variability decreases as the sailfish transitions

out of the foraging behavior seen during the zig-zagging until PSAT release (Figure 3.9 Top Right).

Sailfish 134272 had 3 strong behavioral changes on days 16, 33, and 48 (Figure 3.9 Bottom Left). These change points are clearly visible on the plot and align well with the shifts in migratory patterns in this sailfish from directed to zig-zag and back to more directed. Of all sailfish tagged this represents the most clear delineation of behavioral shifts relative to the animal track map.

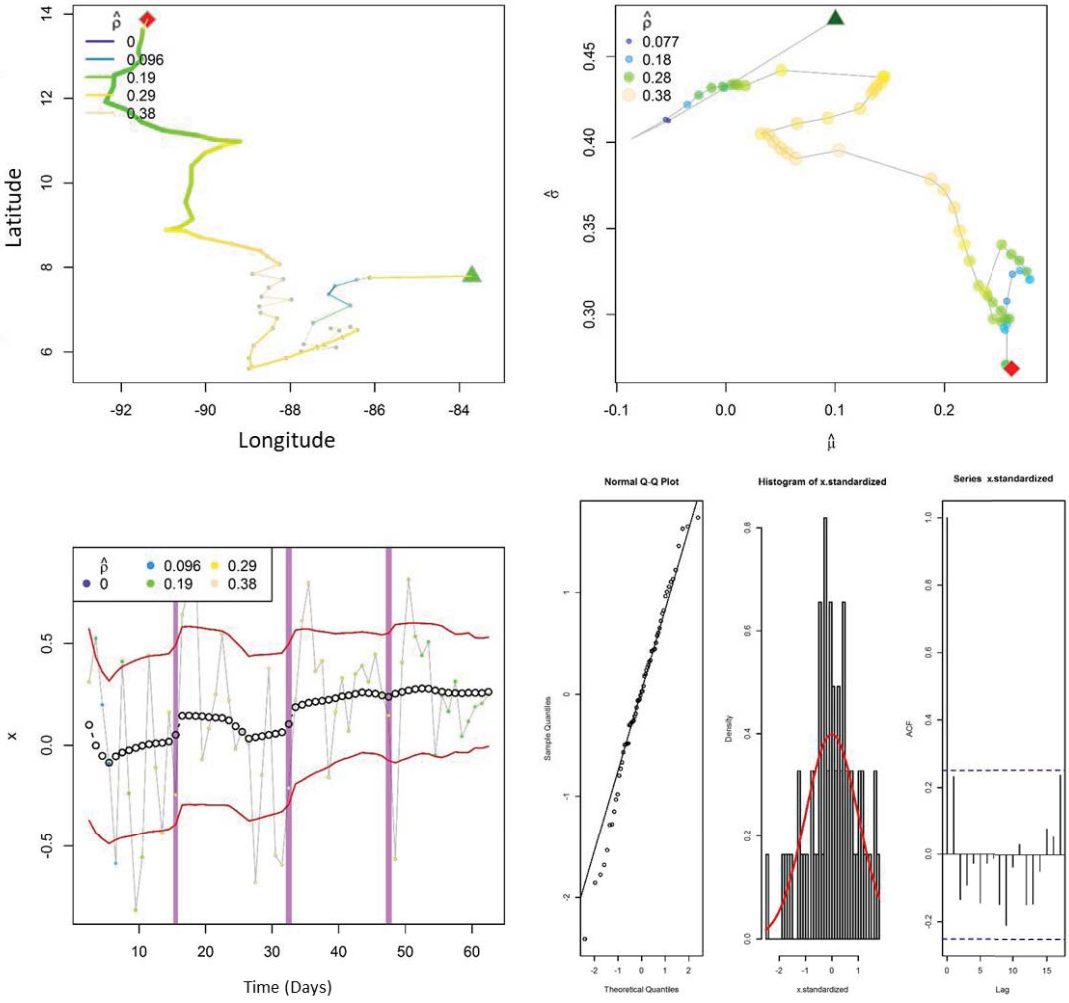

Figure 3.9: Four plots showing the output of the BCPA modeling procedure for sailfish 134272. Top left shows the migratory path where a green triangle marks the PSAT deployment location and a red square the endpoint or PSAT pop-off point.

Color of the line represents the autocorrelation parameter. The top right is a phase plot representing relationship between the 3 parameters estimated from the BCPA with the autocorrelation parameter shown in color and size coded circles. The bottom left plot shows the change points where the pink lines represent the time of the changepoint within the trial and the thickness of the line representing the number of days used for the selection of the change point. The black open circles represent the mean of the BCPA analysis with the red lines indicating the standard deviation. Finally, the bottom right set of diagnostic plots includes a QQ-norm plot, histogram and autocorrelation function of the standardized data from the model.

The diagnostic plots (Figure 3.9 Bottom Right) indicate the assumption of normality of the standardized residuals has been met for Sailfish 134272 in all three of the diagnostics but with the left side of the QQ-Norm plot showing slight deviation on the tail but within acceptable range for this analysis.

Figure 3.10 shows BCPA results for Sailfish 134273 which exhibits overall very low autocorrelation ($\hat{\rho}$) and moderate to high relative tortuosity compared to other tagged sailfish (Figure 3.10 Top Left). Autocorrelation is lowest during the days immediately after deployment and immediately before the endpoint of the trial. As this sailfish travels northwestward, autocorrelation increases as slight meandering movement becomes more directed toward the midpoint of the trial. The track then becomes highly tortuous and less autocorrelated indicating a clear foraging behavior before a return to a more moderately tortuous pattern and an increase in autocorrelation. The highest autocorrelation is seen toward the end of the trial just before the time when autocorrelation becomes lowest. Trackline thickness for this sailfish indicates a small proportional change in the mean BCPA values during the period of foraging behavior and at the start and end of the trial.

The phase plot shows low variability ($\hat{\sigma}$) for the majority of the trial with the exception of the final portion of the track (Figure 3.10 Top Right). This variability reaches its peak toward the end of the trial. This sailfish showed a relative wide range of

speed ($\hat{\mu}$) beginning with the highest velocity followed by a sharp decrease in speed when the sailfish enters the clear foraging period. An increase in speed is then witnessed followed by a slight decrease then slight increase in the final days of the trial.

Sailfish 134273 had 4 behavioral changes with two strong change points found on days 16 and 42 and two weaker changes on days 37 associated with an outlier and on day 51 associated with a strong behavioral change in the two days prior to PSAT release which indicates a significantly different behavioral pattern leading to tag release/shedding (Figure 3.10 Bottom Left). The strong changes appear on the plot as two bars each but can be considered as one change point for the purpose of this analysis that uses a cluster width of 3 days to determine behavioral changes.

The diagnostic plots (Figure 3.10 Bottom Right) show the tails of the QQ-Norm plot to be deviating substantially due to outliers especially those from the days just prior to the end of the trial when parameters become very variable. Although the QQ-Norm plot appears to contain deviations from the normality trendline, the overall normality of the residuals appears to be within acceptable range to proceed with using this animal in the overall analysis. The histogram of residuals also has an important tail on the left side showing a higher density of points on the left tail that may be contributing to the slight lack of residual normality.

The lack of fit in this sailfish is a sign that it undertook relatively abnormal behavioral patterns in speed and directness resulting in BCPA parameter estimates at the start and end of the trial that decrease the quality of the fit. The speed and directness are directly measured from PSAT tag data thus values have only the innate error of the PSAT with no opportunity for estimation error in only a portion of the data meaning parameter

values are real indicators of behavior. Drastic behavioral changes in speed and directness represent the likely issue leading to the lack of fit. The relative values estimated for autocorrelation throughout the entire sailfish track are still valid to estimate time and location of relative behavioral shifts, or change points, within the trial period. For this reason, the change points estimated are included in the discussion with other sailfish parameter values.

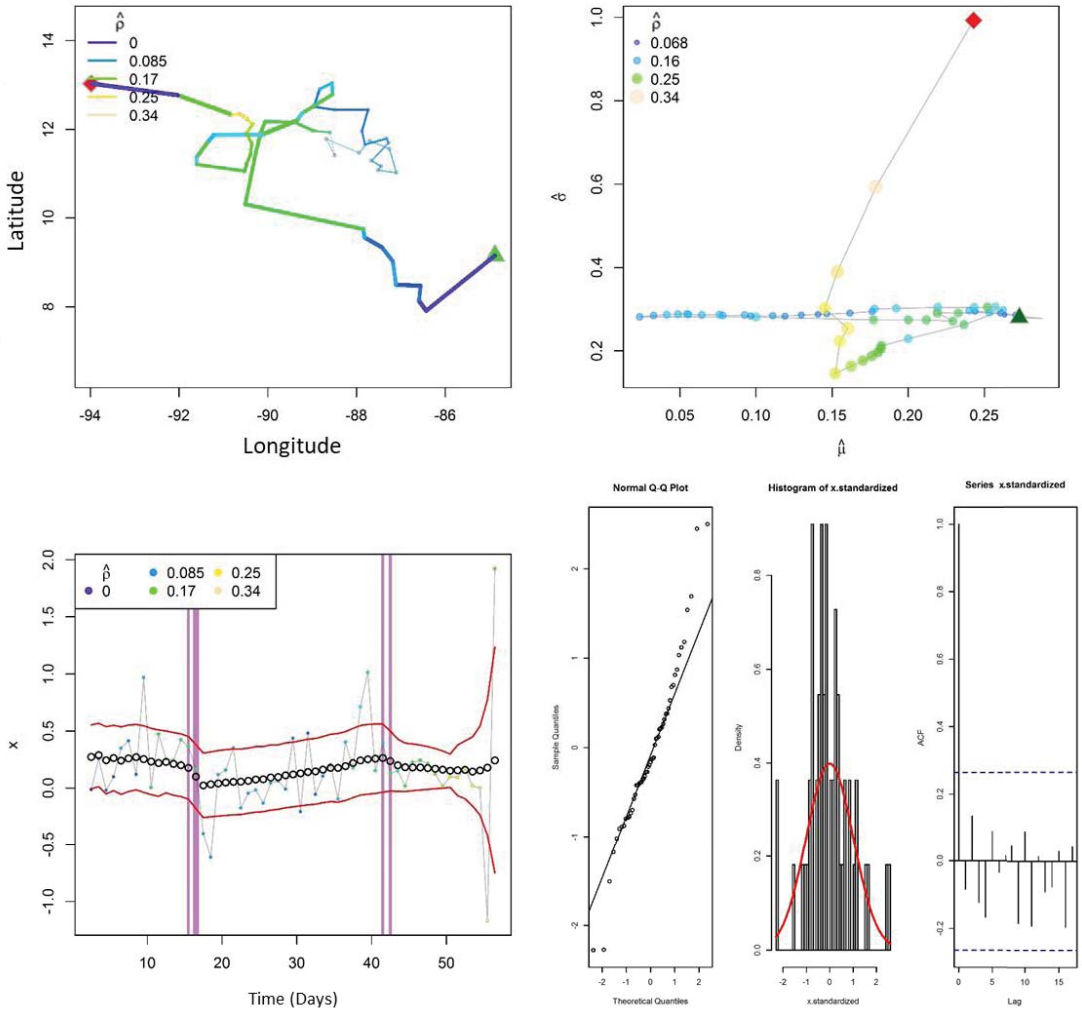

Figure 3.10: Four plots showing the output of the BCPA modeling procedure for sailfish 134273. Top left shows the migratory path where a green triangle marks the PSAT deployment location and a red square the endpoint or PSAT pop-off point. Color of the line represents the autocorrelation parameter. The top right is a phase plot representing relationship between the 3 parameters estimated from the BCPA

with the autocorrelation parameter shown in color and size coded circles. The bottom left plot shows the change points where the pink lines represent the time of the changepoint within the trial and the thickness of the line representing the number of days used for the selection of the change point. The black open circles represent the mean of the BCPA analysis with the red lines indicating the standard deviation. Finally, the bottom right set of diagnostic plots includes a QQ-norm plot, histogram and autocorrelation function of the standardized data from the model.

Figure 3.11 shows BCPA results for Sailfish 134275 which begins the migratory path with low autocorrelation ($\hat{\rho}$) and relative low tortuosity as the sailfish makes an overall northwestward migration consistent with the majority of PSAT tagged sailfish in this study (Figure 3.11 Top Left). This sailfish exhibits the least autocorrelation during the initial migratory path immediately following deployment transitioning to a meandering foraging behavior with slightly increasing autocorrelation. The sailfish then shifts to a traveling mode to the northwest where autocorrelation reaches its highest level until another shift to foraging behavior occurs and autocorrelation decreases prior to the end of the deployment. Trackline thickness for this sailfish indicates a proportional change in the mean BCPA at the midpoint of the truck during the more directed traveling phase indicated by the thicker line.

The phase plot shows an overall lack of variability ($\hat{\sigma}$) at the onset of the trial remains constantly low through the first foraging phase and half of the traveling phase before increasing dramatically until the second foraging phase occurs and variability slightly decreases until the end of the trial (Figure 3.11 Top Right). Speed ($\hat{\mu}$) is low at the start of the trial but immediately begins to increase during the first foraging phase and into the traveling phase where it peaks then begins to decrease until the second foraging phase where it slight increases then decreases just before trial end. the first 15 days before variability increases steadily until day 28 before leveling out.

Sailfish 134275 had 4 behavioral changes on days 16, 19, 24, and 33 with changes on days 16 and 24 being strong behavioral changes indicative of the changes from foraging to traveling to foraging. Weak change points occur on days 19 and 33 and are more associated with outliers and not strong enough to be visualized in the plot (Figure 3.11 Bottom Left).

The diagnostic plots (Figure 3.11 Bottom Right) indicate the assumption of normality of the standardized residuals has been met for Sailfish 134275 in all three of the diagnostics with only slight deviation from normal in the QQ-Norm tails.

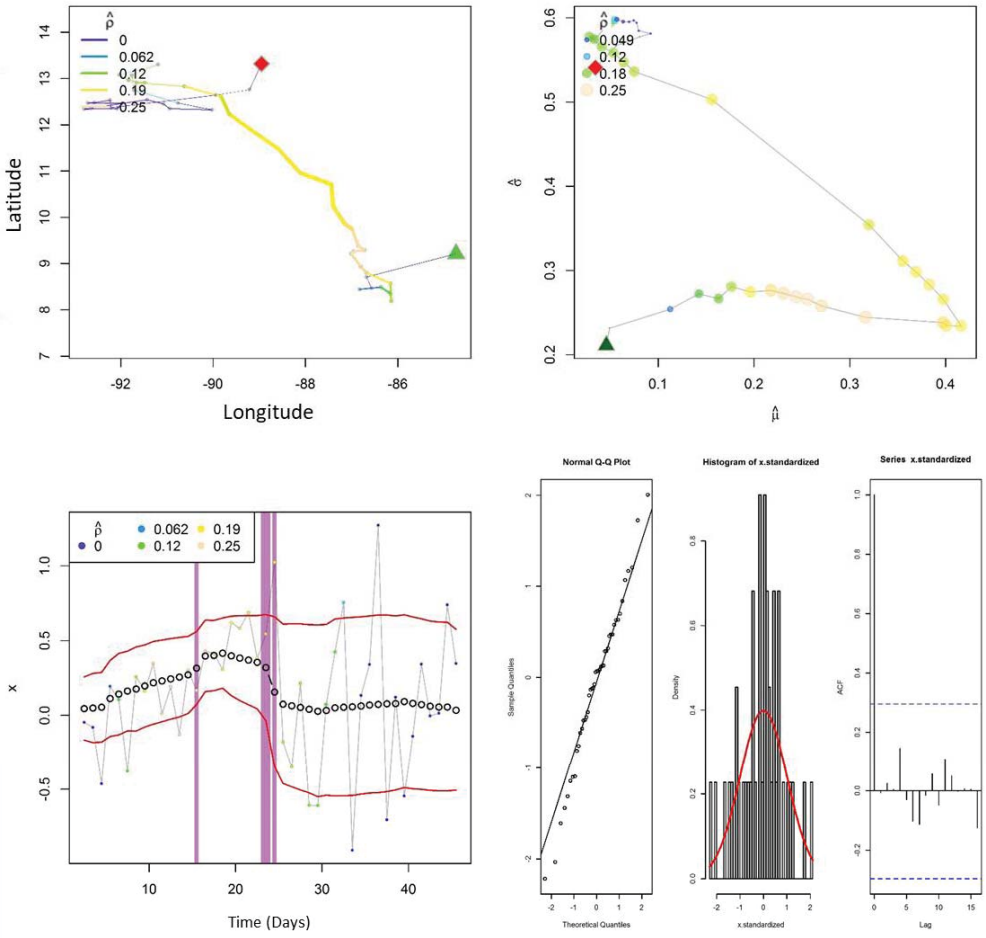

Figure 3.11: Four plots showing the output of the BCPA modeling procedure for sailfish 134275. Top left shows the migratory path where a green triangle marks the PSAT deployment location and a red square the endpoint or PSAT pop-off point.

Color of the line represents the autocorrelation parameter. The top right is a phase plot representing relationship between the 3 parameters estimated from the BCPA with the autocorrelation parameter shown in color and size coded circles. The bottom left plot shows the change points where the pink lines represent the time of the changepoint within the trial and the thickness of the line representing the number of days used for the selection of the change point. The black open circles represent the mean of the BCPA analysis with the red lines indicating the standard deviation. Finally, the bottom right set of diagnostic plots includes a QQ-norm plot, histogram and autocorrelation function of the standardized data from the model.

Figure 3.12 shows BCPA results for Sailfish 134280 which begins with low autocorrelation ($\hat{\rho}$) and relatively direct southwestward movement immediately following deployment (Figure 3.12 Top Left). The sailfish then transitions to a more autocorrelated southeastward path before entering a phase of high tortuosity foraging where autocorrelation decreases slightly before the sailfish transitions to a traveling phase eastward where autocorrelation increases slightly. Autocorrelation decreases slightly then increases as the sailfish turns southwest then southeast before entering a phase of more tortuous movement while maintaining relative high autocorrelated movement toward the northeast. Autocorrelation decreases slightly as the sailfish loops back to the west and southwest prior to the trial end. It is important to note that autocorrelation values are relatively low throughout the trial when compared to other PSAT tagged sailfish. Trackline thickness for this sailfish indicates a proportional change in the mean of the BCPA in the initial phase of the migration and at the midpoint when the sailfish was in the traveling phase indicated by thicker tracklines.

The phase plot reveals a declining trend in variability ($\hat{\sigma}$) and speed ($\hat{\mu}$) during the initial directed phase (Figure 3.12 Top Right). Variability increases as the sailfish enters the foraging phase then levels off during the initial leg of the traveling phase. Variability then increases slightly when the sailfish makes a turn to the southwest before drastically

decreasing as the sailfish travels to the southeast before entering the more tortuous meandering pattern until the end of the trial. Speed remains low during the foraging phase but increases as the sailfish enters the traveling mode toward the east. Speed then decreases slightly and is maintained throughout the final meandering phase.

Sailfish 134280 had 7 behavioral changes on days 14, 25, 28, 35, 87, 62, and 80 (Figure 3.12 Bottom Left). The change points were more easily identified with this sailfish due to clear behavioral changes in both speed and variability and the analysis is aided by the longer duration of the PSAT on the sailfish in this case. The transitions from directed traveling behavior to foraging and vice versa can be easily identified as well as vary levels of traveling and foraging behavior. This sailfish showed distinct traveling phases, one with increasing speed and another relatively constant and these were identified. Foraging modes were also identified with varying levels of directness and speed indicating differing foraging patterns based on spatial and temporal dynamics. Change points for this fish were estimated as strong likely behavioral changes and all are visualized in Figure 3.12. Outliers existed in this dataset as well but do not result in weaker change points.

Although the results of this fish are one the cleanest of the PSAT tagged sailfish, the diagnostic plots (Figure 3.12 Bottom Right) indicate deviation of the model in the tails of the QQ-Norm plot. This deviation is within acceptable limits for the modeled data. The histogram and autocorrelation function do not indicate a drastic deviation from normality.

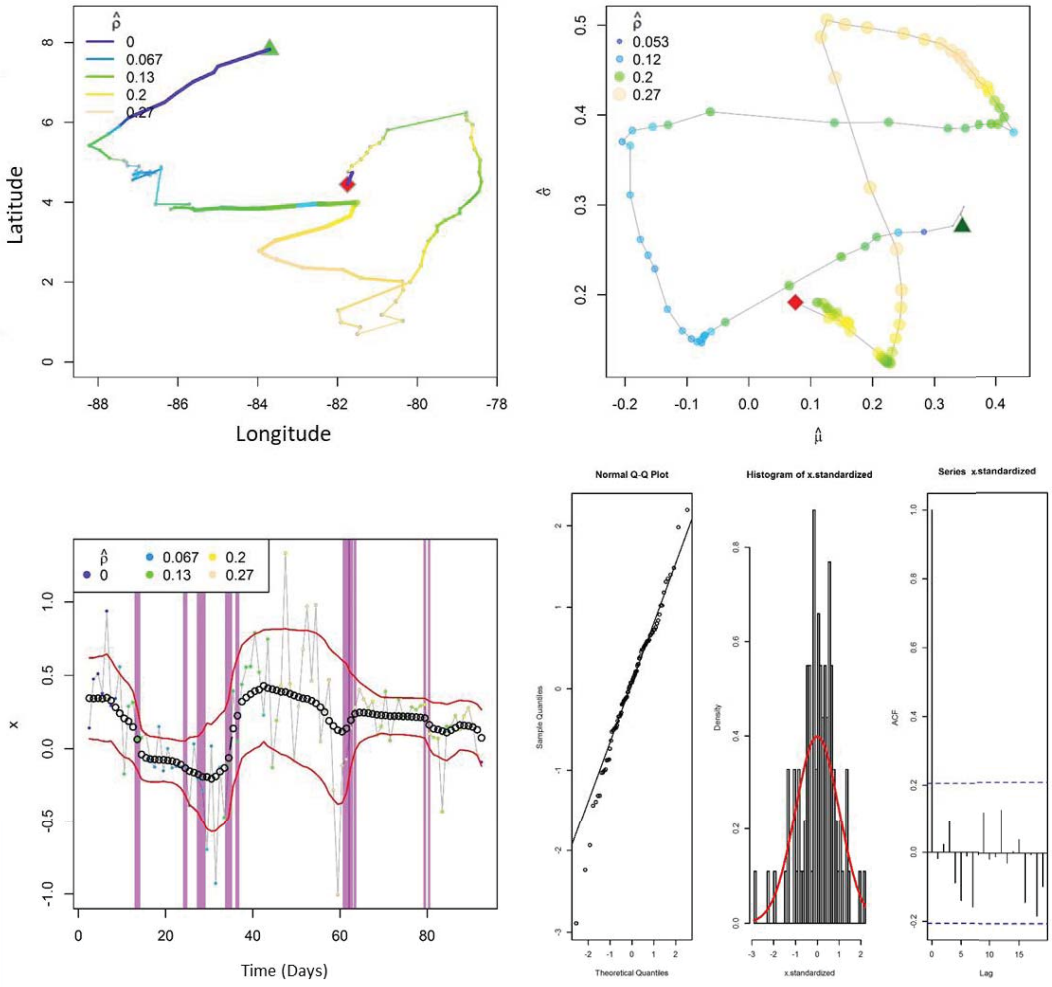

Figure 3.12: Four plots showing the output of the BCPA modeling procedure for sailfish 1342780. Top left shows the migratory path where a green triangle marks the PSAT deployment location and a red square the endpoint or PSAT pop-off point. Color of the line represents the autocorrelation parameter. The top right is a phase plot representing relationship between the 3 parameters estimated from the BCPA with the autocorrelation parameter shown in color and size coded circles. The bottom left plot shows the change points where the pink lines represent the time of the changepoint within the trial and the thickness of the line representing the number of days used for the selection of the change point. The black open circles represent the mean of the BCPA analysis with the red lines indicating the standard deviation. Finally, the bottom right set of diagnostic plots includes a QQ-norm plot, histogram and autocorrelation function of the standardized data from the model.

Figure 3.13 shows BCPA results for Sailfish 134285 which was the second longest deployment period (149 days) of PSAT tagged sailfish. The migratory track

begins with moderate autocorrelation ($\hat{\rho}$) and directed movement just after deployment then transitions to a more tortuous, less autocorrelated, pattern toward the north before gradually turning westward (Figure 3.13 Top Left). A period of moderate to high tortuosity and low autocorrelation is experienced for a majority of the trial with large scale movements to the west and east, and smaller scale movements north and south. Small scale highly tortuous movements are difficult to identify due to the grand temporal and spatial scale of this sailfish migratory track. Just before the midpoint of the trial a period of transition occurs followed by a clear traveling phase and another transition phase before the sailfish reverts back to the large scale moderately tortuous pattern. Overall the autocorrelation for this sailfish is low indicating a lack of persistent directed behavior. Sailfish 134285 shows proportional difference in BCPA mean witnessed by the thick blue line at the midpoint of the trial. This is visible in the longer deployed track data because of the wider range of parameter values witnessed over 149 days compared to the shorter tracks in the majority of sailfish deployments.

The phase plot shows in a very wide range of parameter values especially variability ($\hat{\sigma}$) in this sailfish (Figure 3.13 Top Right). Speed ($\hat{\mu}$) remains relatively high for a majority of the trial before decreasing, reverting back to previous levels, then slightly decreasing before the trial end. Variability shows the widest range of values of any sailfish analyzed. Variability is relatively constant in the first phase of the trial before increasing as the track becomes more tortuous during the initial foraging phase then decreases as the sailfish enters the only clear traveling phase. Variability then increases as the sailfish transitions from the traveling phase back to the foraging pattern and is maintained until a drastic change occurs. During this behavioral shift, variability

dramatically increases, then decreases, then increases before trial end. This phase shows a very tight foraging pattern during this time indicative of some feature in this location where a strong behavioral shift was undertaken from large scale foraging to small scale, very highly tortuous behavior. This behavior is masked by the large scale of the trackplot but may be an important indicator of a unique behavior such as schooling a different type of foraging.

Sailfish 134285 had 15 behavioral changes on days 14, 24, 30, 41, 45, 53, 72, 77, 83, 98, 102, 110, 117, 125, and 132 (Figure 3.13 Bottom Left). Of these change points, all but two are strong behavioral shift where change points on days 14 and 45 are weaker and potentially more associated with strong outliers surrounding those days. The change points in this sailfish are clear and discernible relative to their changes in variability and speed including the transitions from foraging to traveling including the differentiation of the transition periods and especially the period between day 85 and 100 where a strong shift to highly tortuous behavior was witnessed before returning to previous behavioral patterns.

The diagnostic plots reveal a stark departure from normality in the QQ-Norm plot tails which may be a product of the large number of outliers in the relative small range of standard deviation compared to other analyzed sailfish. The histogram and autocorrelation function do not reveal significant issues with normality of residuals indicated by the QQ-Norm plot. Although these QQ-Norm plot reveals a potential issue with normality, the deviations are not so extreme as to disqualify this sailfish from further analysis.

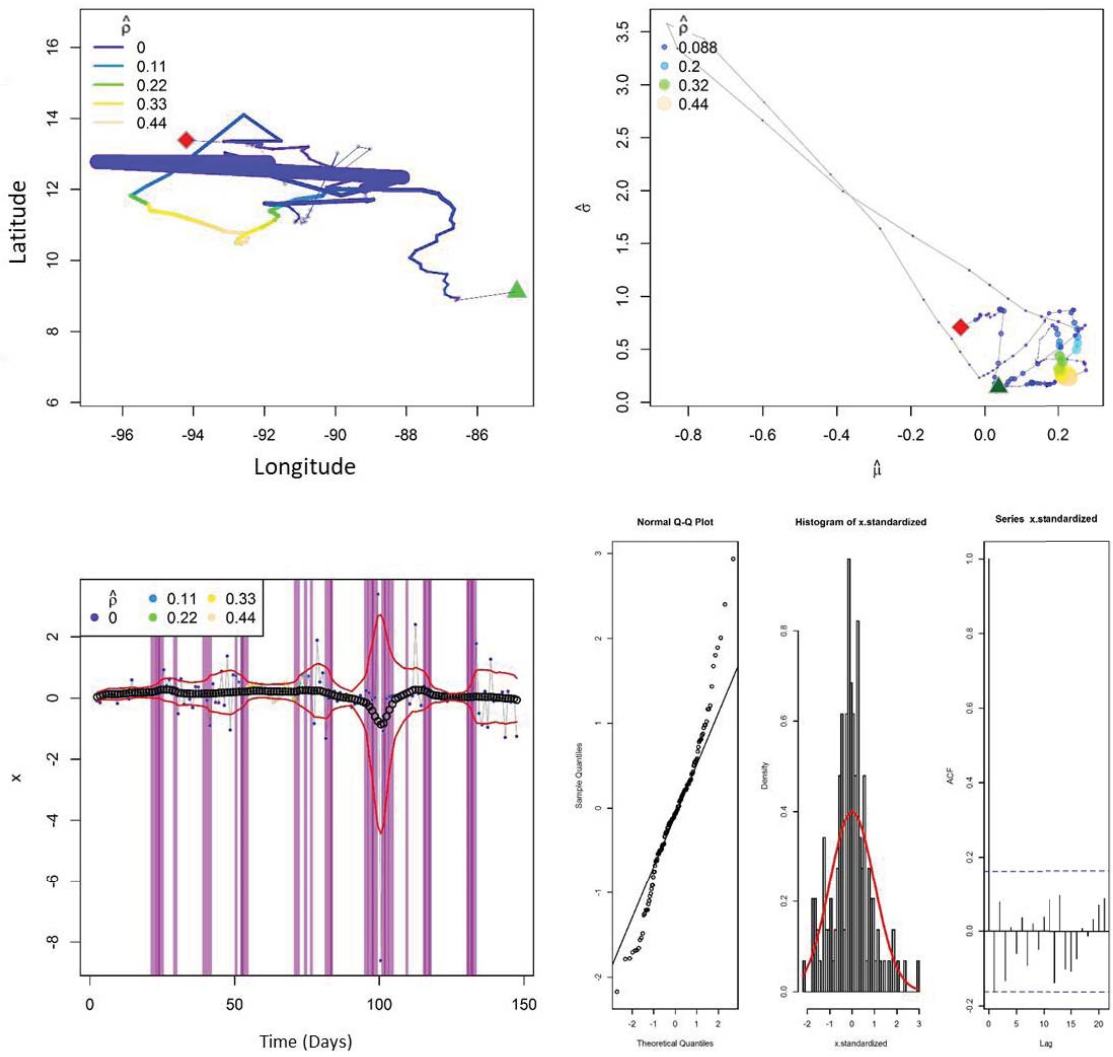

Figure 3.13: Four plots showing the output of the BCPA modeling procedure for sailfish 134285. Top left shows the migratory path where a green triangle marks the PSAT deployment location and a red square the endpoint or PSAT pop-off point. Color of the line represents the autocorrelation parameter. The top right is a phase plot representing relationship between the 3 parameters estimated from the BCPA with the autocorrelation parameter shown in color and size coded circles. The bottom left plot shows the change points where the pink lines represent the time of the changepoint within the trial and the thickness of the line representing the number of days used for the selection of the change point. The black open circles represent the mean of the BCPA analysis with the red lines indicating the standard deviation. Finally, the bottom right set of diagnostic plots includes a QQ-norm plot, histogram and autocorrelation function of the standardized data from the model.

Figure 3.14 shows BCPA results for Sailfish 134258 which was the longest deployment period (179 days) of PSAT tagged sailfish; however, only 120 days were included in this analysis due to an overall lack of datapoints between days 120 and 179. The migratory track begins with relative low autocorrelation ($\hat{\rho}$) and moderate tortuosity in the initial period immediately after deployment while the sailfish meandered around the PSAT deployment location (Figure 3.14 Top Left). Tortuosity increases while autocorrelation remains relatively low as the sailfish continues to undertake a meandering foraging behavioral pattern. Following this foraging phase, a noticeable increase in autocorrelation is witnessed, albeit relatively low compared to other sailfish, and tortuosity begins to decrease. The sailfish then enters a traveling phase with increasing autocorrelation as the sailfish travels toward the northwest with low to moderate tortuosity. After reaching the northernmost point of the migration, the sailfish transitions to a large scale foraging behavior where autocorrelation begins to decrease and tortuosity remains at a moderate level as the fish migrates southeast back toward the tagging location where it remained for half of the trial period before heading west to the endpoint. Overall autocorrelation in this sailfish remained low throughout the deployment. The thickness of the trackline reveals large proportional differences in the mean of the BCPA compared to previously analyzed sailfish tracks with thickest portions during the traveling phase and later foraging phase.

The phase plot shows the wide range of variability ($\hat{\sigma}$) and speed ($\hat{\mu}$) with higher scales than a majority of PSAT tagged sailfish indicating this sailfish underwent more variable behavioral patterns than others in this analysis (Figure 3.14 Top Right). The highest variability is seen when the autocorrelation parameter is also at the highest values

which is unique in that autocorrelated movement should lack variability; however, this sailfish maintained a moderate level of tortuosity throughout. Variability is high throughout but begins at a relatively low value and increases during the traveling phase followed by a decrease as the sailfish transitions from traveling to foraging. The sailfish then maintains the foraging behavior but shows another large increase and subsequent decrease in variability during the later foraging phases prior to trial end. Speed is also variable with a large decrease as the fish enter traveling mode followed by an increase as the fish transitions back to foraging. The speed decreases again during the later foraging phases and increases again to the starting point.

Sailfish 134258 had 15 behavioral changes on days 11, 18, 24, 29, 39, 43, 54, 65, 69, 76, 83, 97, 103, and 109 (Figure 3.14 Bottom Left). Of the 15 change points estimated, only 6 represent strong behavioral shifts in the parameters on days 18, 29, 39, 65, 69, and 76. These strong change points represent the clear behavioral shifts from foraging at the onset of the trial to the transition to traveling and back to varying levels of foraging. The remaining change points are weak behavioral shifts that may be associated with outliers in the mean of the BCPA and may be contributed to very small ranges in autocorrelation while the range of speed and variability were disproportionately higher. Although these are considered weak change points they are not errors thus will remain as part of the analysis moving forward.

With a number of weak change points, the fit of the residuals must be examined in detail; however, the diagnostic plots reveal normality to be acceptable in all three diagnostic plots (Figure 3.14 Bottom Right).

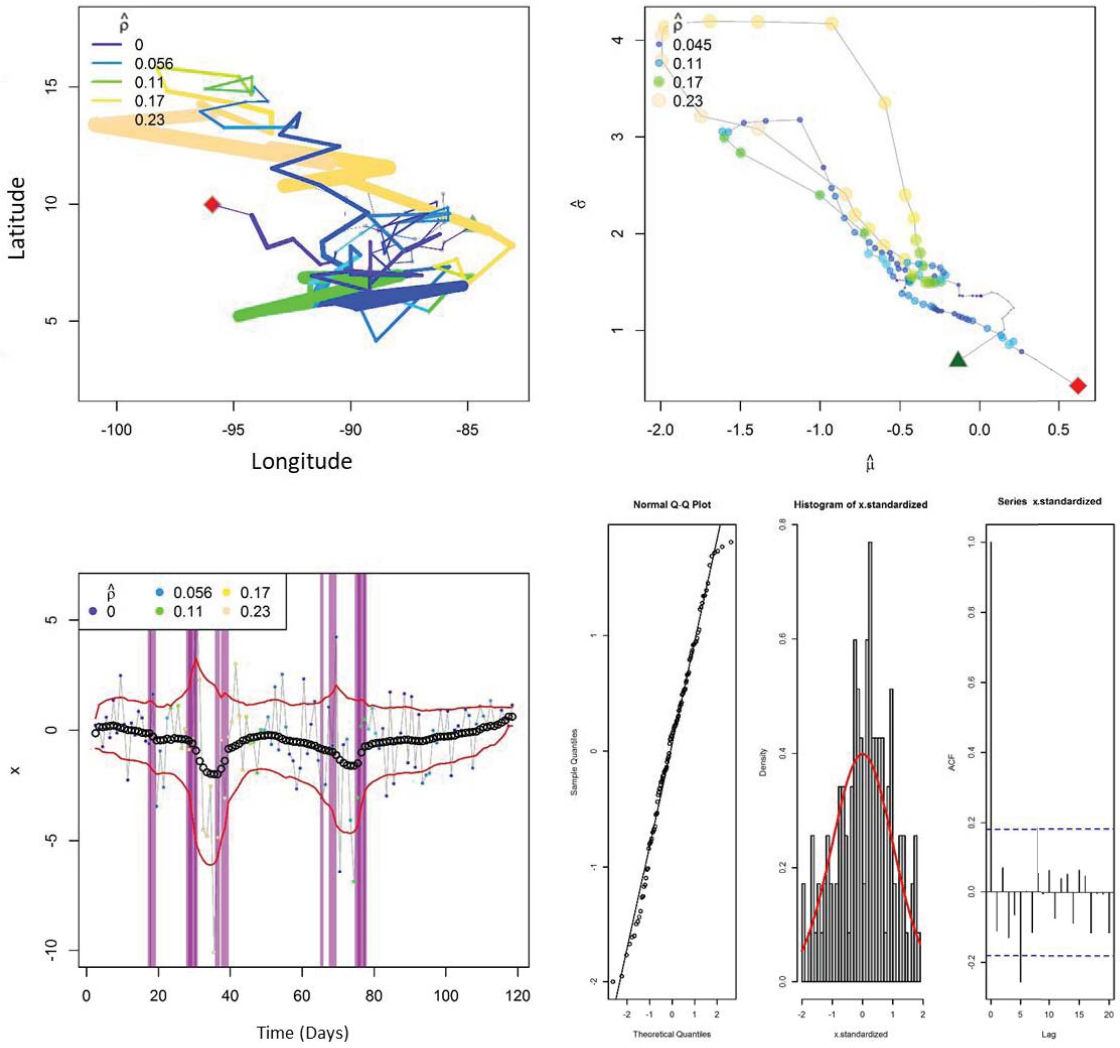

Figure 3.14: Four plots showing the output of the BCPA modeling procedure for sailfish 134258. Top left shows the migratory path where a green triangle marks the PSAT deployment location and a red square the endpoint or PSAT pop-off point. Color of the line represents the autocorrelation parameter. The top right is a phase plot representing relationship between the 3 parameters estimated from the BCPA with the autocorrelation parameter shown in color and size coded circles. The bottom left plot shows the change points where the pink lines represent the time of the changepoint within the trial and the thickness of the line representing the number of days used for the selection of the change point. The black open circles represent the mean of the BCPA analysis with the red lines indicating the standard deviation. Finally, the bottom right set of diagnostic plots includes a QQ-norm plot, histogram and autocorrelation function of the standardized data from the model.

Figure 3.15 shows BCPA results for Sailfish 134241 which exhibited somewhat unique migrational trajectories. At the onset of the deployment, the sailfish makes direct movement westward with the highest autocorrelation ($\hat{\rho}$) value seen during the trial until the track become more tortuous and looping (Figure 3.15 Top Left). Following this moderately tortuous looping the sailfish transitions to a slightly more autocorrelated path to the southeast followed by a short period of tortuosity then a long, very direct but moderately autocorrelated movement to the west southwest before reversing course and heading east with increased autocorrelation. The sailfish then sees a spike in autocorrelation before the trial end. Overall from start to end of migratory path, this sailfish made a net southward migration. Trackline thickness indicates a proportional change in the mean BCPA at the start and end of the trackline as well as during the short period of tortuous foraging behavior indicated by the thin portions of the trackline.

The phase plot reveals relative low variability ($\hat{\sigma}$) and high speed ($\hat{\mu}$) in the first moderately tortuous and looping phase of the migration. This phase is followed by a decrease in speed and increase in variability until the end of the trial period where a speed increase is seen on the last day (Figure 3.15 Top Right).

Sailfish 134241 had 5 behavioral change points on days 19, 23, 39, 44, and 49 (Figure 3.15 Bottom Left). Two of the change points can be considered strong behavioral shifts on days 19 and 44 which clearly separate the foraging phase while the track was looping and the traveling phases. Change points on days 23, 29, and 49 can be considered weaker changes only accounting for a small number of days' worth of parameter estimates. The day 49 change point is of particular interest because of the clear BCPA

mean shift seen in both the thickness of the trackline in Figure 3.15 Top Left, and the variability seen in the mean change point plot. The outliers seen in the final 5 days of the analysis may be contributing to the weakly labeled change point in this case.

The diagnostic plots (Figure 3.15 Bottom Right) reveal a deviation from normality in the tails of the QQ-Norm plot but relatively normal distribution of residuals in the histogram and autocorrelation function.

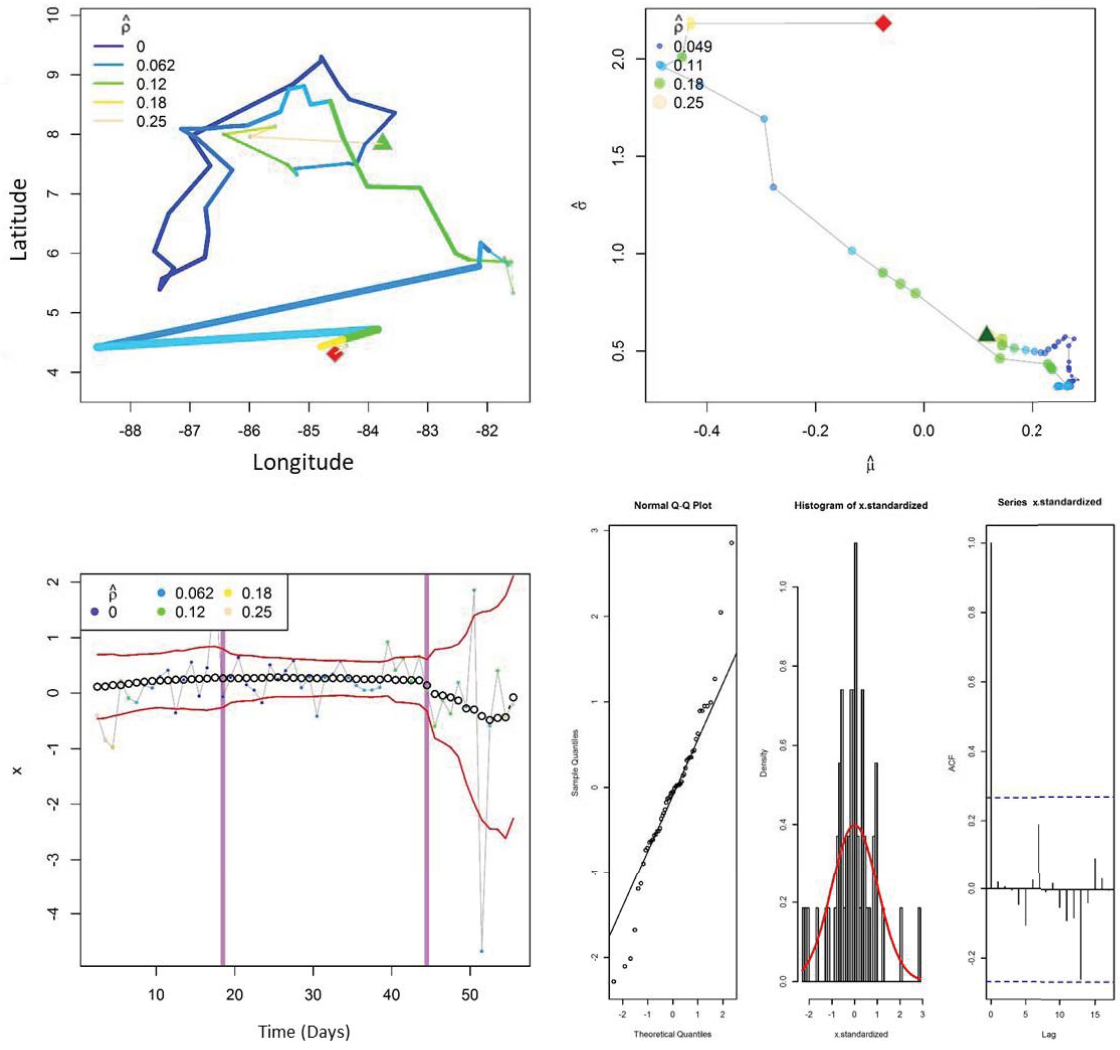

Figure 3.15: Four plots showing the output of the BCPA modeling procedure for sailfish 134241. Top left shows the migratory path where a green triangle marks the PSAT deployment location and a red square the endpoint or PSAT pop-off point. Color of the line represents the autocorrelation parameter. The top right is a phase plot representing relationship between the 3 parameters estimated from the BCPA with the autocorrelation parameter shown in color and size coded circles. The bottom left plot shows the change points where the pink lines represent the time of the changepoint within the trial and the thickness of the line representing the number of days used for the selection of the change point. The black open circles represent the mean of the BCPA analysis with the red lines indicating the standard deviation. Finally, the bottom right set of diagnostic plots includes a QQ-norm plot, histogram and autocorrelation function of the standardized data from the model.

Figure 3.16 shows BCPA results for Sailfish 134252 and shows an initial moderately tortuous movement with high autocorrelation followed by a more directed path with higher autocorrelation ($\hat{\rho}$) (Figure 3.16 Top Left). At the end of the trial period, tortuosity increases until the endpoint as autocorrelation decreases indicating a foraging pattern followed by a slight increase then final decrease just before trial end. Overall, autocorrelation is relatively low throughout the sailfish migratory path which results in a net westward overall movement. The trackline thickness indicates large proportional changes within the mean BCPA in the initial highly autocorrelated phase and again on the last two days of the deployment period.

From the phase plot it can be found that initially the sailfish travelled at slow speed ($\hat{\mu}$) and with increasing variability ($\hat{\sigma}$) in the initial phase of the trial (Figure 3.16 Top Right). Speed increases at the end of the highly autocorrelated phase until the sailfish begins the more tortuous foraging behavior prior to trial end when speed slightly reduces. Variability increases through the initial autocorrelated phase then decreases to the lowest values when the sailfish transitions to foraging before a slight increase just prior to the

end of the trial. The range of variability here is one of the highest seen by sailfish in this study.

Sailfish 134252 was found to have 7 behavioral change points on days 11, 14, 18, 27, 44, 55, and 68 (Figure 3.16 Bottom Left). The strong change points visualized in the plot occur on days 18, 55, and 68 which indicate the transition from the intial tortuous behavior to the autocorrelated phase and finally to the foraging behavior and end point where speed decreased and variability increased in the final few days of the trial. The weak change points are associated with the very high variation in BCPA mean in the first 18 days of the trial. The change point on day 27 is somewhat of an oddity in that there does not appear to be a dramatic change in any parameter or the mean BCPA but there is a slight outlier at that location that may be contributing to the inclusion of this time period in the behavior change methodology. On day 44 there is a weak change point that again indicates a small behavioral change and a slight change in the pattern of the mean BCPA can be seen at this point indicating a slight change in behavior.

The diagnostic plots (Figure 3.16 Bottom Right) indicate the assumption of normality of the standardized residuals has been met for Sailfish 134252 in all three of the diagnostics with only the QQ-Norm plot showing slight deviation from normal on one tail and the histogram indicating a very slight skew of the bell curve toward the left of the distribution. The autocorrelation function appears satisfactory.

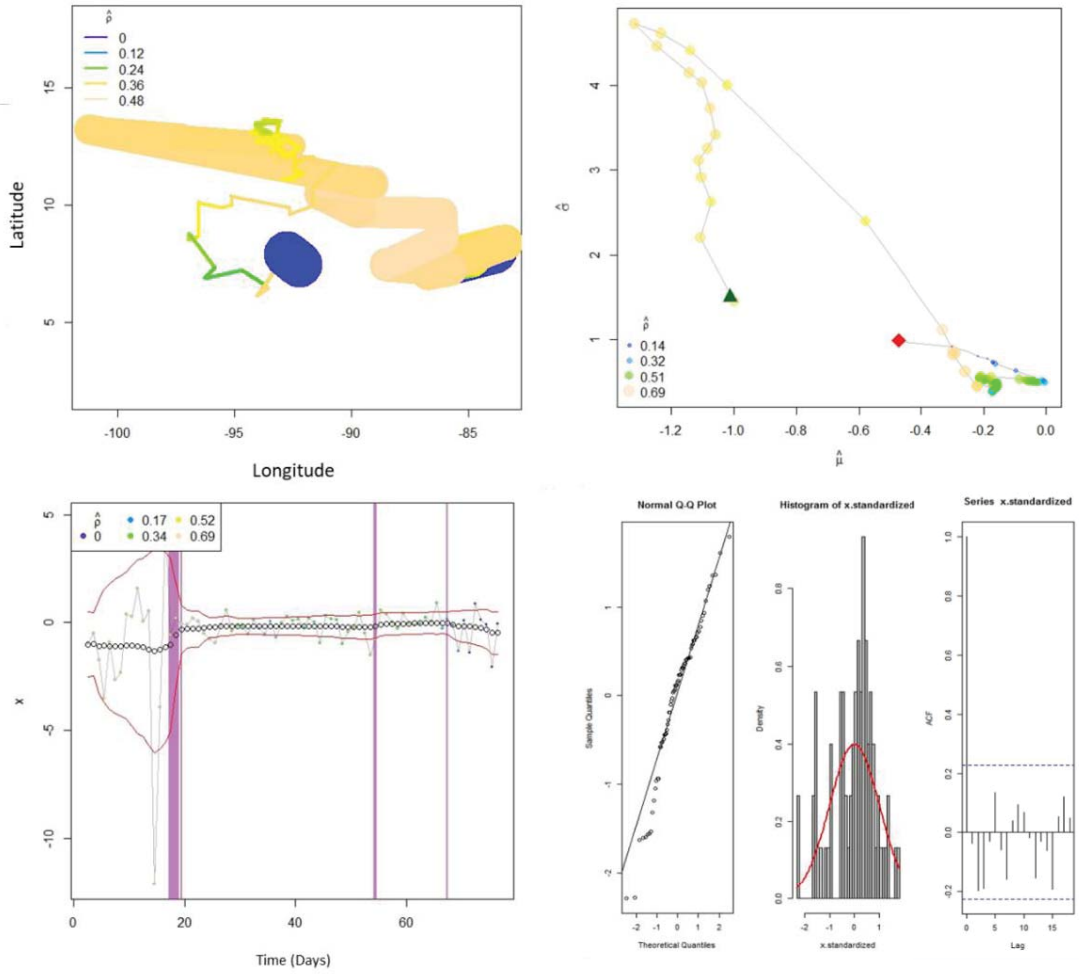

Figure 3.16: Four plots showing the output of the BCPA modeling procedure for sailfish 134252. Top left shows the migratory path where a green triangle marks the PSAT deployment location and a red square the endpoint or PSAT pop-off point. Color of the line represents the autocorrelation parameter. The top right is a phase plot representing relationship between the 3 parameters estimated from the BCPA with the autocorrelation parameter shown in color and size coded circles. The bottom left plot shows the change points where the pink lines represent the time of the changepoint within the trial and the thickness of the line representing the number of days used for the selection of the change point. The black open circles represent the mean of the BCPA analysis with the red lines indicating the standard deviation. Finally, the bottom right set of diagnostic plots includes a QQ-norm plot, histogram and autocorrelation function of the standardized data from the model.

Figure 3.17 shows BCPA results for Sailfish 134263 revealing an increasing pattern of tortuosity and in the initial phase of the trial while the sailfish undertook a

foraging meandering pattern around the tagging location (Figure 3.17 Top Left). Following this foraging phase, the sailfish transitions to a very slightly increased autcorrelation as the sailfish travels to the northwest in a slightly more tortuous route. Autocorrelation values in this fish are extremely low indicating an overall lack of persistence of movement or clear traveling behavioral pattern. The trackline thickness indicates large proportional changes in the BCPA mean during the first foraging phase, again at the midpoint of the track and the last portion of the migratory track just before PSAT release from the fish.

From the phase plot it can be found that initially the sailfish travelled at very slow but increasing speed ($\hat{\mu}$) for the first days postrelease followed by a reduction in speed then a large increase until the end of the trial end (Figure 3.17 Top Right). Overall speed values are low comparatively to other PSAT tagged sailfish in this study. Increasing variability ($\hat{\sigma}$) is witnessed immediately following PSAT deployment followed by a dramatic decrease as the sailfish transitions away from the foraging behavior into the more autocorrelated movement prior to the trial end.

Sailfish 134263 was found to have 7 behavioral change points on days 7, 10, 19, 31, 37, 46, and 61(Figure 3.17 Bottom Left). Of the 7 change points estimated, 3 are considered strong behavioral changes on days 19, 31, and 46 which indicate the transitions between differing foraging modes with varying tortuosity and speeds. Weak change points were found on days 7, 10, 37, and 61that can be attributed to some relatively large deviations in the estimated BCPA as seen in the outliers on the change point plot.

Although a number of outliers occur than may indicate small behavioral changes or simply a lack of model fit, the diagnostic plots show relatively normally distributed residuals in all 3 diagnostic plots (Figure 3.17 Bottom Right).

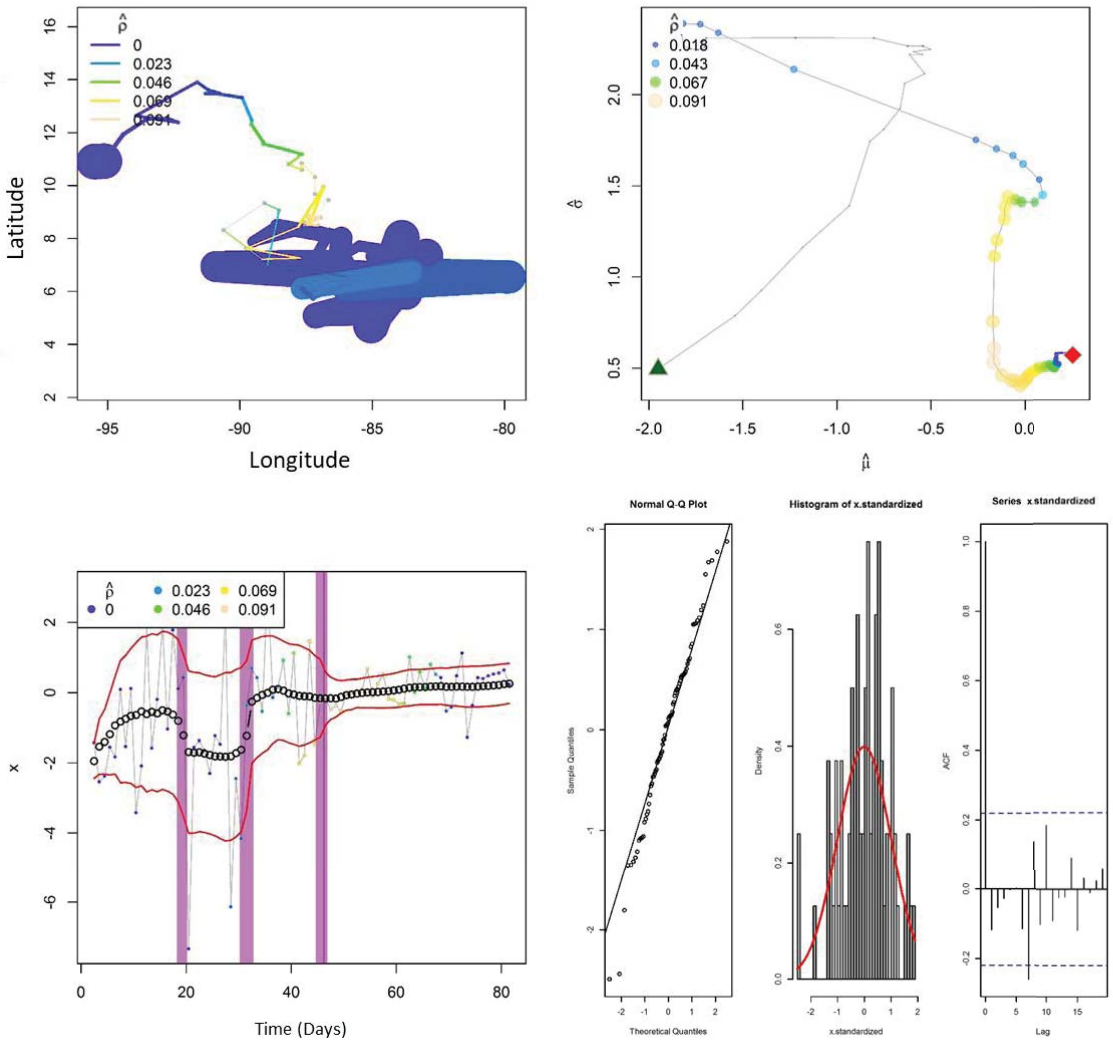

Figure 3.17: Four plots showing the output of the BCPA modeling procedure for sailfish 134263. Top left shows the migratory path where a green triangle marks the PSAT deployment location and a red square the endpoint or PSAT pop-off point. Color of the line represents the autocorrelation parameter. The top right is a phase plot representing relationship between the 3 parameters estimated from the BCPA with the autocorrelation parameter shown in color and size coded circles. The bottom left plot shows the change points where the pink lines represent the time of the changepoint within the trial and the thickness of the line representing the number of days used for the selection of the change point. The black open circles represent the mean of the BCPA analysis with the red lines indicating the standard

deviation. Finally, the bottom right set of diagnostic plots includes a QQ-norm plot, histogram and autocorrelation function of the standardized data from the model.

Figure 3.18 shows the BCPA resulting plots for Sailfish 134266 which began its migration with tortuous movement resulting in low autocorrelation coefficient ($\hat{\rho}$) values in the initial phase of the track indicating a foraging behavioral pattern (Figure 3.18 Top Left). Following this foraging phase around the tagging location, the sailfish then begins a slightly more autocorrelated behavioral trend while maintaining moderate tortuosity but exhibiting zig-zag movements. Following this foraging type behavior, the sailfish exhibits a northwestward movement that becomes slightly less autocorrelated and less tortuous. As the sailfish turns west, the autocorrelation begins to increase and the tortuosity decreases until the sailfish turns south and the autocorrelation decreases steadily while tortuosity slightly increases until the end of the trial period. Autocorrelation values for this sailfish are low comparatively to other sailfish indicating a lack of persistent movement overall. Trackline thickness indicates large proportional changes in mean BCPA during the initial foraging pattern and during the final period of tortuosity just prior to trial end.

The phase plot (Figure 3.18 Top Right) shows the relatively high variability ($\hat{\sigma}$) increasing initially to a peak during the most tortuous portion of the track followed by a decrease in variability as the track becomes more directed. Variability increases slightly again when the track becomes more tortuous after the period of directed movement then decreases prior to trial end. Sailfish speed ($\hat{\mu}$) shows a small range in this particular sailfish track, beginning at its slowest speed and increasing as the sailfish transitions away from the initial foraging pattern. The speed remains relatively constant throughout the remainder of the trial.

Sailfish 134266 generated 7 change points on days 9, 23, 29, 41, 47, 69, and 79 of the trial period (Figure 3.18 Bottom Left). Of the 7 change points estimated, 5 can be considered strong behavioral changes on days 23, 29, 41, 47, and 69 representing the behavioral shifts in differing foraging behaviors and more directed pattern at the midpoint of the trial. Weak change points were found on days 9 and 79 most likely associated with major outliers at those time periods.

The diagnostic plots (Figure 3.18 Bottom Right) indicate the assumption of normality of the standardized residuals has been met for Sailfish 134266.

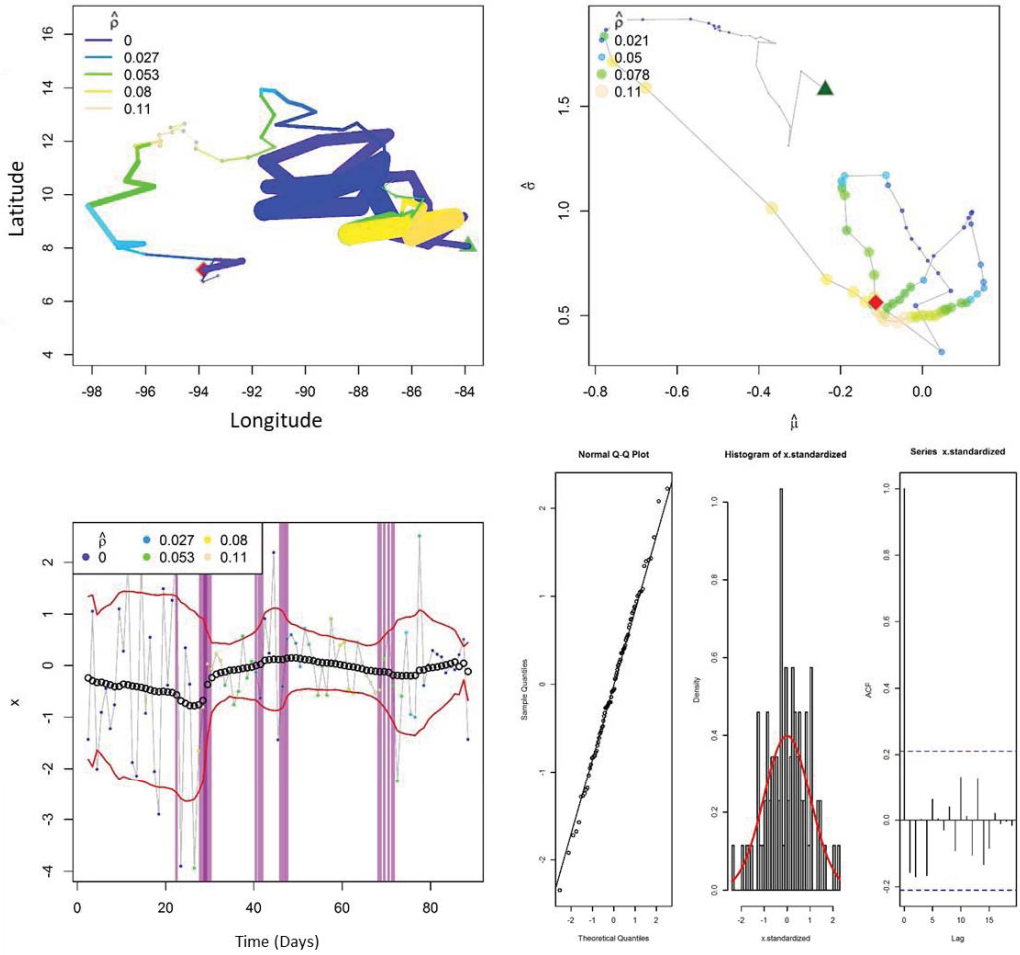

Figure 3.18: Four plots showing the output of the BCPA modeling procedure for sailfish 134266. Top left shows the migratory path where a green triangle marks the

PSAT deployment location and a red square the endpoint or PSAT pop-off point. Color of the line represents the autocorrelation parameter. The top right is a phase plot representing relationship between the 3 parameters estimated from the BCPA with the autocorrelation parameter shown in color and size coded circles. The bottom left plot shows the change points where the pink lines represent the time of the changepoint within the trial and the thickness of the line representing the number of days used for the selection of the change point. The black open circles represent the mean of the BCPA analysis with the red lines indicating the standard deviation. Finally, the bottom right set of diagnostic plots includes a QQ-norm plot, histogram and autocorrelation function of the standardized data from the model.

Individual Behavior Analysis: Blue Marlin

Figure 3.19 shows BCPA results for Blue Marlin 134283 revealing an overall tortuous movement pattern resulting in a low autocorrelation ($\hat{\rho}$) parameter estimate as the track meanders around the tagging location in a foraging mode (Figure 3.19 Top Left). Autocorrelation remains low throughout with the exception of one phase of the track where this blue marlin transitions to a zig-zag pattern with slightly less tortuosity and increase autocorrelation in the southwestern portion of the blue marlin track indicating a less tortuous foraging pattern. Outside of this one behavioral shift, a similar level of tortuosity is seen throughout and the BCPA mean remains relatively constant based on the trackline thickness.

This can be quantified by examining the phase plot where variability ($\hat{\sigma}$) occurs in a very small range of values indicating a lack of differing behavior modes (Figure 3.19 Top Right). On this small scale, this blue marlin begins the trial with relative high variability but decreasing for the first highly tortuous foraging mode. Variability increases slightly before decreasing as the blue marlin enters the less tortuous phase and continues to decrease until the end of the trial. Speed ($\hat{\mu}$) increases during the initial

foraging mode before decreasing just prior to the more directed, less tortuous pattern finally showing an increase in the days just prior to trial end.

Blue marlin 134283 was estimated to have 4 behavioral change points on days 44, 58, 63, and 67 with the strongest behavioral changes occurring on days 44 and 58 distinguing the phase of less tortuous, higher autocorrelation from the rest of the track (Figure 3.19 Bottom Left). Weak behavioral change points were found on days 63 and 67 coinciding with the abrupt shift from high autocorrelation to low and a relative sharp decrease in speed just before this time period.

The diagnostic plots show relatively normally distributed residuals and acceplatble ACF in the 3 diagnostic plots (Figure 3.19 Bottom Right).

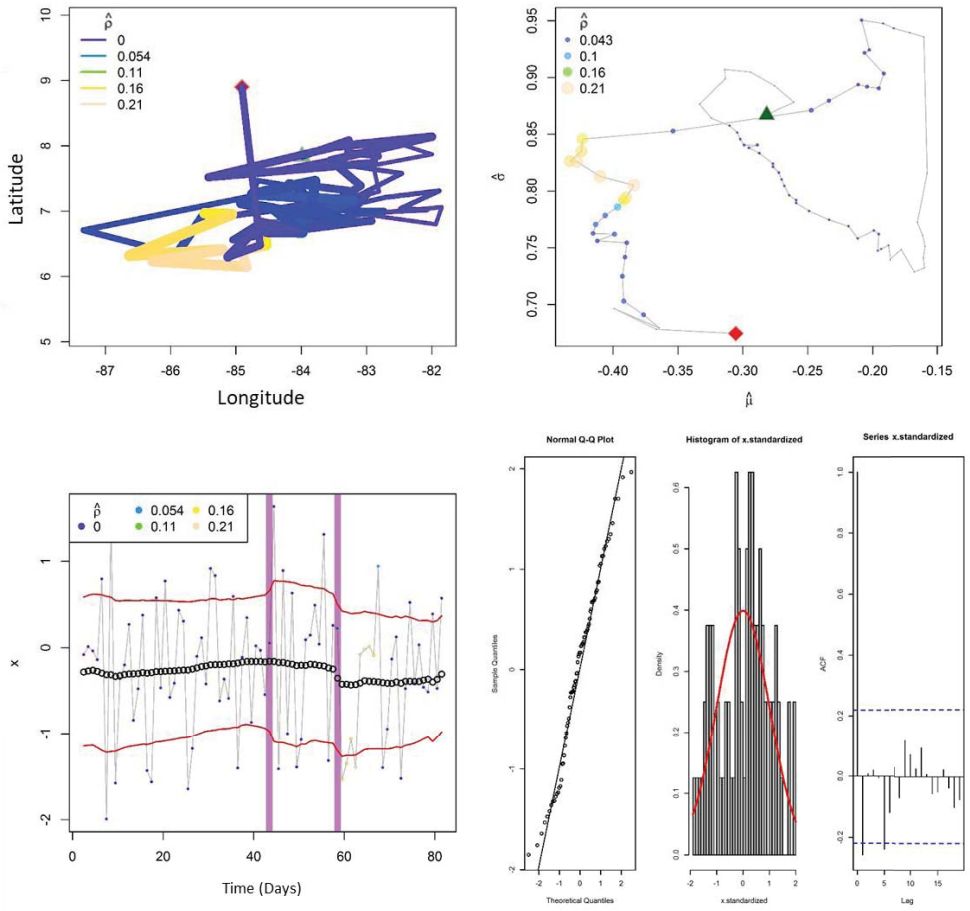

Figure 3.19: Four plots showing the output of the BCPA modeling procedure for blue marlin 134283. Top left shows the migratory path where a green triangle marks the PSAT deployment location and a red square the endpoint or PSAT pop-off point. Color of the line represents the autocorrelation parameter. The top right is a phase plot representing relationship between the 3 parameters estimated from the BCPA with the autocorrelation parameter shown in color and size coded circles. The bottom left plot shows the change points where the pink lines represent the time of the changepoint within the trial and the thickness of the line representing the number of days used for the selection of the change point. The black open circles represent the mean of the BCPA analysis with the red lines indicating the standard deviation. Finally, the bottom right set of diagnostic plots includes a QQ-norm plot, histogram and autocorrelation function of the standardized data from the model.

Figure 3.20 shows BCPA results for Blue Marlin 134277 which was the longest deployed PSAT (200 days) of any included in the analysis in this chapter. Only the first 140 days were included in the analysis for comparisons between blue marlin results. The track plot reveals a highly tortuous movement pattern in the initial portion of the trial followed by a shift to more directed movements while maintain a lesser but moderate level of tortuosity throughout the rest of the trial. This indicated and transition from foraging to a more directed path following the midpoint of the trial. Movement occurs around the tagging location with an overall westward movement from start to end of the trial period. Autocorrelation ($\hat{\rho}$) of the path is relatively low in the initial highly tortuous phase until movement becomes more directed and autocorrelation increases for a short time before decreasing again at the midpoint of the trial. Following the midpoint, autocorrelation increased dramatically until just prior to the trial end when autocorrelation decreases. The widest track thickness, which is proportional to the BCPA mean, is found where autocorrelation is at a minimum indicating mean BCPA values are different when autocorrelation of the track is lowest which is unique to this tagged blue marlin.

From the phase plot it can be found that initially the blue marlin travelled at slow speed ($\hat{\mu}$) and with high variability ($\hat{\sigma}$) at the onset of the trial followed by increasing speed and maintenance of variability over the first highly tortuous segment (Figure 3.20 Top Right). Following this foraging behavior at the onset, speed increases while variability dramatically decreases. After this decrease in variability and increase in speed, the parameter values meander about much the way the blue marlin meandered about the general tagging area without making any long migratory paths in any one direction. This results in parameter values that increase and decrease on short time scales but having an overall moderate speed and low variability. Of the blue marlin analyzed in this study, this blue marlin showed the widest range of variability parameter estimates by a large degree.

Blue marlin 134277 was found to have 13 behavioral change points on days 16, 27, 35, 47, 55, 61, 66, 78, 89, 105, 113, 120, and 129 (Figure 3.20 Bottom Left). All but 4 of the behavioral change points are strong except on days 55, 113, 120, and 129. These strong change points indicate transitions to differing levels of foraging with only one section that could be implied to be a traveling, highly autocorrelated, phase. These weak change points are all associated with outliers but represent slight deviations from typical behavioral activity enough to be considered important.

The diagnostic plots (Figure 3.20 Bottom Right) indicate the assumption of normality of the standardized residuals has been met for Blue Marlin 134277 in all three plots.

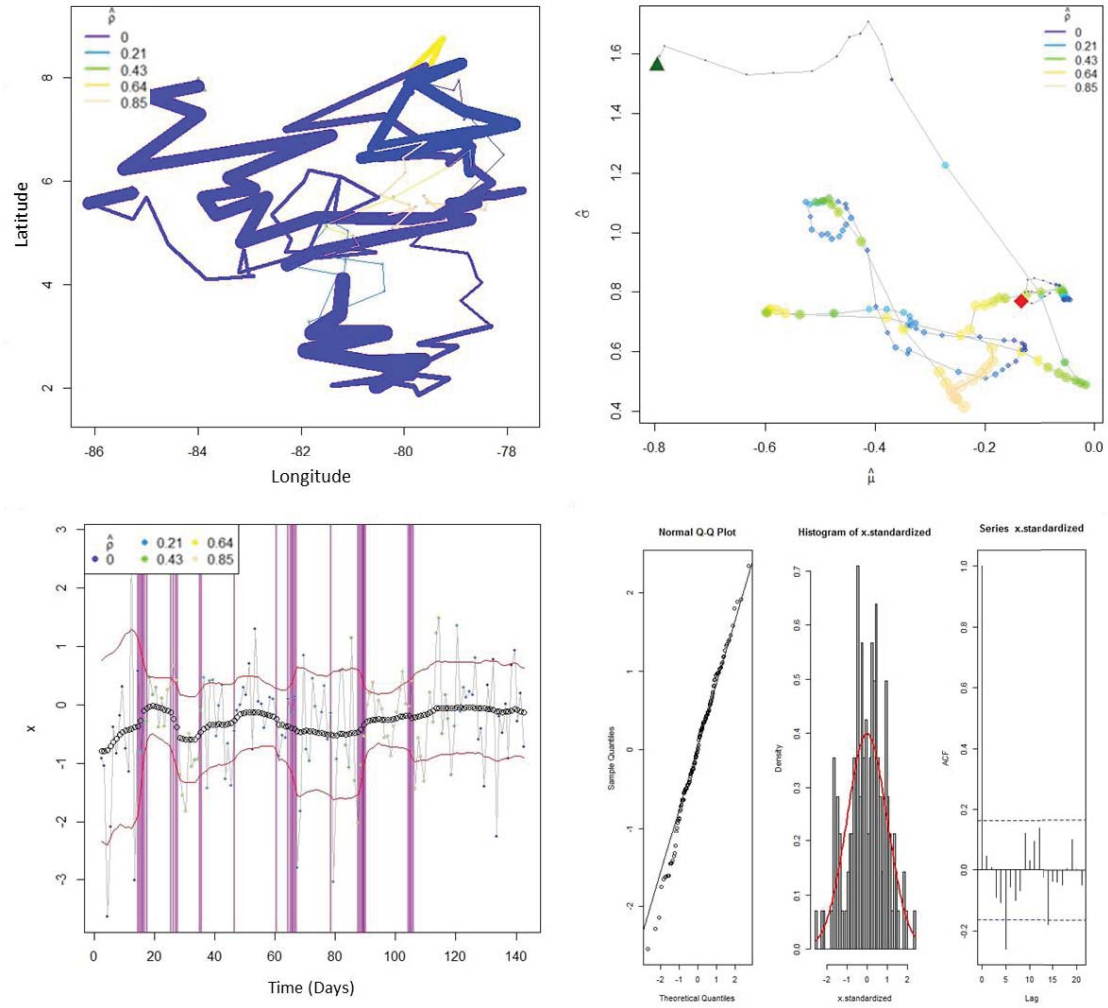

Figure 3.20: Four plots showing the output of the BCPA modeling procedure for blue marlin 134277. Top left shows the migratory path where a green triangle marks the PSAT deployment location and a red square the endpoint or PSAT pop-off point. Color of the line represents the autocorrelation parameter. The top right is a phase plot representing relationship between the 3 parameters estimated from the BCPA with the autocorrelation parameter shown in color and size coded circles. The bottom left plot shows the change points where the pink lines represent the time of the changepoint within the trial and the thickness of the line representing the number of days used for the selection of the change point. The black open circles represent the mean of the BCPA analysis with the red lines indicating the standard deviation. Finally, the bottom right set of diagnostic plots includes a QQ-norm plot, histogram and autocorrelation function of the standardized data from the model.

Figure 3.21 shows BCPA results for Blue Marlin 134254 which undertook a migratory path beginning with direct movements north, then south, then west with very low levels of autocorrelated ($\hat{\rho}$) movement during the first phase of the trial period but

also with low levels of tortuosity (Figure 3.21 Top Left). As the fish turns to the north at the midpoint of the trial, autocorrelation begins to increase and the blue marlin transitions to a period of highly autocorrelated, very low tortuosity, traveling behavior in a large looping motion. A major shift in behavior is present and although this looping behavior appears to be artifact, it was confirmed to be true migratory behavior of this particular blue marlin. Trackline thickness indicated a proportional difference in the first- and last-time step of the trial, shown by thicker blue lines during these time steps. This blue marlin track has unique migratory path features not witnessed in any of the other blue marlin or sailfish tagged with PSATs for this study. The long looping, highly autocorrelated path suggests highly directed movement with little deviation from the line which is highly uncommon as witnessed here in this chapter.

From the phase plot it can be found that initially the blue marlin travelled at slow speed ($\hat{\mu}$) immediately after PSAT deployment and with high variability ($\hat{\sigma}$) (Figure 3.21 Top Right). In the days following deployment speed increases proportionally to a decrease in variability until the end of the initial southward movement when variability shows a small spike then slight decrease until the transition to traveling phase when variability maintains a minimum value and speed very slightly increases until the endpoint of the trial.

Blue marlin 134254 was found to have 5 behavioral change points on days 7, 17, 24, 33, and 56 (Figure 3.21 Bottom Left). Only 2 of the 5 change points are considered strong and these occur on days 17 and 24 indicating the transition from lower autocorrelation to traveling phase. The change point on day 24 appears in the plot to contain multiple change points but, as mentioned previously, a cluster width of 3 days

was implemented thus can be considered one change point over a 3-day period. The weak change point on day 7 can be attributed to a large deviation in the model on the day prior and days 33 and 56 represent the endpoints of the time period of highest autocorrelation during the looping activity.

The diagnostic plots (Figure 3.21 Bottom Right) do not indicate the assumption of normality of the standardized residuals has been broken.

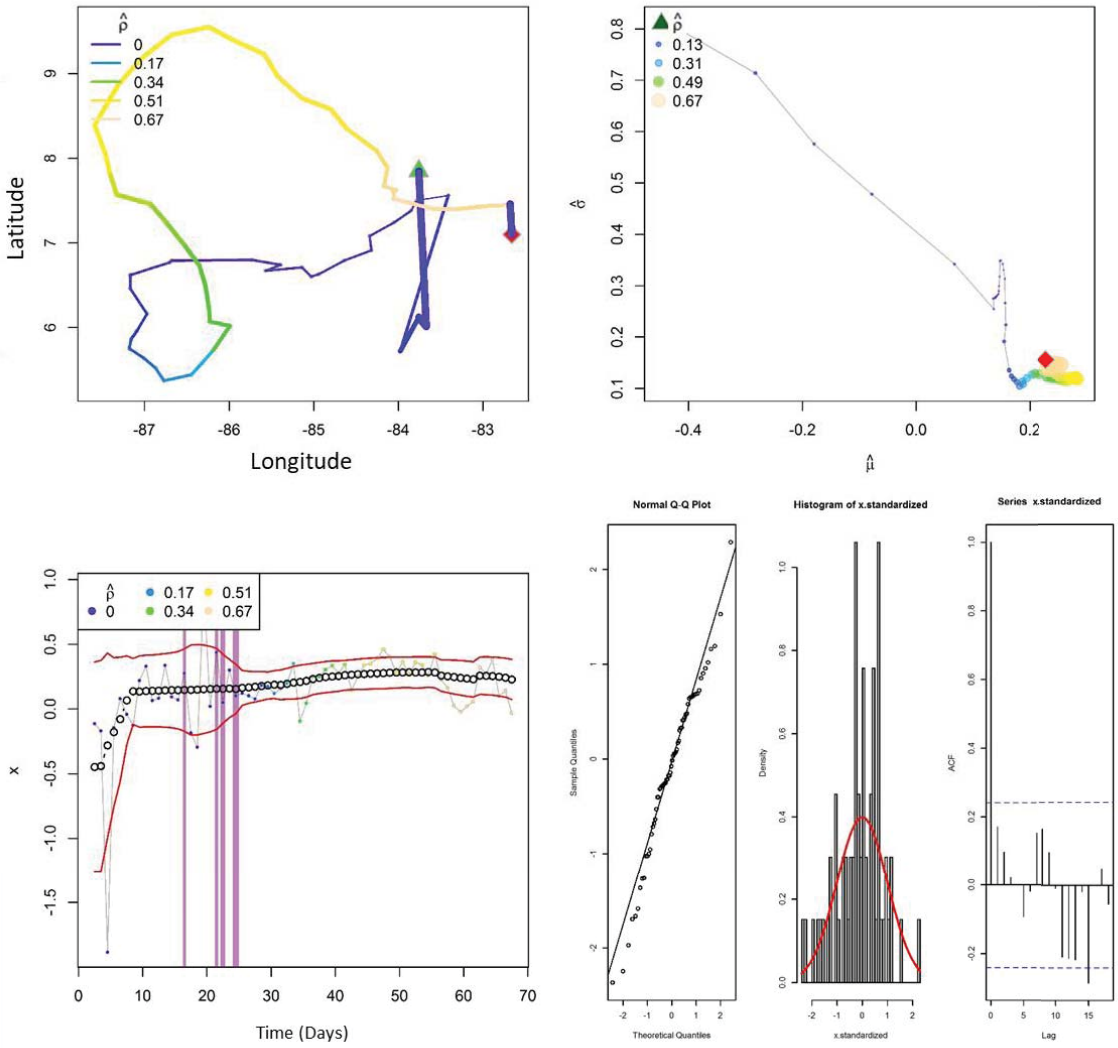

Figure 3.21: Four plots showing the output of the BCPA modeling procedure for blue marlin 134254. Top left shows the migratory path where a green triangle marks the PSAT deployment location and a red square the endpoint or PSAT pop-off point. Color of the line represents the autocorrelation parameter. The top right

is a phase plot representing relationship between the 3 parameters estimated from the BCPA with the autocorrelation parameter shown in color and size coded circles. The bottom left plot shows the change points where the pink lines represent the time of the changepoint within the trial and the thickness of the line representing the number of days used for the selection of the change point. The black open circles represent the mean of the BCPA analysis with the red lines indicating the standard deviation. Finally, the bottom right set of diagnostic plots includes a QQ-norm plot, histogram and autocorrelation function of the standardized data from the model.

Figure 3.22 shows BCPA results for Blue Marlin 134251 which undertook a highly directed path with very little tortuosity overall which represents the majority of blue marlin behavior. Initially the blue marlin travels with low levels of autocorrelation ($\hat{\rho}$) typical of foraging as it meanders about the tagging location before traveling westward where it transitions to a clear traveling phase toward the north and northwest (Figure 3.22 Top Left). Following the traveling phase, the blue marlin transitions back to a less autocorrelated, more tortuous behavior just prior to trial end. Overall this blue marlin had a net northwestward migratory path. Trackline thickness indicates no proportionally strong changes in the mean BCPA occur during the trial period. Much like the previous blue marlin analyzed the lack of tortuosity is somewhat unique but instead of looping, this blue marlin appears to move in more direct paths.

From the phase plot it can be found that initially the blue marlin travelled at moderate speed ($\hat{\mu}$) immediately after PSAT deployment and with high variability ($\hat{\sigma}$) during the initial foraging phase (Figure 3.22 Top Right). As the blue marlin transitions to the traveling phase, speed increases while variability decreases until the transition back to foraging when speed begins to decrease substantially while variability only slightly increases until the end of the PSAT deployment period.

Blue marlin 134251 was found to have 3 behavioral change points on days 16, 19, and 35, all of which were estimated as strong behavioral shifts (Figure 3.22 Bottom Left). These represent the clear delineation between foraging at the start, transitioning to travel and finally back to foraging.

The diagnostic plots (Figure 3.22 Bottom Right) indicate a slight skew shown by the QQ-Norm plot and the histogram where the left tail shows slight deviation from the normal distribution. The autocorrelation function appears acceptable.

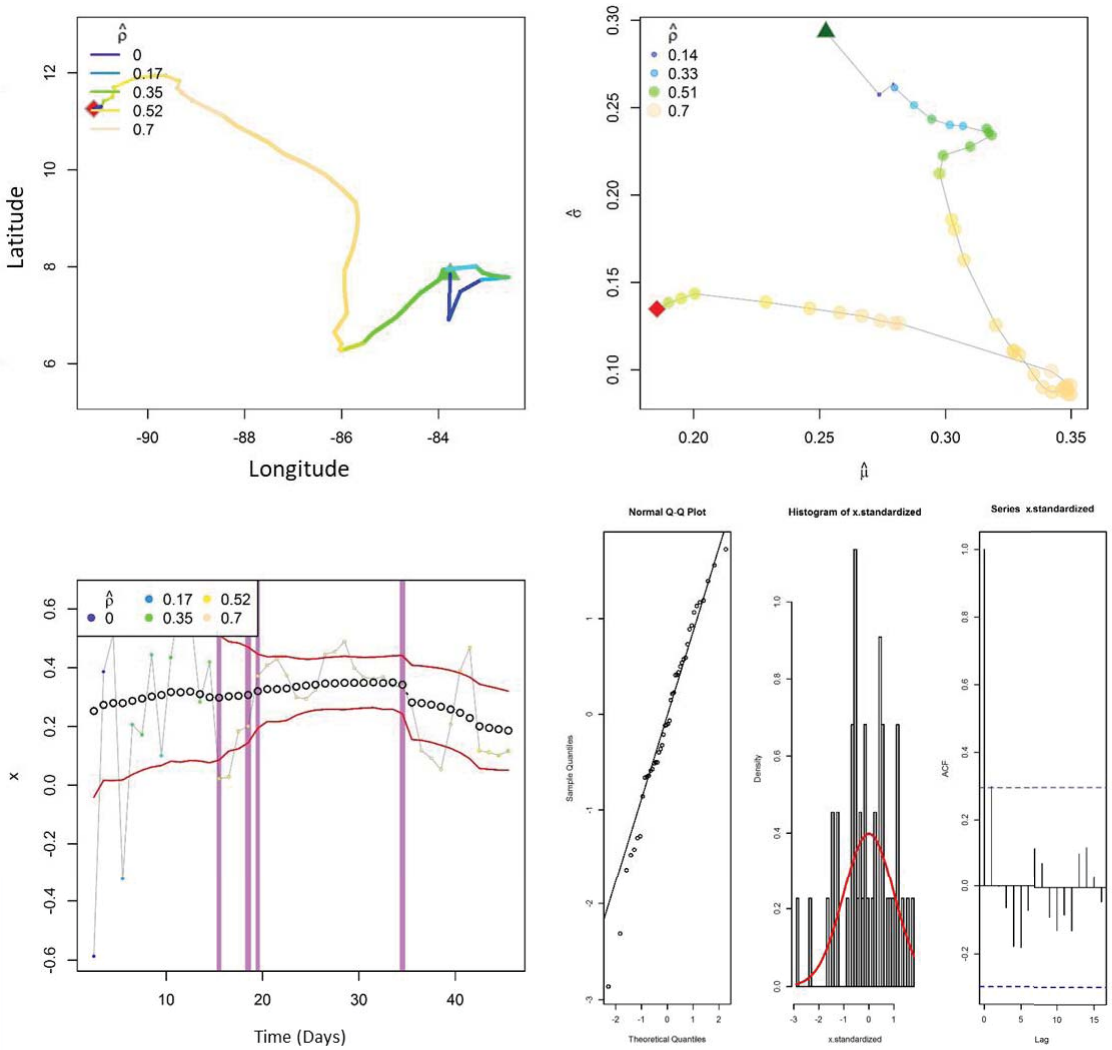

Figure 3.22: Four plots showing the output of the BCPA modeling procedure for blue marlin 134251. Top left shows the migratory path where a green triangle

marks the PSAT deployment location and a red square the endpoint or PSAT pop-off point. Color of the line represents the autocorrelation parameter. The top right is a phase plot representing relationship between the 3 parameters estimated from the BCPA with the autocorrelation parameter shown in color and size coded circles. The bottom left plot shows the change points where the pink lines represent the time of the changepoint within the trial and the thickness of the line representing the number of days used for the selection of the change point. The black open circles represent the mean of the BCPA analysis with the red lines indicating the standard deviation. Finally, the bottom right set of diagnostic plots includes a QQ-norm plot, histogram and autocorrelation function of the standardized data from the model.

Figure 3.23 shows BCPA results for Blue Marlin 134248 which maintained relatively high autocorrelation ($\hat{\rho}$) throughout its migratory path (Figure 3.23 Top Left). This blue marlin makes a clockwise loop immediately after PSAT deployment where autocorrelation is moderate and tortuosity is slightly increased compared to the remainder of the trial. Following this loop, the blue marlin and travels east with increasing directness and low tortuosity before turning west and looping to the north with high autocorrelation and low tortuosity for the remainder of the PSAT deployment trial. This westward movement in the second half of the trial represents the period of highest autocorrelation where almost no tortuosity occurs. Trackline thisckness indicated a lack of proportional difference in the mean BCPA.

From the phase plot it can be found that initially the blue marlin travelled at slow speed ($\hat{\mu}$) immediately after PSAT deployment and with low variability ($\hat{\sigma}$) (Figure 3.23 Top Right). In the first clockwise loop, speed decreases slightly but increases continuously after the sailfish transitions to a clear traveling phase until the endpoint. Variability, although starting at the lowest point, continuously increases throughout the trial until just prior to PSAT tag release from the fish.

Blue marlin 134248 was found to have only 1 weak behavioral change point on day 22 which coincides with a time period just before a large outlier in the BCPA model

(Figure 3.23 Bottom Left). Overall, this blue marlin does not indicate any major behavioral regimes with relative small scales for all parameter estimates indicating a lack of differing behavioral patterns in the data.

The diagnostic plots (Figure 3.21 Bottom Right) indicate a deviation from normal at both the tails and slightly in the center of the distribution but not outside the bounds of acceptance for the purpose of this analysis, especially considering no strong change points were estimated. The ACF does not appear to contain the exponential decline we expect thus we can infer this blue marlin track was not an ideal fit for the BCPA due to an overall lack of behavioral variability.

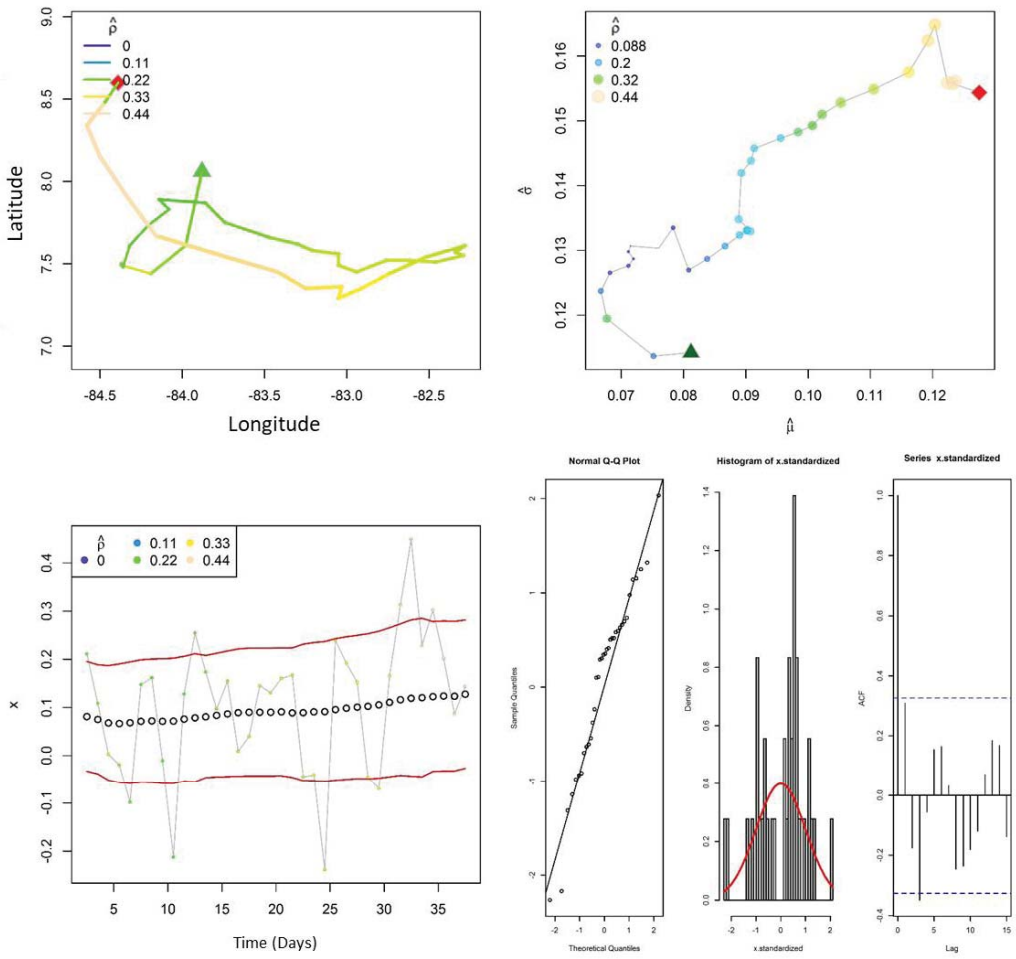

Figure 3.2312: Four plots showing the output of the BCPA modeling procedure for blue marlin 134248. Top left shows the migratory path where a green triangle marks the PSAT deployment location and a red square the endpoint or PSAT pop-off point. Color of the line represents the autocorrelation parameter. The top right is a phase plot representing relationship between the 3 parameters estimated from the BCPA with the autocorrelation parameter shown in color and size coded circles. The bottom left plot shows the change points where the pink lines represent the time of the changepoint within the trial and the thickness of the line representing the number of days used for the selection of the change point. The black open circles represent the mean of the BCPA analysis with the red lines indicating the standard deviation. Finally, the bottom right set of diagnostic plots includes a QQ-norm plot, histogram and autocorrelation function of the standardized data from the model.

Figure 3.24 shows BCPA results for Blue Marlin 134244 which migrated in a net southward direction overall and with moderate tortuosity and very low autocorrelation ($\hat{\rho}$) through the first southward and westward movement of the trial before turning to the southeast when autocorrelation began to increase during a less tortuous traveling mode (Figure 3.24 Top Left). The blue marlin traveled southeast until just before trial end before looping back toward the north and northwest. During this northwesterly movement, the highest autocorrelation values were witnessed indicating a transition to a more traveling mode as the track progressed to the south and southeast. Trackline thickness does not indicate proportional difference in the mean BCPA.

The phase plot reveals initially the blue marlin was traveling at a slow speed ($\hat{\mu}$) and with relatively high variability ($\hat{\sigma}$) although it is important to note the small range of variability values (Figure 3.24 Top Right). As the trial progresses, speed increases overall while variability decreases until the endpoint of the trial.

Blue marlin 134241 was found to have only 1 weak behavioral change point on day 26 which coincides with a very slight bump in the mean BCPA as well as a previous outlier on day 22 (Figure 3.24 Bottom Left). Overall, this blue marlin does not indicate

any major behavioral regimes with relative small scales for all parameter estimates indicating a lack of differing behavioral patterns in the data. The diagnostic plots (Figure 3.24 Bottom Right) indicate only a slight deviation from normal at the tails of the QQ-Norm plot and a slight skew to the histogram bell curve but nothing to suggest the assumptions have not been met.

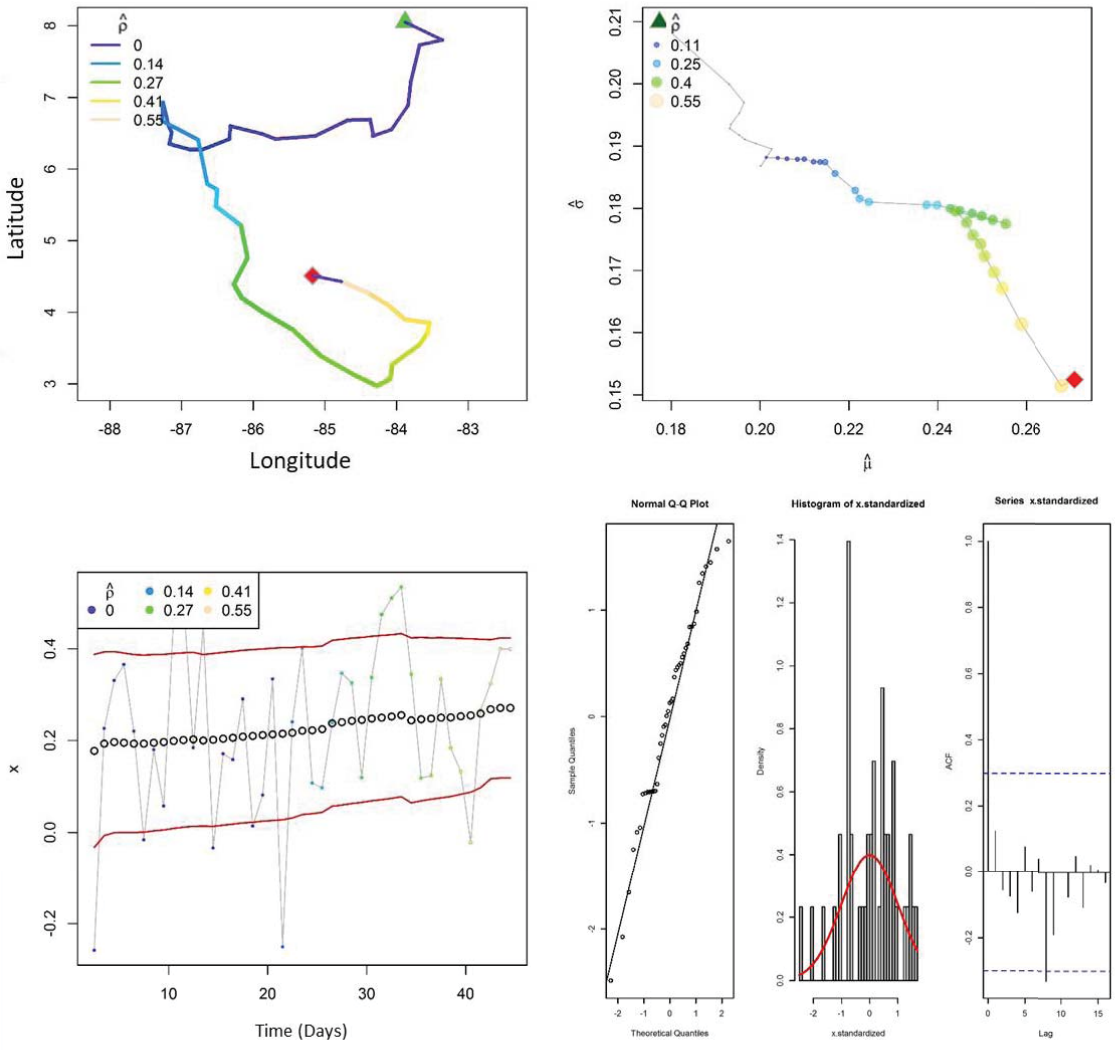

Figure 3.24: Four plots showing the output of the BCPA modeling procedure for blue marlin 134244. Top left shows the migratory path where a green triangle marks the PSAT deployment location and a red square the endpoint or PSAT pop-off point. Color of the line represents the autocorrelation parameter. The top right is a phase plot representing relationship between the 3 parameters estimated from

the BCPA with the autocorrelation parameter shown in color and size coded circles. The bottom left plot shows the change points where the pink lines represent the time of the changepoint within the trial and the thickness of the line representing the number of days used for the selection of the change point. The black open circles represent the mean of the BCPA analysis with the red lines indicating the standard deviation. Finally, the bottom right set of diagnostic plots includes a QQ-norm plot, histogram and autocorrelation function of the standardized data from the model.

Figure 3.25 shows BCPA results for Blue Marlin 134240 which undertook a moderately tortuous and moderately autocorrelated ($\hat{\rho}$) path immediately after PSAT deployment (Figure 3.25 Top Left). Following this initial travceling type behavior, autocorrelation decreases until the midpoint of the trial and tortuosity remains at a moderate level indicating a potential foraging phase as the blue marlin travels southward. As the blue marlin turns to the north, autocorrelation increaseswhile tortuosity remains at a moderate level until the blue marlin transitions to more directed path and turning east with the highest autocorrelation witnessed prior to the end of the trial period. Trackline thickness indicates no proportionally strong changes in the mean BCPA occur during the trial period.

From the phase plot it can be found that initially the blue marlin travelled at moderate speed ($\hat{\mu}$) immediately after PSAT deployment and with high variability ($\hat{\sigma}$) (Figure 3.25 Top Right). In the days following deployment speed decreases through the initial traveling type phase when it begins to increase as the fish heads south and transitions to foraging. Speed decreases as the blue marlin turns to the north then begins to steadily increase until the end of the trial during the final traveling phase. Variability decreases steadily until it abruptly increases coinciding with the period of highest autocorrelation during the late traveling phase. Overall, the range value for both speed and variability are comparatively low for this blue marlin.

Blue marlin 134240 was found to have 5 behavioral change points on days 15, 30, 36, 48, and 51 (Figure 3.25 Bottom Left). Of the 5 change points estimated, 3 are strong changes that indicate the transition from traveling to foraging and back to traveling while 2 can be considered weak change points on days 48 and 51 and these are most likely associated with the period of high autocorrelation and increase number of outliers from days 48 to the end of the trial.

Diagnostic plots (Figure 3.25 Bottom Right) indicate a slight skew shown by the QQ-Norm plot and the histogram where the left tail shows deviation from the normal distribution. The autocorrelation function appears acceptable.

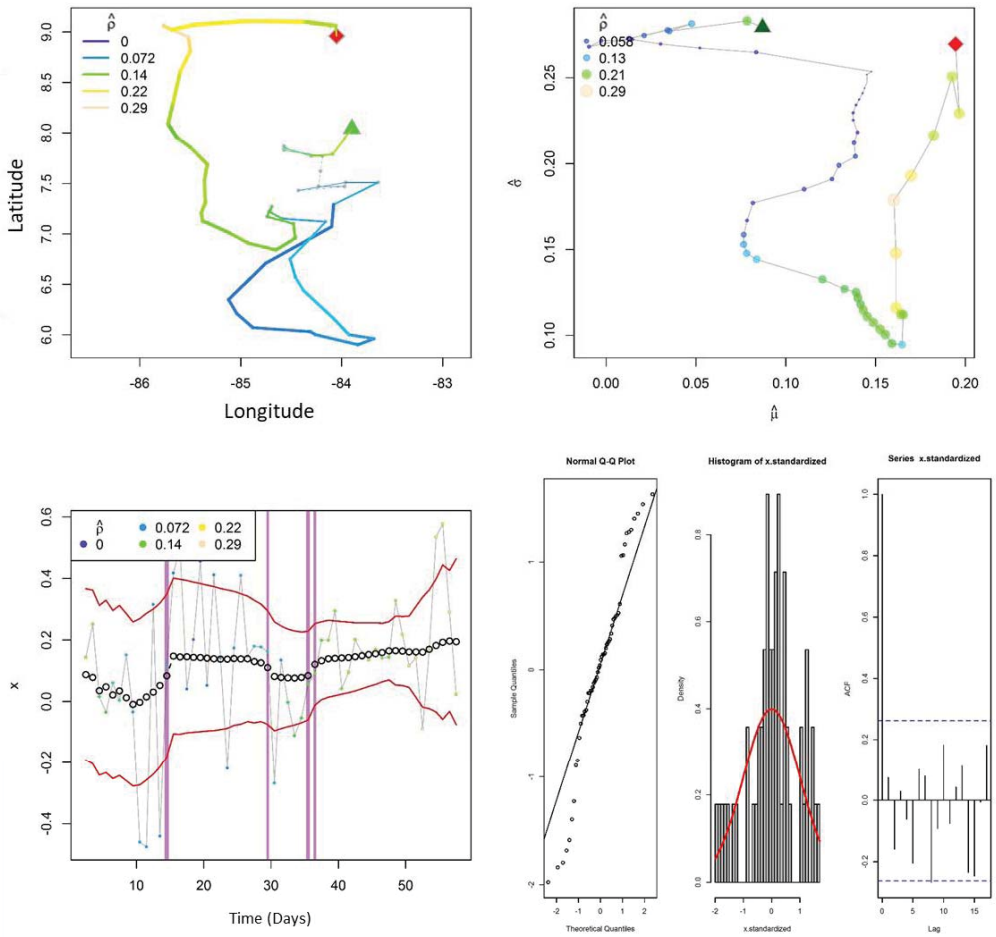

Figure 3.25: Four plots showing the output of the BCPA modeling procedure for blue marlin 134240. Top left shows the migratory path where a green triangle marks the PSAT deployment location and a red square the endpoint or PSAT pop-off point. Color of the line represents the autocorrelation parameter. The top right is a phase plot representing relationship between the 3 parameters estimated from the BCPA with the autocorrelation parameter shown in color and size coded circles. The bottom left plot shows the change points where the pink lines represent the time of the changepoint within the trial and the thickness of the line representing the number of days used for the selection of the change point. The black open circles represent the mean of the BCPA analysis with the red lines indicating the standard deviation. Finally, the bottom right set of diagnostic plots includes a QQ-norm plot, histogram and autocorrelation function of the standardized data from the model.

Figure 3.26 shows BCPA results for Blue Marlin 134255 which undertook a highly autocorrelated ($\hat{\rho}$) path throughout the trial period resulting in a net southward migration with a general lack of tortuosity (Figure 3.26 Top Left). The blue marlin can be considered to be in traveling mode throughout the track with only a slight decrease in autocorrelation during a phase at the midpoint that would still qualify as traveling as opposed to foraging. The highly autocorrelated, directed path continues after this midpoint lesser autcorrelated traveling phase until the endpoint of the trial.

From the phase plot it can be found that initially the blue marlin travelled at low speed ($\hat{\mu}$) immediately after PSAT deployment and with relatively high variability ($\hat{\sigma}$) (Figure 3.26 Top Right). In the days following deployment speed increases until the midpoint traveling phase begins when speed begins to decrease until the end of this midpoint traveling phase before increasing again until the end of the deployment period. Variability range is low but consistently decreases from the start until the midpoint phase when it levels out and only increases slightly from the end of the midpoint phase until the endpoint.

Blue marlin 134255 was found to have 2 behavioral change points on days 22 and 28, both of which represent weak behavioral change points (Figure 3.26 Bottom Left). Although not visible as a bar because of the weak status, the difference in mean BCPA from days 22 to 28 is visible and may be skewed by four outlying points during that time period.

Diagnostic plots (Figure 3.26 Bottom Right) indicate a fairly significant skew in both the QQ-Norm plot and the histogram of standardized residuals. The autocorrelation function appears appropriate and acceptable.

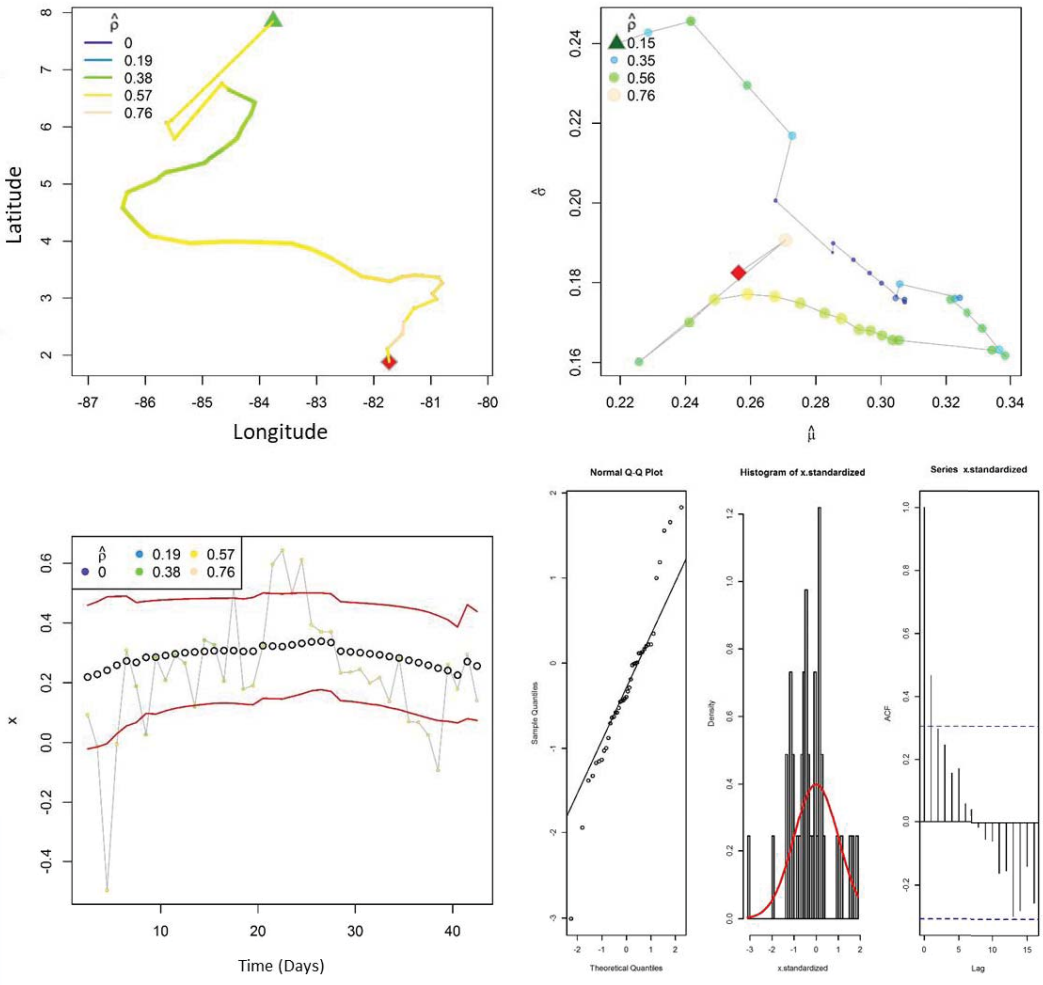

Figure 3.26: Four plots showing the output of the BCPA modeling procedure for blue marlin 134255. Top left shows the migratory path where a green triangle

marks the PSAT deployment location and a red square the endpoint or PSAT pop-off point. Color of the line represents the autocorrelation parameter. The top right is a phase plot representing relationship between the 3 parameters estimated from the BCPA with the autocorrelation parameter shown in color and size coded circles. The bottom left plot shows the change points where the pink lines represent the time of the changepoint within the trial and the thickness of the line representing the number of days used for the selection of the change point. The black open circles represent the mean of the BCPA analysis with the red lines indicating the standard deviation. Finally, the bottom right set of diagnostic plots includes a QQ-norm plot, histogram and autocorrelation function of the standardized data from the model.

Distribution of Change Points

The spatial distribution of behavioral change points in both sailfish and blue marlin provide little information as to the factors leading to behavioral changes (Figure 3.27). Although these changes are well identified to be true behavioral shifts, their distribution lacks clustering that would indicate shifts occurring due to spatial differences. The only indication of regional clustering could be interpreted from blue marlin change points occurring along the Coco's Ridge seamount area off Costa Rica, but this is likely a product of increased presence of PSAT tagged blue marlin in this region during the deployment periods of the study.

Comparison of BCPA Parameters Among Species

Sailfish

An examination of parameter changes over time between individual sailfish provides information on behavioral traits shared among the species (Figure 3.28). First, examining speed ($\hat{\mu}$ or mu.hat), sailfish 134252, 134258, 134263, and 134285 were unique where other sailfish maintained similar velocity related behavior. Interestingly, of these four sailfish, three were the longest deployment periods and the fourth was above average duration, indicating PSAT deployment duration is a critical factor in parameter estimation. In the examination of variability ($\hat{\sigma}$ or s.hat) these same four sailfish exhibit a

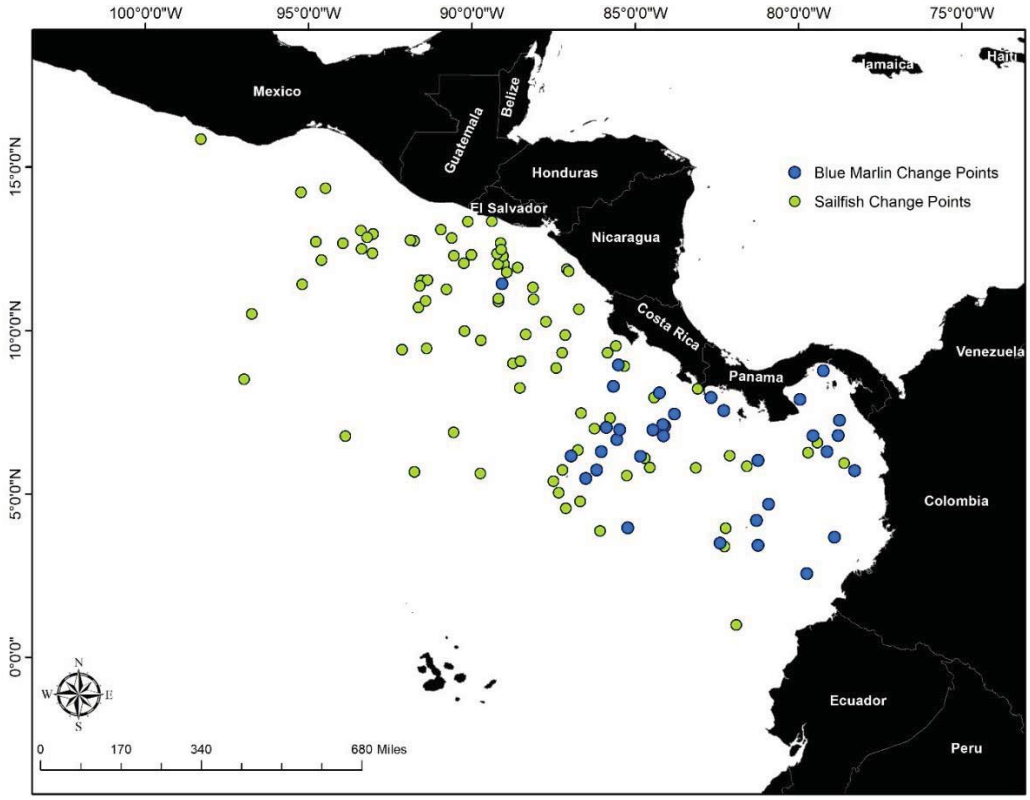

Figure 3.27: Map showing behavioral change point location for both sailfish (Green Circles) and blue marlin (Blue Circles).

wider range of values along with 134266 and 134241. The most important parameter for biological analysis moving forward is the movement inertia or autocorrelation ($\hat{\rho}$ or rho.hat) which does not indicate deployment duration to be a contributing factor. Although not all sailfish undergo this trend, a majority of PSAT tagged sailfish begin with relative low autocorrelation paths followed by immediate increases in the autocorrelation parameter from the onset of the deployment until days 25-40 and another peak from days 45 to 75. This is a biologically relevant contribution of the BCPA model in that the movement inertia parameter may indicate sailfish have similar migratory patterns relative to post-release behavior and the more autocorrelated persistent movement away from the tagging location.

The lack of estimated change points for 6 of the sailfish indicate their behavioral parameters did not change significantly enough to registers as a shift in the BCPA model. This is ecologically relevant as these fish did not indicate differential behavior over the course of their entire migration maintaining speed, track variability and momentum.

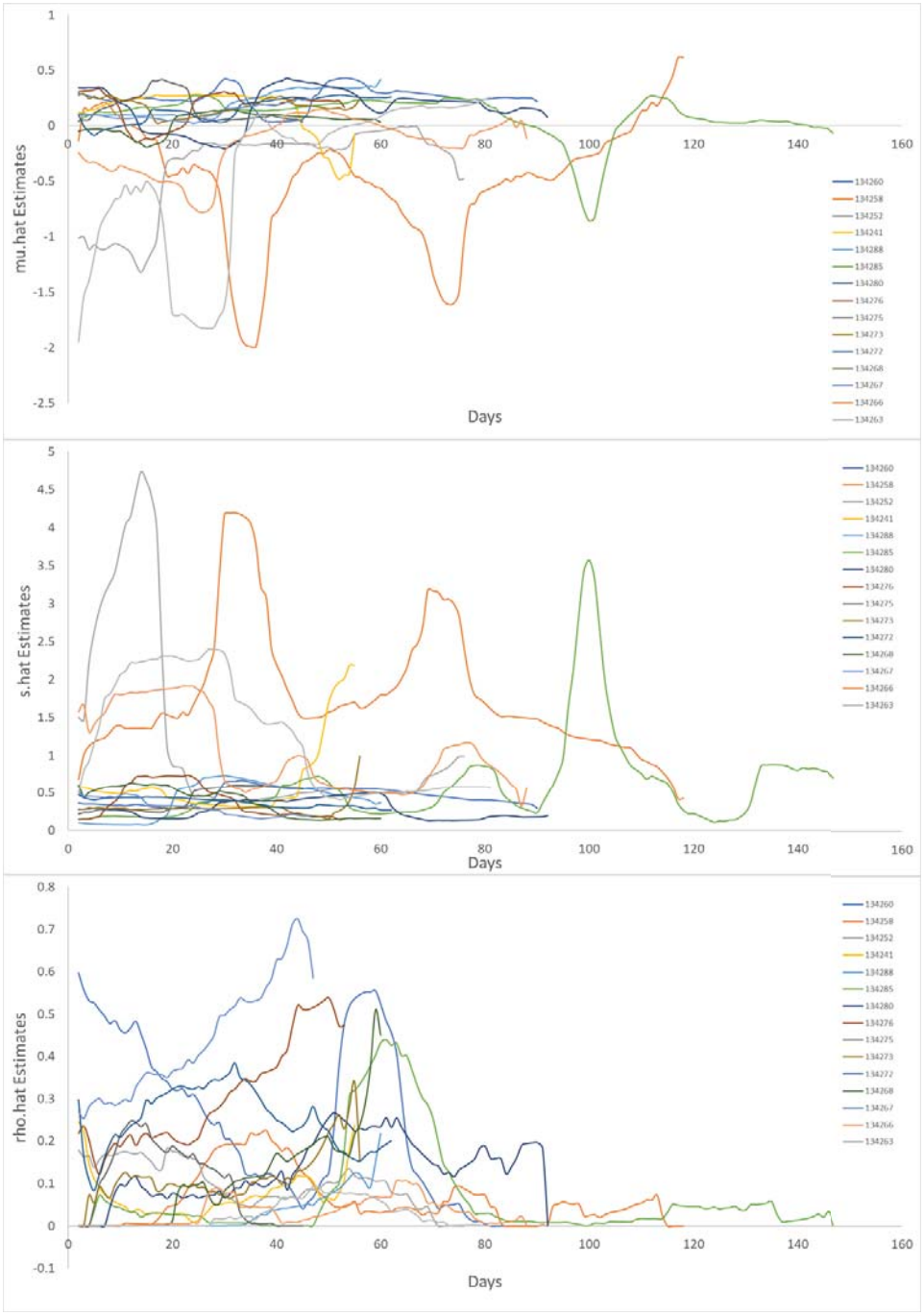

Figure 3.28: Plots showing parameter estimated for all modeled sailfish. Top: Plot of mu.hat equivalent to speed; Middle: Plot of s.hat equivalent to variability of movement; Bottom: Plot of rho.hat equivalent to "movement inertia" or autocorrelation.

Blue Marlin

An examination of parameter changes over time between individual blue marlin provides information on behavioral traits shared among the species (Figure 3.29). First, examining speed ($\hat{\mu}$ or mu.hat), two blue marlin had substantially different behavioral patterns and lower speed compared to other PSAT tagged blue marlin and, similar to sailfish, these different patterns are attributed to the longest PSAT durations. Blue Marlin 134277 and 134283 are also differently behaved in terms of the variability parameter ($\hat{\sigma}$ or s.hat) where migrations in these two were estimated to be much more variable throughout. Although these two are outliers in the sample of blue marlin, the consistency of the others is somewhat striking in both speed and variability. This implies a majority of blue marlin follow similar trends in behavior post-release. The similar deployment durations allow for comparisons among the consistent blue marlin and indicate this behavior to be typical of PSAT tagged blue marlin. The movement inertia or autocorrelation ($\hat{\rho}$ or rho.hat) parameter again does not distinguish behavioral difference between those two outlying blue marlin as seen in the other comparisons. An important feature among all blue marlin is the overall increasing autocorrelation over the initial 25 to 40 days of the trial period with some blue marlin exhibiting a decreased and others continuously increasing their autocorrelation path.

Figure 3.29: Plots showing parameter estimated for all modeled blue marlin. Top: Plot of mu.hat equivalent to speed; Middle: Plot of s.hat equivalent to variability of movement; Bottom: Plot of rho.hat equivalent to "movement inertia" or autocorrelation.

Using BCPA and acceleration to explore post-release behavior

Combining the information from acceleration studies and depth results discussed in Chapter 2 of this Dissertation with the results of the BCPA explores the relationship between time post-release and changes in behavioral characteristics.

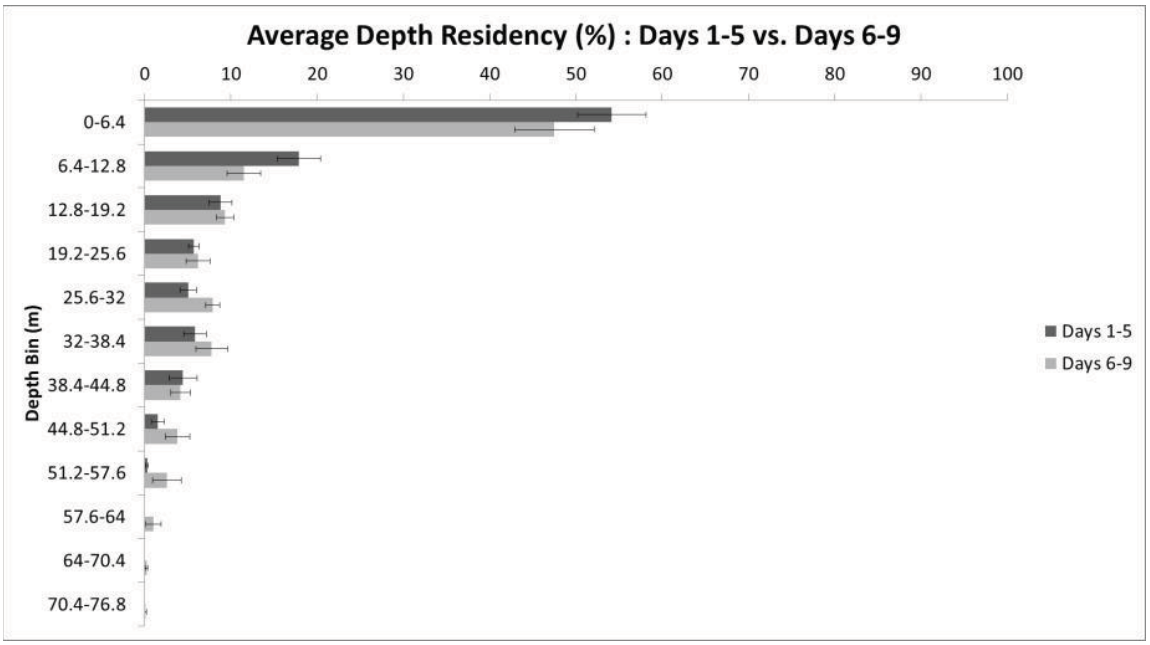

Figure 3.30: Plot of sailfish depth residency for 7 tagged sailfish off the Guatemalan coast during April 2012.

Depth residency obtained for sailfish indicated increased diving behavior following the 5th day post-release up to the 9th day with tag release on the 10th day of this short-term study (Figure 3.30). Acceleration values for the same PSAT tagged sailfish corroborate depth findings and show a declining trend in overall activity from day 1 to day 5 followed by an increase in activity until day 8 when activity levels begin to decline again until day 10 (Figure 3.31). In the immediate short-term post-release, there is a clear behavioral shift in activity and diving behavior; however, the need to examine behavioral

trends after the 10 day trial is necessary. To accomplish this, the inclusion of the first behavioral change point for each sailfish is considered. An average of 14.8 days with a range from 7 days to 24 days to the first behavioral change point was found with a standard deviation of ±4.4 days (Figure 3.32). This implies a slightly longer recovery period before the first behavioral change when compared with the short-term study. Overall, the PSAT tagged sailfish exhibited a post-release recovery period of at least 5 days.

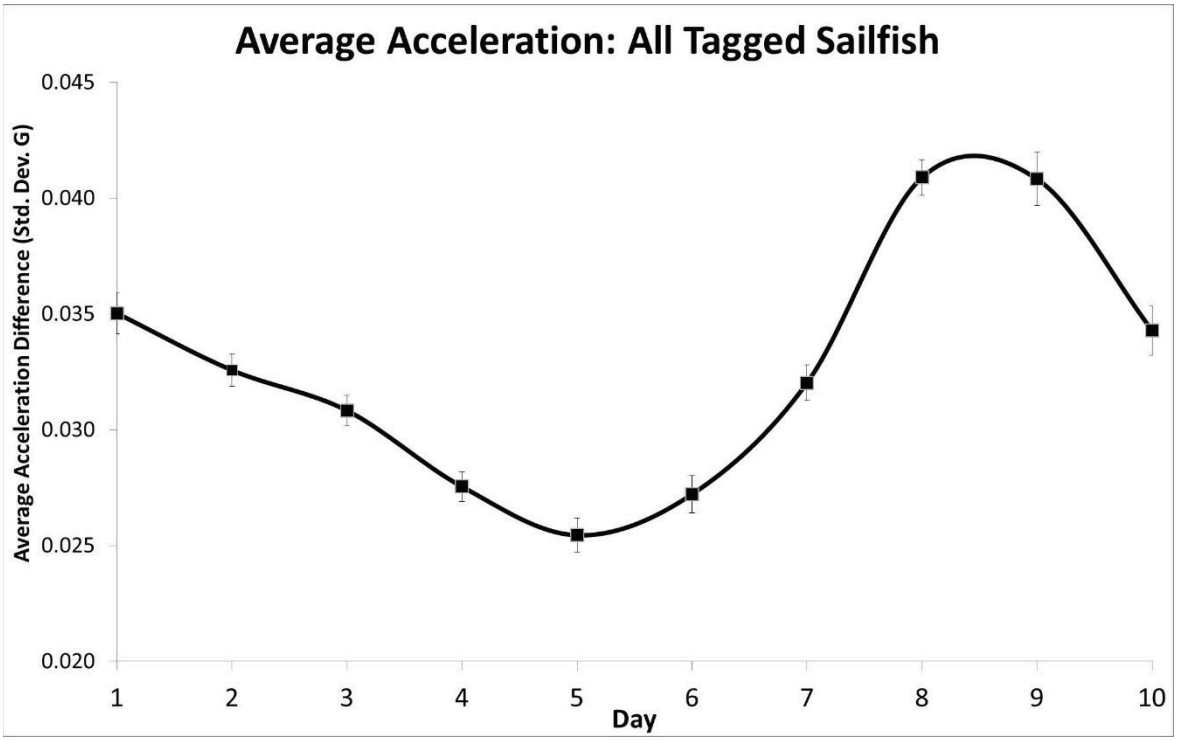

Figure 3.31: Plot of average acceleration activity for 7 PSAT tagged sailfish of the Guatemalan coast during April 2012.

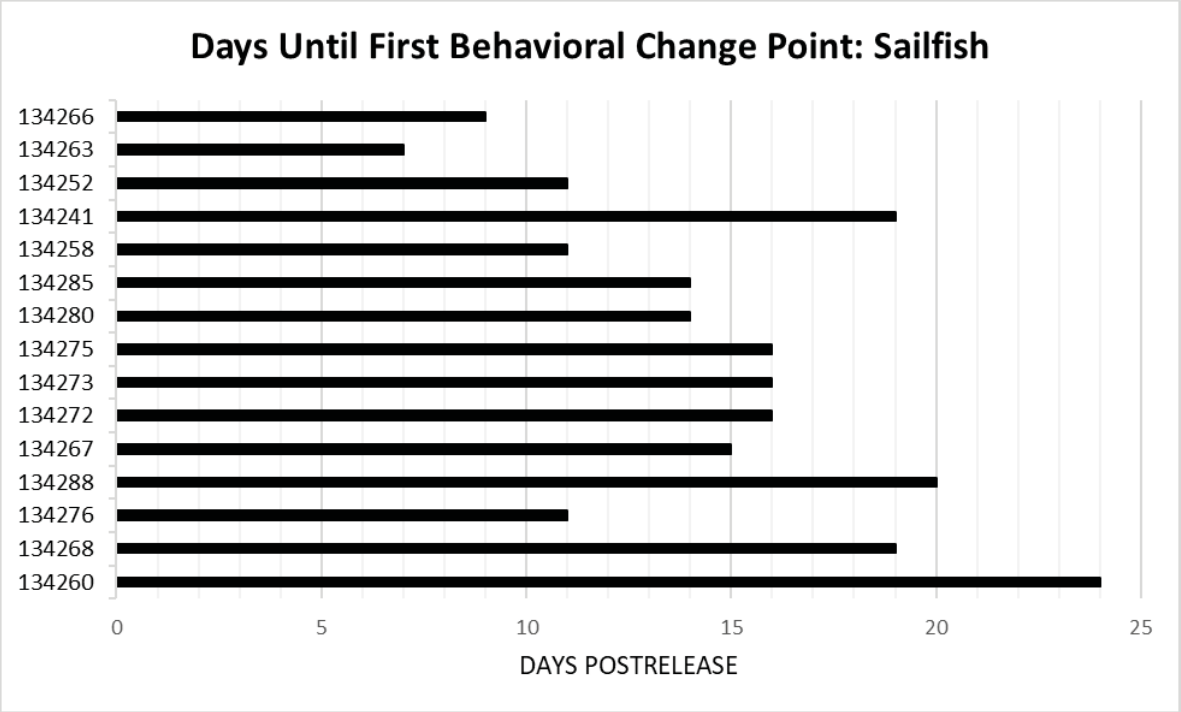

Figure 3.32 Plot of all tagged sailfish and their resulting BCPA results showing the number of days before the first behavioral change point occurred. This indicates a behavioral shift hypothesized as the postrelease recovery period before the sailfish returns to typical behavior.

Although no activity or depth data is available for blue marlin to examine post-release recovery, the BCPA estimated an average time to first change point at 20.6 days with a range of 7-44 days and a standard deviation of ±10.2 (Figure 3.33). This implies blue marlin require more time after catch and release to exhibit a significant behavioral shift.

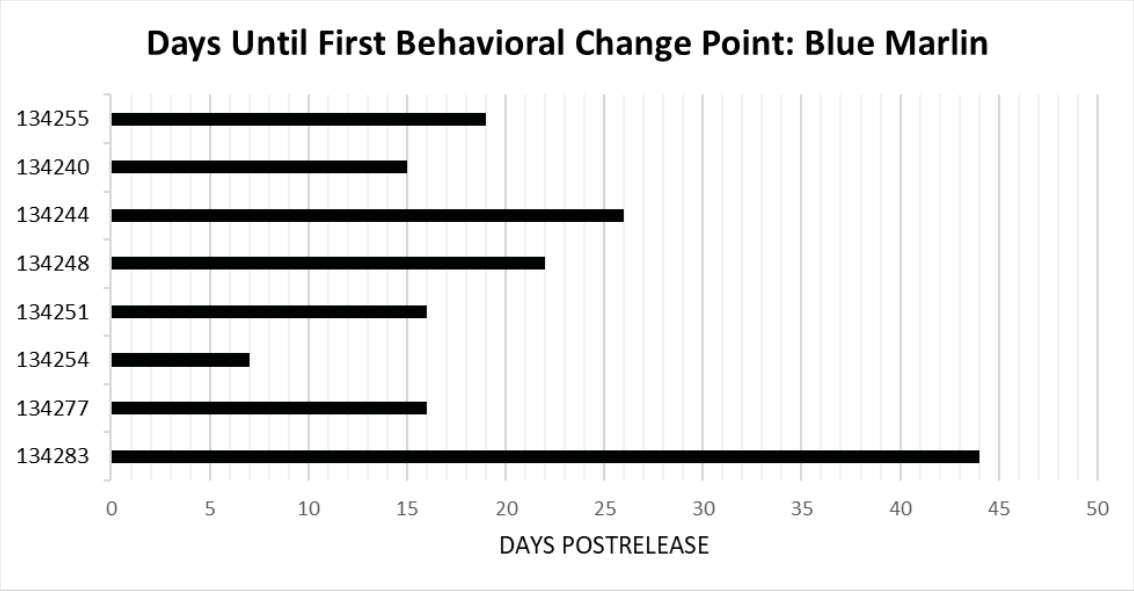

Figure 3.33 Plot of all tagged sailfish and their resulting BCPA results showing the number of days before the first behavioral change point occurred. This indicates a behavioral shift hypothesized as the postrelease recovery period before the sailfish returns to typical behavior.

Discussion

Satellite Tagging Program Implementation

The use of PSATs represents the only means of assessing behavior and habitat use of billfish species such as sailfish and blue marlin that live in the pelagic environment. The combination of behavioral modeling, depth analysis, and the inclusion of an accelerometry activity study provide a unique and innovative look into the daily lives of these billfish species.

To ensure PSAT deployments were successful, many steps were taken to improve traditional methods of tag attachment and retention. The use of Desert Star SeaTags was the initial technological decision as the MOD tag allowed the use of accelerometry while

the GEO is significantly smaller and lighter than standard PSATs available. This choice came with two compromises, the first being, the MOD tag is very large compared to other PSAT designs and much too large for long term deployments on sailfish thus could only be implemented for 10-15 day trial periods. The second compromise was the lack of depth data recording on the GEO tag. For obvious reasons, depth provides the 3rd dimension to habitat use, which was not possible with the current technological status at the time of tagging. For this reason, only depth from short term MOD tags was available for depth analyses. Future work should focus on the depth residency of sailfish and blue marlin on longer time scales.

An important distinction using SeaTags was the data return. Compared to other satellite tagging efforts where 1 out of 10 PSATs return a data level meeting expectations (Musyl et al. 2011) SeaTags returned more than expected data sets in over 90% of the PSAT deployments. The economic value of this more affordable option and the increased likelihood of data return provide distinct benefits to a budget-friendly research project. With the expectation that longer deployment times increase the likelihood of tag failure (Hays et al. 2007), the improved data return with the GEO compared to other tag brands was an unexpected benefit.

Tag retention was a focus throughout the deployment efforts. Initial use of a stainless floy tag was determined to be viable only for the shortest deployment durations of 10-15 days. A separate long-term MOD study was attempted as part of a different project, and all MOD tags with floy attachment shed prior to 25 days. This is likely due to a combination of the heavy tag and blade-like floy attachment that was thought to physically cut its way back out of the fish due to the pressure from the heavy tag.

Because of these initial results, a drastic change had to be undertaken, and the tether was completely redesigned. Musyl et al. 2011 suggests nylon dart heads such as the Domeier dart are more likely to detach early from the fish. This was not the case in sailfish as the stainless floy dart performed poorly in comparison to the Domeier dart, at least with MOD tags. Later GEO deployments transitioned to the exclusive use of the Domeier dart but sought to improve any potential infection or biomaterial rejection response that has been suggested as potential means mortality or early tag detachment (Graves et al. 2002, Jellyman and Tsukamoto 2002, Domeier et al. 2003, Kerstetter et al. 2003, De Metrio et al. 2004, Wilson et al. 2005, Wilson et al. 2006, Sasso and Epperly 2007, Musyl et al. 2011). Although monofilament fishing line is a biocompatible material, the rejection response of the fish could create a capsule surrounding the monofilament that does not promote tissue regrowth. The use of Dacron material supplied with the Domeier dart provides a scaffolding within which tissue can grow and, hopefully, promote healing and tag anchoring. To further promote healing and limit rejection response and infection, a medical-grade surgical heat shrink tube prevented contact of the monofilament line and any section of the tether with the animal tissue. Each of these improvements are thought to be beneficial to improving tag retention at relatively low cost. Another important factor in the tag tether was the use of standardized materials (Jinkai brand) known to be of highest quality and limiting errors due to mechanical failure in the tether.

In sailfish, smaller specimens occasionally saw the dart head come through the opposite side of the fish where the dart head was on the right side of the fish while the tag was tethered to the left. In these cases, there was an increased retention as the three longest duration tags on sailfish all had the tag head on the outside of the fish. Having the

Domeier dart on the outside issue has benefits and drawbacks. Firstly, the ability to stay in the fish over 100 days is a major benefit and, with only the medical grade tubing in contact with the interior tissue of the fish, the likelihood for infection is decreased. However, the likelihood for infection on the skin is increased with two open wounds compared to one. Infection was limited with Neosporin and oxytetracylin but these would eventually wash off the dart head once outside the body of the sailfish and the dacron covered head may be a possible location for increased biofouling or potential infection. The increased duration of these tags suggest infection does not occur at a faster rate compared to sailfish tagged without the tether traveling through the fish but this has not be specifically tested. An important distinction here is that no mortality events occurred due to infection with only one fish dying immediately following tagging due to a lack of proper revival and much too long fight time. Fish death can be determined with the GEO tag via light levels assuming a dead fish will stop moving and sink to darkness.

Overall, the steps taken to reduce infection, increase deployment durations, and provide good data were effective and beneficial to the satellite tagging program. Future work should examine the possibility of employing a tag tether designed to reach through the fish with some type of stopper on the side opposite the tag.

Tag shedding represented the main reason why deployment durations did not reach full term; however, this was not the only reason for the disappearance of tags. One case was found in tag 134250, which was at large for 47 days before disappearing and reappearing in a river in Panama where commercial fishing boats bring fish back to market. Even with a $300 reward, this tag was not returned but, luckily, was thrown back into the river and left to transmit data as it flowed toward the ocean. It could be possible that other tags

were caught by commercial fishermen, but no obvious patterns such as in tag 134250 occurred. It is certainly possible other billfish were caught, and the tag removed at the time of capture and returned to the ocean which would mimic a tag shedding event. The pressure of fishing should be considered whenever placing PSATs in the EPO as longlining and other commercial fishing is likely to cause unexpected mortality events.

Using PSAT Data in the BCPA to Examine Behavioral Modes

The BCPA was used to examine the behavioral trends in sailfish and blue marlin and to determine whether differing behavioral modes could be identified. The analysis was successful in determining behavioral differences in space and time in a vast majority of the PSAT tracks for both sailfish and blue marlin. The BCPA parameter values were used to infer the behavioral mode start and end points indicated by estimated behavioral change points. The change points are especially relevant because they occur at a time and location where some feature of the environment caused the animal to change behavior. These times and locations could provide information on behavioral preference, and the viability of this is examined further later in this dissertation.

In the sailfish and blue marlin that generated behavioral change points, the BCPA was successful at distinguishing differing behavioral pattern types or modes that could be attributed to foraging or traveling. Overall, sailfish tended to be more likely to undertake tortuous patterns leading to the designation of foraging while blue marlin, on average, were more directed and moved a higher speed. Parameter scales for variability reached value over 4.0 in some cases where most blue marlin variability scales maxed at 0.3 with only one blue marlin variability scale reaching values greater than 1.0. This implies blue

marlin travel with less tortuous paths. Blue marlin were also found to travel at a slower rate and, as a whole, over shorter migratory distances than sailfish in this study. The average number of days at large were comparable between the two species at 70.29 for sailfish and 71.90 for blue marlin; however, sailfish traveled 3638.62nm while blue marlin traveled 2163.3nm. Because of this difference, the distance traveled per day for blue marlin (25.61nm) was nearly half of that for sailfish at 50.77. This distinction is critically important to understanding the difference between the species occupying the same region but employing substantially different population dynamics. This statement is especially true considering methodology for data collection and analysis in the BCPA was performed in an identical manner between the two species which provides insight into how sailfish use the EPO ecosystem compared to blue marlin.

The differentiation between species must be attributed to differing population dynamic factors. Although these species share prey items (Olson and Watters 2003, Hinke et al. 2004), blue marlin that were caught and tagged were associated with schools of small tuna too large for sailfish to eat. This different prey preference in the EPO off Costa Rica could lead to the differences in behavior seen between the species in this study. Examining the migratory behavior of small tuna school versus smaller pelagic schools targeted by sailfish would clarify whether the behavioral trends are related to food availability.

The behavioral modes were defined as one of two types (traveling and foraging) within which includes a variety of subtypes that were not specifically analyzed in this study. Differing levels of autocorrelation, speed, and variability result in a plethora of potentially identifiable foraging modes as well as traveling modes. For example, one

could attribute a slightly tortuous, highly autocorrelated track as an intermediate searching mode that would fall between foraging and traveling. These small differences make clear distinction between foraging and traveling sometimes tricky. As this is the first time billfish location data has been modeled in the BCPA, the designation between parameter values related to behavioral modes is still ongoing and requires further effort to clarify via increased PSAT samples. Another example on a more specific behavioral phase designation could be a very slow, highly tortuous pattern occurring over more extended time periods as indicating some behaviorally specific pattern such as feeding or spawning based on further knowledge of the behavior. Although this situation would be designated as foraging, future clarification could provide the ability to attribute highly specific behavioral modes. This level of examination is beyond the scope of this dissertation, but further work using BCPA on sailfish and blue marlin would benefit from a more complex classification system for behavioral modes.

An important note is the necessity for longer durations of PSATs as the window size of 20 days is suggested as a minimum. This limited the number of PSATs that could be incorporated into the analysis. Long durations are notoriously difficult in sailfish and blue marlin making analyses such as the BCPA more difficult requiring more investment in PSAT deployments. Every potential means to increase duration of PSAT deployments was incorporated; however, shorter PSAT durations than expected were still obtained in both sailfish and blue marlin. Increased duration of PSAT deployments provide more data to be incorporated into the BCPA modeling effort, and the tagged fish that had longest durations tended to provide more sensible and recognizable behavioral shifts in parameter values. For this reason, this researcher recommends BCPA only be used for

billfish research using the longest PSAT durations and eliminating short term (<30 days) deployments from the analysis.

The Potential Influence of Fish Aggregating Devices (FADs)

The entirety of blue marlin PSAT deployments occurred off the coast of Costa Rica where the implementation of recreational FADs has been ongoing for nearly a decade. The blue marlin PSATs were placed in the region dominated by FADs known as the Coco's Ridge seamount regions between the Coco's Island and the coast of Costa Rica. Although both sailfish and blue marlin were tagged in similar locations, blue marlin appear to be more associated with this seamount regions as tagged sailfish traveled away from the region where blue marlin remained in the area significantly longer with the majority never leaving. This is confirmed by captains who fish the FADs for blue marlin regularly that insist sailfish are rarely caught surrounding the FADs but rather are found closer to the coast (Personal Communication). Based on these personal communications with charter boat captains in Costa Rica, the seamount region has been bombarded with FADs since 2010 with potentially hundreds present at the time of the PSAT deployments. Blue marlin PSAT results suggest this influence of FADs may be generating the localized environments necessary for blue marlin population dynamics to persist without the necessity to migrate out of the FAD/seamount area. As opposed to sailfish BCPA results, blue marlin do not indicate clear foraging modes in a majority of the fish. This could be due to feeding behavior around FADs where blue marlin simply travel to and from different FADs as they meander about the FAD region. This situation would imply a

separate classification system be in place for FAD associated blue marlin compared to examples from other regions of the world.

Blue marlin literature suggest spatial movements on much larger scales than what was found in this PSAT blue marlin study (Kerstetter et al. 2003, Prince and Goodyear 2006, Goodyear et al. 2008, Prince et al. 2010). Hawaiian tagged blue marlin suggest movement toward the south and east indicating a potential connection between the Hawaiian stock and EPO; however, this connection does not appear to be mutual as none of the blue marlin tagged off Costa Rica appeared to travel toward the central Pacific. This lack of expansive migrations compared to other stocks of blue marlin may suggest this FAD region is developing a specialized lone FAD stock. Of course, without PSAT deployments reaching full term data collection up to a year, it is impossible to fully suggest the FAD associated blue marlin never leave the area; however, recreational catch rates now suggest blue marlin are available to the recreational fishery throughout the year. Whether these blue marlin were previously available in this region year-round prior to FAD placement is unknown due to a lack of recreational effort prior to FAD deployments.

Overall, research on EPO blue marlin should consider the outside factors affecting the distribution of the stock. Although speculative, it is possible the tremendous effort at FAD implementation has provided blue marlin the opportunity to feed throughout the year, removing the need to leave and convoluting the population dynamics. Furthermore, aggregation of this species provides the opportunity for exploitation of the stock as they are more available to extractive fishing practices such as longline fishing especially

considering the habitat compression keeping these animals in only the upper water column which is discussed in detail in Chapters 4 and 5 of this dissertation.

Post-release Behavior and Recovery

Although never a specific intention of this research study, the opportunity to take a holistic view of post-release behavior using a variety of data sources provides insight into what occurs following the traumatic event of catch, tag, and release from a recreation vessel. Results of acceleration studies suggest increase and peak in activity following release of around eight days on average. Without accelerometry studies beyond ten days post-release, the BCPA behavioral traits were used to determine behavioral differences that occur after the initial ten days of the trials. Examination of the BCPA results for the number of days until first behavioral change suggests a recovery period is represented by first behavioral phase as the fish recovers then switches behavior to a more typical behavioral pattern once recovery has concluded. Figure 28 reveals an overall trend in sailfish autocorrelation from the onset of the PSAT deployments where autocorrelation begins at low levels and increases immediately as the fish travels outside of the tagging area. This change in autocorrelation suggests sailfish do not remain in the immediate vicinity of the tagging location immediately after deployment; however, sailfish may return to the tagging location at a later date after recovery has occurred. Blue marlin data suggest a trend in autocorrelation that does not indicate a similar recovery pattern to sailfish. Blue marlin begin their migratory paths with relative variable autocorrelation levels among the individuals. A majority of these blue marlin see a decline in autocorrelation following release followed by a steady increase. This result suggests blue

marlin recovery by remaining close to the tagging location and exhibiting an overall lack of active movement away immediately post-release.

Many references allude to post-release behavior of sailfish, blue marlin, and other billfish; however, few studies were designed specifically to elucidate the behavioral pattern through satellite tag data collection (Holland et al.., 1990; Holts and Bedford, 1990; Block et al.., 1992; Pepperell and Davis, 1999; Hoolihan, 2005, Skomal 2007, Hoolihan et al. 2011). Hoolihan et al. 2011 developed a review of post-release behavior for a variety of species and found 15 of 21 sailfish not to exhibit irregular post-release behavior indicating a recovery period is not necessary. The findings of this study suggest sailfish do require a recovery period of at least five days when using accelerometry and 14.8 days via the BCPA. The Musyl et al. 2011 study also estimated blue marlin recovery time to be 8.2 days on average with 19 of 50 blue marlin not showing signs of a recovery period. In comparison to these findings, this study estimated blue marlin to have a recovery period of 20.6 days, which is significantly longer than literature suggests. It could be inferred from the results of this study that sailfish appear to show a more clear recovery period than blue marlin, at least using autocorrelation data, which stands in contrast to Musyl et al. 2011 study.

To elucidate details of a post-release recovery period, a very specific research program is required with high resolution data collection for a minimum of 30 days to discover true activity levels and depth residency over the entire potential range of the recovery period. Until a study of this type is completed, it is difficult to estimate true recovery periods for any billfish species. In light of this fact, this study provides a first look at using BCPA

and acceleration research as a means to examine post-release behavior in PSAT tagged billfish species.

Chapter 4: An examination of environmental signals effecting billfish behavior

Overview

An understanding of behavior and habitat use relative to the environment is critical for conservation and proper management of an animal as a natural resource for human consumption or recreational use. Much like understanding the movements of endangered mammals inhabiting the African plains to protect against poaching, understanding the movements of open ocean animals such as sailfish and blue marlin can provide the ability to better assess the status of the resource as well as the potential for extraction beyond sustainable levels. To examine these movement patterns relative to local environmental conditions is to analyze the sailfish of blue marlin moving through space and time relative to outside factors that may affect said movement. Behavioral change points represent an animal's identification of some change in their habitat that can be identified through ecosystem based analyses where individual fish behavioral parameters are mapped on environmental variables to determine those most affecting behavioral changes. As discussed in detail in Chapter 3 of this dissertation, available Pop-up Satellite Archival Tag (PSAT) data was analyzed to obtain behavioral parameters associated with persistence velocity and turning angles as well as spatial and temporal information of behavioral changepoints. To investigate the migrations of sailfish and blue marlin relative to these behavioral changes, environmental and oceanographic data obtained through available online databases are analyzed along with commercial fishery catch in the industrial tuna purse seine fisheries.

Oceanic conditions affect the distribution of small pelagic prey species most sought after by billfish and other larger pelagics (Olson et al. 2014) thus drive the

distribution of predators such as sailfish and blue marlin. A fish in the ocean, whether it be predator or prey, is only aware of its immediate surroundings and, with the exception of some migratory species, must adapt to small changes in the immediate habitat by remaining present if those conditions are favorable, or leaving if they are not. As discussed in Chapter 1 of this dissertation, the tropical Eastern Pacific Ocean (EPO) off Central America ecosystem is characterized by numerous upwelling regions forced by gap winds accelerated through the low lying passages along Central America at Tehuantepec (Mexico), the low lands associated with the Great Lake of Nicaragua referred to as the Papagayo wind jet (Nicaragua/Costa Rica), and the Panama Canal Passage creating a parceling effect of the coastal marine habitat. This environmental forcing drives productivity and, in turn, effects the foraging of billfish species making it imperative to examine how environmental variables effect the migration and catch of sailfish and blue marlin in this unique upwelling driven ecosystem. The parceling of habitat is further affected by the availability of dissolved oxygen at depth which has been well documented to play a role in billfish distribution (Ehrhardt and Fitchett 2006, Pohlot and Ehrhardt 2017, Prince et al. 2006).

Daily behavioral data estimated from satellite tagging and the analyses presented in Chapter 3 of this dissertation as well as the publically available Inter-American Tropical Tuna Commission (IATTC) monthly and spatially defined tuna targeting purse seine catch data provides two different spatial and temporal resolution data sets that can be compared against available oceanographic variables. Using the behavioral parameters which provide knowledge of directional persistence along with the catch distribution of

sailfish and blue marlin caught incidentally in the industrial tuna purse seine fishery, it is possible to determine which, if any, environmental variables are driving billfish presence.

Availability of such environmental data on appropriate spatial and temporal scales is lacking in many cases; however, fine scale animal behavior data presents an opportunity to examine individual animal migratory characteristics on a sub-mesoscale level. This opportunity required the examination of oceanographic features typically not analyzed in fisheries research such as divergence and vorticity. Table 4.1 shows the list of oceanographic variables thought most likely to impact sailfish and blue marlin migration patterns and tuna purse seine catch. Sea Surface Height (SSH) data is used to analyze the geostrophic flow and presence of oceanic fronts such as those occurring along eddies and meanders caused by wind jets. As opposed to the standard SSH parameter, it was determined the zonal component (u) and meridional component (v) would be ecologically relevant if differentiated as divergence and vorticity estimations. The surface divergence represents the outward flow from higher pressure indicating upwelling where divergence occurs and downwelling at convergence points. The relative vorticity or circulation can be caused by curvature or shear and can indicate edges of eddy systems or meanders where productive habitats may be found. Integrating and estimating divergence and relative vorticity is assumed in the analyses to better relate the three-dimensional effects of differences in SSH as seen by an animal in the ocean than using SSH alone (Personal Communication Arthur Mariano). Chlorophyll concentration along with Sea Surface Temperature (SST) is used to indicate the level of upwelling and available nutrients for lower trophic levels that accumulate prey biomass.

Table 4.1: Environmental data used in regression analyses and sources

Environmental Data
Divergence and Vorticity: Ocean Surface Current Analysis Real-time (OSCAR)
Chlorophyll Concentration: Aqua Moderate Resolution Imaging Spectroradiometer (MODIS)
Sea Surface Temperature: Optimum Interpolation Sea Surface Temperature (OISST)

Methods and Materials

In these analyses, migration patterns of sailfish and blue marlin are characterized according to time stratifications to elucidate seasonality of migration behavior relative to the changing EPO environment. The patterns of seasonal changes in model parameter estimates will indicate the habitat use and preference for specific oceanographic conditions based movement within given habitats. The behavioral parameters: speed (μ), movement variability (σ), and autocorrelation of movement (ρ) are regressed against environmental data: divergence, vorticity, and sea surface temperature, first to determine individual preferences for each condition then as a group to determine the combination of variables most affecting billfish migratory behavior as a whole. The combination of individual and group migration modeling and ecosystem variable analyses should provide the ability to explain Sailfish and Blue Marlin migratory characteristics relative to their potential habitat use.

As mentioned in Chapter 1 of this Dissertation, upwelled waters with low Dissolved Oxygen (DO) compresses the habitat for large predators, such as billfish species, and their prey in the Eastern Pacific Ocean (EPO); however, such data is not available in enough spatial or temporal resolution necessary for localized EPO analyses.

In addition, estimation process for DO data from online databases such as World Ocean Atlas which is not able to differentiate small scale DO changes that may be biologically relevant. For the purpose of examining the effect of dissolved oxygen on sailfish and blue marlin distribution, mapping of World Ocean Atlas DO data overlaid with billfish depth histograms and catch provides insight into how this habitat limiting condition effects distribution both horizontally and vertically.

PSAT and Catch Data

Satellite tag locations were modelled using the behavioral change point analysis performed in Chapter 3 of this dissertation. The results of this analysis, behavioral parameters and change points in space and time, were organized and combined in Microsoft Excel for the purpose of matching each location with the associated oceanographic features at that location and on that day or month. Dates, latitudes and longitudes were formatted to link through R software with any available oceanographic parameters that matched the resolution of the behavioral data. Microsoft Excel CSV files consisted of behavioral parameters (μ, σ, ρ) for all sailfish in one file with associated: latitude, longitude, date, days post-release, and PSAT identification. A separate file was created for blue marlin with the same information.

Monthly tuna purse seine catch and fishing effort data for sailfish and blue marlin was obtained from the IATTC website public domain data (https://www.iattc.org/Catchbygear/IATTC-Catch-by-species1.htm). This data is found in a CSV file including year, month, flag and set type gridded by one degree latitude and longitude. Dates were filtered to include the range of years from 2003 to 2015 based on

availability of monthly oceanographic data from this time range. Sailfish and blue marlin are combined with other billfish species in the same file and this file was formatted to link through the R statistical computing program (R Program 2013) by date and location to environmental datasets. Catch Per Unit Effort (CPUE) was obtained for sailfish and blue marlin by dividing monthly catch by the number of sets within that one-degree grid for that month. Fishing effort statistics were not standardized due to the confidential nature of IATTC public domain data, which does not include vessel characteristics or information on sets other than a total monthly number for each grid square. Catch per set without standardization was determined to be more relevant for this analysis as the presence of sailfish and blue marlin is the factor of interest as well as the fact that billfish are caught in extremely low numbers as bycatch in the tuna purse seine fishery targeting Yellowfin Tuna (YFT). On the other hand, fishing effort standardization procedures would seek to remove the important environmental effects that this analysis seeks to discover.

Environmental Data Organization and Preference Analysis

All environmental data was organized in NetCDF format and required unpackaging using R statistical software, specifically the package "ncdf4" (Pierce 2015). This package was used to isolate and extract environmental parameters based on location and date to match Behavioral Change Point Analysis (BCPA) parameters of speed, variability, and autocorrelation data as well as tuna purse seine catch files. Divergence and vorticity information was calculated from data obtained from the Ocean Surface Current Analyses Real-Time (OSCAR) website (http://www.esr.org/oscar_index.html).

Horizontal surface current velocities were obtained as a 1/3 degree grid with 5 day averages and a 10 day smoothing component. These horizontal velocities include the zonal component (u) and the meridional component (v) as vertical averages over the surface layer down to 30m. The u and v estimation from OSCAR incorporates multiple data types including Archiving Validation and Interpretation of Satellite Oceanographic (AVISO) sea surface height information, surface wind data, and sea surface temperature. OSCAR u and v components were loaded into R statistical software and differentiated over time and space resulting in two parameters, one for divergence and another for vorticity. Divergence is estimated by the equation du/dx+dv/dy representing changes in the u and v velocities in the x and y directions respectively, while the local vertical component of relative vorticity can be represented as dv/dx-du/dy.

Sea surface temperature data was obtained in two formats, daily and monthly. Both datasets were National Oceanographic and Atmospheric Administriation (NOAA) optimum interpolation version 2 data where the daily was High Resolution Sea Surface Temperature (SST) data provided by the NOAA/NOAA Oceanographic and Atmospheric Research (OAR)/NOAA Earth System Research laboratory (ESRL)/Physical Sciences Division (PSD) (Boulder, Colorado, USA) while the monthly data was obtained from the same location as averages of daily values over the duration of the month. Daily SST data resolution was a 0.25 degree grid to ensure as high a spatial resolution as possible where monthly data was available in a 1 degree grid which matched the spatial resolution of the IATTC tuna purse seine data it was to be analyzed against.

Aqua MODIS chlorophyll-a composite information was obtained from NOAA Coastwatch Environmental Research Division Data Access Program (ERDDAP) website and consisted of monthly data from 2003 to 2016 at 4km scale. Chlorophyll-a data was

averaged over 1 degree latitude and longitude for comparison of one degree gridded tuna purse seine catch data. Sub-monthly time series data was determined not analyzable due to incomplete coverage in the EPO due to cloud cover effects and lack of ability to interpolate across the region. For this purpose, chlorophyll-a information was only included in analyses of monthly datasets and not included in preference analyses with PSAT BCPA data. Chlorophyll-a data was linked by date and location to each occurrence of sailfish and blue marlin catch from the IATTC public domain tuna purse seine data discussed previously. The resulting dataset included all sailfish and blue marlin caught as bycatch with an associated chlorophyll-a value for each monthly data point.

The resulting organized dataset includes an excel .CSV for the tuna purse seine catch with sailfish and blue marlin CPUE that includes: Year, Month, Latitude, Longitude, Sailfish Catch, Blue Marlin Catch, Number of Sets, Sea Surface Temperature, Chlorophyll-a Concentration, Divergence, Vorticity. For the behavioral change point results, the species were split into two .CSV files with each containing: Three Behavioral Parameters (μ, σ, ρ), Date, Days Post-release, Latitude, Longitude, PSAT ID, Sea Surface Temperature, Divergence, Vorticity.

Each of these environmental variables is first examined qualitatively using histograms of each environmental variable. This is analyzed by overlaying the histogram of values actually witnessed by PSAT tagged sailfish and blue marlin over histograms of that variable's occurrence throughout the entire EPO system. Thus, the qualitative step provides insight into the range of total values preferred by sailfish and blue marlin in the region, and potentially infers species specific usage of differing environmental variables.

Vertical Habitat Use Information

Depth histograms were obtained from the April 2012 PSAT deployment discussed in detail in Chapter 2 of this dissertation with a total of six SeaTag-MOD tags recording depth histograms at 12 hour intervals from 6AM to 6PM local time in Guatemala. One PSAT was placed in March 2013 off Costa Rica that collected 15 days of depth histogram information in the same format as those in Guatemala. Depth histograms were compared to oceanographic variables of DO level at depth, temperature at depth, and salinity at depth in both Guatemala and Costa Rica where the tags were deployed to determine the vertical habitat use of sailfish. These three oceanographic transect datasets were obtained from World Ocean Atlas (WOA 2013). DO data was not available specifically collected from 2012; however, an average for the month of April is provided from the WOA website incorporating available data from all years for that month.

Generalized Additive Modeling

To explore environmental preference for sailfish and blue marlin using behavioral characteristics and catch type, Generalized Additive Modeling (GAM) was used (Hastie and Tibshirani 1986, Hastie and Tibshirani 1990, Wood 2006). The GAM provides flexibility in ecological analysis when compared to linear generalized models without covariate smoothing functions. GAMs represent non-parametric and semi-paramteric regression that are used to determine relationships between the response variables, in this case, the BCPA parameters values and IATTC tuna purse seine catch and the matching explanatory variables comprised of environmental variables along with time and space. Speed, variability, and autocorrelation parameters from the BCPA are analyzed via

GAMs separately; however, the autocorrelation parameter must be kept as the primary variable implying sailfish and blue marlin preference to remain in a region or leave thus emphasis is placed on BCPA autocorrelation results. The GAM methodology was chosen over linear modeling due to the relaxation of assumptions of the relationship between response and explanatory variables, allowing these to be modeled via smoothing functions. Model selection was performed using the "gam" package in R, specifically the model selection routine "step.Gam" that estimated Akaike 1973 index (AIC) for each model, allowing the model the option to remove, include unsmoothed, or smooth each explanatory variable (Hastie 2018). This process is completed both forward and backward relative to explanatory variable selection. Once the best model was chosen from the "step.Gam" function, the GAM methodology was performed using R software and the "mgcv" package allowing family functions ,such as gamma or Gaussian, with a link function to be applied (Wood and Wood 2016). When data is strictly positive, the gamma distribution can be used; however, negative response variable values are not possible to analyze using the gamma distribution within the GAM. Speed, or mu.hat is the only variable estimated with a range including negative values which requires the gaussian distribution with identity link function. This somewhat limiting as the distributions that may fit the data best are not always available within the "mgcv" framework. For this reason, the gaussian distribution is used in an effort to keep GAM analyses between variables as consistent and simplified as possible. Family and link functions were chosen based on a combination of distribution of response variable data and resulting best fit. Gamma distributions were accompanied by log link functions in all

cases. Resulting GAMs are then analyzed for their fit and level of deviance explained using built in diagnostic tools in the "mgvc" package.

Results of BCPA parameter GAM modeling are examined to determine if sailfish and blue marlin behaviors can be linked to environmental characteristics and whether or not these results can be applied for conservation purposes. As GAMs are additive models, interaction between explanatory variables are not explored in this analysis as the goals of this chapter focus specifically on exploring the use of GAMs and their viability for analysis using two data types not commonly used for habitat based analyses, stock assessment, or CPUE standardization methods.

Commercial catch data analysis to remove effects not associated with stock abundance using generalized modeling is well documented in the literature (Gavaris 1980, Kimura 1981, Punt et al. 2001, Maunder and Punt 2004, Perryman 2017). The process of standardizing catch and effort data to remove effects of environmental variables is the goal of this research; however, this study seeks to elucidate which environmental variables have an impact on sailfish and blue marlin presence, and not to remove the effect. The GAM methodology has been employed in a variety of commercial catch studies and represents a non-parametric means to examine the potentially additive effects of explanatory variables with more flexibility in assumptions (Bigelow et al. 1999, Rodriguez-Marin et al. 2003, Martinez-Rincon et al. 2012, Perryman 2017). IATTC tuna purse seine data does not contain individual set data thus making binomial analyses of presence/absence in catch impossible in this scenario. For that reason, only positive catch data was used for this analysis, focusing only on the environmental conditions where catch of sailfish or blue marlin actually occurred. In the absence of zero catch data, only

the positive catch analysis can be completed and this is commonly referred to as a Delta framework for standardization and normal or gamma distributions can be used (Andrade 2009).

Tuna purse seine catch database is structured such that catch of sailfish and blue marlin data distributions are not normally distributed, with a majority of values closer to zero. For this reason, two approaches were taken, first, GAMs were employed using log-normalized catch data and a gaussian distribution with identity link, and second, non-normalized catch data with a gamma distribution and log link.

In all GAM analysis, both using BCPA and catch data, environmental variable selection is performed using AIC scores as variables are added, removed, or smoothed. The AIC criteria for explanatory variable selection is well accepted in the scientific literature (Maunder and Watters 2003, Maunder and Punt 2013). Once the best model is determined, the GAM procedure is employed to examine relationships between billfish behavior or catch and environmental variables not associated with stock size.

Results

PSAT Environmental Preference

Examination of qualitative preference for differing environmental variables suggests ranges preferred by sailfish and blue marlin in the EPO. PSAT tracked sailfish and blue marlin suggest differing preference for habitat that can be attributed to differing habitat usage and strategies employed between the two species; therefore, separate analyses are presented below.

Sailfish

The range of values experienced by sailfish in their preference for divergent locations suggest an overall lack of preference for any specific level of divergence (Figure 4.1). Overall there exists a lack of sailfish presence in regions where divergence was at the extreme. This lack of preference with high or low levels of divergence coincides with results found in other chapters of this dissertation where areas of extreme upwelling were either avoided or passed straight through to limit exposure such as in the region known as the Costa Rica Dome (CRD) that was discussed in detail in Chapter 1. This is further evidenced by the left skew of sailfish preference histogram to the lesser divergent range.

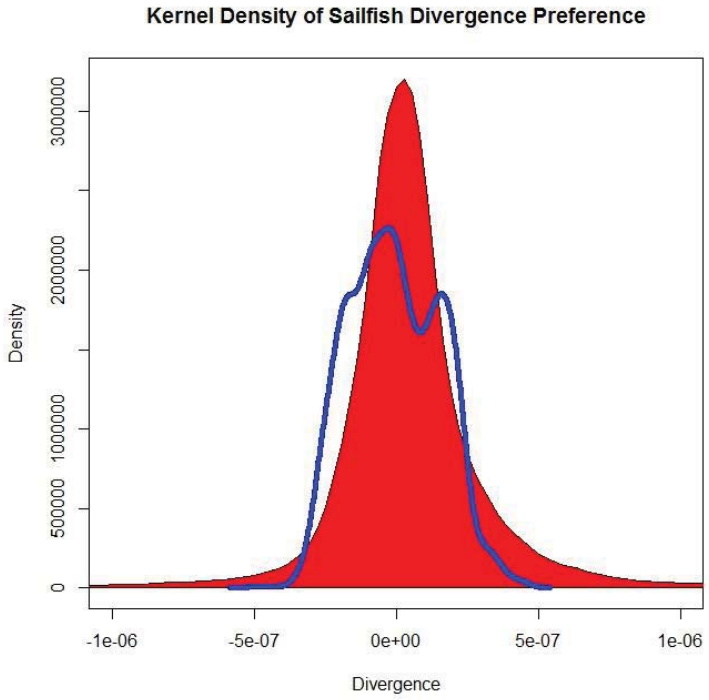

Figure 4.1. Two adaptations of histograms with a red polygon of the density of values of divergence throughout the tropical EPO, and a blue line of the density of divergence values actually visited by PSAT tagged sailfish.

Sailfish preference for vorticity suggests a clear preference for high vorticity regions suggesting sailfish may seek out these regions (Figure 4.2). The nearly full range of vorticity value found in the region was seen by PSAT tagged sailfish suggesting the sailfish inhabit regions where large fluctuations of the grandest scale in the EPO are found. This finding coincides with commonly belief that sailfish show preference to the edges of eddy systems where vorticity is high. This higher vorticity associated with eddy systems aligns with the region's propensity to spin up massive eddy systems associated with gap winds at Tehuantepec, Papagayo, and Panama.

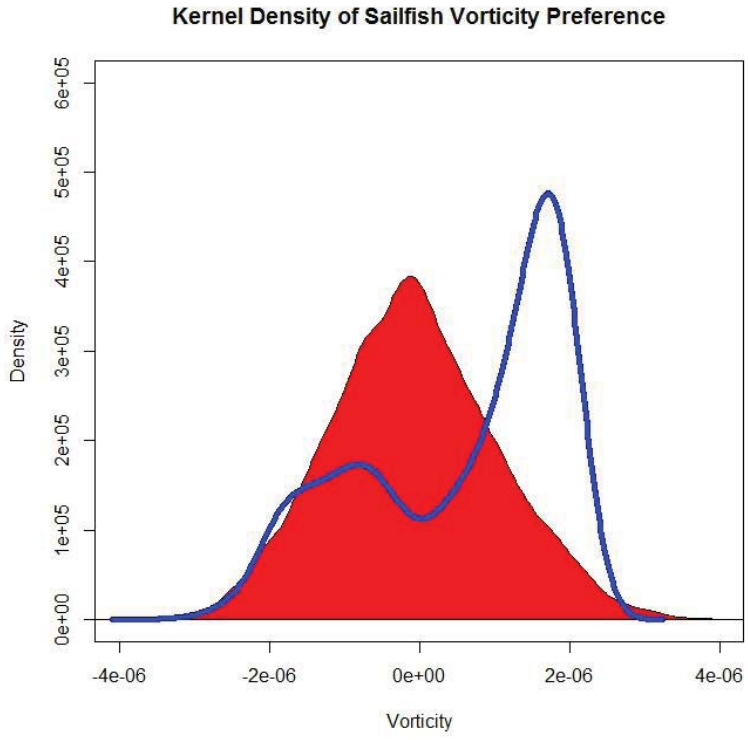

Figure 4.2 Two adaptations of histograms with a red polygon of the density of values of vorticity throughout the tropical EPO, and a blue line of the density of vorticity values actually visited by PSAT tagged sailfish.

Sea surface temperature ranges found in PSAT tagged sailfish suggest a propensity to remain in the warm pools formed off Costa Rica and Guatemala and an overall avoidance of the regions of highest upwelling such as the Costa Rica Dome (CRD) where SSTs would be lowest as cold water is being upwelled to the surface where data is sampled (Figure 4.3). The range of SSTs suggest sailfish are capable of inhabiting areas of lower SST; however, the tagged individuals clearly preferred only the warmest SSTs available in the EPO region. An important note is the relationship between upwelling and temperature and DO in this scenario and whether sailfish have preference for SST or are limited by availabile DO at the equivalent depth to the lend end of the SST curve. This relationship is discussed in detail in the next section of this chapter.

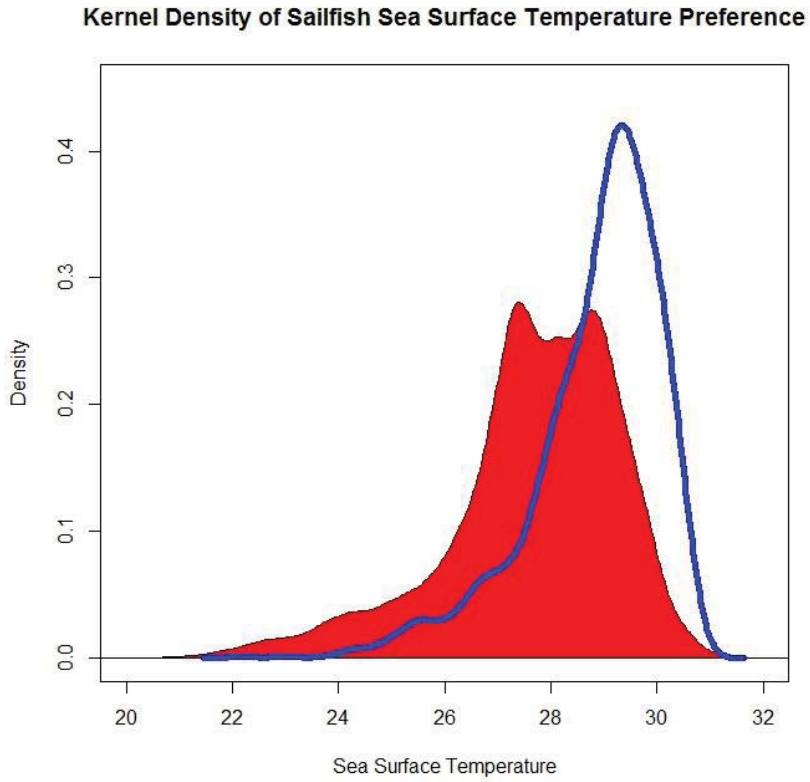

Figure 4.3 Two adaptations of histograms with a red polygon of the density of values of SST throughout the tropical EPO, and a blue line of the density of SST values actually visited by PSAT tagged sailfish.

Blue Marlin

Divergence values experienced by blue marlin compared to those of the whole tropical EPO suggest a similar pattern to sailfish in that there does not appear to be a clear preference for any given divergence range (Figure 4.4). Overall there is a lack of preferred range at the extremes of divergence not unlike sailfish, the preference is centrally distributed within the range of tropical EPO divergence suggesting no preference for positive or negative values.

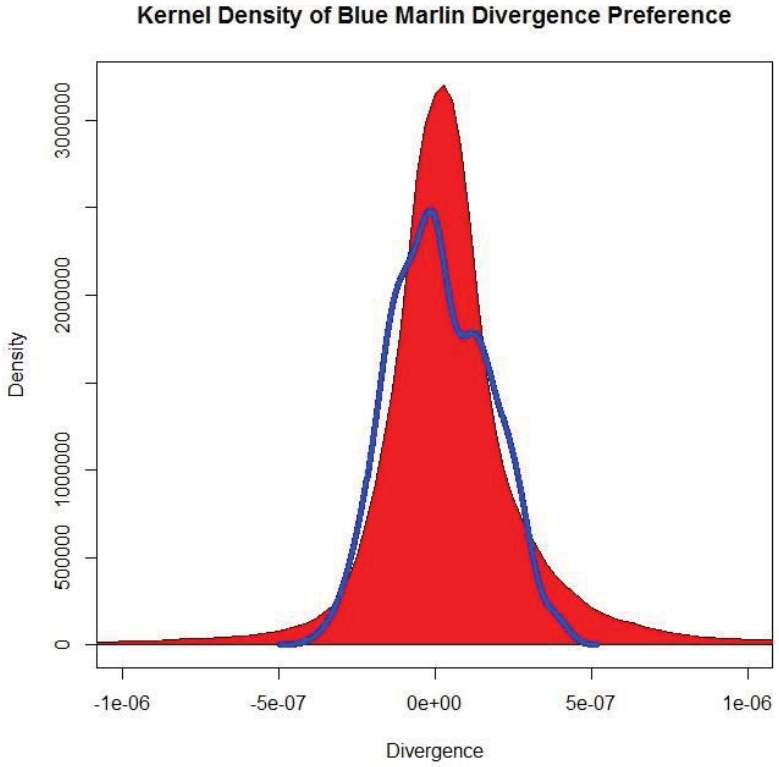

Figure 4.4 Two adaptations of histograms with a red polygon of the density of values of divergence throughout the tropical EPO, and a blue line of the density of divergence values actually visited by PSAT tagged blue marlin.

Vorticity preference of blue marlin is in stark contrast to sailfish with a clear preference for lower levels of vorticity (Figure 4.5). This preference implies blue marlin seek out regions where eddy systems are not present, which is confirmed by the fact that

blue marlin examined in this study remained in the Coco's Island Ridge seamount region inside the warm pool off Costa Rica where gap wind induced upwelling does not occur. There is an overall lack of presence within the highest levels of vorticity, also unlike sailfish in this study.

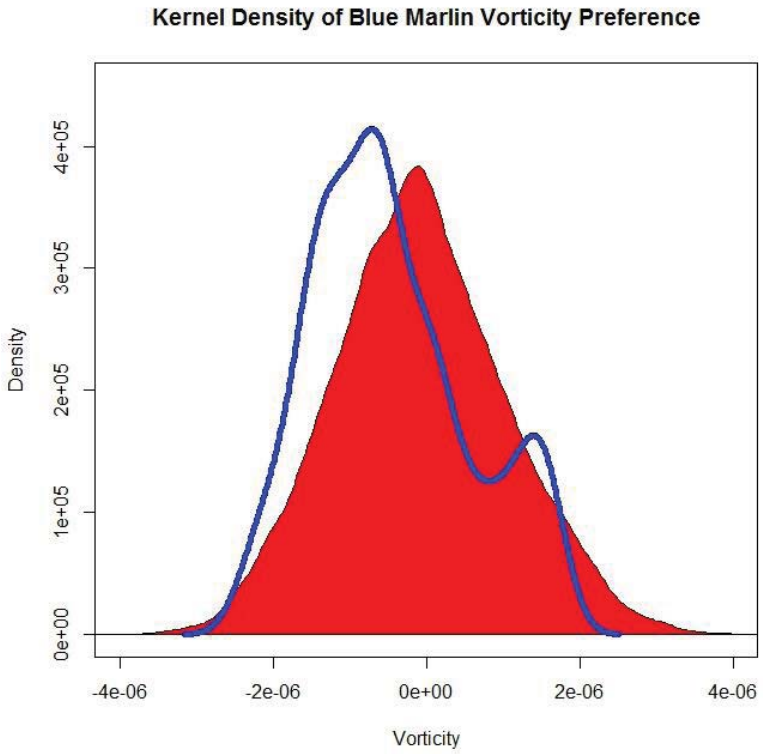

Figure 4.5 Two adaptations of histograms with a red polygon of the density of values of vorticity throughout the tropical EPO, and a blue line of the density of vorticity values actually visited by PSAT tagged blue marlin.

In this study, blue marlin was found inhabiting within a smaller range of SST values than sailfish and showed preference for the higher SST values between 27 and 30 degrees C (Figure 4.6). Unlike sailfish, blue marlin were not found where SST was at the maximum but rather remained in a smaller range of values. This smaller range witnessed is likely a product of less extensive migrations compared with sailfish that crossed extensive SST regimes along the continental coastal regions.

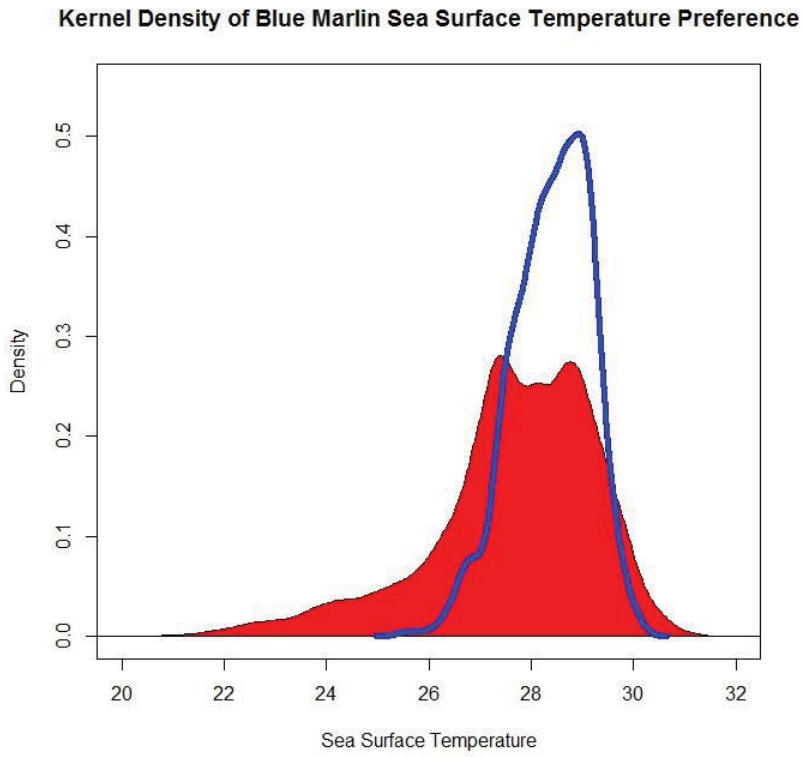

Figure 4.6 Two adaptations of histograms with a red polygon of the density of values of SST throughout the tropical EPO, and a blue line of the density of SST values actually visited by PSAT tagged blue marlin.

Vertical Habitat Use of Sailfish from Short Term PSAT Deployment

Using depth data obtained from PSAT tagging in Guatemala and Costa Rica, the preference of water with highest dissolved oxygen at depth is evident (Figures 4.7 & 4.8). In Guatemala, no sailfish dove deeper than 76.8m and 58m in Costa Rica, which coincides with a decrease in oxygen to levels below what might be possible for long term presence. The 1ml/l minimum Dissolved Oxygen (DO) level is widely considered the absolute lowest level of DO within which a fish species can inhabit (Ehrhardt and Fitchett 2006). The level of DO in this region may represent the most important environmental factor limiting sailfish vertical migration to only levels capable of survival.

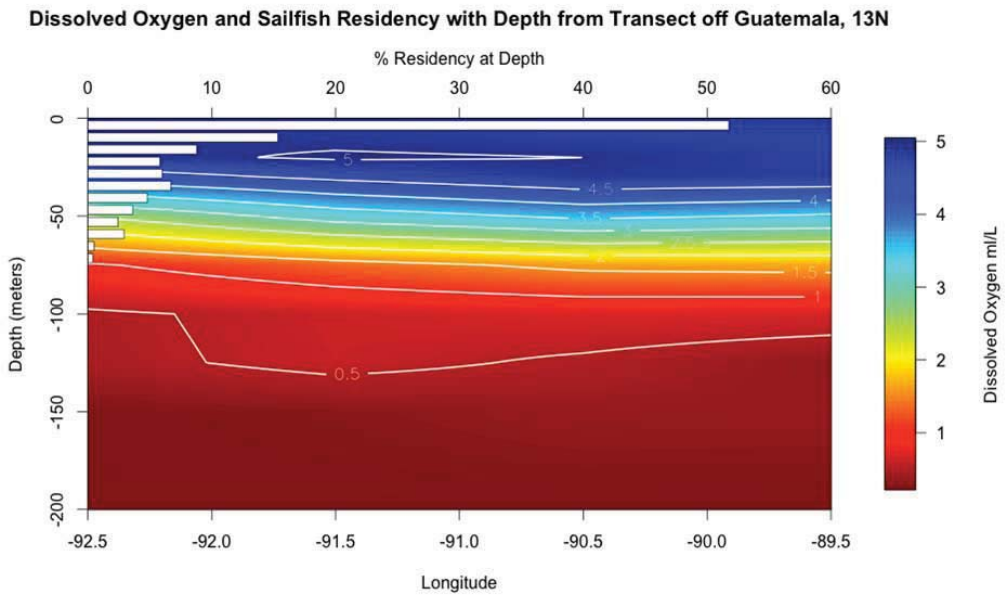

Figure 4.7 Plot of the depth residency of sailfish tagged off Guatemala in 2012 (white bars) overlaid on DO data at latitude 13N obtained from World Ocean Atlas.

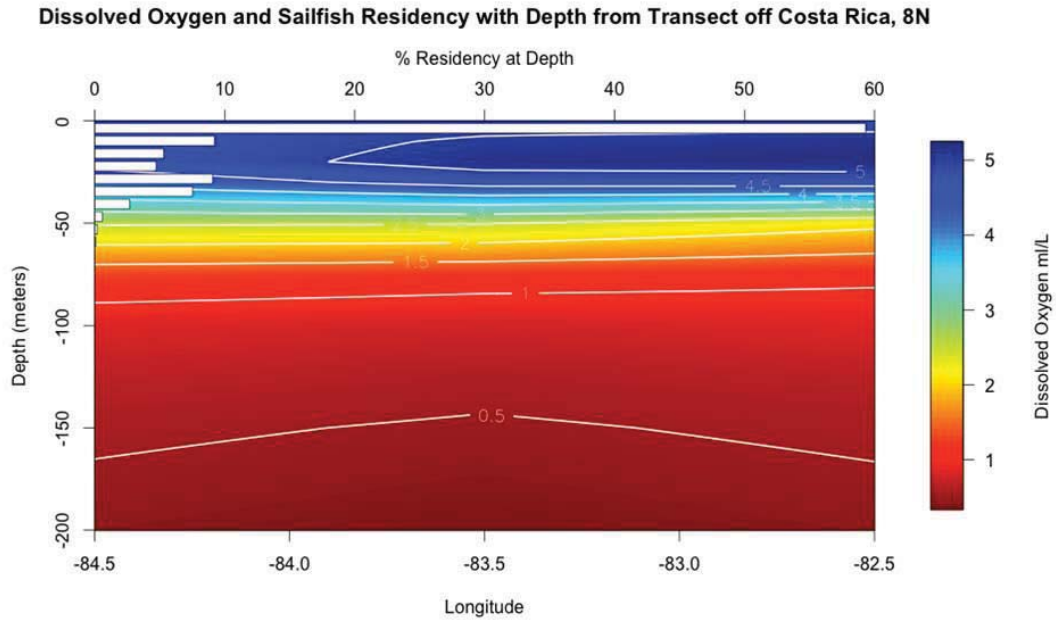

Figure 4.8 Plot of the depth residency of sailfish tagged off Costa Rica in 2013 (white bars) overlaid on DO data at latitude 8N obtained from World Ocean Atlas.

Depth analysis of sailfish preference for temperature (SST) suggest a lower limit of 18 degrees C with no fish in either Guatemala or Costa Rica diving deeper than this temperature level (Figures4. 9 & 4.10). The low temperature seen at depth are upwelled in a similar manner to the low levels of DO thus these two variables should be considered linked in this region. Although this lower limit of SST represents the maximum depth at which the tagged sailfish dove, the habitat compression caused by DO cannot be ignored when considering the temperature limitation seen in Figures 4.9 and 4.10. Overall sailfish presence in the depth of highest SST coincides with the range of temperature seen in spatial analysis previously where sailfish were found to prefer the highest temperatures found in the EPO.

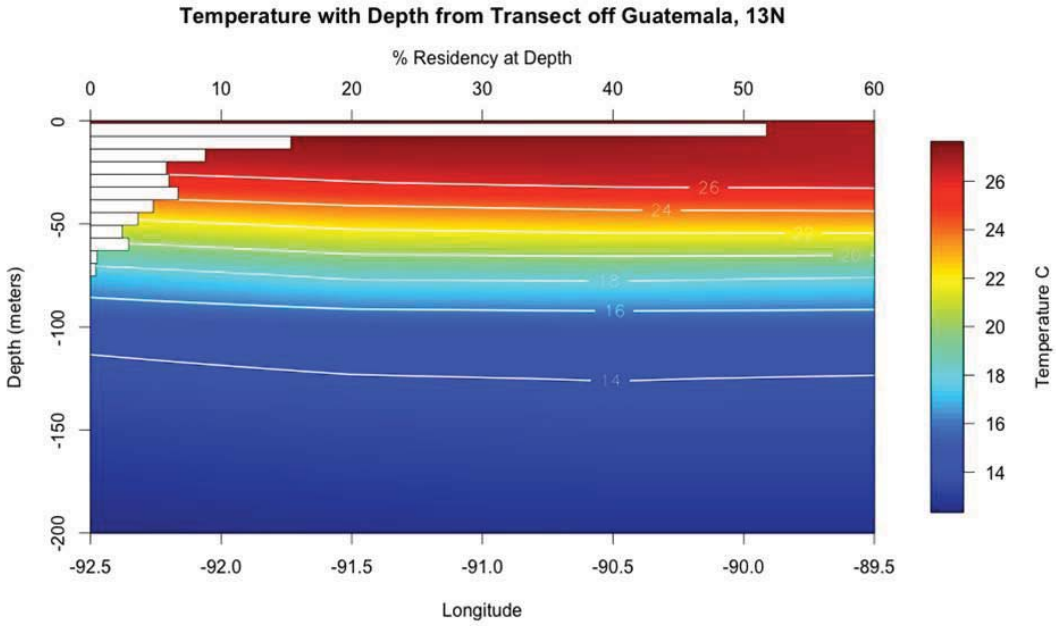

Figure 4.9 Plot of the depth residency of sailfish tagged off Guatemala in 2012 (white bars) overlaid on SST data at latitude 13N obtained from NOAA OISST.

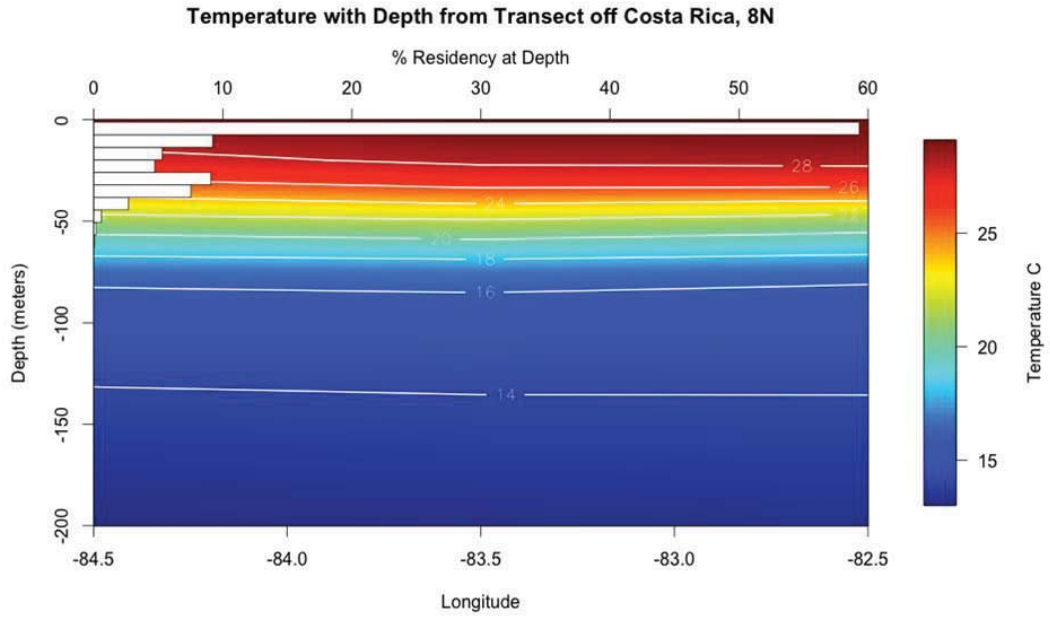

Figure 4.10 Plot of the depth residency of sailfish tagged off Costa Rica in 2013 (white bars) overlaid on SST data at latitude 8N obtained from NOAA OISST.

Sailfish GAM Results

BCPA Parameter GAM Model Selection

Distributions of the three BCPA parameters associated with speed (mu.hat), variability (s.hat), and autocorrelation (rho.hat) are found in Figure 4.11. The histogram for speed suggest a right skew with higher speeds making up the majority of values. The opposite if true for variability and autocorrelation where data is skewed left with low values making up the majority of the data set. For this reason, variability and autocorrelation are modeled similarly within the GAM methodology where speed applies different distributional and link analysis.

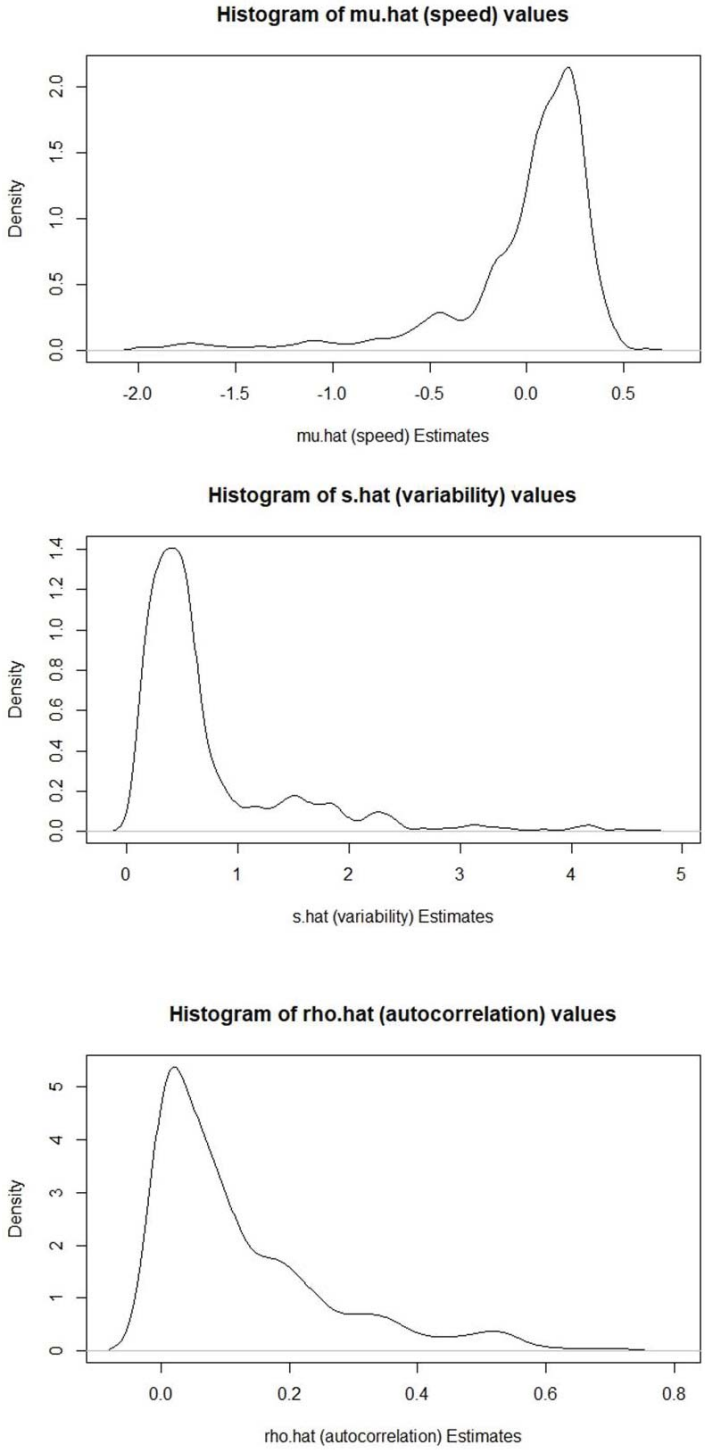

Figure 4.11 Histogram density plots for each of the response variables: speed or mu.hat (top), movement variability or s.hat (middle), and autocorrrelation of movement or rho.hat (bottom).

The distributions of explanatory variables can be found in Figure 4.12 and are used to examine the distribution of values not shown in the histograms of preference in the previous section of this chapter. The distribution of values for Time (# Days Postrelease) suggests left skew with majority of values occurring less than 100 days which is expected based on the deployment times of PSATs. Latitude and longitude are both relatively normally distributed with wide ranges given the large migratory paths undertaken by sailfish in this study.

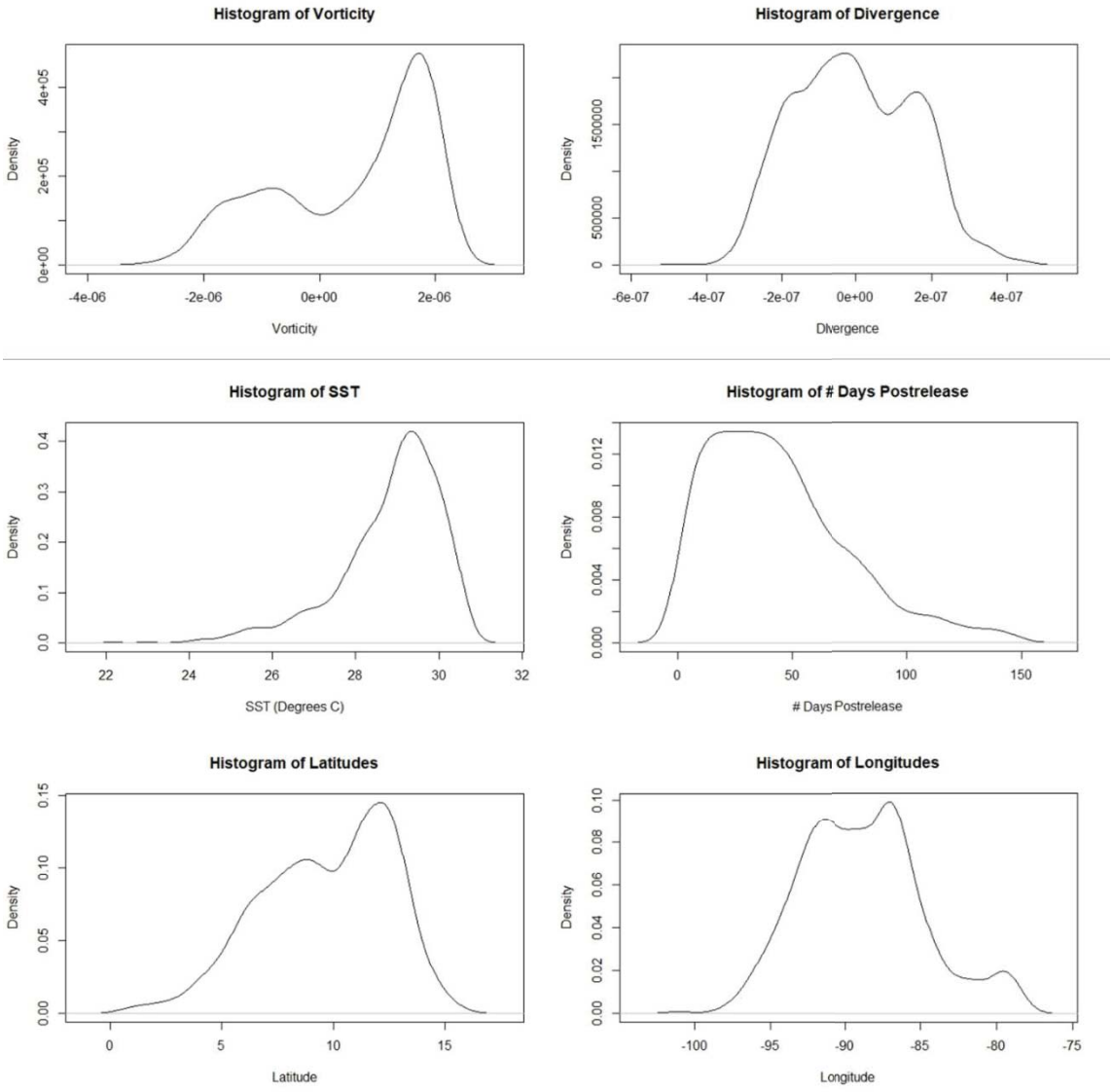

Figure 4.12 Histogram density plots for each of the explanatory variables: vorticity (top left), divergence (top right), SST (middle left), Time or # of days postrelease (middle right), Latitude (bottom left), and longitude (bottom right).

Table 4.2 shows the correlation matrix for explanatory variables incorporated into the sailfish BCPA GAM analysis. Correlation results suggest a lack of correlated explanatory variable with one exception: Latitude and longitude are negatively correlated at -0.6906 and given the disperse nature of the data origins, correlation value is fairly high thus consideration of the coupling of these two variables must be taken into account when both variables are included in analysis. This analysis seeks to examine specific environmental features associated with sailfish presence thus latitude and longitude significance combined in the GAM is not the primary goal of this research. Latitudinal and longitudinal difference in environmental factors will be incorporated into the differences in values of such environmental variables; however; there does not appear to be correlation with these variables and latitude or longitude. A correlation between divergence and SST was expected as changes in divergence should lead to upwelling or downwelling resulting in SST changes; however, this association was not found in the subset of data points incorporated into this analysis with a correlation value of 0.2182. Vorticity and divergence, which use the same data show a correlation of -0.3374 which reveals a level of correlation that should be expected given the estimation procedure and the data source. Time and vorticity and time and divergence represent the most unexpected correlations at -0.5414 and 0.4137 respectively, meaning the number of days post-release is correlated with the level of vorticity and divergence experienced by the

sailfish. This implies sailfish to show a different preference for vorticity and divergence levels as time progressed beyond the initial PSAT deployment date.

Table 4.2 Correlation matrix showing explanatory variables used for sailfish BCPA GAM analysis.

	Vorticity	Divergence	SST	Latitude	Longitude	Time
Vorticity	1.0000	-0.3374	-0.1827	-0.0619	0.0242	-0.5414
Divergence	-0.3374	1.0000	0.2182	0.4271	-0.3014	0.4137
SST	-0.1827	0.2182	1.0000	0.1632	-0.3924	0.3610
Latitude	-0.0619	0.4271	0.1632	1.0000	-0.6906	0.1373
Longitude	0.0242	-0.3014	-0.3924	-0.6906	1.0000	-0.2676
Time	-0.5414	0.4137	0.3610	0.1373	-0.2676	1.0000

Model selection using the step.GAM function supplied 6 steps for each BCPA parameter estimate as response variables (Table 4.3). Explanatory variables were allowed to be removed, included unsmoothed, or smoothed, and each step is associated with a different model, each improving upon the previous in terms of AIC. The model developed for the GAM of speed found smoothing of each variable improved the AIC with the best model only removing the explanatory variable longitude in the best model. Similar to speed, variability models showed improved AIC by smoothing all terms and removing the variable longitude in the best model. Autocorrelation improved with smoothing; however, the best model included a smoothed longitude term meaning the longitude had more of an impact on sailfish autocorrelation or “movement inertia” than speed or variability. This may be due to long migrations that occurred in the far west of the study region in EPO where migrations were direct, meaning less tortuosity of the path, and more highly correlated.

Table 4.3 List of sailfish BCPA GAM models created by the step.GAM function in R program. Steps are listed in order for each response variable with descending values of AIC.

Mu.hat (Speed)	
Start: mu.hat ~ Vorticity + Divergence + SST + Time + Lat + Lon;	AIC= 1094.263
Step:1 mu.hat ~ Vorticity + Divergence + SST + Time + s(Lat) + Lon ;	AIC= 1031.212
Step:2 mu.hat ~ Vorticity + Divergence + SST + Time + s(Lat) + s(Lon) ;	AIC= 982.867
Step:3 mu.hat ~ s(Vorticity) + Divergence + SST + Time + s(Lat) + s(Lon) ;	AIC= 961.5066
Step:4 mu.hat ~ s(Vorticity) + Divergence + SST + s(Time) + s(Lat);	AIC= 943.2542
Step:5 mu.hat ~ s(Vorticity) + Divergence + s(SST) + s(Time) + s(Lat);	AIC= 930.2947
Step:6 mu.hat ~ s(Vorticity) + s(Divergence) + s(SST) + s(Time) + s(Lat) ;	AIC= 922.2397
S.hat (Variability)	
Start: s.hat ~ Vorticity + Divergence + SST + Time + Lat + Lon;	AIC= 2457.093
Step:1 s.hat ~ Vorticity + Divergence + SST + Time + Lat + s(Lon) ;	AIC= 2386.884
Step:2 s.hat ~ s(Vorticity) + Divergence + SST + Time + Lat + s(Lon) ;	AIC= 2343.411
Step:3 s.hat ~ s(Vorticity) + Divergence + SST + Time + s(Lat) + s(Lon) ;	AIC= 2299.717
Step:4 s.hat ~ s(Vorticity) + Divergence + s(SST) + Time + s(Lat);	AIC= 2273.54
Step:5 s.hat ~ s(Vorticity) + Divergence + s(SST) + s(Time) + s(Lat);	AIC= 2259.458
Step:6 s.hat ~ s(Vorticity) + s(Divergence) + s(SST) + s(Time) + s(Lat);	AIC= 2254.519
Rho.hat (Autocorrelation)	
Start: rho.hat ~ Vorticity + Divergence + SST + Time + Lat + Lon;	AIC= -1281.088
Step:1 rho.hat ~ Vorticity + Divergence + SST + Time + Lat + s(Lon) ;	AIC= -1401.024
Step:2 rho.hat ~ Vorticity + Divergence + SST + s(Time) + Lat + s(Lon) ;	AIC= -1441.888
Step:3 rho.hat ~ Vorticity + Divergence + SST + s(Time) + s(Lat) + s(Lon) ;	AIC= -1468.282
Step:4 rho.hat ~ s(Vorticity) + Divergence + SST + s(Time) + s(Lat);	AIC= -1494.505
Step:5 rho.hat ~ s(Vorticity) + s(Divergence) + SST + s(Time) + s(Lat);	AIC= -1500.512
Step:6 rho.hat ~ s(Vorticity) + s(Divergence) + s(Time) + s(Lat) + s(Lon);	AIC= -1502.024

BCPA Parameter GAM Analysis

Mu.hat (Speed)

The best model for speed analyzed using a gaussian distribution and identity link confirmed the significance of all the explanatory variables but with a low coefficient of determination (R^2) value of 0.196, low deviance explained at 21.7% but fairly good minimized generalized cross-validation (GCV) score of the GAM fitted at 0.13383 (Figure 4.13). The GCV here can be considered similar to AIC with lower values representing an improved fit of the smoothing parameters limiting prediction error of the explanatory variable in the GAM. Overall the results here suggest a lack of fit of the model for speed. The resulting lack of fit uses Gaussian distribution where truly the

distribution of speed is not normal (W=0.92, p=1.4 e-15 Shapiro Test); however, GAM methodology in R is limiting due to distributional requirements of gamma with log link not permitting the presence of negative values. This facilitated the only viable option for analysis that aligns with others performed throughout this chapter.

```
Family: gaussian
Link function: identity

Formula:
mu.hat ~ s(Vorticity) + s(Divergence) + s(SST) + s(Time) + s(Lat)

Parametric coefficients:
            Estimate Std. Error t value Pr(>|t|)
(Intercept) -0.01903    0.01080  -1.762   0.0784 .
---
Signif. codes:  0 ‘***’ 0.001 ‘**’ 0.01 ‘*’ 0.05 ‘.’ 0.1 ‘ ’ 1

Approximate significance of smooth terms:
                edf Ref.df      F  p-value
s(Vorticity)  5.153      9  4.735 3.97e-09 ***
s(Divergence) 5.669      9  3.553 1.69e-06 ***
s(SST)        3.962      9  2.422 4.77e-05 ***
s(Time)       7.855      9  6.356 9.01e-10 ***
s(Lat)        7.055      9 12.067  < 2e-16 ***
---
Signif. codes:  0 ‘***’ 0.001 ‘**’ 0.01 ‘*’ 0.05 ‘.’ 0.1 ‘ ’ 1

R-sq.(adj) =  0.196   Deviance explained = 21.7%
GCV = 0.13383  Scale est. = 0.13015   n = 1115
```

Figure 4.13 Model result for sailfish speed parameter BCPA GAM.

Figure 4.14 shows the first set of diagnostic plots for the GAM produced by the “mgcv” package. The qq-norm plot suggests an overall lack of fit and deviation from normal of the model residuals. This is confirmed in the histogram of residuals showing an overall lack of normality and a skew to the right of the distribution. Plots of the residuals

of the model versus the linear predictor and response variable against the fitted values suggest lack of fit with points spread about in not discernible pattern.

Figure 4.15 shows the second set of diagnostic plots with residuals of the model plotted against the speed variable which shows lower speeds deviate substantially in terms of residual error away from the 0 line. Squared residuals against speed values again suggests lower speeds have more variable residual patterns. The plot of standardized residuals against fitted values suggests deviations greater than 2 standardize residual units.

Plots of the smoothers applied to explanatory variables can be found in Figure 4.16 and shows the variables are better fitted at the midpoints, as expected in regressional modeling, of their range but quality of fit declines at the tails of the value range. Vorticity, divergence, SST, and Latitude show lack of fit at lower values where Time variable is well modeled at the start and but fit declines at higher values which were rarer in the data.

Overall speed is not well fit using GAM with gaussian distribution and the explanatory variables in the best model chosen. Speed in the BCPA was variable and this may cause the overall lack of fit given the lack of consistency with speed relative to behavioral conditions.

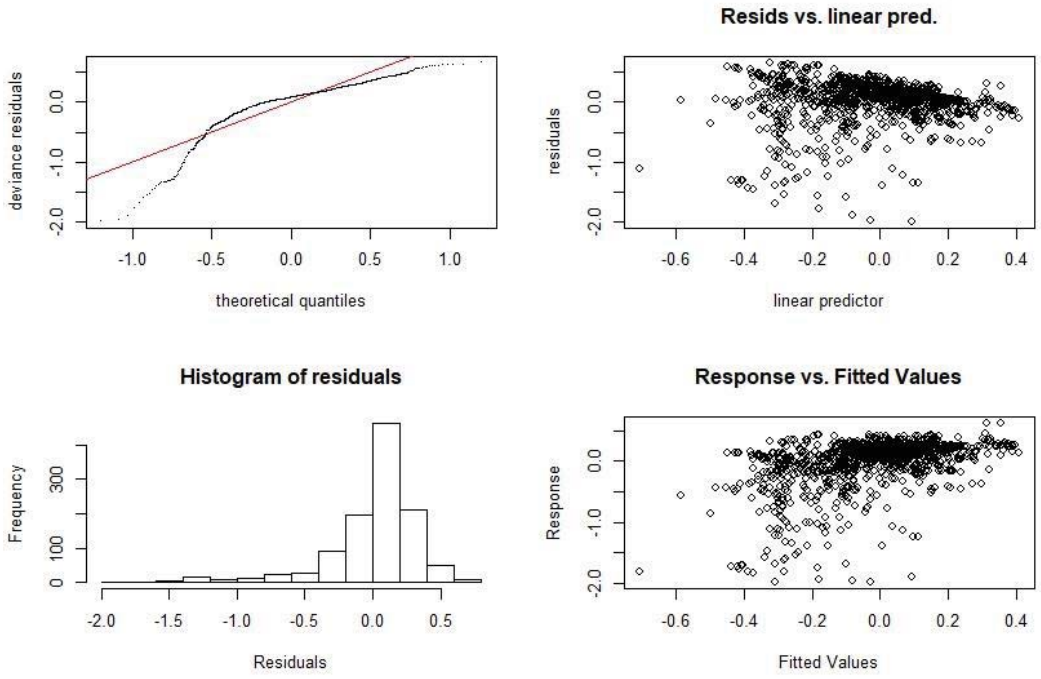

Figure 4.14: Sailfish speed parameter GAM model diagnostics including QQ-norm plot (top left), residuals versus linear predictor (trop right), histogram of model residuals (bottom left), and response variable against model fitted values (bottom right).

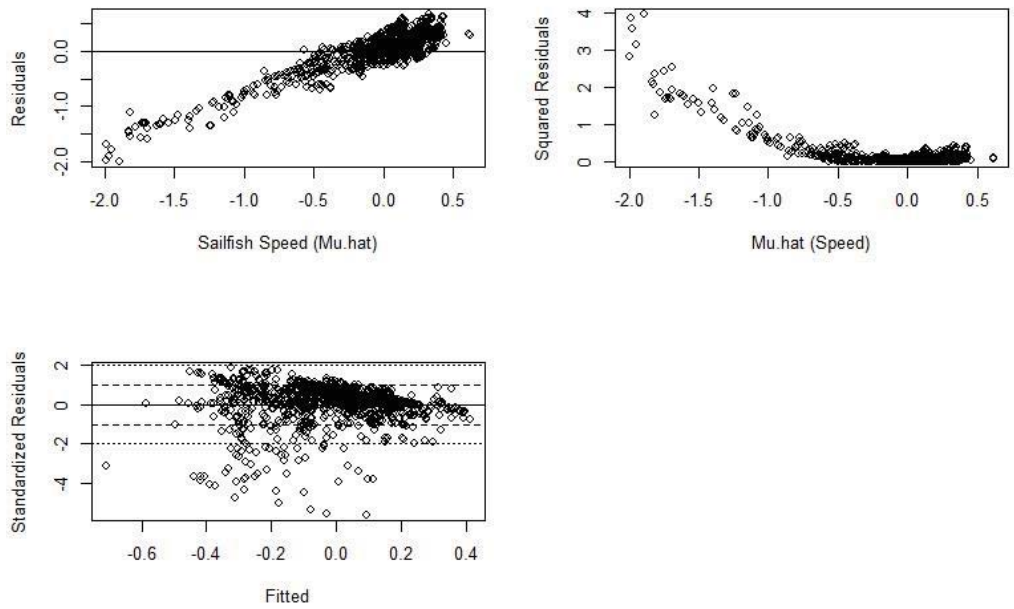

Figure 4.15 Sailfish speed parameter GAM model diagnostics including plot of model residuals against the speed variable (top left), squared residuals against speed variable (top right), and standardized residuals against model fitted values.

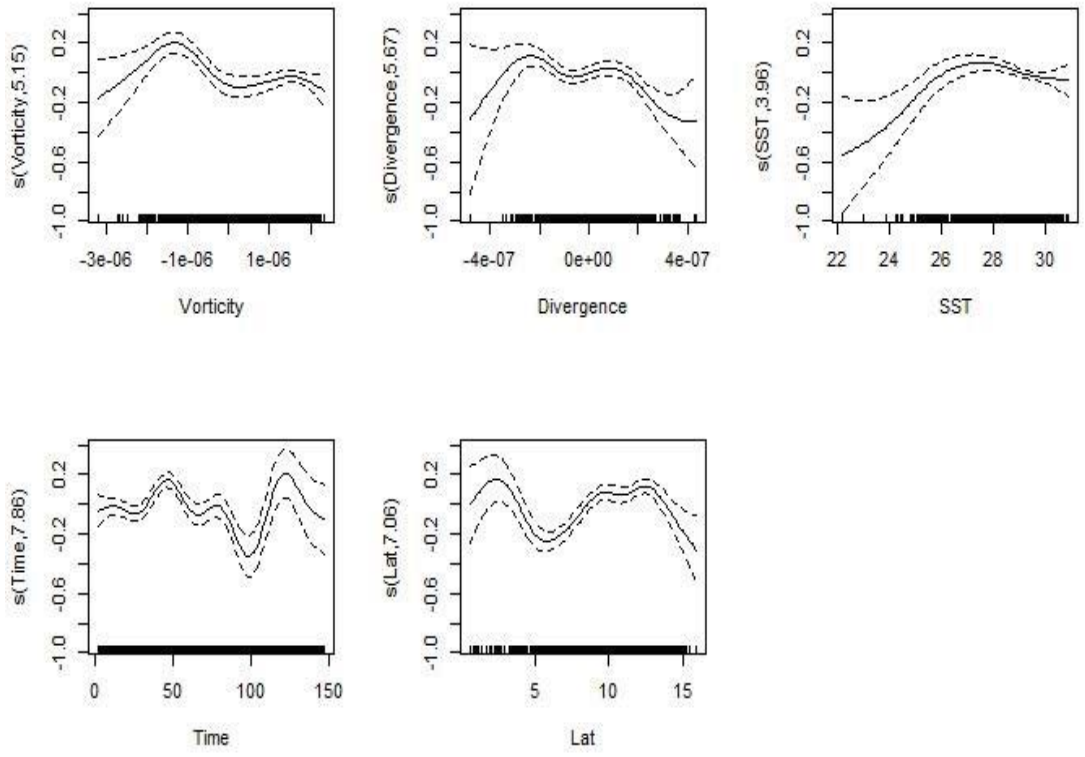

Figure 4.16: Sailfish speed parameter GAM model smoother diagnostics.

S.hat (Variability)

The best model for variability analyzed using a gamma distribution and log link confirmed the significance of all the explanatory variables but with a low R^2 value of 0.191, low deviance explained at 26.5% which is slightly higher than the deviance explained by the GAM for speed but with a decreased generalized cross-validation (GCV) score of the GAM fitted at 0.55557 (Figure 4.17). The GCV suggest the fit of the smoothing parameters has increased prediction error in the model compared to the model for speed. Overall the results here suggest a lack of fit of the model for variability.

```
Family: Gamma
Link function: log

Formula:
s.hat ~ s(Vorticity) + s(Divergence) + s(SST) + s(Time) + s(Lat)

Parametric coefficients:
            Estimate Std. Error t value Pr(>|t|)
(Intercept) -0.41010    0.02631  -15.59   <2e-16 ***
---
Signif. codes:  0 ‘***’ 0.001 ‘**’ 0.01 ‘*’ 0.05 ‘.’ 0.1 ‘ ’ 1

Approximate significance of smooth terms:
                edf Ref.df     F  p-value
s(Vorticity)  7.429      9 7.719 3.23e-13 ***
s(Divergence) 7.111      9 3.836 6.33e-06 ***
s(SST)        2.500      9 1.646 0.000337 ***
s(Time)       8.879      9 5.764 3.51e-08 ***
s(Lat)        6.168      9 5.951 9.50e-11 ***
---
Signif. codes:  0 ‘***’ 0.001 ‘**’ 0.01 ‘*’ 0.05 ‘.’ 0.1 ‘ ’ 1

R-sq.(adj) =  0.191   Deviance explained = 26.5%
GCV = 0.55557  Scale est. = 0.77171   n = 1115
```

Figure 4.17 Model result for movement variability or s.hat BCPA GAM.

Figure 4.18 shows the fit is improved compared to the GAM for speed as residual error is more like the traditional bell curve of normal distributions. The qq-norm plot suggests an overall lack of fit and deviation from normal of the model residuals at the tails of the data distribution with relatively good fit at the midpoint. The histogram of residuals suggests an overall bell-shaped distributed but with a skew to the left of the distribution. Plots of the residuals of the model versus the linear predictor and response variable against the fitted values suggest lack of fit with points spread about in no discernible way other than a shotgun blast type pattern.

Figure 4.19 shows the second set of diagnostic plots with residuals of the model plotted against the movement variability (s.hat) which shows more spread and deviation in terms of residual error away from the 0 line. Squared residuals against movement variability values again suggests higher movement variability levels show more spread in residual patterns. The plot of standardized residuals against fitted values suggests deviations greater than 2 to 3 standardized residual units.

Plots of the smoothers applied to explanatory variables can be found in Figure 4.20 and shows the variables are well modeled at the midpoints of their range but quality of fit declines at the tails of the value range especially lower values to the left of the distribution. Vorticity, divergence, SST, and Latitude show lack of fit at lower values but fit fairly well at the midpoint of the data range. Divergence and latitude both show lack of fit at the higher range of values. The Time variable provides interesting results as variability changes substantially with time post release with large scale changes occurring after day 100 causing a slight decrease in the quality of the smoothing fit.

Overall variability is not well fit using GAM with gamma distribution and the explanatory variables in the best model chosen. Much the same as speed, the tortuosity of the movement track is not indicative of the preference for environmental conditions using the specified available environmental characteristics. This implies a truly wandering pattern in sailfish movement with little outside factors affecting the level of movement variability or movement path tortuosity. This may be due to some physiological or genetic condition where the sailfish changes behavioral modes based on some physiological need such as feeding or spawning.

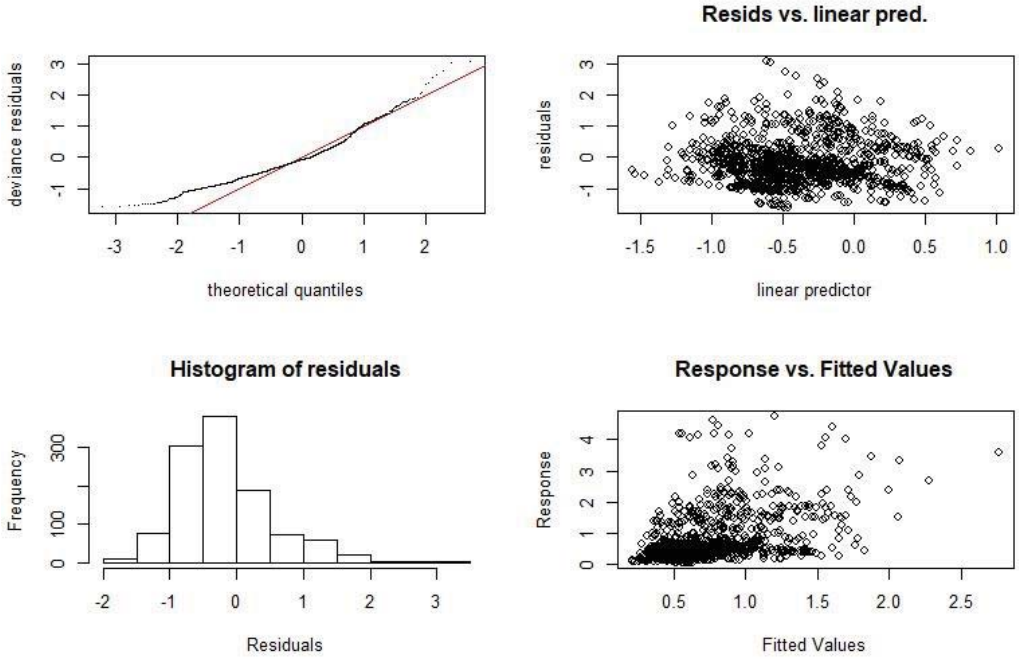

Figure 4.18 Sailfish variability parameter GAM model diagnostics including QQ-norm plot (top left), residuals versus linear predictor (trop right), histogram of model residuals (bottom left), and response variable against model fitted values (bottom right).

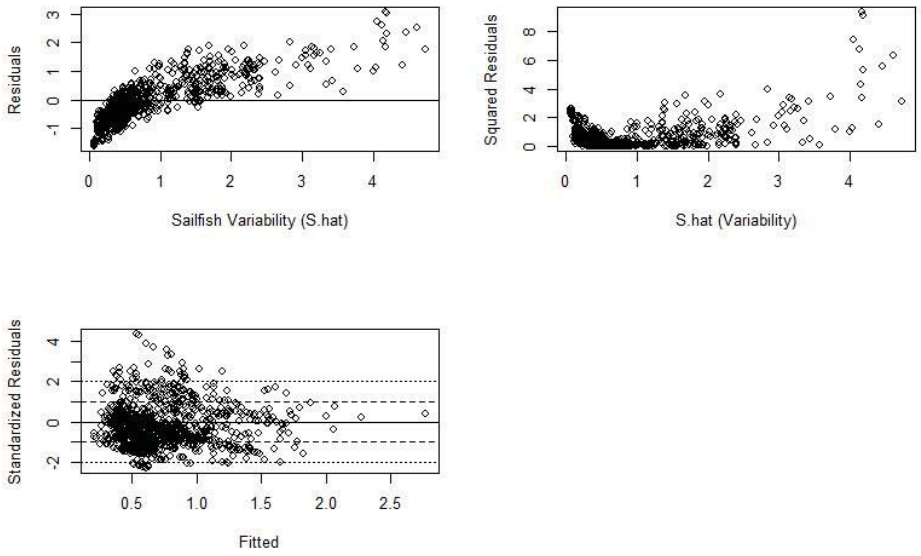

Figure 4.19 Sailfish variability parameter GAM model diagnostics including plot of model residuals against the variability variable (top left), squared residuals against variability variable (top right), and standardized residuals against model fitted values.

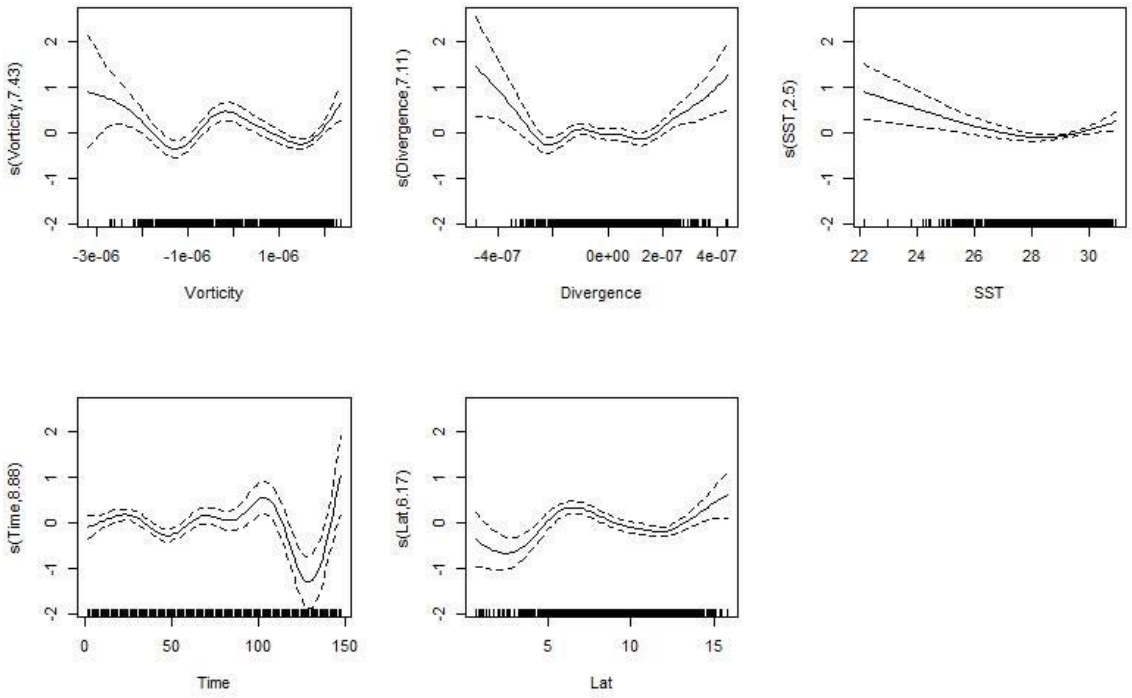

Figure 4.20 Sailfish variability parameter GAM model smoother diagnostics.

Rho.hat (Autocorrelation)

The best model for autocorrelation analyzed using a gamma distribution and log link confirmed the significance of all the explanatory variables but with an improved but still low R^2 value of 0.21, low deviance explained at 22.1% and a high generalized cross-validation (GCV) score of the GAM fitted at 1.8473, which indicated the fit of smoothers is lacking (Figure 4.21). The GCV suggests the fit of the smoothing parameters has increased prediction error in the model compared to the model for speed or variability. Overall the results here suggest a lack of fit of the model for the autocorrelation parameter. It is critically important to note here that the lack of fit is not simply an artifact of an improper analysis or error in estimation of the data, the lack of fit is indicative of behavioral traits in sailfish that do not allow for clear predictive modeling of preference due to the lack of information incorporated by the fish in the choice of whether to

continue moving with equal inertia/momentum or move toward a more searching behavioral mode.

The propensity for sailfish to wander over long distances with little recurring patterns in speed and variability create distributions of BCPA parameters with very small ranges of values for a majority of PSAT tagged sailfish. For this reason, the GAM model does little to differentiate between searching versus traveling modes as discussed in Chapter 3 of this dissertation. It is this structure of the data combined with the ecology and behavioral aspects of sailfish that results in poorly fitted GAM models.

```
Family: Gamma
Link function: log

Formula:
rho.hat ~ s(Vorticity) + s(Divergence) + s(Time) + s(Lat) + s(Lon)

Parametric coefficients:
            Estimate Std. Error t value Pr(>|t|)
(Intercept) -2.33684    0.02822  -82.82   <2e-16 ***
---
Signif. codes:  0 ‘***’ 0.001 ‘**’ 0.01 ‘*’ 0.05 ‘.’ 0.1 ‘ ’ 1

Approximate significance of smooth terms:
                edf Ref.df      F  p-value
s(Vorticity)  6.5197      9  8.152 5.57e-15 ***
s(Divergence) 0.6757      9  0.246     0.04 *
s(Time)       8.2024      9 39.548  < 2e-16 ***
s(Lat)        6.4549      9  6.489 1.29e-11 ***
s(Lon)        6.1742      9 18.584  < 2e-16 ***
---
Signif. codes:  0 ‘***’ 0.001 ‘**’ 0.01 ‘*’ 0.05 ‘.’ 0.1 ‘ ’ 1

R-sq.(adj) =   0.21   Deviance explained = 22.1%
GCV = 1.8473  Scale est. = 0.88777   n = 1115
```

Figure 4.21 Model result for autocorrelation or rho.hat BCPA GAM.

Figure 4.22 shows the fit is improved compared to the GAM for speed and variability as residual error is more normally distributed although again is not statistically qualified as a normal distribution (Shapiro Test p value=2.2e-16). The qq-norm plot

suggests an overall lack of fit at lower theoretical quantiles but more normally distributed at the midpoint and tails than speed of variability GAMS. The histogram of residuals suggests an overall bell shape but with a skew to the left of the distribution with a slight peak on the left tail of the distribution. Plots of the residuals of the model versus the linear predictor suggest less variability in residual error as the linear predictor increases and the response variable against the fitted values suggests increased variance in the response variable as fitted values increase..

Figure 4.23 shows the second set of diagnostic plots with residuals of the model plotted against the autocorrelation (rho.hat) variable which shows midrange autocorrelation values to have most variability in terms of residual error. Squared residuals against autocorrelation values again suggests midrange autocorrelation values to have more variable residual patterns. The plot of standardized residuals against fitted values suggests deviations much less extreme than for speed or variability with maximum deviation in residual patterns less than 3 standardize units.

Plots of the smoothers applied to explanatory variables can be found in Figure 4.24 and shows the variables are well modeled at the midpoints of their range but quality of fit declines at the tails of the value range. All explanatory variables showed larger error in the lower range of the values and improved fit at the midpoint; however, Time was found to cause large scale changes in the autocorrelation parameter and has a wider range of error in fitting. Divergence has a very small range relative to autocorrelation thus if fit fairly well. Latitude and longitude both show increased error in fit of the smoothers at the tails of the value range indicating lack of fit at the extremes of the migratory tracks spatially for the BCPA autocorrelation parameter which coincides with long distance

migrations toward the end of the track when sailfish were more likely to undergo highly autocorrelated movement patterns.

The autocorrelation parameter of the BCPA is the main variable of interest, and as mentioned previously, indicates the “movement inertia” of the sailfish path. The likelihood for a sailfish to continue moving along a migratory path with autocorrelation to the previous geolocated data point should provide insight into environmental factors that cause sailfish to discontinue an autocorrelated movement. Results of the GAM model suggest the available environmental variables may not be the main variables of interest to sailfish behavioral changes. In general, billfish physiology, especially their endothermy of eye and brain would suggest the species as a whole is capable of traveling through a wide range of temperature gradients (Block 1986) Given that temperature is driven variable relative to upwelling, it implies that billfish can travel long distances through significant temperature regime changes as demonstrated by the results presented here.

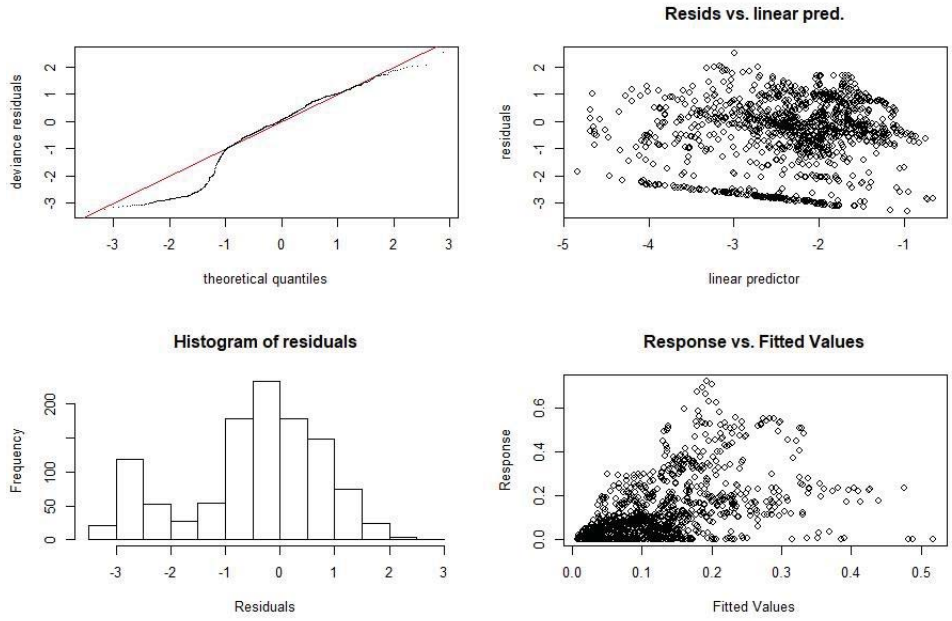

Figure 4.22 Sailfish autocorrelation parameter GAM model diagnostics including QQ-norm plot (top left), residuals versus linear predictor (trop right), histogram of

model residuals (bottom left), and response variable against model fitted values (bottom right).

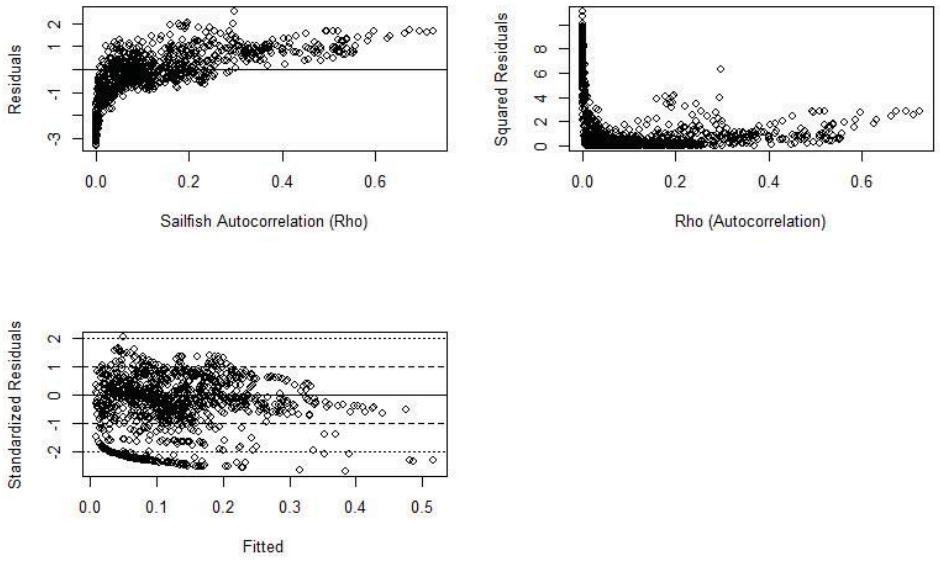

Figure 4.23 Sailfish autocorrelation parameter GAM model diagnostics including plot of model residuals against the autocorrelation variable (top left), squared residuals against autocorrelation variable (top right), and standardized residuals against model fitted values.

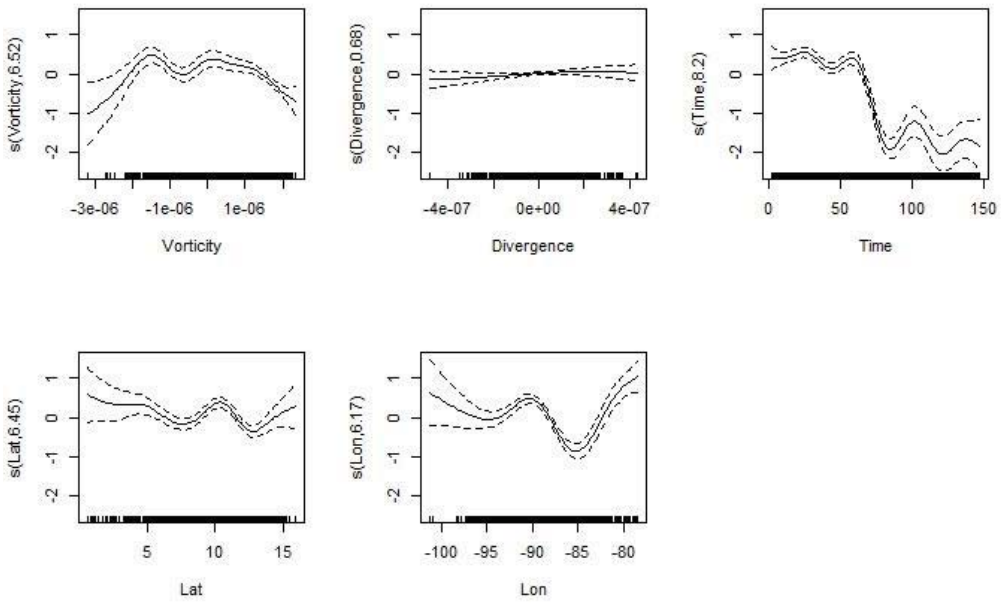

Figure 4.24 Sailfish autocorrelation parameter GAM model smoother diagnostics.

IATTC Purse Seine GAM Model Selection

Figure 4.25 shows the histograms of sailfish CPUE in the purse seine fishery in the EPO with non-transformed CPUE data in the top histogram showing the left skewed distribution expected from the catch in the purse seine fishery and the bycatch nature of billfish species within said fishery, and the log-transformed CPUE data in the bottom plot. Log transforming the CPUE data appears to normalize the data be transforming to a traditional bell curve; however highly significant Shapiro test (p value=2.996e-10) confirms the distribution not to be normal. For this reason, the Gaussian distribution is not implemented in the GAM in favor of the gamma distribution with log link that better matches the data structure.

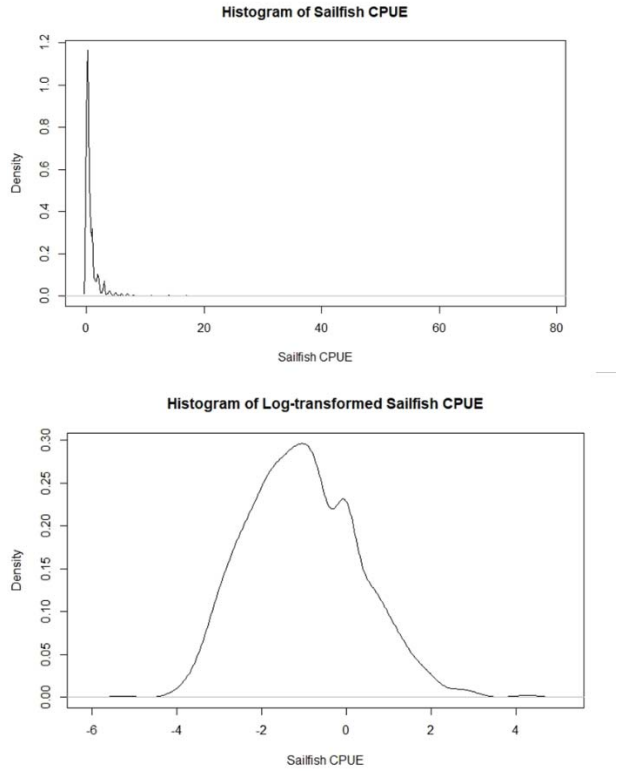

Figure 4.25 Histogram density plots for the response variable sailfish CPUE in original non-transformed state (top) and log-transformed (bottom).

Histograms of the explanatory variables from this purse seine sailfish catch GAM can be found in Figure 4.26 with vorticity, divergence, SST, latitude, and longitude all showing the structure of a traditional bell curve associated with normally distributed data. Chlorophyll-a data however showed a significant left skew with incidences of high values of chlorophyll but with extremely low density almost not visible in the plot.

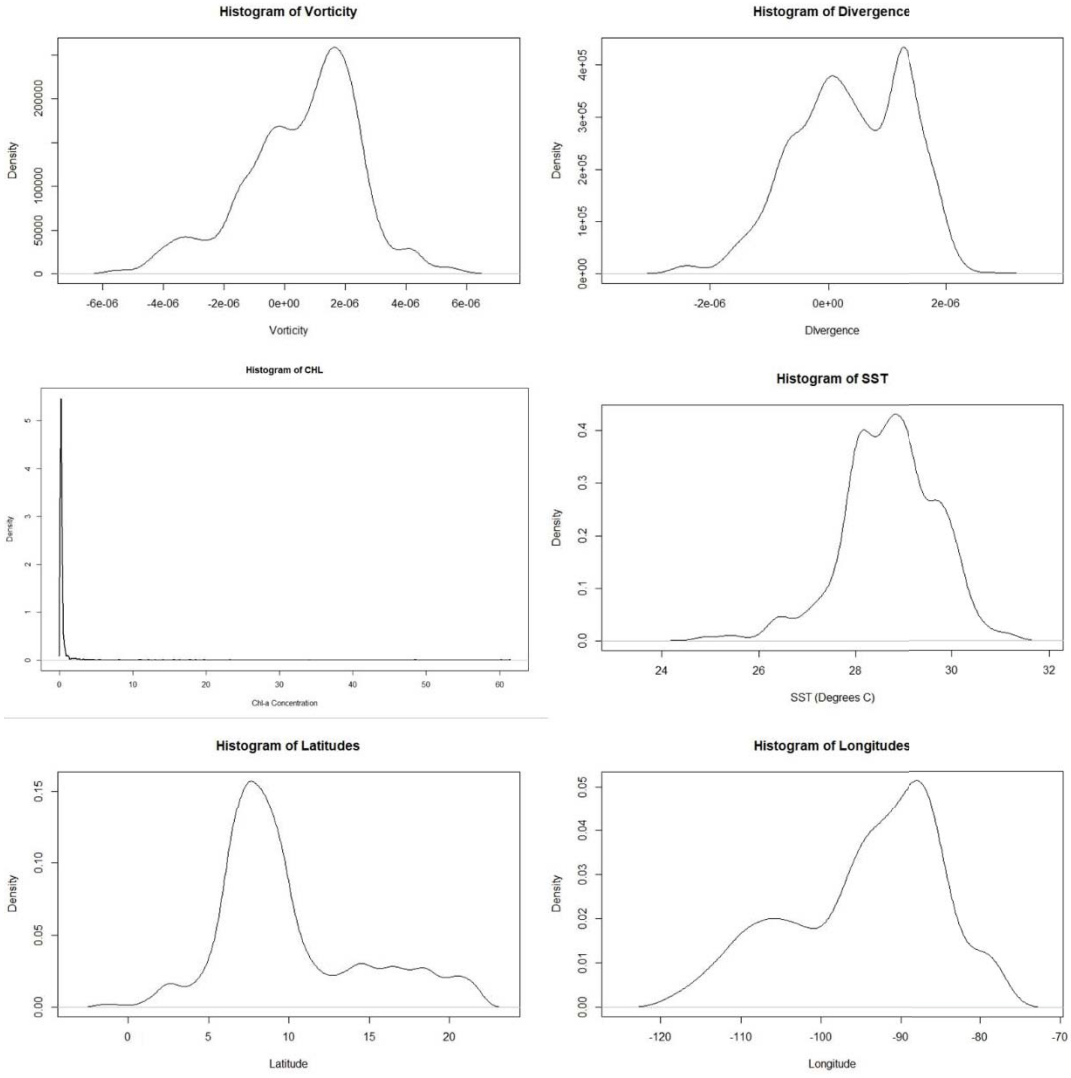

Figure 4.26 Histogram density plots for each of the explanatory variables: vorticity (top left), divergence (top right), Chlorophyll-a (middle left), SST (middle right), Latitude (bottom left), and longitude (bottom right).

The correlation matrix for the sailfish catch GAM shows a complete lack of correlation between any of the explanatory variables in the subset of catch data in the EPO where sailfish were caught in the tuna purse seine sets (Table 4.4). The highest level of correlation among explanatory variables occurs between latitude and SST at 0.3342 followed by the relationship between SST and divergence at -0.3165. Both of these correlations are sensible as SST changes with latitude as a whole, and divergence should results in SST changes based on scale and time of divergence. All other correlations are relatively low comparatively.

Table 4.4 Correlation matrix for explanatory variables in sailfish catch data GAM.

	SST	CHL	Divergence	Vorticity	Latitude
SST					
CHL	-0.0398				
Divergence	-0.3165	-0.0313			
Vorticity	-0.1012	0.0034	-0.0078		
Latitude	0.3342	-0.0405	-0.0267	0.0017	
Longitude	-0.011	0.1877	-0.0168	0.0189	-0.3182

The model selection procedure for the sailfish catch GAM suggest environmental factors have little to no influence on sailfish catch in the tuna purse seine fishery (Table 4.5). The best model contained only the explanatory variables of latitude and longitude with smoothing applied only to latitude. This result provides little insight into the environmental factors associated with sailfish preference thus the best model is not ideal for this chapter's analysis. Values for AIC decrease as a decreasing rate with each step in the model selection procedure. The removal of divergence in step 4 only decreased AIC by les than 2 thus the model chosen for the analysis includes divergence and is represented by the model in Table 4.5 as step 3.

Table 4.5 List of sailfish catch data GAM models produced by the step.GAM function in R software in order of decreasing AIC.

Start: SFACPUE ~ Vorticity + Divergence + SST + CHL + as.factor(Year) + as.factor(Month) + Lat + Lon;	AIC= 9474.862
Step:1 SFACPUE ~ Vorticity + Divergence + SST + CHL + as.factor(Month) + Lat + Lon;	AIC= 9455.422
Step:2 SFACPUE ~ Vorticity + Divergence + SST + CHL + Lat + Lon ;	AIC= 9446.897
Step:3 SFACPUE ~ Vorticity + Divergence + SST + CHL + s(Lat) + Lon ;	AIC= 9439.285
Step:4 SFACPUE ~ Vorticity + SST + CHL + s(Lat) + Lon ;	AIC= 9437.377
Step:5 SFACPUE ~ Vorticity + CHL + s(Lat) + Lon ;	AIC= 9435.612
Step:6 SFACPUE ~ CHL + s(Lat) + Lon ;	AIC= 9433.951
Step:7 SFACPUE ~ s(Lat) + Lon ;	AIC= 9432.472

IATTC Purse Seine GAM analysis

Both log transformed sailfish CPUE data and non-transformed CPUE were analyzed through GAM models with differing distributions and link functions with dramatically improved results using non-transformed CPUE data and a gamma distribution and log link function. For the purposes of this chapter, only the non-transformed CPUE GAM will be discussed in results as the transformed gaussian GAM revealed a complete lack of fit with less than 6% deviance explained, a low R^2, and a high GCV score indicating lack of fit of smoothing functions and increased predictive error. The lack of normality of the log-transformed CPUE data combined with the lack of fit negates the proper use of this model (Figure 4.27).

The fact that the best model does not include environmental characteristics suggest tuna purse seine catch data for sailfish reveals no signals of environmental influence likely due to the bycatch aspect of sailfish in the tuna purse seine fishery and the lack of targeting sailfish preferential habitat by the tuna directed fishery. Because this chapter seeks to elucidate environmental impacts on sailfish catch, the results of the best model that incorporated the chosen environmental characteristics is presented in this chapter.

Results from the GAM model suggest the fit using gamma distribution with log link and non-transformed CPUE data is only marginally better than those of the gaussian distribution GAM and log-transformed data. The only smoothed term, as expected, shows significance, as does longitude which was not smoothed. The R^2 statistic suggest this model does not fit the response variable at 0.0168 by any means. Oddly, the deviance explained is substantially larger than the R^2 statistic suggests but is still low at 12.2%. The GCV score is far from 0 thus suggest smoothers are estimated with relatively high predictive error. Overall this GAM model does not represent an informative analysis of specific environmental characteristics relative to sailfish presence in purse seined tuna catch.

```
Family: Gamma
Link function: log

Formula:
SFACPUE ~ Vorticity + SST + CHL + Divergence + s(Lat) + Lon

Parametric coefficients:
              Estimate Std. Error t value Pr(>|t|)
(Intercept)  1.918e+00  2.219e+00   0.864  0.38744
Vorticity   -1.914e+04  2.986e+04  -0.641  0.52163
SST          2.193e-02  6.968e-02   0.315  0.75300
CHL         -2.326e-02  2.030e-02  -1.146  0.25207
Divergence  -5.816e+02  6.619e+04  -0.009  0.99299
Lon          2.817e-02  9.039e-03   3.116  0.00186 **
---
Signif. codes:  0 ‘***’ 0.001 ‘**’ 0.01 ‘*’ 0.05 ‘.’ 0.1 ‘ ’ 1

Approximate significance of smooth terms:
         edf Ref.df     F  p-value
s(Lat) 7.491      9 4.112 5.04e-06 ***
---
Signif. codes:  0 ‘***’ 0.001 ‘**’ 0.01 ‘*’ 0.05 ‘.’ 0.1 ‘ ’ 1

R-sq.(adj) =  0.0168   Deviance explained = 12.2%
GCV = 1.8105  Scale est. = 5.6599    n = 1792
```

Figure 4.27 Results of sailfish catch data GAM.

Figure 4.28 shows the result of the sailfish CPUE GAM model which is overall poorly fitting using the model chosen. The qq-norm plot shows strong deviation from normal throughout, especially at the tails of the distribution. The histogram of residuals suggests an overall bell shape but with a skew to the left of the distribution. Plots of the residuals of the model versus the linear predictor suggest increased variance in residual error as the linear predictor increases and the response variable against the fitted values suggests increased variance in the response variable as fitted values increase.

Figure 4.29 shows the second set of diagnostic plots for the purpose of further evaluating the distribution of residuals and overall fit of the model. The residuals of the model plotted against the response sailfish CPUE variable, which shows that a small sample of high catches biases the model with increased variance due to incidences of very high catches relative to typical CPUE levels. Squared residuals against sailfish CPUE also suggests few isolated high catches that represent outliers in the data that may cause lack of fit in the modeling procedure. The plot of standardized residuals against fitted values suggests extreme deviations exist in the data with values reaching nearly 8 standardized units away from expected. This result also suggests that the nature of the data generates a lack of fit of the model. Plots of the smoother applied only to latitude in this model shows the tails of the data distribution to have much less ideal fits than the central portion of the distribution (Figure 4.30).

Results of the GAM model suggest tuna purse seine catch combined with the choice of explanatory environmental variables is not a useful method to discern preference for habitat characteristics of a bycatch species such as sailfish. Little

information is gleaned from this tuna purse seine catch analysis resulting in such a non-significant fit of the model to the data.

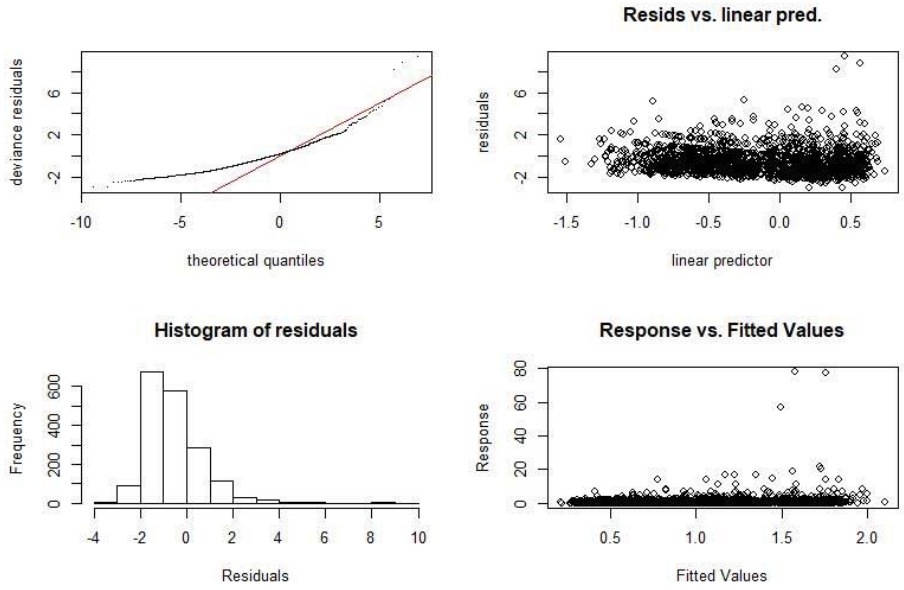

Figure 4.28 Sailfish catch data GAM model diagnostics including QQ-norm plot (top left), residuals versus linear predictor (trop right), histogram of model residuals (bottom left), and response variable against model fitted values (bottom right).

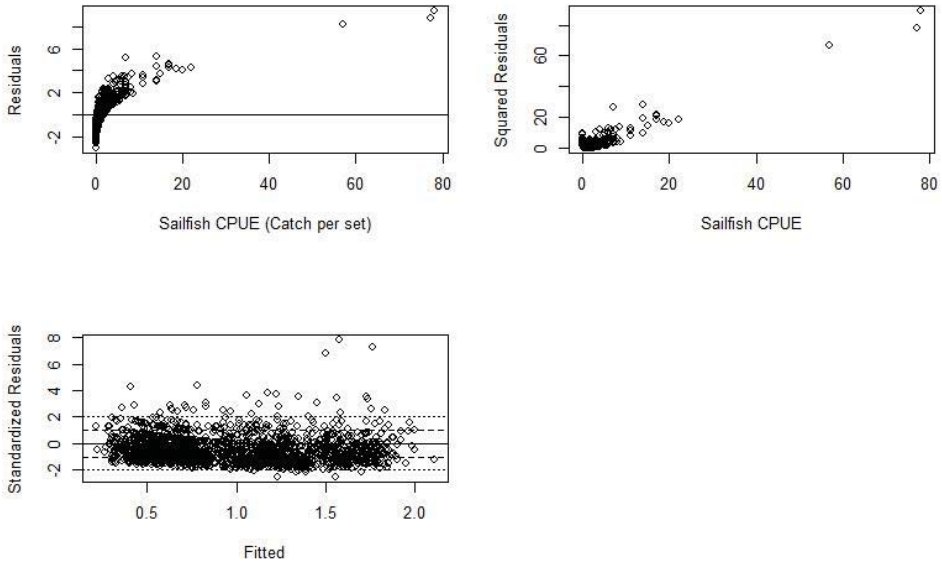

Figure 4.29 Sailfish catch data GAM model diagnostics including plot of model residuals against sailfish CPUE (top left), squared residuals against sailfish CPUE (top right), and standardized residuals against model fitted values.

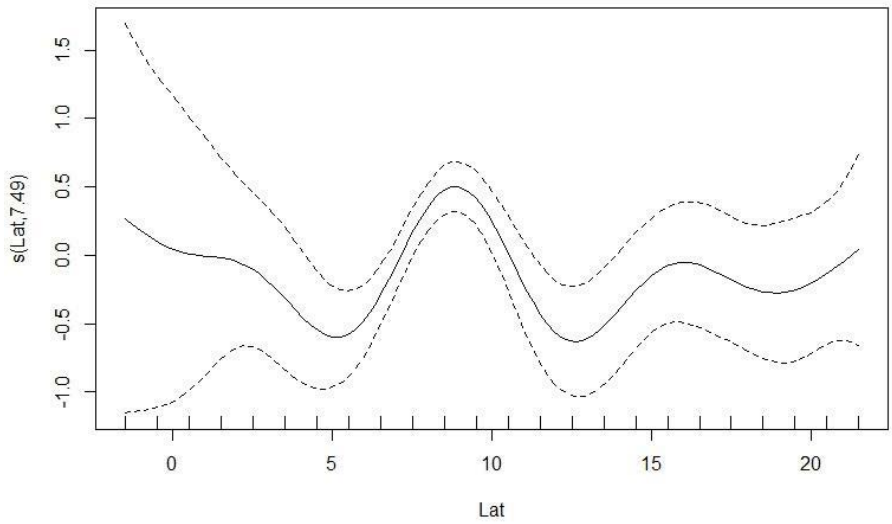

Figure 4.30 Diagnostic of smoother applied to latitude in sailfish catch data GAM.

Blue Marlin GAM Results

BCPA Parameter GAM Model Selection

Distributions of the three BCPA parameters associated with speed (mu.hat), variability (s.hat), and autocorrelation (rho.hat) are found in Figure 4.31. The histogram for speed suggests a right skew with higher relative speeds making up the majority of values; however negative values exist, eliminating the gamma distribution with log link GAM as an option for analysis. The opposite is true for variability and autocorrelation where data is skewed left with low values making up the majority of the data set. For this reason, variability and autocorrelation are modeled similarly within the GAM methodology where speed applies different distributional and link analysis.

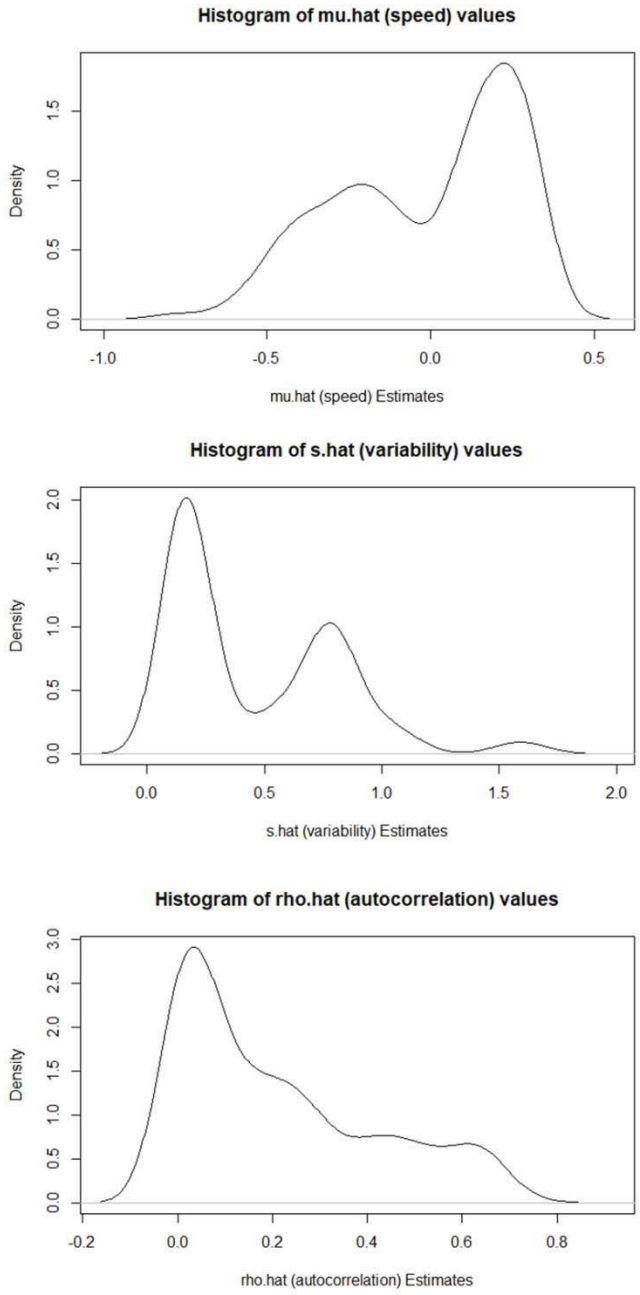

Figure 4.31 Histogram density plots for each of the response variables: speed or mu.hat (top), movement variability or s.hat (middle), and autocorrrelation of movement or rho.hat (bottom).

The distributions of explanatory variables can be found in Figure 4.32 and are used to examine the distribution of values. The distribution of values for Time (# Days Postrelease) suggests left skew with majority of values occurring less than 100 days which is expected based on the deployment times of PSATs for blue marlin and the

decreasing probability of retention as deployment times increase. Latitude and longitude are both relatively normally distributed with narrower ranges compared to sailfish due to the more confined migratory paths and lack of sustained travel outside of the Coco's Island Ridge region of the tropical EPO.

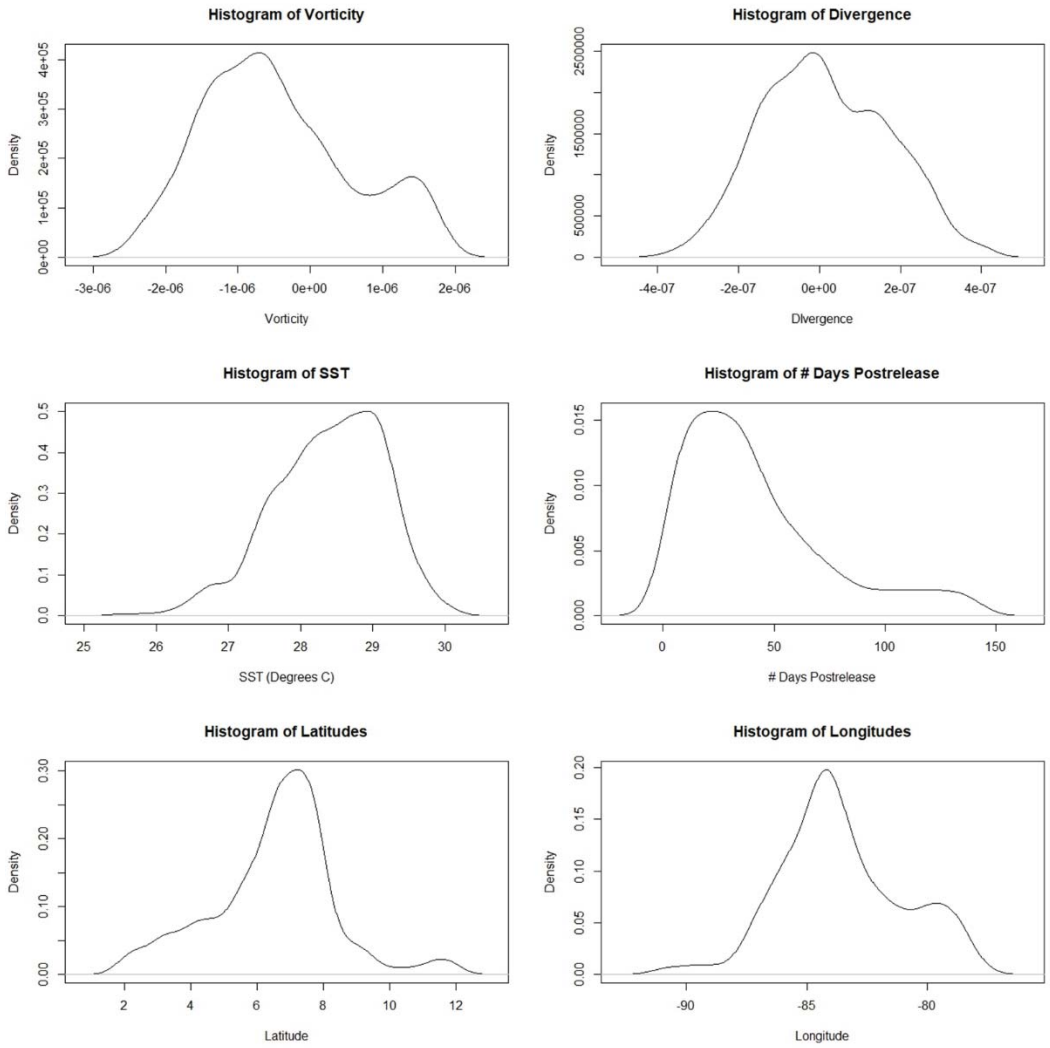

Figure 4.32: Histogram density plots for each of the explanatory variables: vorticity (top left), divergence (top right), SST (middle left), Time or # of days postrelease (middle right), Latitude (bottom left), and longitude (bottom right).

Table 4.6 shows the correlation matrix for explanatory variables incorporated into the blue marlin BCPA GAM analysis. Correlation results suggest a lack of correlated

explanatory variables in all cases with highest correlation seen being between latitude and longitude at -0.4641. No significant correlations exist that need to be addressed in the statistical model moving forward in the analysis. An interesting negative correlation of 0.3540 exists between time and SST. This is likely the effect of seasonal difference in SST as the majority of PSATs were deployed in spring and as time increased, moved toward warmer SST summer months.

Table 4.6 Correlation matrix showing explanatory variables used for blue marlin BCPA GAM analysis.

	Vorticity	Divergence	SST	Latitude	Longitude	Time
Vorticity	1.0000	-0.2609	0.1707	-0.1088	-0.0182	-0.2447
Divergence	-0.2609	1.0000	-0.0498	0.2211	0.0318	-0.2005
SST	0.1707	-0.0498	1.0000	0.2675	-0.1514	-0.3540
Latitude	-0.1088	0.2211	0.2675	1.0000	-0.4641	-0.1326
Longitude	-0.0182	0.0318	-0.1514	-0.4641	1.0000	0.3945
Time	-0.2447	-0.2005	-0.3540	-0.1326	0.3945	1.0000

Model selection using the step.GAM function supplied 5 steps for speed and variability GAM models and 6 steps for autocorrelation (Table 4.7). Best models for speed and variability include all environmental variables but SST is left as a parametric coefficient because of its more linear relationship to the response variable as suggest by the step.GAM procedure, while other variables are smoothed. The autocorrelation GAM best model removes longitude from the model and places smoothing functions on all 3 environmental variable including SST.

Table 4.7 List of blue marlin BCPA GAM models created by the step.GAM function in R program. Steps are listed in order for each response variable with descending values of AIC.

Mu.hat (Speed)	
Start: mu.hat ~ Vorticity + Divergence + SST + Time + Lat + Lon;	AIC= -212.4244
Step:1 mu.hat ~ Vorticity + Divergence + SST + s(Time) + Lat + Lon ;	AIC= -284.1536
Step:2 mu.hat ~ s(Vorticity) + Divergence + SST + s(Time) + Lat + Lon ;	AIC= -326.9207
Step:3 mu.hat ~ s(Vorticity) + s(Divergence) + SST + s(Time) + Lat;	AIC= -361.7099
Step:4 mu.hat ~ s(Vorticity) + s(Divergence) + SST + s(Time) + s(Lat);	AIC= -386.7790
Step:5 mu.hat ~ s(Vorticity) + s(Divergence) + SST + s(Time) + s(Lat) + s(Lon) ;	AIC= -397.7028
S.hat (Variability)	
Start: s.hat ~ Vorticity + Divergence + SST + Time + Lat + Lon;	AIC= 144.2564
Step:1 s.hat ~ Vorticity + Divergence + SST + s(Time) + Lat + Lon ;	AIC= 29.1396
Step:2 s.hat ~ Vorticity + s(Divergence) + SST + s(Time) + Lat + Lon ;	AIC= -39.8794
Step:3 s.hat ~ s(Vorticity) + s(Divergence) + SST + s(Time) + Lat ;	AIC= -100.3724
Step:4 s.hat ~ s(Vorticity) + s(Divergence) + SST + s(Time) + s(Lat);	AIC= -114.9224
Step:5 s.hat ~ s(Vorticity) + s(Divergence) + SST + s(Time) + s(Lat) + s(Lon) ;	AIC= -125.6444
Rho.hat (Autocorrelation)	
Start: rho.hat ~ Vorticity + Divergence + SST + Time + Lat + Lon;	AIC= -332.8684
Step:1 rho.hat ~ s(Vorticity) + Divergence + SST + Time + Lat + Lon ;	AIC= -422.7776
Step:2 rho.hat ~ s(Vorticity) + Divergence + SST + Time + s(Lat) + Lon ;	AIC= -483.9080
Step:3 rho.hat ~ s(Vorticity) + s(Divergence) + SST + Time + s(Lat) + Lon ;	AIC= -528.2637
Step:4 rho.hat ~ s(Vorticity) + s(Divergence) + SST + s(Time) + s(Lat) + Lon ;	AIC= -561.5726
Step:5 rho.hat ~ s(Vorticity) + s(Divergence) + SST + s(Time) + s(Lat) + s(Lon) ;	AIC= -567.4644
Step:6 rho.hat ~ s(Vorticity) + s(Divergence) + s(SST) + s(Time) + s(Lat);	AIC= -574.4235

BCPA Parameter GAM Analysis

Mu.hat (Speed)

The best model for speed analyzed using a gaussian distribution and identity link confirmed the significance of the explanatory variables and a drastically improved model fit compared to sailfish speed GAM results. The GAM produced an R^2 statistic of 0.743, a deviance explained of 75.9%, and a very low GCV score of 0.020429 (Figure 4.33). These results suggest GAM modeling of BCPA parameter of speed in blue marlin provides useful insight into the variance in speed explained by environmental characteristics both parametric and nonparametric. Results suggest speed is regulated by blue marlin relative to vorticity, divergence, SST, chlorophyll and location in time and space.

```
Family: gaussian
Link function: identity

Formula:
mu.hat ~ s(Vorticity) + s(Divergence) + SST + s(Time) + s(Lat) +
    s(Lon)

Parametric coefficients:
            Estimate Std. Error t value Pr(>|t|)
(Intercept)  1.32329    0.38431   3.443 0.000626 ***
SST         -0.04705    0.01353  -3.476 0.000555 ***
---
Signif. codes:  0 ‘***’ 0.001 ‘**’ 0.01 ‘*’ 0.05 ‘.’ 0.1 ‘ ’ 1

Approximate significance of smooth terms:
                edf Ref.df      F  p-value
s(Vorticity)  7.788      9 18.825  < 2e-16 ***
s(Divergence) 5.643      9 17.949  < 2e-16 ***
s(Time)       6.866      9 34.503  < 2e-16 ***
s(Lat)        8.178      9  9.592 7.72e-16 ***
s(Lon)        2.245      9  3.337 2.96e-08 ***
---
Signif. codes:  0 ‘***’ 0.001 ‘**’ 0.01 ‘*’ 0.05 ‘.’ 0.1 ‘ ’ 1

R-sq.(adj) =  0.743   Deviance explained = 75.9%
GCV = 0.020429  Scale est. = 0.019111  n = 507
```

Figure 4.33 Model result for blue marlin speed parameter BCPA GAM.

Figure 4.34 shows the first set of diagnostic plots for the blue marlin speed GAM analysis. The qq-norm plot suggests moderate fit in the majority of the observational range with the exception of the leftmost tail of the theoretical quantiles. Although this deviation appears in the qq-norm plot, the histogram of residuals suggests an overall normal distribution of residuals which represents substantial improvement of model fit when compared to sailfish GAM models for BCPA parameters. This is likely due to the more constrained region of presence and the overall lack of behavioral shifts in blue marlin compared to sailfish. Plots of the residuals of the model versus the linear predictor show an overall decrease in residual variance with increasing values of the linear predictor. The response variable, speed, or mu.hat in this case, against the fitted values suggest speed increases with increased fitted values of the model.

Figure 4.35 shows the second set of diagnostic plots with residuals of the model plotted against the speed variable revealing a relatively tight grouping about the zero line which implies residuals lack variance suggesting a model that fit to the data well. The squared residual plot reveals increased variation in squared residuals at lower levels of speed and a slight increase in variation at the highest speed values. The plot of standardized residuals against fitted values suggests deviations up to 4 standardize residual units but with a tighter grouping than previously seen in other GAM analysis in this chapter; however, two groupings exist in the plot separated by lower and higher fitted values. This grouping may suggest bimodal speed characteristics in the blue marlin GAM model.

Plots of the smoothers applied to explanatory variables can be found in Figure 4.36. Vorticity appears well modeled with consistent fit while vorticity shows characteristic regressional tight bounds at the midpoint but lack of fit at the tails of the distribution. The Time variable model is fit to the data fairly well at low values but the bound increase in spread as values increase. Latitude smoothing reveals an overall good fit but as latitude increases, the fit appears to degrade. Longitude shows characteristically good fit at the mid-range of values and a decreased model fit at the tails of the value range.

Overall speed is well fit using the GAM with gaussian distribution and the explanatory variables in the best model chosen. Blue marlin exhibit relatively consistent speed throughout their migratory tracks with lesser range of values compared to sailfish which may improve the modeling fitting procedure and improve the amount of variance explained by the environmental variables.

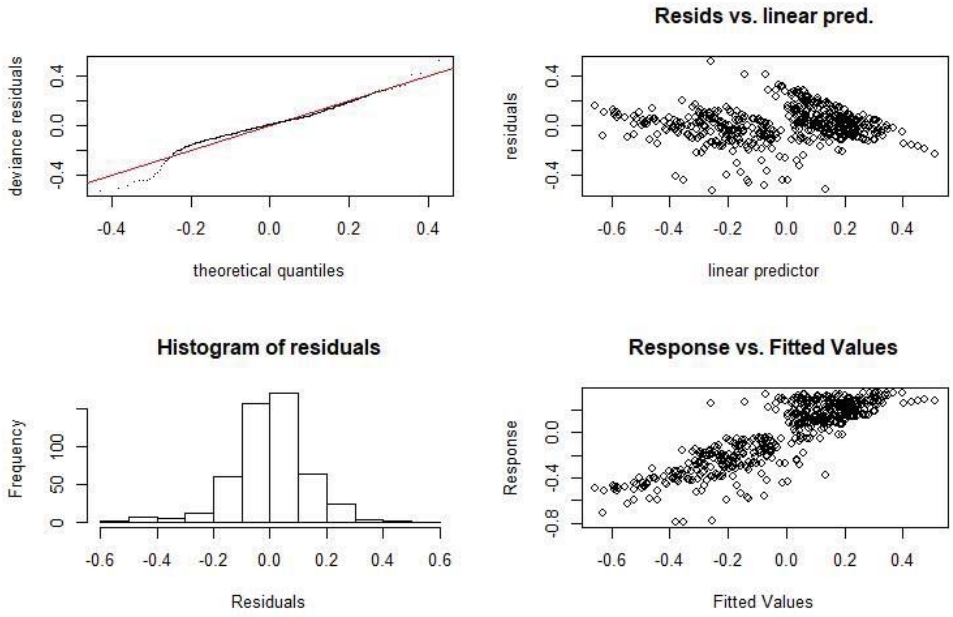

Figure 4.34 Blue marlin speed parameter GAM model diagnostics including QQ-norm plot (top left), residuals versus linear predictor (trop right), histogram of model residuals (bottom left), and response variable against model fitted values (bottom right).

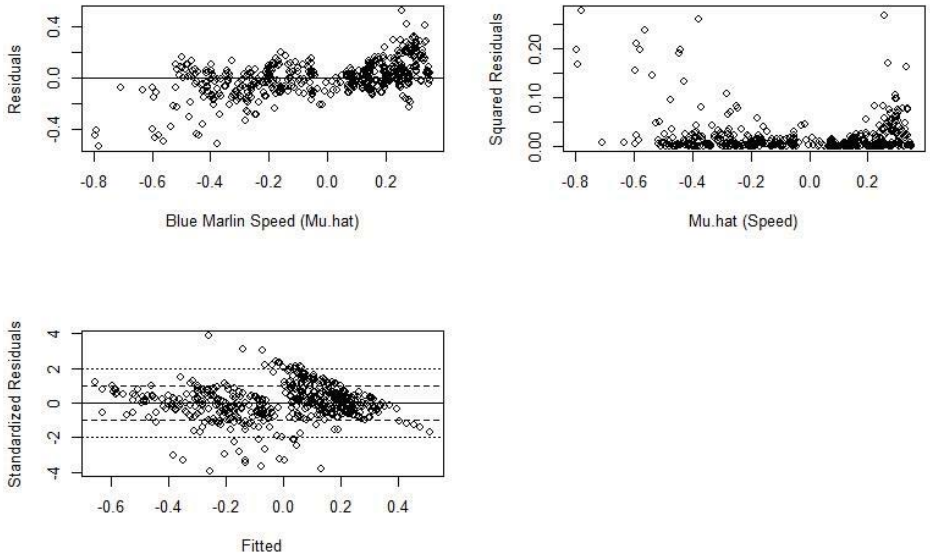

Figure 4.35 Blue marlin speed parameter GAM model diagnostics including plot of model residuals against the speed variable (top left), squared residuals against speed variable (top right), and standardized residuals against model fitted values.

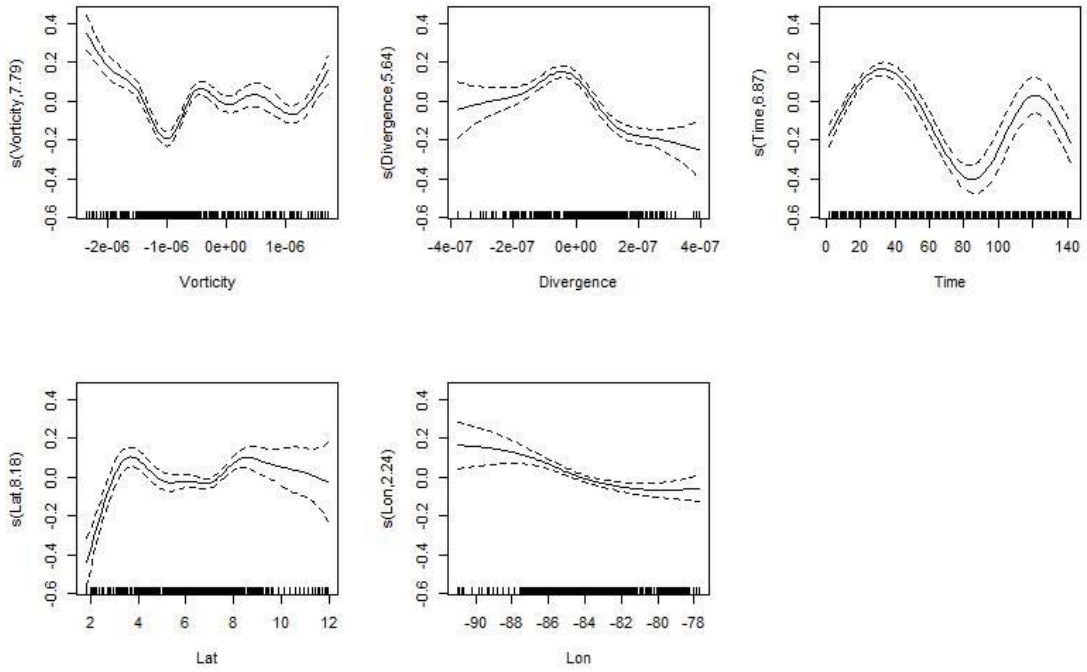

Figure 4.36 Blue marlin speed parameter GAM model smoother diagnostics.

S.hat (Variability)

The best model for variability analyzed using a gamma distribution and log link confirmed the significance of all the explanatory variables (Figure 4.37). Explanatory variables were used in the GAM model with all characterized as non-parametric relative to the response with the only exception being SST which was designated as parametric due to the linear relationship with blue marlin movement path variability or s.hat. The GAM resulted in an adjusted R^2 of 0.721 indicating variance in variability, or s.hat, is explained well using the explanatory variables in the best model. Deviance explained is highest of any GAM run in this chapter at 81.2% and a GCV score of 0.1442 suggest relatively low predictive error in the smoothing procedure.

```
Family: Gamma
Link function: log

Formula:
s.hat ~ s(Vorticity) + s(Divergence) + SST + s(Time) + s(Lat) +
    s(Lon)

Parametric coefficients:
            Estimate Std. Error t value Pr(>|t|)
(Intercept) -4.86549    1.03857  -4.685 3.68e-06 ***
SST          0.13467    0.03658   3.682 0.000258 ***
---
Signif. codes:  0 ‘***’ 0.001 ‘**’ 0.01 ‘*’ 0.05 ‘.’ 0.1 ‘ ’ 1

Approximate significance of smooth terms:
                edf Ref.df      F p-value
s(Vorticity)  8.014      9 18.168  <2e-16 ***
s(Divergence) 4.770      9 32.874  <2e-16 ***
s(Time)       8.118      9 31.825  <2e-16 ***
s(Lat)        8.122      9 14.615  <2e-16 ***
s(Lon)        6.413      9  9.815  <2e-16 ***
---
Signif. codes:  0 ‘***’ 0.001 ‘**’ 0.01 ‘*’ 0.05 ‘.’ 0.1 ‘ ’ 1

R-sq.(adj) =  0.721   Deviance explained = 81.2%
GCV = 0.1442  Scale est. = 0.1307    n = 507
```

Figure 4.37 Model result for blue marlin movement variability or s.hat BCPA GAM.

Figure 4.38 shows the fit and normality of residuals is quite good with little to no deviation in the qq-norm plot and tradition bell curve shaped residuals in the histogram. Plots of the residuals of the model versus the linear predictor reveals a somewhat concerning level of clustering and a systematic relationship with the residuals which may suggest this model may not be as well fit to the data as the R^2 and deviance explained values suggest. The response variable against the fitted values plot suggests increasing values in variability as fitted values increase.

Figure 4.39 shows the second set of diagnostic plots with residuals of the model plotted against the variability (s.hat) variable showing an overall good distribution of residuals about the zero line. The squared residuals against variability values indicate increased range of squared residuals when variability is at low levels, at high levels, and at the midpoint of the variability range with decreased squared residuals in between these 3 values regions. The plot of standardized residuals against fitted values suggests the model fit the data well with distributed standardized residuals about the zero line and within 3 standard residual units.

Plots of the smoothers applied to explanatory variables can be found in Figure 4.40 and shows the variables to be well modelled overall. Vorticity, divergence, and longitude show lack of fit or poor modelling of variables at the lowest range of values with improved fit toward the midpoint and end of the value range, which is characteristic of regression, for vorticity where divergence and longitude also has a slight less well fit tail at higher values. Time and latitude variables have well fit smoothers through the midpoint of value range but with decreasing quality of fit from midpoint to the end of the trial. This is consistent with previous Time variable smoothing as this represent the number of days postrelease with few long duration tags limiting number of data points at the upper range.

Overall, blue marlin movement path variability estimated by the BCPA appears well modeled using the GAM methodology with gamma distribution and log link function. Blue marlin variability range, like the range for speed, is reduced compared to sailfish, possibly improving the quality of model fitting but creating systematic and clustering residual relationship against the linear predictor.

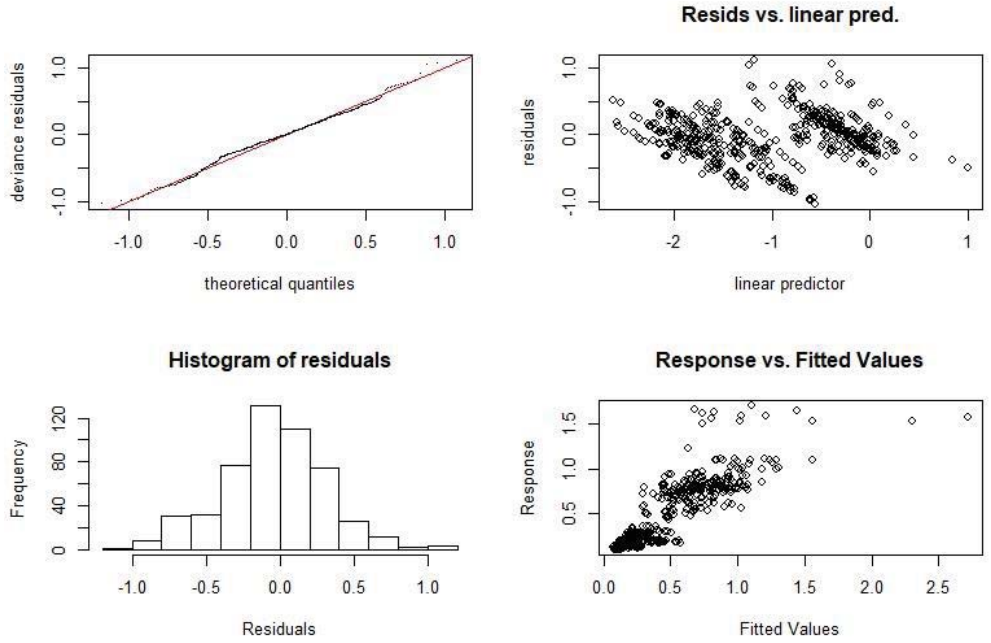

Figure 4.38 Blue marlin variability parameter GAM model diagnostics including QQ-norm plot (top left), residuals versus linear predictor (trop right), histogram of model residuals (bottom left), and response variable against model fitted values (bottom right).

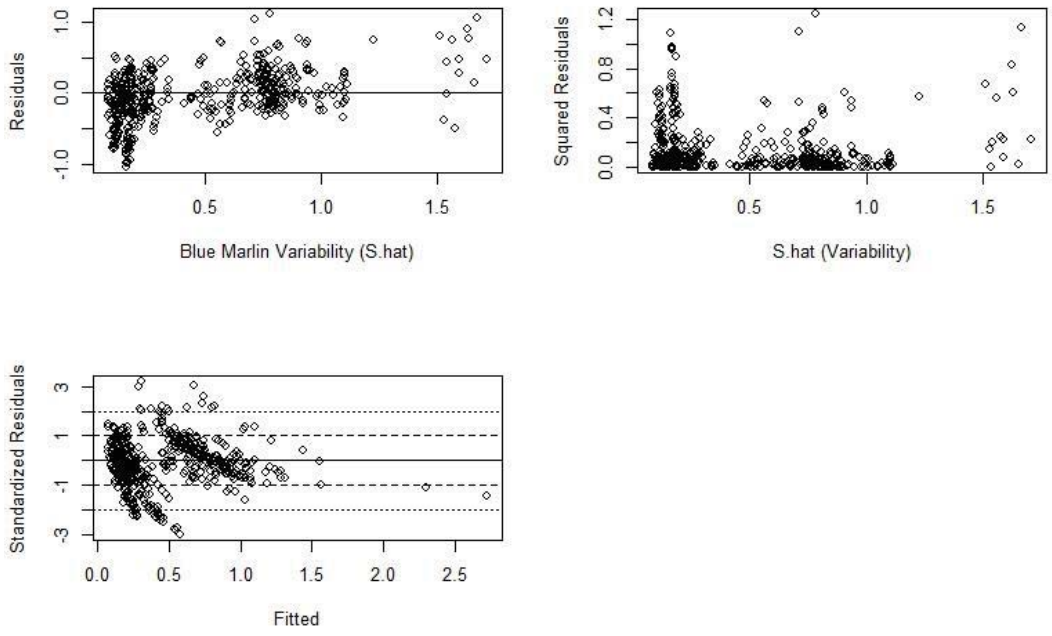

Figure 4.39 Blue marlin variability parameter GAM model diagnostics including plot of model residuals against the variability variable (top left), squared residuals

against variability variable (top right), and standardized residuals against model fitted values.

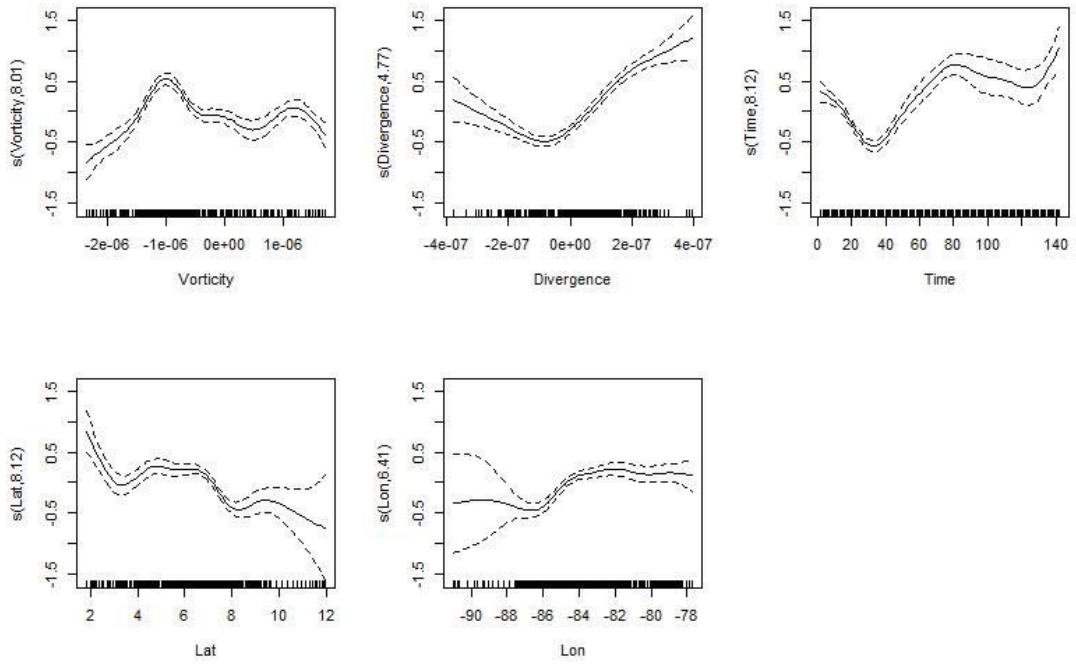

Figure 4.40 Blue Marlin variability parameter GAM model smoother diagnostics.

Rho.hat (Autocorrelation)

The best model for autocorrelation analyzed using a gamma distribution and log link confirmed the significance of all the explanatory variables except SST which was determined not to be significant in the GAM model (Figure 4.41). Model fit of this GAM is very poor although the deviance explained is 47.8%, the adjusted R^2 statistic is -3.34 indicating the unadjusted R^2 to be very low meaning the explanatory variables do not model the response variable. This lack of fit is further exemplified by a high GCV score indicating high levels of potential predictive error in the smoothing procedure. Compared to speed and movement path variability, autocorrelation values have more variable patterns within individual blue marlin tracks potentially creating a similar situation as

seen in sailfish autocorrelation GAM results. This suggests the possibility of autocorrelation, or movement inertia, may not have sptial or temporal relationships with the explanatory variables and is linked to sailfish and blue marlin behavioral traits such as hunger or the need to spawn that is not quantified in this study.

```
Family: Gamma
Link function: log

Formula:
rho.hat ~ s(Vorticity) + s(Divergence) + s(SST) + s(Time) + s(Lat)

Parametric coefficients:
            Estimate Std. Error t value Pr(>|t|)
(Intercept) -2.09027    0.04048  -51.64   <2e-16 ***
---
Signif. codes:  0 ‘***’ 0.001 ‘**’ 0.01 ‘*’ 0.05 ‘.’ 0.1 ‘ ’ 1

Approximate significance of smooth terms:
                   edf Ref.df      F p-value
s(Vorticity)  6.979e+00      9  9.773  <2e-16 ***
s(Divergence) 7.210e+00      9 42.795  <2e-16 ***
s(SST)        4.191e-05      9  0.000   0.375
s(Time)       8.558e+00      9 46.511  <2e-16 ***
s(Lat)        8.462e+00      9 23.599  <2e-16 ***
---
Signif. codes:  0 ‘***’ 0.001 ‘**’ 0.01 ‘*’ 0.05 ‘.’ 0.1 ‘ ’ 1

R-sq.(adj) =  -3.34   Deviance explained = 47.8%
GCV = 1.3371  Scale est. = 0.83079   n = 507
```

Figure 4.41 Model result for blue marlin autocorrelation or rho.hat BCPA GAM.

Figure 4.42 reveals the normality of residuals from the GAM model and suggests a slight deviation on the left tail of the qq-norm plot and the histogram of residuals where a bell shape with left skew exists. The plot of residuals of the model versus the linear predictor suggests an overall lack of a distinct pattern while the response variable against the fitted values suggests increased variance in the response variable as fitted values increase. Autocorrelation parameter GAM results are substantially less well fitted than

speed or variability BCPA parameters, similar to the GAM analyses for sailfish, have more discernible trends on the GAM diagnostics than speed or variability GAMs.

Figure 4.43 shows the second set of diagnostic plots with residuals of the model plotted against the autocorrelation (rho.hat) variable which shows a relative wide range in residuals as autocorrelation values increase but with equal distribution about the zero line. Squared residuals against autocorrelation values again suggests increased variance in residuals as autocorrelation values increase. The plot of standardized residuals against fitted values shows a clustering of residuals at the lowest range of fitted values with a lack of distribution about the zero line and abnormal residual points at high fitted values.

Plots of the smoothers applied to explanatory variables can be found in Figure 4.44 and shows the variables are well modeled with the exception of SST. Further examination of the oddity that is the SST smoother reveals an estimated degrees of freedom of 0.0004 which indicates a potential problem with the smoothing procedure or choice of SST as a smoothed term. The GAM was rerun with SST as a parametric term; however, the GAM modeling actually decreased in quality of fit suggesting the SST should be a smoothed term. Values within SST were double checked for validity and all aspects appeared appropriate thus the GAM model with SST as a smoothed term was maintained as the best possible model. Vorticity, Time, and latitude are well fit in terms of smoothing; however, divergence see lack of fit at low and high values.

The autocorrelation parameter of the BCPA is the main variable of interest, and as mentioned previously, indicates the “movement inertia” of the blue marlin path. The likelihood for a blue marlin to continue moving along a migratory path with autocorrelated movement from the previous geolocated data point should provide insight

into environmental factors that cause blue marlin to discontinue an autocorrelated movement. Results of the GAM model suggest the use f BCPA developed autocorrelation values may not indicate behavioral preference for environmental signals in sailfish or blue marlin as the autocorrelation GAMs did not provide discernible evidence of preference for vorticity, divergence, SST, or spatial and temporal characteristics using the chosen methodology. Oddly the model claims to describe almost half of the explained deviance but this statistic should not be considered more important than the highly negative adjusted R^2 that indicated a lack of model fit.

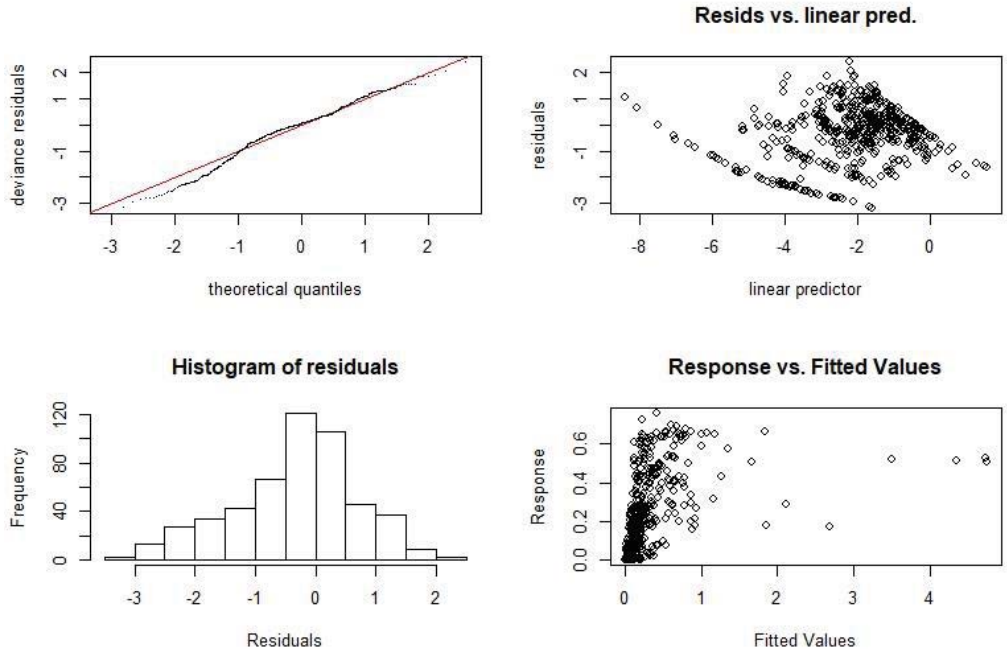

Figure 4.42 Blue marlin autocorrelation parameter GAM model diagnostics including QQ-norm plot (top left), residuals versus linear predictor (trop right), histogram of model residuals (bottom left), and response variable against model fitted values (bottom right).

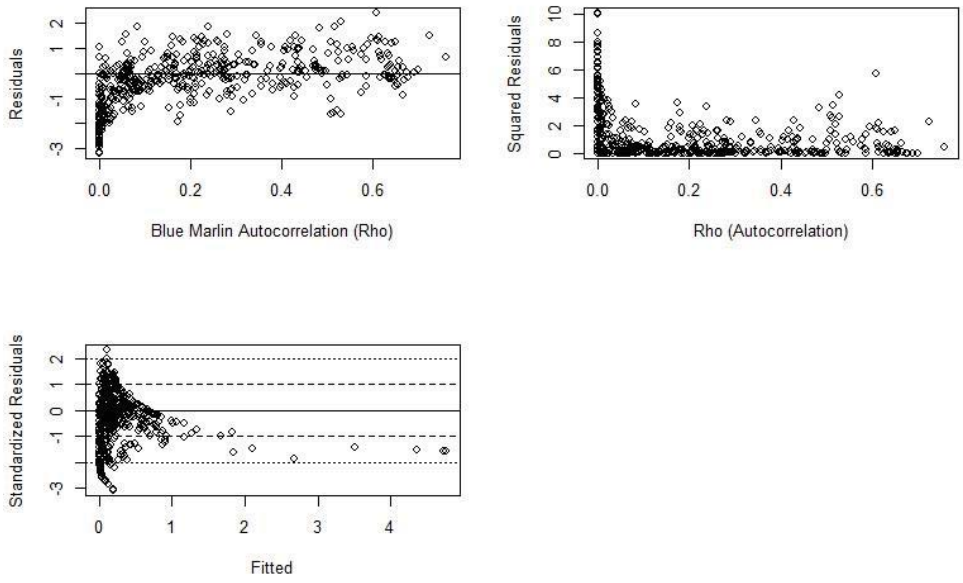

Figure 4.43 Blue marlin autocorrelation parameter GAM model diagnostics including plot of model residuals against the autocorrelation variable (top left), squared residuals against autocorrelation variable (top right), and standardized residuals against model fitted values.

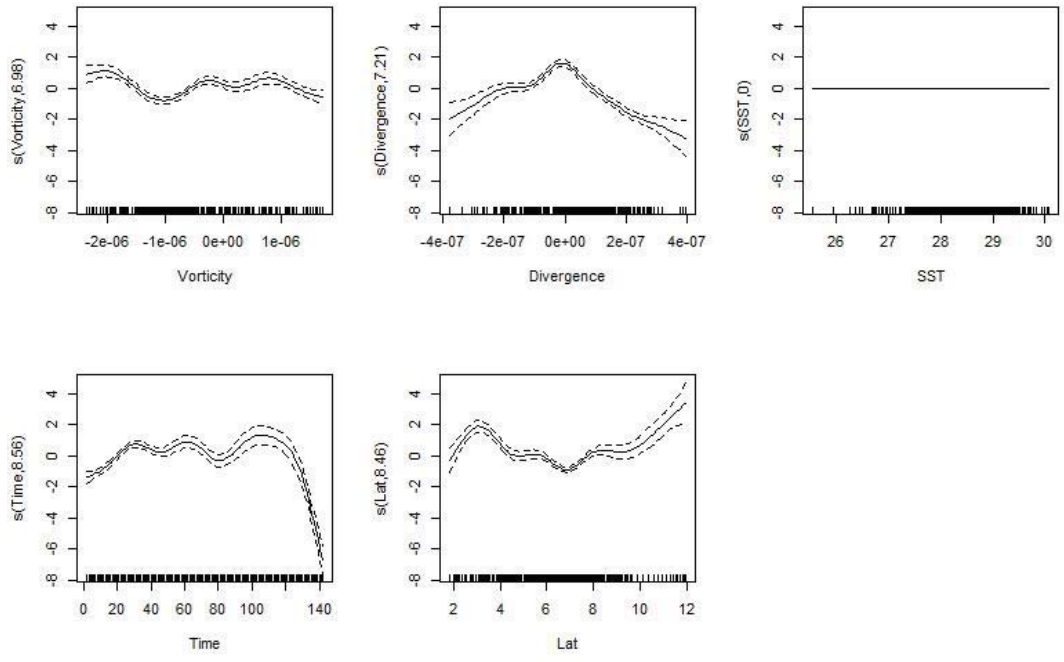

Figure 4.44 Blue marlin autocorrelation parameter GAM model smoother diagnostics.

IATTC Purse Seine GAM Model Selection

Figure 4.45 shows the histograms of blue marlin CPUE in the tuna purse seine fishery in the study area in the EPO with non-transformed CPUE data in the top histogram showing the left skewed distribution expected from the catch in the tuna purse seine fishery and the bycatch nature of billfish species within said fishery, and the log-transformed CPUE data in the bottom plot. Log transforming the CPUE data appears to normalize the data; however, a highly negative Shapiro test confirms the distribution not to be normal (W=0.96, p value=2.2e-16). For this reason, only the GAM run with non-transformed CPUE data is included in this analysis although model fit using Gaussian normal distribution and log transformed CPUE is slightly improved compared to the gamma distribution GAM results presented here. This is opposite to the results found for sailfish where the normal distribution GAM resulting in a much poorer fit compared to gamma with log link. This may be due to sailfish undertaking more random searching with increased range of explanatory variable ranges due to increased migratory range compared to blue marlin which were constrained in migration to a smaller region of the EPO.

Histograms of the explanatory variables from this tuna purse seine sailfish catch GAM can be found in Figure 4.46 with vorticity, divergence, SST, Latitude, and longitude all showing somewhat normal distributions and lacking any major concerning issues in the data structure. Chlorophyll-a data however showed a significant left skew with incidences of high values of chlorophyll but with extremely low density almost not visible in the plot.

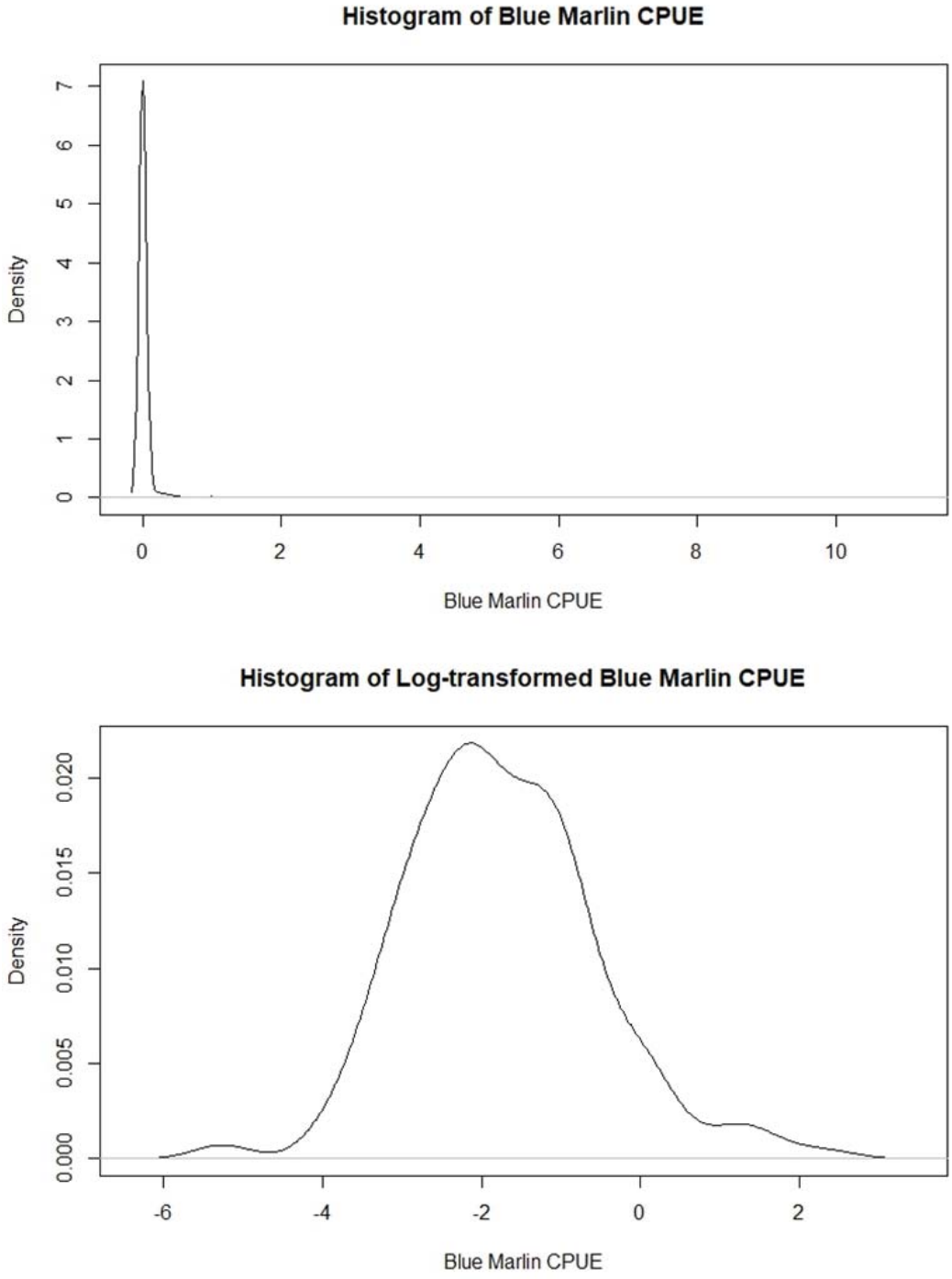

Figure 4.45 Histogram density plots for the response variable blue marlin CPUE in original non-transformed state (top) and log-transformed (bottom).

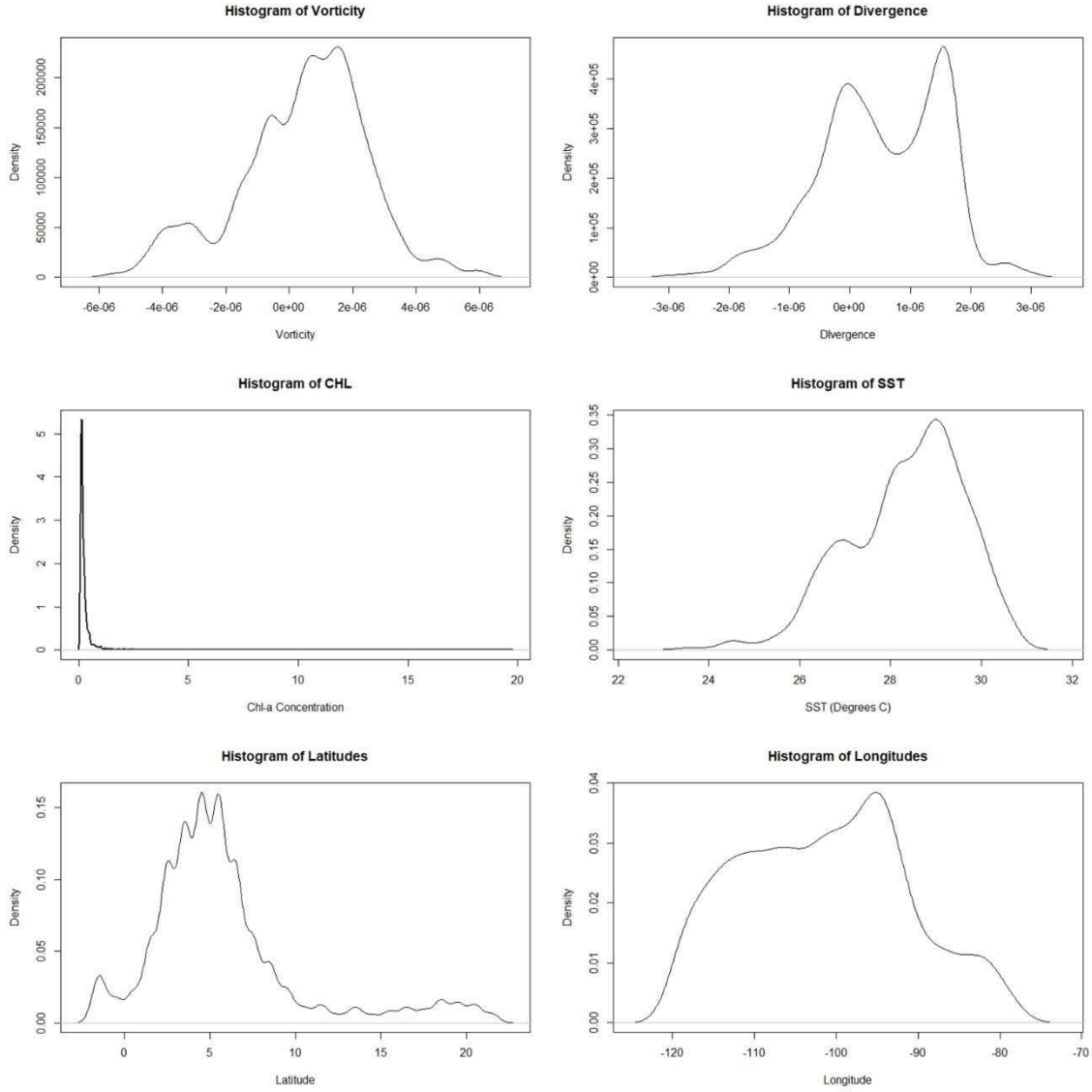

Figure 4.46 Histogram density plots for each of the explanatory variables: vorticity (top left), divergence (top right), Chlorophyll-a (middle left), SST (middle right), Latitude (bottom left), and longitude (bottom right).

The correlation matrix for the blue marlin catch GAM shows a complete lack of correlation between any of the explanatory variables in the subset of the EPO where sailfish were caught in the purse seine (Table 4.8). The highest level of correlations occur

between latitude and SST at 0.3342 and divergence and SST at -0.3165 which should be expected given how overall SST changes with latitude on Earth and divergence leads to SST changes through upwelling. Other correlations in this GAM are lower comparatively to other GAM models discussed in this analysis.

Table 4.8 Correlation matrix for explanatory variables in blue marlin catch data GAM.

	SST	CHL	Divergence	Vorticity	Latitude
SST					
CHL	-0.0398				
Divergence	-0.3165	-0.0313			
Vorticity	-0.1012	0.0034	-0.0078		
Latitude	0.3342	-0.0405	-0.0267	0.0017	
Longitude	-0.011	0.1877	-0.0168	0.0189	-0.3182

The model selection procedure for the blue marlin catch GAM suggest environmental factors vorticity and divergence have little to no influence on blue marlin catch in the tuna purse seine (Table 4.9). The best model contained the explanatory variables of SST, CHL, year, month, latitude, and longitude with smoothing applied only to SST, latitude and longitude. This result provides little insight into the environmental factors associated with blue marlin preference thus the best model is not ideal for this chapter's analysis. Values for AIC decrease as a decreasing rate with each step in the model selection procedure with minute changes beyond step 2 of the step.GAM procedure. The removal of vorticity in step 4 and divergence in step 5 only decreased AIC by less than 2 thus the model chosen for the analysis includes vorticity and divergence and is represented by the model in Table 4.9 as step 3.

Table 4.9 List of blue marlin catch data GAM models produced by the step.GAM function in R software in order of decreasing AIC.

Start: BUMCPUE ~ Vorticity + Divergence + SST + CHL + as.factor(Year) + as.factor(Month) + Lat + Lon;	AIC= 7722.877
Step:1 BUMCPUE ~ Vorticity + Divergence + SST + CHL + as.factor(Year) + as.factor(Month) + s(Lat) + Lon ;	AIC= 7683.663
Step:2 BUMCPUE ~ Vorticity + Divergence + SST + CHL + as.factor(Year) + as.factor(Month) + s(Lat) + s(Lon) ;	AIC= 7664.235
Step:3 BUMCPUE ~ Vorticity + Divergence + s(SST) + CHL + as.factor(Year) +as.factor(Month) + s(Lat) + s(Lon) ;	AIC= 7660.428
Step:4 BUMCPUE ~ Divergence + s(SST) + CHL + as.factor(Year) + as.factor(Month) + s(Lat) + s(Lon) ;	AIC= 7658.445
Step:5 BUMCPUE ~ s(SST) + CHL + as.factor(Year) + as.factor(Month) + s(Lat) + s(Lon) ;	AIC= 7656.528

IATTC Purse Seine GAM analysis

Using only non-transformed CPUE data for tuna purse seine caught blue marlin in the EPO, GAM results suggest an overall lack of fit of the model including all environmental variables (Figure 4.47). For the purposes of this chapter, only the non-transformed CPUE GAM will be discussed in results as the distribution of log-transformed CPUE data did not truly normalize the data similar to sailfish. The resulting GAM suggests chlorophyll-a, latitude, longitude, years 2011-2015, and months 2,3,7, and 12 were found to be significant. This significance is relatively meaningless given the lack of variance explained by the model with adjusted R^2 of 0.0811 and a deviance explained of 12.9%. The GCV score indicates lack of fit of smoothing functions and increased predictive error. The most likely reason may be a disassociation of blue marlin from yellowfin tuna habitat use and the allocation of fishing search in the tuna directed purse seine fishery.

The lack of impact of including vorticity and divergence suggest neither of these variables impact tuna purse seine blue marlin CPUE in the EPO. Although the best model is not presented here in favor of exploring environmental signals, it was run and the resulting fit was nearly identical in R^2, deviance explained, and GCV score. This implies the model as a whole does a poor job of modeling blue marlin CPUE from the tuna purse seine fisheries in the EPO. Much like sailfish, blue marlin as only caught as bycatch in

the purse seine and there is a lack of targeting blue marlin preferential habitat by the tuna directed fishery.

```
Family: Gamma
Link function: log

Formula:
BUMCPUE ~ Vorticity + Divergence + s(SST) + CHL + as.factor(Year) +
    as.factor(Month) + s(Lat) + s(Lon)

Parametric coefficients:
                      Estimate Std. Error t value Pr(>|t|)
(Intercept)          1.177e-01  1.402e-01   0.840  0.40117
Vorticity            4.435e+03  1.103e+04   0.402  0.68756
Divergence           1.373e+04  2.289e+04   0.600  0.54877
CHL                 -1.079e-01  2.687e-02  -4.015 6.09e-05 ***
as.factor(Year)2004  1.216e-02  9.826e-02   0.124  0.90150
as.factor(Year)2005 -1.496e-02  8.570e-02  -0.175  0.86147
as.factor(Year)2006 -1.337e-01  1.102e-01  -1.214  0.22491
as.factor(Year)2007 -1.230e-01  1.171e-01  -1.050  0.29387
as.factor(Year)2008 -1.601e-01  1.220e-01  -1.313  0.18936
as.factor(Year)2009 -1.082e-01  1.136e-01  -0.953  0.34084
as.factor(Year)2010 -1.323e-01  1.106e-01  -1.196  0.23174
as.factor(Year)2011 -2.938e-01  1.098e-01  -2.675  0.00751 **
as.factor(Year)2012 -3.330e-01  1.142e-01  -2.917  0.00356 **
as.factor(Year)2013 -3.143e-01  1.071e-01  -2.934  0.00337 **
as.factor(Year)2014 -2.991e-01  1.045e-01  -2.863  0.00423 **
as.factor(Year)2015 -3.246e-01  1.108e-01  -2.930  0.00341 **
as.factor(Month)2   -3.139e-01  1.254e-01  -2.504  0.01233 *
as.factor(Month)3   -2.952e-01  1.285e-01  -2.297  0.02170 *
as.factor(Month)4   -1.419e-01  1.334e-01  -1.063  0.28765
as.factor(Month)5   -6.208e-03  1.275e-01  -0.049  0.96117
as.factor(Month)6   -1.488e-01  1.212e-01  -1.227  0.21986
as.factor(Month)7   -2.433e-01  1.153e-01  -2.111  0.03487 *
as.factor(Month)8   -1.478e-01  1.182e-01  -1.251  0.21115
as.factor(Month)9   -1.512e-01  1.180e-01  -1.281  0.20021
as.factor(Month)10  -1.485e-01  1.160e-01  -1.279  0.20086
as.factor(Month)11  -1.815e-01  1.168e-01  -1.554  0.12032
as.factor(Month)12  -3.373e-01  1.310e-01  -2.574  0.01010 *
---
Signif. codes:  0 ‘***’ 0.001 ‘**’ 0.01 ‘*’ 0.05 ‘.’ 0.1 ‘ ’ 1

Approximate significance of smooth terms:
         edf Ref.df      F  p-value
s(SST) 1.760      9  0.406   0.0996 .
s(Lat) 4.361      9 22.702  < 2e-16 ***
s(Lon) 8.893      9  6.917 3.36-10 ***
---
Signif. codes:  0 ‘***’ 0.001 ‘**’ 0.01 ‘*’ 0.05 ‘.’ 0.1 ‘ ’ 1

R-sq.(adj) =  0.0811   Deviance explained = 12.9%
GCV = 0.88767  Scale est. = 0.99952   n = 3024
```

Figure 4.47 Results of blue marlin catch data GAM.

Figure 4.48 shows the diagnostics of the fit of the GAM model which is confirmed to be poorly fitted. The qq-norm plot shows deviation from normal at the tails of the distribution. The histogram of residuals suggests an overall normally distributed shape but with a skew to the left of the distribution. Plots of the residuals of the model versus the linear predictor suggest increased variance in residual error as the linear predictor increases but an overall shotgun blast pattern with little indicative pattern. The response variable against the fitted values suggests increased variance in the response variable as fitted values increase especially toward the midpoint of fitted values.

Figure 4.49 shows the second set of diagnostic plots with residuals of the model plotted against the response, blue marlin CPUE variable, which shows a small sample of high catches biases the model with increased variance due to incidences of very high catches relative to typical CPUE levels. Squared residuals against blue marlin CPUE also suggests high catches cause lack of fit in the modeling procedure. The plot of standardized residuals against fitted values suggests deviations exist in the data with values reaching over 4 standardized units away from expected. This result also suggests a lack of fit of the model.

Plots of the smoother applied only to SST, latitude, and longitude in this model shows the tails of the data distribution to have much less ideal fits than the central portion of the distribution but overall have relatively tight bounds compared to other GAMs in this chapter (Figure 4.50).

Results of the GAM model suggest purse seine catch combined with the choice of explanatory environmental variables is not a useful method to discern preference for habitat characteristics in blue marlin. Little information is gleaned from this purse seine

catch analysis resulting in such a poorly fit model especially considering the GAM methodology chosen produced the best fit of all statistical analyses employed including but not limited to: generalized linear modeling, principal component analysis, classification trees, and boosted regression trees. Each of these methodologies produced results not discussed in this chapter due to lack of fit or failure of the model to produce informative results.

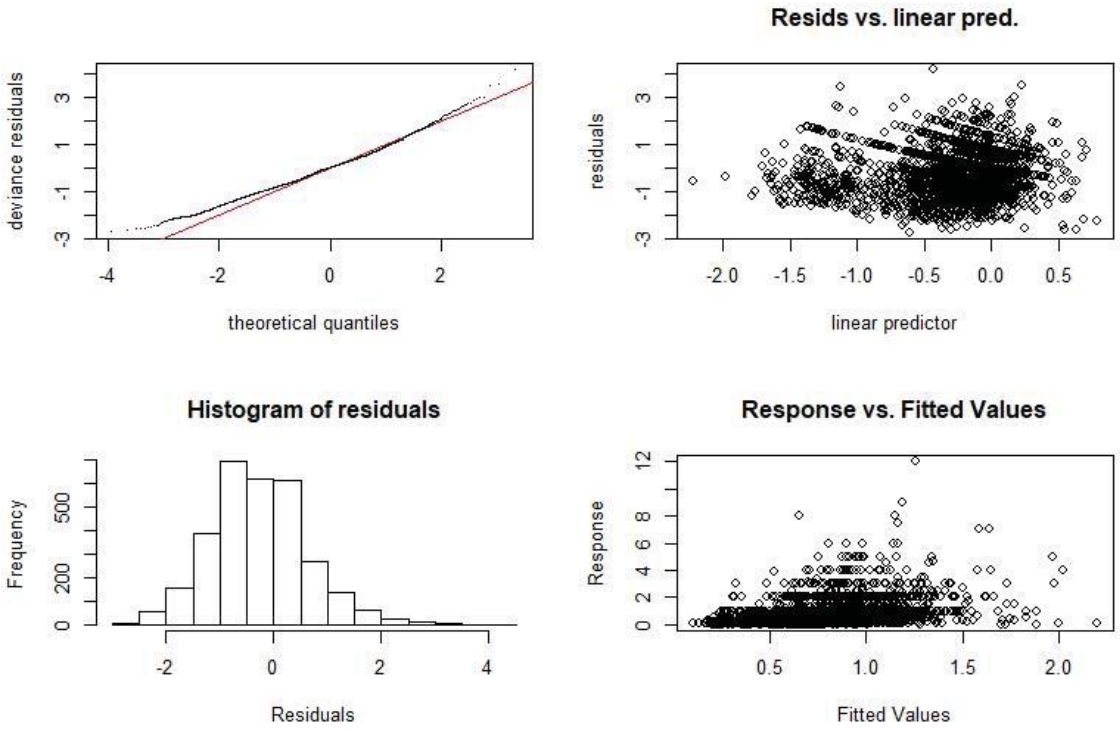

Figure 4.48 Blue marlin catch data GAM model diagnostics including QQ-norm plot (top left), residuals versus linear predictor (trop right), histogram of model residuals (bottom left), and response variable against model fitted values (bottom right).

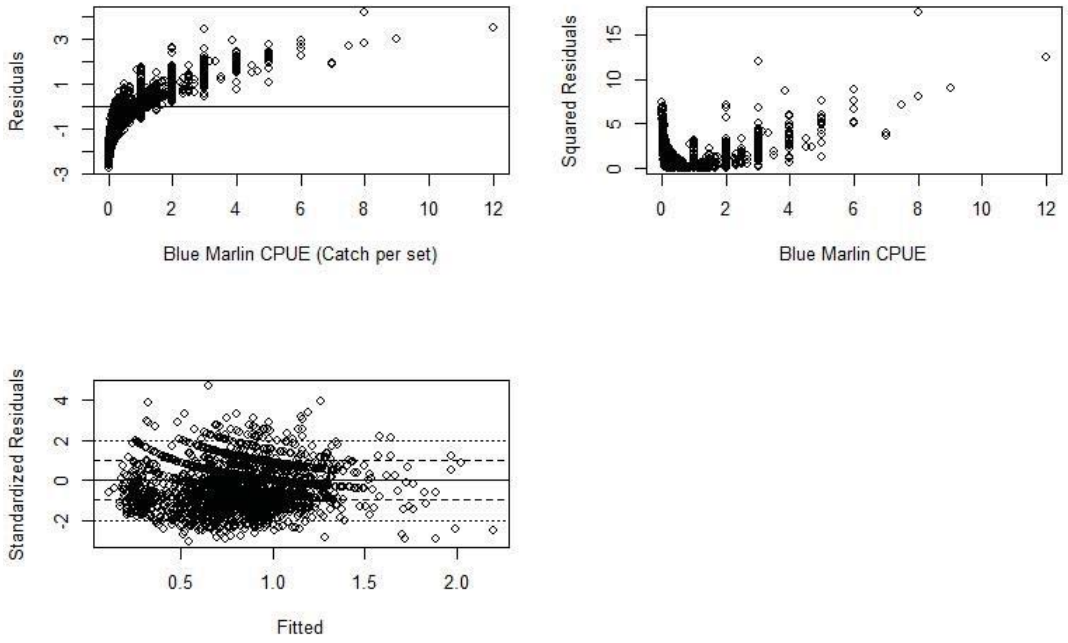

Figure 4.49 Blue marlin catch data GAM model diagnostics including plot of model residuals against blue marlin CPUE (top left), squared residuals against blue marlin CPUE (top right), and standardized residuals against model fitted values.

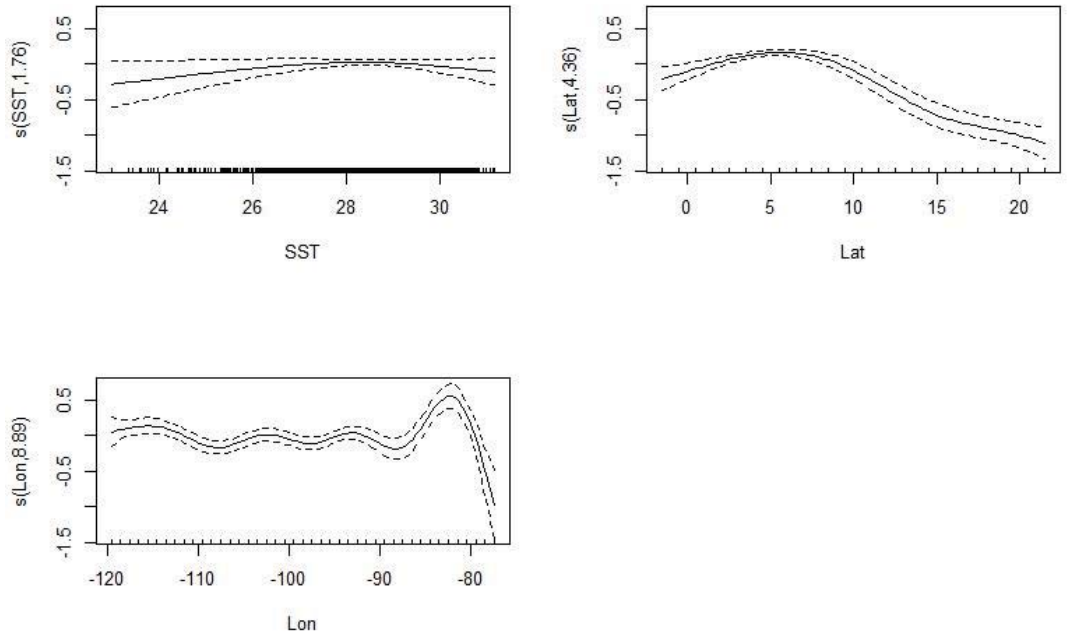

Figure 4.50 Diagnostic of smoothers applied to explanatory variables in blue marlin catch data GAM.

Discussion

Environmental Preference

Histograms of the preferred range of environmental variables suggest differing behavioral strategies between sailfish and blue marlin. Vorticity preference represents the main difference as sailfish preferred high vorticity associated with eddy systems, while blue marlin preferred low vorticity in areas separated from the main migratory routes found for sailfish. Sailfish preferred the maximum values of SST and blue marlin showed similar preference for higher SST values but not to the absolute extreme such as in sailfish. This difference matches their differing spatial distributions as blue marlin preferred the region known as the Coco's Island Ridge seamount area with little movement away from this region. In contrast to blue marlin, sailfish traveled throughout the tropical EPO with no one location seemingly preferred although the area off Guatemala appears to be important. This region off Guatemala saw a proportionally large number of sailfish PSAT data points, especially considering all sailfish tags used in the analysis were deployed off Costa Rica. Blue marlin lack of movement away from a preferred region is not merely an artifact of low sample size of short tag durations. Blue marlin tags had a similar average deployment time with the most extended PSAT deployment for all species tagged being a blue marlin. Longer deployment periods in blue marlin did not indicate movement away from the region but rather indicated the seamount area to be a location this local stock returns regularly.

Preference of sailfish for high vorticity regions and lower divergence values confirms previously held knowledge (Personal Communication Fishing captains, traditional knowledge) that sailfish in the EPO are associated with eddy systems and avoid the

regions of highest upwelling activity, for example, the Costa Rica Dome (CRD). Satellite tagging results suggest sailfish travel across the CRD regularly from Costa Rica moving toward the west and northwest. While sailfish cross this upwelling region, they move more directly, and at a faster rate of speed than on the edges of the CRD where eddies are generated and convergent boundaries form. Sailfish behavior off upwelling areas can be characterized as a searching mode that does not show fast direct movements (Figure 4.51). In contrast, blue marlin does not show any differential behavior due to upwelling because a majority of blue marlin PSATs remained far away from the CRD. One blue marlin crossed the CRD just before being shed and while in the upwelling region, moved in a highly directional manner. With only one blue marlin result in a region of high upwelling, exposing the preference, or lack thereof, for the CRD in blue marlin can only be hypothesized from these results. These results suggest an overall avoidance of the central portion of the upwelling system at the CRD by sailfish and potentially by blue marlin that travel into this region.

Depth results from short term deployments provide insight into habitat use vertically in the water column and Dissolved Oxygen (DO) appears to be the single most restricting environmental variable in terms of billfish presence. These results confirm previous research into habitat compression caused by low DO at depth (Ehrhardt and Fitchett 2006, Pohlot and Ehrhardt 2017, Prince et al. 2006). The resolution of DO data in space and time is extremely limiting, eliminating this variable from use in spatial analyses in this chapter; however, depth result suggest 1ml/l is a conservative minimum for sailfish DO values. The minimum DO level is suggested to be 1ml/l (Ehrhardt and Fitchett 2006), but it is likely that sailfish preference would fall within the higher values

of DO in surface waters where sailfish spend a vast majority of the time. Sailfish were found to spend 83% of their residence within the upper 25.6m and 67% above 12.8m, indicating a strong affinity for surface waters where DO is at maximum levels.

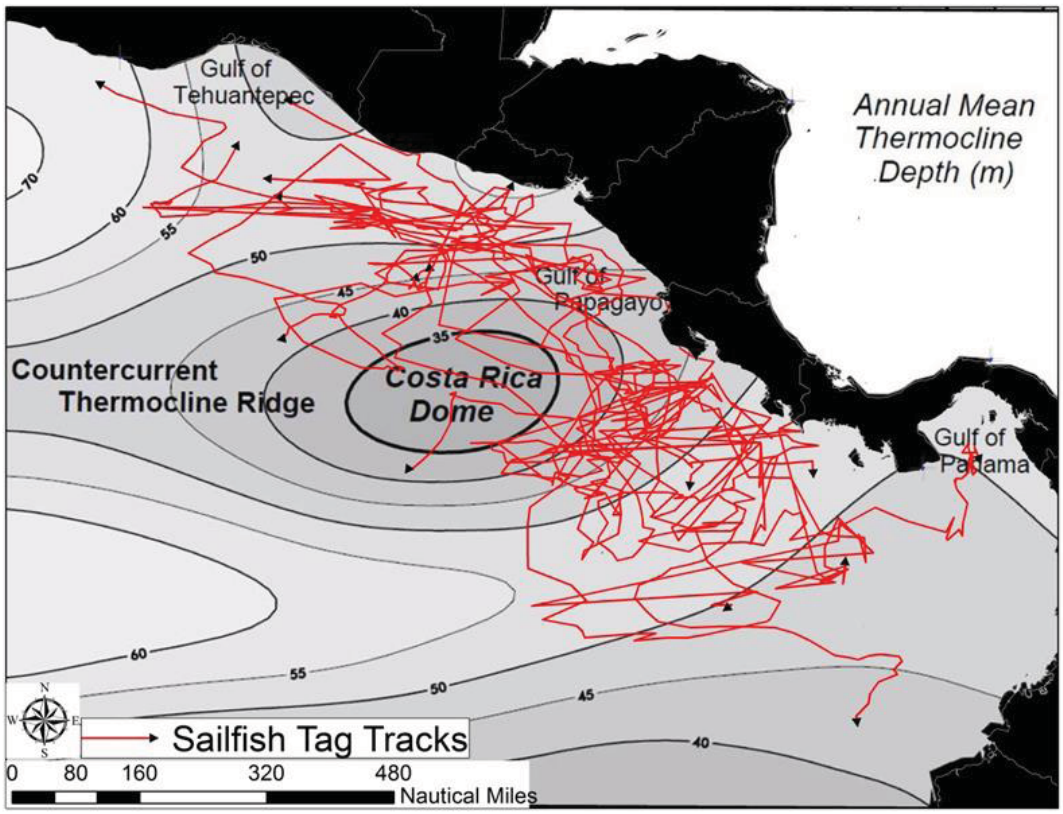

Figure 4.51 Satellite tag tracks from the March 2013 PSAT deployment period showing the distribution of sailfish around the Costa Rica Dome during the spring of 2013. The tracks are overlaid on the average location of the CRD adapted from Fiedler 2002.

Lack of depth recording PSATs placed on blue marlin precluded the analysis of vertical distribution in this species; however, DO minimum levels at depth effect both sailfish and blue marlin and habitat compression will have similar effects on both species. As the climate changes and oxygen minimum zones continue to increase in size and scale, the necessity for a better understanding of the effect of DO on migratory pelagic

species such as the billfish is even more critical for conservation. As sailfish and blue marlin are limited to only the upper water column, they are more at risk for exploitation in surface commercial fishing practices.

It is likely that the presence of low DO at depth is not itself limiting the distribution of sailfish and blue marlin but rather, the low DO effects the distribution of prey species of these predators thus eliminating the necessity to search for food and travel below the minimum oxygen barrier. Results from Chapter 2 of this dissertation suggest sailfish and blue marlin have eyesight optimized for depths greater than those witnessed by depth collecting PSAT tagged sailfish. This suggests the limiting DO barrier is effectively limiting the predatory capability of sailfish, prompting billfish predatory behavior to more effectively locate and consume prey herded by the habitat compression. Clearly, the high catch rates of sailfish and blue marlin in the recreational fisheries suggest these animals are still capable of attaining the necessary food; however, further reduction of habitat due to compression could pose a risk to the billfish stocks in the EPO through increased fishing pressure and lack of habitat for population dynamic processes

The increased availability of billfish to surface fisheries increases their catchability resulting in convolution of stock assessment standardization methods making proper assessment of stock conditions difficult. Future work should focus on collecting DO data spatially and temporally to facilitate analyses that incorporate DO into examination of both sailfish and blue marlin. Understanding the level of habitat compression and the resulting increased catchability is critically important moving forward as DO is expected to continue to decline at depth with climate change. The ecological consequences of an increasing lack of DO could lead to regime changes with low oxygen capable species out-

competing those species currently occupying the food web. The only benefit seen from habitat compression is economic in nature and refers to increased catchability within the recreational fleet throughout the EPO. Catch rates have been maintained at extremely high levels for over a decade influencing business development and economic injections to Central American economies.

Generalized Additive Modelling

The implementation of GAMs to analyze environmental preference in sailfish and blue marlin provides some level of insight into factors other than abundance that influence distribution of sailfish and blue marlin stocks as well as their behavioral preference relative to their habitat. This was analyzed by examining two data types traditionally not used for sailfish and blue marlin assessment modeled PSAT behavioral characteristics and purse seine commercial catch.

In blue marlin BCPA parameter GAMs, model fits were found to be improved compared to sailfish; however, autocorrelation was the most important variable of interest, but neither sailfish nor blue marlin GAM results suggest autocorrelation (rho.hat) variance is explained by the environmental variables chosen for the analysis. Speed and movement path variability from the BCPA analysis is modeled better using GAM analysis with blue marlin that has less variability of parameter values compared to sailfish. The wide range of parameter values seen in sailfish for speed and variability decreases the quality of the GAM analysis for sailfish compared to blue marlin.
The availability of satellite-derived environmental data at spatial scales congruent with PSAT tracking data is rare for a majority of environmental factors such as chlorophyll in

the high cloud region of the EPO. Further exacerbating the issue is the fact that error in PSAT geolocation can range from 35 miles in the SeaTags used in this study to 60 miles with traditional PSATs. This situation results in geolocation error on scales larger than the resolution of the environmental data especially considering the use of traditional tags with a 60-mile error radius effectively creating a 120-mile diameter circle within which the PSAT most likely was found. In the case of the SeaTag, this circle diameter is 70 miles which is a substantial improvement compared to traditional light-based tags but remains an issue when analyses include spatial data of finer resolution which is usually the case.

In sailfish and blue marlin, the purse seine catch GAM analysis was very poorly fitting when compared to the GAM using BCPA parameters. The purse seine fishery represents the only available sailfish and blue marlin catch data in the EPO that is available publicly. The structure of purse seine data for sailfish and blue marlin is problematic due to incidences of very high catch in some months. These values are real catch statistics that represent purse seine sets that came across large schools of sailfish and to a lesser extent, blue marlin. This caused further reduction in the quality of GAMs for purse seine data. The resulting poorly fit GAMs using purse seine data suggest purse seine not be used as an indicator of billfish presence given the rarity of incidental catch in the purse seine. Lack of fit of some of the GAM modeling suggests the explanatory variables used may not be the primary drivers of billfish behavior and that GAM modeling in this fashion may not be the best procedure to investigate preference. Generalized linear modeling, classification trees, and boosted regression trees among many others methods were used to examine the relationship between variables included in the model and results were

fully inconclusive and were not included in this chapter due to lack of findings. This would suggest that available satellite data is not sufficient to explain billfish behavior and the modeling environment may be ignoring some of the more important considerations regarding behavior and habitat use. Billfish do not know where preferential habitat exists. They simply find preferred locations or something preferential and remain the region until the preference is no longer available such as schools of prey for feeding. For this reason, there is no means to predict where a billfish will travel as it is a function of where it has been, the direction it is traveling, and what population dynamic process is most important at that given time. Feeding is hypothesized in this dissertation as the primary motivation for movement of billfish species, but spawning and other processes affect behavior in ways that have never been studied in sailfish or blue marlin in the EPO region.

This chapter sought to assess sailfish and blue marlin preference for habitat and the potential of using BCPA parameters and purse seine catch as a means to statistically evaluate the impact of environmental conditions on behavioral traits and CPUE indices. This goal was attempted by incorporating rarely used oceanographic variables in fishery research, including vorticity and divergence estimations. Overall, ranges for habitat preference for vorticity, divergence, SST, was evaluated qualitatively via overlaid histograms resulting in the confirmation of widely held beliefs among fishermen regarding the preference for eddy systems in sailfish and the preference for blue marlin to remain in the seamount region of the Coco's Island Ridge. Generalized additive modeling attempted to elucidate these finding quantitatively but was limited by spatial and temporal resolution availability of explanatory variables and the only available CPUE

indices being from a fishery that rarely finds sailfish or blue marlin in large numbers represented in the catch statistics. Although GAM modeling did not result in clear definitions of billfish presence, the lack of viability of GAM modeling used in the manner described in this chapter is a result in itself. Sailfish and blue marlin do not benefit from foresight or knowledge of their destination thus using “movement inertia” to elucidate where sailfish and blue marlin preferred habitat exists may not be the ideal research endeavor at current resolutions of environmental data.

Chapter 5: Assessing the extent of sailfish and blue marlin migratory range relative to management boundaries and protected areas

Overview

Sailfish and blue marlin are caught recreationally and commercially in the Eastern Pacific Ocean (EPO) within all of the exclusive economic zones of Central American countries (Figure 1). Recreational and artisanal billfish fisheries management in this region is the responsibility of individual countries, however all members of the IATTC have to enact legislation to follow the recommendations of the Commission. These countries rarely have fishery statistics or the means to assess such fisheries, resulting in a lack of fishery dependent catch data especially for billfish species typically valued less than Yellowfin Tuna (YFT), a highly sought-after species in commercial fisheries. Additionally, there is a complete lack of fishery independent surveys for the purpose of quantifying abundance due to the high cost of data collection and relative remoteness and size of the region. This lack of historical catch data in the EPO, has hindered stock assessment for sailfish and blue marlin in the region (Hinton and Maunder 2011, Hinton et al. 2014).

Commercial fisheries targeting tuna and mahi-mahi include: the industrial purse seine, industrial longline, artisanal longline and small scale pole and line fisheries. Longline fisheries have the highest level of bycatch and industrial longline data is publicly unavailable but is collected by the Inter-American Tropical Tuna Commission (IATTC) and summarized in their reports. These data sources suggest billfish represent the majority of longline bycatch in the EPO and that the purse seine fishery is not a major contributor to billfish fishing mortality (Figure 5.2). Statistics from 2012 EPO industrial longline data reveal a catch of total Billfish (minus Swordfish) to be 7,306mt where in

that year the total longline catch for YFT, a target species, was 9,956mt (Figure 5.2b). In contrast, the purse seine fishery in 2012 caught 198,468mt of YFT and 329mt of billfish bycatch (Figure 5.2a). Artisanal fisheries throughout Central America rely on longlining as an efficient means of exploiting mahi–mahi and tuna species, resulting in significant amounts of billfish caught and killed as bycatch that enter local markets for human consumption; not all of which are counted in stock assessment statistics.

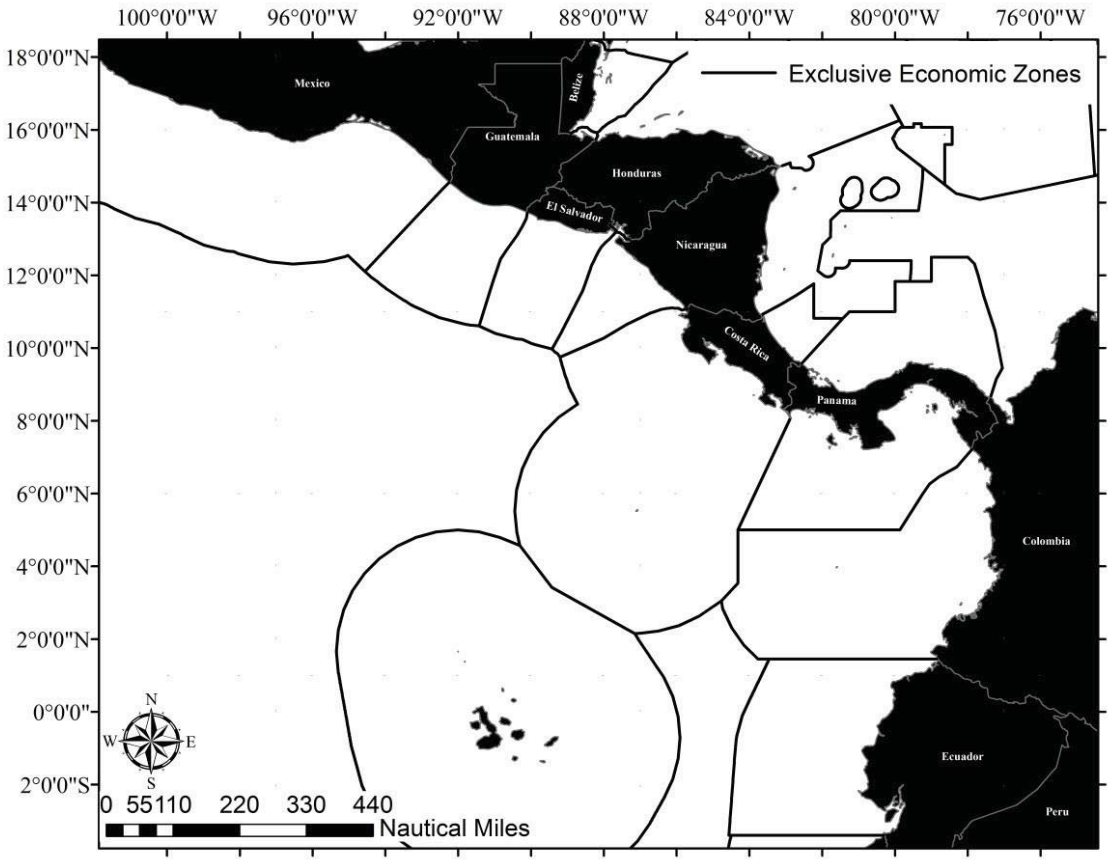

Figure 5.1 Map showing the study area of the Eastern Pacific Ocean and exclusive economic zones associated with each nation indicated by black lines.

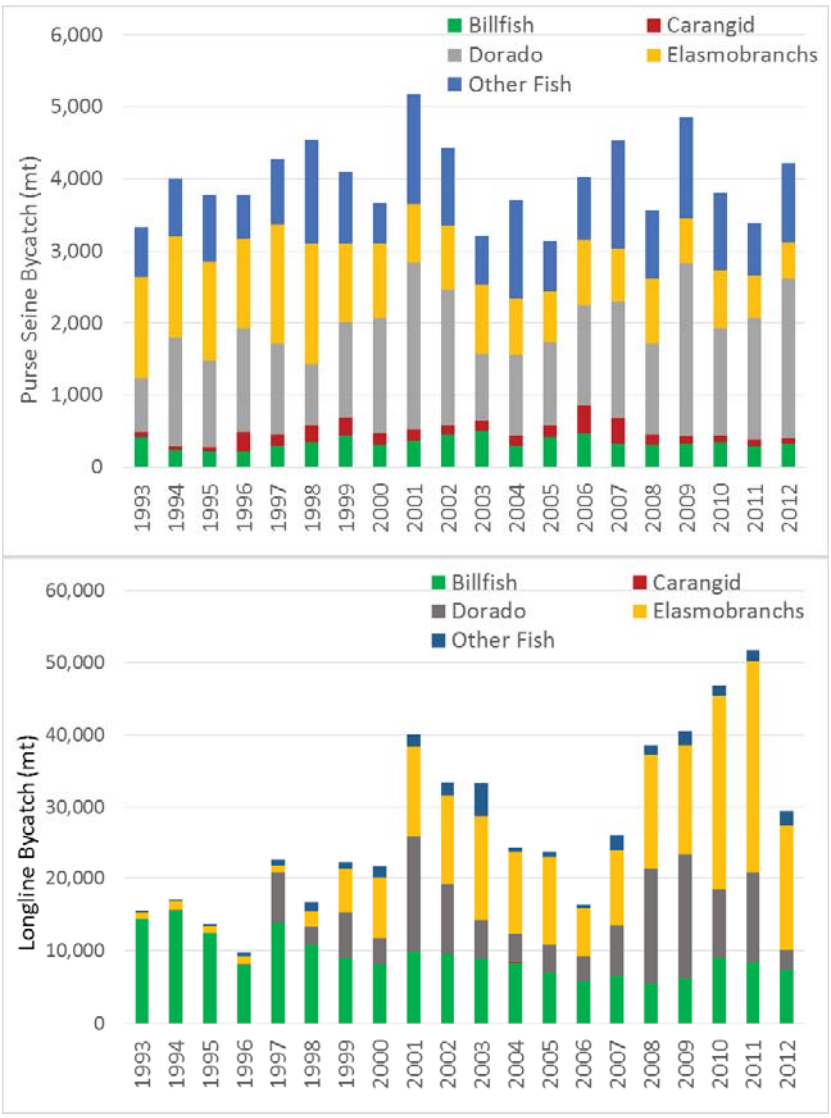

Figure 5.2 Top: Distribution and amount of bycatch in the purse seine fishery from 1993 to 2012 showing relatively low levels of billfish bycatch in the fishery compared to longline fishing. Bottom: Longline bycatch amount and distribution from 1993 to 2012 indicating the large level of billfish bycatch especially in the early years presented.

Some Central American countries retain records of landings of billfish, tuna, sharks, and mahi-mahi because of their commercial value and export but this data is rarely made available to the public and these landings do not include artisanal fisheries not selling their catch to large markets and for export. Also important is the fact that these landings are rarely geolocated thus could come from any location open to fishing

including illegal fishing in other countries EEZ. The prevalence of illegal, unreported, and unregulated fishing within Central American EEZs has been witnessed and reported by many fishermen as well as researchers working in the region (Personal Communication, Golfito, Costa Rica Captains). One particular research expedition found Panamanian longline vessels fishing illegally within Costa Rican waters and another found Ecuadorian purse seiners operating within Panama's EEZ. Additional evidence of illegal fishing was found in satellite tagging experiments where a tagged sailfish was caught in Costa Rica and brought back to market in Panama. Furthermore, landings occur in many locations not monitored by national fishery officials. To date, levels of exploitation within Central America's EEZs can only be explored through analyses of vulnerability of the species through habitat analysis or through statistical estimation based on size and growth of the species (e.g. Fitchett 2015).

Fitchett (2015) estimated sailfish fishing mortality in the EPO based on size and growth analysis that was higher than the estimated natural mortality for the species indicating overfishing is likely occurring on sailfish. Results from Chapters 2 and 4 of this dissertation indicate a high vulnerability of pelagic predators to fishing pressure due to high population density as a result of a limitation of available vertical habitat caused by habitat compression where low levels of oxygen occur at shallow depths in the EPO (Ehrhardt and Fitchett 2006, Prince and Goodyear 2006). The increased density of billfish in surface ocean layers gives the false impression of that relative abundance does not change in response to fishing pressure because catch per unit of effort does not represent local abundance. This concept is referred to as hyperstability (Erisman et al. 2011, Harley et al. 2001, Hillborn and Walters 1992, Walters and Martell 2004) and is a major issue in

statistical data available for stock assessments such as those in the EPO (Hamilton et al. 2016). The hyperstability of sailfish and blue marlin in the EPO is difficult to quantify and has yet to be fully incorporated into stock assessments.

Evaluation of the management strategies necessary to deliver effective conservation of billfish species is a difficult but necessary process. Fishery independent and dependent sources of data providing insight into distribution and habitat use of pelagic fish are a fundamental for ecological assessment and are critical for management (Bigelow and Maunder 2007, Brill and Lutcavage 2001, Carlisle et al. 2017). Spatial analysis such as dispersal range and mean center statistics provide knowledge of the position, extent, and residency of species within specific areas such as EEZs of Central American countries as well as protected areas implemented by individual management regimes (Scott and Janikas 2009, Vokoun 2003). Equally important is to associate habitat use of the species with the regional fishing intensity deployed by the fishing fleets. In that way, risks of mortality and the value of marine protected areas can be assessed. Such analysis requires representative fishery independent data collected through an appropriate statistical design. Satellite tagging results from this research presented in Chapters 2, 3, and 4 are the only fishery independent data available for sailfish and blue marlin, relative to migratory characteristics and habitat preferences at the time of this writing. These results are used in this Chapter to examine species' residency in the region.

The charismatic nature of billfish species and their value as targets of recreational catch and release fisheries has provided a launching point for billfish conservation in the EPO. Recreational fishing tourist and stakeholders are taking charge to help protect their resource. Most countries in the region use presidential or ministerial decrees to enact

change but these are rarely made laws thus creating a difficult political decision making process that can be easily changed by newly elected governments. This is occurring especially in Guatemala and Costa Rica where fishing lodge owners have developed conservation organizations to create new regulations to protect billfish. For example, in Guatemala, stakeholders and researchers worked collaboratively for the creation of the Guatemala Sailfish Conservation Commission which was instrumental in passing laws making possession of sailfish illegal. In Costa Rica, the Federación Costarricense de Pesca (FECOP) and the Instituto Costarricense de Pesca y Acuicultura (INCOPESCA) were instrumental in convincing their government to exclude certain areas to tuna purse seiners in an effort to protect juvenile tunas in the Costa Rican EEZ and to make tuna more available for local fishermen. The management actions also included implementation of restricted areas to limit longlining in near shore areas where tourist fish recreationally for billfish from economically important vacation lodges.

As a result of these efforts a presidential decree was enacted in 2014 in Costa Rica splitting the Costa Rican EEZ into zones, each with a specific purpose and each restricting purse seining in those zones (Figure 2). A coastal and buffer zone (Zones A and B) was created to limit purse seining in this coastal polygon to provide opportunity for recreational and local artisanal fishing without competition and interaction from industrial, technologically more advanced, purse seine operations. Zone C limits purse seining and is an oceanic zone where more capable national commercial and recreational operations are permitted to fish for tunas and billfish. Zone D is a special circumstance area that also limits but does not restrict purse seine operations and was implemented for the purpose of protecting juvenile tuna and improving recruitment. This decree was

created based on results of catch analysis from IATTC observer program data collected aboard purse seiners operating within the Costa Rican EEZ. The efficacy of a closed area on the scale of Zone D for a highly migratory species is unknown.

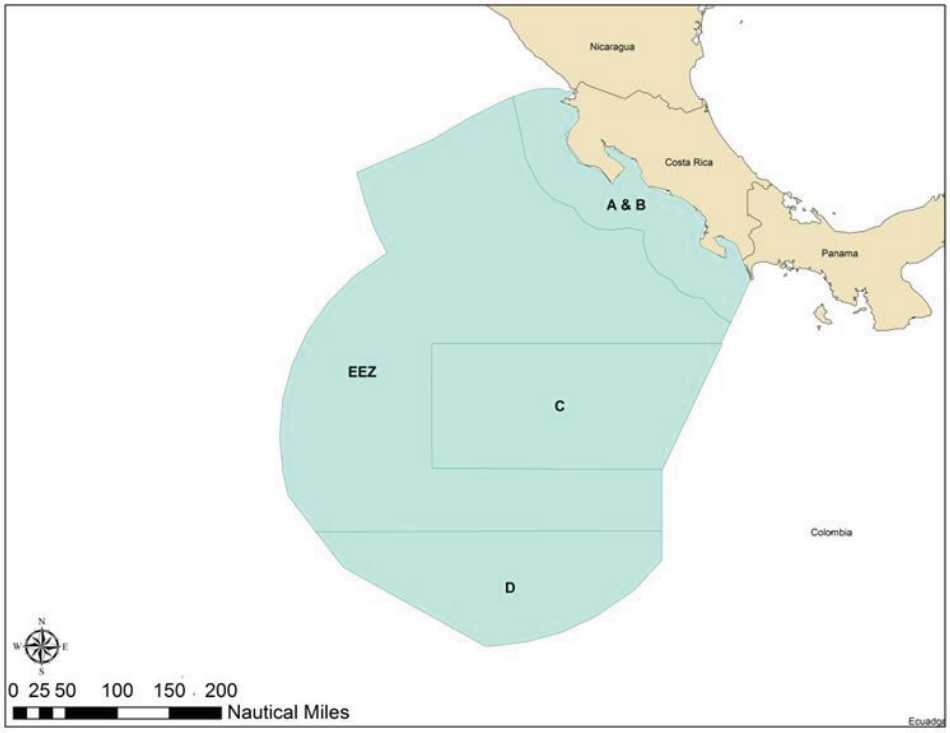

Figure 5.3 Map of the fishing zones designated by the Presidential Decree in Costa Rica in 2014.

To assess the effectiveness of this presidential decree and whether small scale marine closed areas provide effective conservation measures for large pelagic predators in the EPO, an analysis of residency within each zone from satellite tagged sailfish and blue marlin was performed along with an examination of YFT purse seine catch before and after the decree. This analysis is performed with the purpose of achieving Goal #5 of this dissertation which was defined as an exploration of the effectiveness of fishery management of the Yellowfin Tuna purse seine fleet relative to billfish vulnerability in Costa Rica under current (Post-2014) management strategies.

Methods and Materials

The examination of patterns of spatial behavior in animals is made possible with the use of ArcGIS, spatial analysis software packages, and R statistical programming software. These features allow data handling and visualization to discover patterns and trends in spatial data, in this case, commercial catch and satellite tag locations (Scott and Janikas 2009). Sailfish satellite tagging results from Chapters 2, 3 and 4 were incorporated and placed in ArcGIS for spatial analysis. This process included the plotting of satellite tag track files produced by Desert Star Systems' SeaTrack software in Google Earth Pro to convert file format into a .KMZ format compatible with Microsoft Excel. Upon uploading the track data into Excel, a .CSV file was created which could be loaded and projected into ArcGIS' ArcMap software package. Satellite tagging data from 21 sailfish and 10 blue marlin tags were uploaded into the mapping software, geolocated and projected to match the basemap geographic coordinate system, and exported as shapefiles. Also uploaded into ArcMap was a file containing all location estimations from tagging data with each species as single files for the purpose of estimating the migratory range and residency of sailfish and blue marlin as individual groups.

IATTC purse seine observer and catch data is made available in the public domain through their website as mentioned in Chapter 4 of this dissertation. This data is in monthly format and spatially aggregated as 1°x1° latitude and longitude grids for sailfish, blue marlin, and YFT. This catch data was in .CSV format and was combined for all years containing billfish catch which began in 1993 and continues to present day with the final year of the public domain data including 2015. Yellowfin tuna purse seine catch was used from 2000-2015 but required to be split into decadal groups, from 2000-2010

and the second from 2010-2015 for mean center analysis. These were separated only for computing and mapping purposes due to the large size of data files. Also available for comparative analysis was the purse seine catch of striped marlin and black marlin from 1993-2015. Data was then loaded and projected in ArcMap by year as well as a spatial average of all years. The purse seine has three basic operational modes for their set types in the EPO. Sets can be made on dolphin schools, over fish aggregating devices, or on free swimming tuna (Figure 4). Data were analyzed for dolphin associated sets for two reasons; first, only dolphin associated sets were found to catch billfish as bycatch in the EPO, and second, a vast majority of all sets within the EPO north of the equatorial upwelling region were performed on dolphin associated schools (Figure 5.4).

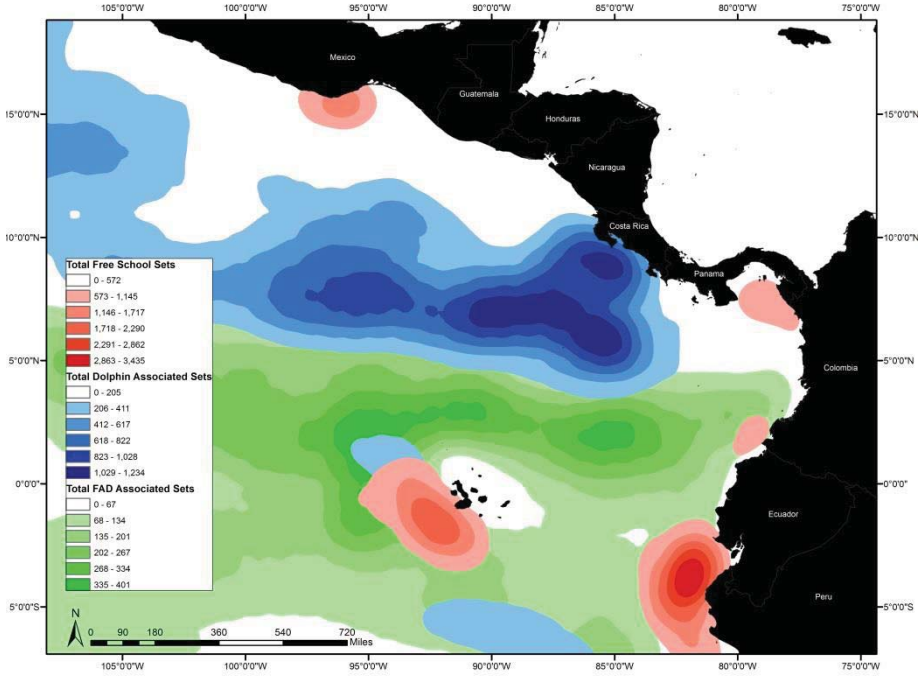

Figure 5.4 Map showing the distribution of set types in the EPO purse seine fishery with red shades indicating free school/unassociated sets, blue shades indicating dolphin associated sets, and green shades indicating object oriented/fish aggregating device sets.

The conglomerate of integrated tagging and catch data was then available for comparison and analysis using the ArcToolbox functions provided by ArcMap. These functions included the determination of the geographic center of the populations and the kernel densities which can be used to determine dispersal range extent.

Distributional Mean Center Estimation

Estimation of mean centers of a population distribution is useful for comparison of distributions from differing data sources such as purse seine catch and satellite tagging data (e.g. Mitchell 2005). Distributional mean center analyses may reflect species ecosystem dynamics and the effects of exploitation as mean centers can change due to resource availability relative to biomass. To determine the geographic center of a population in ArcMap, one needs to load in a feature class such as the files with all tagging locations for each species. The mean center is calculated from tagging data points using the equations for latitude (Y) and longitude (X) where x_i and y_i are longitude and latitude coordinates within the feature class (i) and n is the number of grid squares within the file (Equation 5.1).

Equation 5.1

$$\bar{X} = \frac{\sum_{i=1}^{n} x_i}{n} \quad , \quad \bar{Y} = \frac{\sum_{i=1}^{n} y_i}{n}$$

For purse seine datasets, a weighted mean center was calculated using the number of animals caught per month within a one degree grid square. This estimation procedure used a weighted formulation (Equation 5.2) with the same parameter definitions but this

time adding a weight w_i, in this case weighting by number of fish caught within that month and grid square.

Equation 5.2

$$\bar{X}_w = \frac{\sum_{i=1}^{n} w_i x_i}{\sum_{i=1}^{n} w_i} \quad , \quad \bar{Y}_w = \frac{\sum_{i=1}^{n} w_i y_i}{\sum_{i=1}^{n} w_i}$$

Mean population centers were calculated separately for sailfish and blue marlin with data from all tag location estimates. Mean centers were also estimated for sailfish, blue marlin, YFT, striped marlin, and black marlin from monthly purse seine catch to discern if the tagging data population centers coincide with those of the purse seine and how they relate to YFT, which is the purse seine target species. If coincidence occurred within the same species between data types, it could be concluded that the tagging data may represent habitat range and thus could be applied to the full extent of dispersal range analysis using ArcMap software. This is especially important knowing that the EPO purse seine fishes the full extent of the potential range of these species throughout the tropical and sub-tropical Pacific. If there is no coincidence between purse seine distribution and satellite tagging points we can conclude that satellite tagging data does not represent the full extent of that species range but rather the local range for the tagging location in Costa Rica. Mean center estimations between data types and species, as well as over time, are also useful to examine the behavior of species relative to their exploitation.

Kernel Density Dispersal Range Analysis

Aggregated spatial information for many individuals can provide information relative to an animal's total habitat use defined as the dispersal range (Burt 1943, Powell and Mitchell 2012, White and Garrott 2012). Kernel density estimates are commonly used to estimate the spatial area and residence of an animal using location or telemetry data in ecological studies. Kernel densities are one of the best estimators of animal dispersal range and have been used for this purpose since the 1950s, mostly in marine and terrestrial mammal species studies (Powell 2000, Silverman 1986, Seaman and Powell 1996, Seaman et al. 1999, Worton 1987, Worton 1989). Animal spatial data especially telemetry data is not distributed in statistical patterns required for parametric analysis thus nonparametric methods are necessary to explore statistical relationships found in animal location data such as residence and habitat use which include kernel density estimation (Laver and Kelly 2008, Powell and Mitchell 2012, Powell 2000). The main benefit of kernel density estimators for dispersal range analysis is the ability to objectively demarcate the most used areas of a habitat based on some percentage of residence (Vokoun 2003). The resulting dispersal range percent residence levels can be used to assess habitat usage by the animal (Kernohan et al. 1998, Mitchell 1997, Vokoun 2003).

Kernel densities are taken from point data where the number of point features, or point density, is calculated following the quadratic kernel function of Silverman (1986). This kernel density is not affected by the size of the grid or placement and is an unbiased estimate obtained directly from the data (Powell 2000). Kernel densities can also be estimated from fishery catch data where a point includes more information including the

number of fish caught at said point. These densities are estimated in the same way with a slightly different routine. First, a circular smooth surface is fit to a point or animal location where the surface value is highest directly over the point and decreases with increasing distance from the point until it reaches zero at a defined distance known as the search radius which is defined below. The population field adds value to a point so it can be counted in a weighted manner based on the designated population field, in the case of the purse seine catch data this is designated as catch in numbers. Basically, if the population field is added, the point will have volume equal to the value of the population field where in satellite tagging densities the volume is one and population field is not selected. In the case of this research, the number of fish caught at any point will increase the times that point is counted equal to the number of fish.

The kernel density estimation is heavily influenced by the inputted search radius also referred to as the bandwidth (Fieberg 2007, Kernohan et al. 2001, Worton 1995). Because of the importance of this parameter, an algorithm is built in to the kernel density toolbox to automatically estimate a search radius; however, this is not always appropriate for all data types thus it needs to be analyzed for appropriateness. The default algorithm first estimates the mean center of the points including those weighted by catch then calculates the distances from each point to the mean center. The median (D_m) and standard distance (SD) are estimated next from these distance measurements and applied to the following formula

Equation 5.3

$$SearchRadius = 0.9 * \min\left(SD, \sqrt{\frac{1}{\ln(2)}} * D_m \right) * n^{-0.2}$$

where *n* is the number of points to be estimated, weighted or not. Each density map is required to be validated visually to ensure the default search radius produces proper spatial extent and coverage.

To perform a kernel density analysis with the given data requires a number of steps to produce a billfish dispersal range map showing the 95% residence of the tagging locations. The first step is to create an ocean mask to restrict the analysis to only ocean areas for the purpose of comparing different species distributions across the same region as well as remove the possibility of densities occurring on land. This step includes using a land shapefile which is used as a basemap as well the identification of country boundary lines for later analyses. This land shapefile is imported and a new mask is created using the extent of all data points minus the land coverage. The next step is to create the kernel density raster files. This process uses the previously described spatial analyst tools in ArcMap's ArcToolbox specifically the density tool for kernel density analysis. Tagging data files including all sailfish and blue marlin satellite tag locations are loaded into this analysis separately using the default estimation of bandwidth or search radius. Once the kernel densities are estimated it is necessary to create isopleths of the kernel densities which requires analysis outside of the ArcMap program. Kernel densities are exported from ArcMap and opened in the Geospatial Modeling Environment (GME) which requires the installation of R statistical software as well as the "ks" package for kernel smoothing (Beyer 2017). The GME contains an isopleth tool that loads in the kernel

density file and produces density values based on the quantiles inputted into the tool, in this case, for the 95% dispersal range, the quantiles were set for convenience as: 0.25, 0.5, 0.75, 0.95. The density quantile values produced by the GME tool are then recorded and these values used to reclassify the original kernel density estimation in ArcMap. Five classes are defined, coinciding with the quantiles but adding a 1.0 (100%) value which corresponds to the 5% of tagging locations outside of the 95% dispersal range.

Break values corresponding to the GME isopleth results are input for mapping of the 95% kernel densities. Dispersal range maps are validated by adding isoline files produced by the GME to ArcMap to ensure the kernel density percentages match their respective isolines. This is confirmed for all density files created using this dispersal range method. Finally, kernel density raster files are reclassified into polygons for further analysis and the estimation of total area.

Kernel Density Overlap of Sailfish and Yellowfin Tuna

A kernel density raster containing the IATTC EPO purse seine catch data was loaded into ArcMap separately for both YFT and sailfish. The kernel density values in each raster were then normalized on a scale from 0 to 10 and multiplied against each other using ArcMap's providing a level of "correlation" between the files ranging from 0 to 100 where 100 would refer to two completely identical kernel density rasters. This method does not produce a true "correlation" statistic but is useful because it produces low(high) values where low(high) values occur in both rasters compared to a true correlation which would show high correlation where densities were low(high) in both

raster files. This method produces a third kernel density map of the effective "correlation" or perhaps would be best considered as "association".

Exclusive Economic Zones and Closed Area Residence

To examine the residency of sailfish and blue marlin within Central American EEZs as well as within the Costa Rica zones closed to purse seine fishing, the satellite tag locations of each fish were analyzed for percent residence within specific areas. These areas included the country EEZs of Mexico, Guatemala, El Salvador, Nicaragua, Costa Rica, and Panama. Also included but separate to the EEZ analysis was a determination of individual fish residence within the exclusion zones defined by the 2014 presidential decree in Costa Rica.

This analysis was performed using ArcMap by using the aforementioned individual sailfish and blue marlin tag location shapefiles. This method requires selecting points within an individual fish shapefile using the spatial selection tool in ArcMap and selecting only points that fall "completely within the source layer feature" which, in this case, was the EEZ of Costa Rica zone. Following the selection, the attribute table for the individual fish shapefile was examined and the number of points within that layer as well as total number of points were recorded. The percentage within that layer was estimated by dividing the number of points within the layer by the total number of points available. This method was performed for each fish and for each EEZ and Costa Rica closed areas.

Catch Analysis of YFT in Costa Rican Closed Areas

Yellowfin tuna catch data shapefiles created from yearly purse seine records were projected over a shapefile corresponding to the location of closed areas within the Costa Rican EEZ. A viewing window was chosen for summation of catches within and outside of Costa Rica's EEZ for the purpose of spatial and temporal catch analysis before and after the presidential purse seine area exclusions decree in 2014. The extent of this analysis included catch data by one degree squares ranging from 1^{O} to 12^{O} North latitudes and from 80^{O} to 93^{O} West longitudes. Catch and effort was summed over this grid to determine total catch, total number of sets, and a non-standardized Catch Per Unit Effort (CPUE) by dividing total catch by number of sets in each year. Also performed was a qualitative analysis of catch within Zones C and D which were closed to YFT targeted purse seine effort.

Results

Distributional Mean Center Estimation

A total of 21 sailfish and 10 blue marlin PSAT tags were included in the mean center analysis that included migratory tracks greater than 35 days in duration and up to 200 days post-release. Sailfish satellite tag locations ranged throughout the tropical EPO from Southern Mexico (16º N) to Northern Ecuador (1º N) and from nearshore out to 561 miles off the coast of Central America. The purse seine catch used for this comparison ranged from 22º N to 3º S and 77º W out to 115º W with a majority of catches nearshore and substantially lower catch greater than 500nm from shore. The distributional mean center estimated from this range of locations falls 175 miles west of Costa Rica and is

within 75nm from the distributional mean center of sailfish catch for the purse seine fishery 244nm west of Costa Rica (Figure 5.5). Because the purse seine covers the full extent of the EPO, nearby mean centers between tagging locations and purse seine catch validate that tagging locations can be used for dispersal range analysis. Figure 5 shows the matching extent of catch and sailfish satellite tag locations revealing the spatial association of coastal habitat shared between the tuna purse seine fishery and sailfish. The tag locations are coincident with the purse seine catch in that both suggest sailfish habitat range lies mainly nearshore. The coastal region between Mexico and Ecuador makes up a majority of Eastern Pacific Sailfish habitat.

Unlike the more coastal sailfish, blue marlin are commonly caught in the purse seine just north of the equator and in the open ocean and are less common in the northern EPO off Mexico, Guatemala, El Salvador and Nicaragua; however, tagged blue marlin remained in the easternmost regions of the EPO (Figure 5.6). Catches of blue marlin in the purse seine are dominated by catches in the open ocean between 0 N and 8 N while the tagging data suggest those caught off Costa Rica remain in the nearshore region where they were caught ranging from 2º N to 12º N and 78º W to 91º W. Consequently, the tagged blue marlin population mean center was disproportionately located toward the east relative to the blue marlin population center expressed by purse seine catch analysis. For this reason, the dispersal range analysis of tagged blue marlin cannot be used to describe the entire stock over many years due to a lack of spatial coverage or time at large in satellite tagging results. This result; however, could indicate that blue marlin form seasonal hotspots in the Pacific within their habitat range.

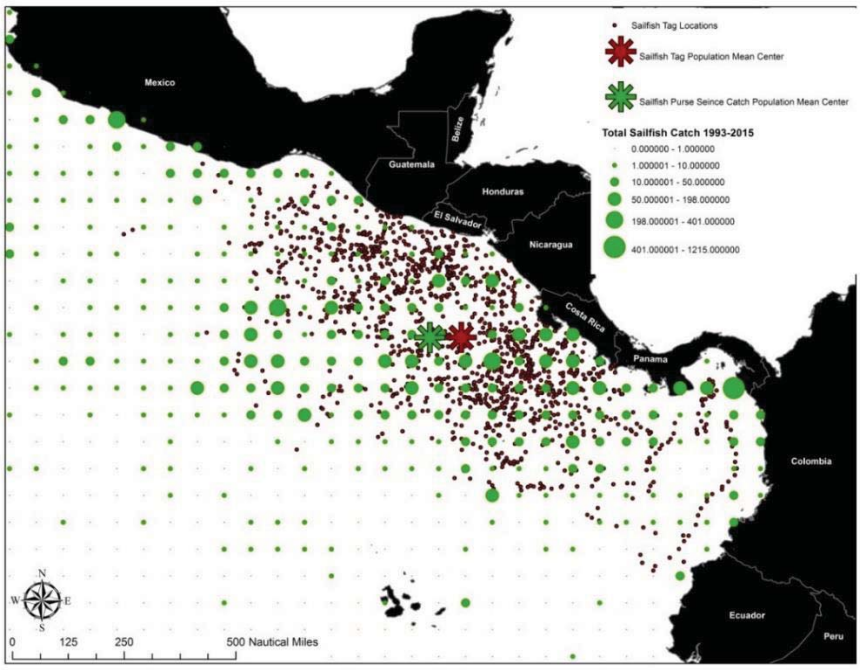

Figure 5.5 Map of sailfish satellite tagging locations (red dots), total sailfish catch in the purse seine (green circles), and mean centers of population distribution for each of these data types (green asterisk refers to purse seine catch mean center and red asterisk to satellite tag location mean center.

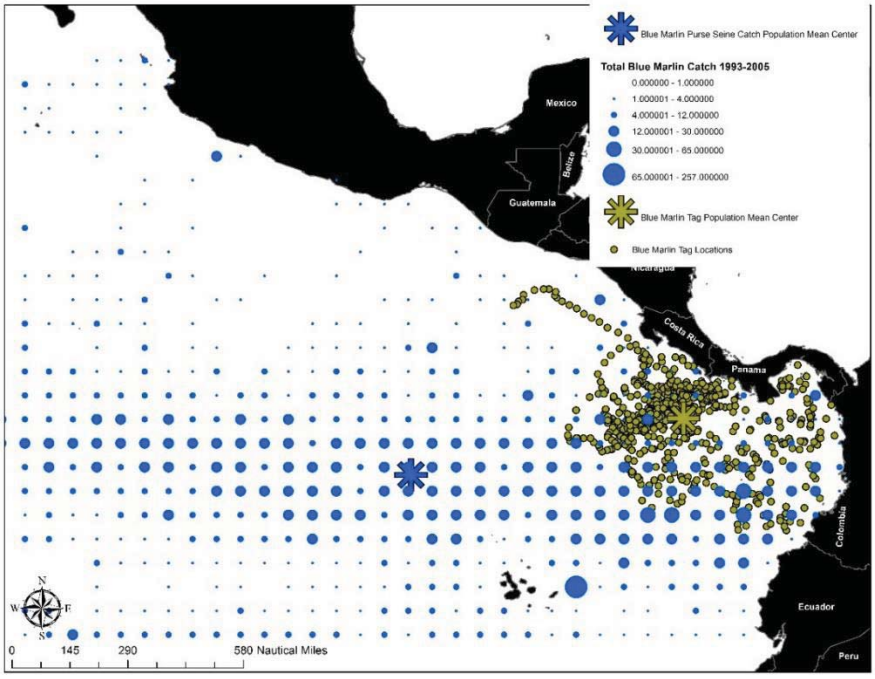

Figure 5.6 Map of blue marlin satellite tagging locations (yellow dots), total blue marlin catch in the purse seine (blue circles), and mean centers of population

distribution for each of these data types (blue asterisk refers to purse seine catch mean center and yellow asterisk to satellite tag location mean center.

In addition, sailfish and blue marlin purse seine catch and tagging distribution mean centers were compared to YFT purse seine spatial catch distribution mean centers using data for two periods, 2000-2010 and 2010-2015 (Figure 5.7). These decadal periods were chosen to separate a decade of consistent spatial fishing distribution for YFT versus the recent decade when spatial restrictions were implemented. The centers of distribution of catches of YFT were found to be much further west and variable within the 15 year period than all billfish examined. This area coverage of YFT fishing effort could be disproportionate relative to blue marlin if they have formed multiple hotspots within the distribution of YFT purse seine effort. The more coastal distribution of sailfish would negate this disproportionality.

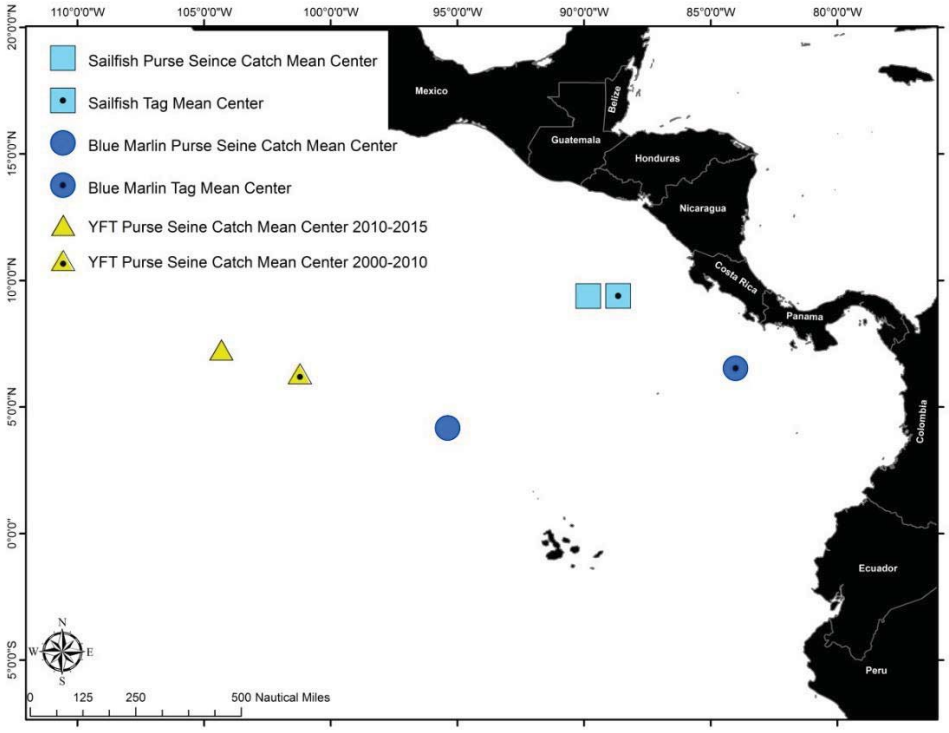

Figure 5.7 Map of mean centers of distribution for sailfish (light blue square=purse seine catch mean center, light blue square with dot=sailfish satellite tag location mean center) and blue marlin (blue circle=purse seine catch mean center, blue circle with dot=blue marlin satellite tag mean center) and yellowfin tuna(YFT)(yellow triangle=purse seine catch mean center from 2010-2015, yellow triangle with dot=purse seine catch mean center from 2000-2010).

Kernel Density Dispersal Range Analysis and EEZ Residence

Sailfish

The sailfish estimated dispersal range in the EPO was found to extend across the EEZs of all Central American Countries as well as Mexico, Panama, Colombia and one fish travelled to Ecuador (Figure 5.8). The highest density of tag locations (25% level) corresponds to the regions where 75% of tagging locations are found in the region off Costa Rica, El Salvador, and Guatemala as well as two small regions in the open ocean just outside of the Guatemalan and El Salvadorian EEZ. The 50% level densities were found in these countries as well as the open ocean region and in the Nicaraguan, Mexican, and Panamanian EEZs. Of the countries included, Mexico, Colombia and Ecuador have the lowest density of satellite data points most likely due to insufficient time for more complete (35-179 days) tag dispersal. In total, the 95% dispersal range of sailfish satellite tagging data points shown in Figure 8 spans eight international borders during the length of the study.

Although all of these sailfish were tagged within the Costa Rica EEZ, all but one sailfish travelled outside of this EEZ to some extent with 12 sailfish spending proportionally more time (>53.97%) residing outside of Costa Rica's EEZ than within it (Table 5.1). Of the 21 sailfish tags 45.42% of the days at large were found within the Costa Rica EEZ, 4.25% in Nicaragua's EEZ, 11.53% in El Salvador's EEZ, 10.43% in

Guatemala's EEZ, 6.82% in Mexico's EEZ, 5.21% in Panama's EEZ, 2.59% in Colombia's EEZ, 0.31% in Ecuador's EEZ, and finally the remaining 13.44% in the open ocean. These percentages are indicating that sailfish carries out extensive migrations away from the sites where tags were released. An important result ecologically is the proportionally lower residence within the Nicaraguan EEZ compared to other, more distant Central American EEZs. This relative lack of residence may be attributed to the presence of unfavorable environmental conditions related to the upwelling caused by the Costa Rican Dome (CRD).

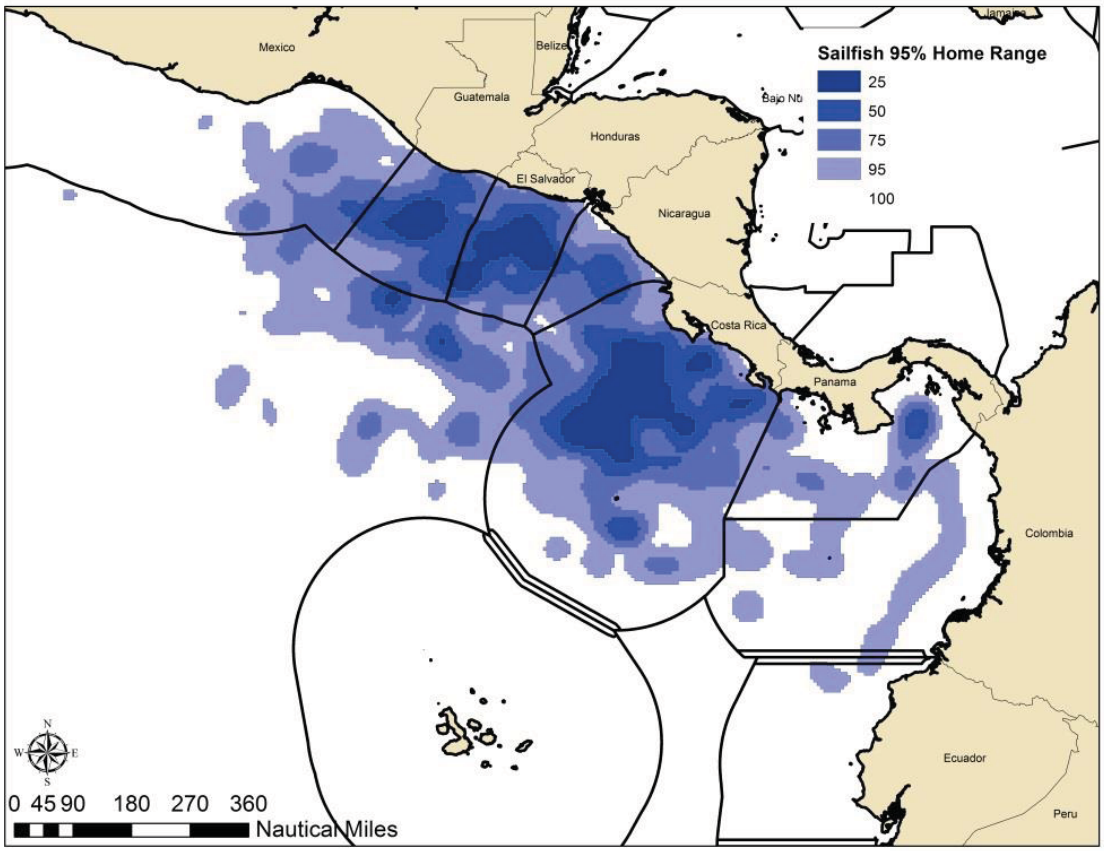

Figure 5.8 Map showing the extent of the estimated sailfish dispersal range from satellite tagging locations. The shades of blue range from 25% to 100% darkest to lightest. The darkest blue indicates the highest density of satellite tag locations corresponding to the 25% dispersal range where 75% of tagging locations fall. The

next darkest shade of blue indicates the 50% dispersal range referring to 50% of tagging locations etc.

A majority of tagged sailfish travelled north and west from the tagging location in Costa Rica with only 5 of the tagged sailfish visiting the EEZ of Panama which was the nearest international border to the east of the tagging location. One sailfish travelled as far south as Ecuador and three sailfish resided for a time in Colombia. On the other end of the spectrum, 10 sailfish travelled as far to the north and west as Mexico with one sailfish spending 48.57% of its track within the Mexican EEZ and 5 sailfish spending over 15% of the residence within the same EEZ. Compared to the size of the EEZ, Guatemala, El Salvador, and Costa Rica have the highest proportion of the dispersal range of sailfish within their respective EEZs.

Table 5.1 Table indicating the percent (%) residency of 21 tagged sailfish in the Exclusive Economic Zones of countries where tag tracks occurred.

Sailfish Tag ID	Days At Liberty	Mexico	Guatemala	El Salvador	Nicaragua	Costa Rica	Panama	Colombia	Ecuador
134241	58	0.00	0.00	0.00	0.00	80.36	17.86	1.79	0.00
134252	104	16.88	33.77	3.90	0.00	12.99	0.00	0.00	0.00
134258	179	15.13	5.04	5.04	0.84	47.90	0.00	0.00	0.00
134260	91	19.78	6.59	27.47	5.49	4.40	0.00	0.00	0.00
134263	82	1.22	12.20	6.10	6.10	57.32	7.32	0.00	0.00
134266	89	2.25	14.61	5.62	7.87	33.71	0.00	0.00	0.00
134267	48	10.42	18.75	41.67	14.58	10.42	0.00	0.00	0.00
134268	61	0.00	0.00	0.00	0.00	36.07	63.93	0.00	0.00
134272	63	0.00	19.05	12.70	0.00	53.97	0.00	0.00	0.00
134273	57	1.75	8.77	50.88	22.81	15.79	0.00	0.00	0.00
134275	46	0.00	39.13	15.22	6.52	36.96	0.00	0.00	0.00
134276	54	0.00	3.70	11.11	12.96	20.37	0.00	0.00	0.00
134280	93	0.00	0.00	0.00	0.00	41.94	6.45	45.16	6.45
134285	149	2.68	34.90	32.89	6.04	11.41	0.00	0.00	0.00
134288	61	24.59	8.20	8.20	3.28	54.10	0.00	0.00	0.00
134242	41	0.00	0.00	0.00	0.00	100.00	0.00	0.00	0.00
134250	47	0.00	0.00	0.00	0.00	97.87	0.00	0.00	0.00
134257	35	48.57	14.29	11.43	2.86	22.86	0.00	0.00	0.00
134270	36	0.00	0.00	0.00	0.00	86.11	13.89	0.00	0.00
134279	42	0.00	0.00	0.00	0.00	61.90	0.00	0.00	0.00
134281	40	0.00	0.00	10.00	0.00	67.50	0.00	7.50	0.00
Average	70.29	6.82	10.43	11.53	4.25	45.42	5.21	2.59	0.31

Blue Marlin

Although the blue marlin 95% dispersal range estimated from satellite tagging data was not found to correspond spatially to the full extent of catch distribution in the EPO purse seine fishery, the possibility of a localized hotspot off Costa Rica exists and was analyzed. The localized dispersal range estimation may not be indicative of the full extent of the blue marlin population migratory capability due to the mismatch of YFT fishing effort relative to blue marlin bycatch but directly relates to local stock abundance/transient residency within this specific area during the time of tag deployment. The tagged blue marlin population dispersal range includes the EEZs of Costa Rica, Panama, Colombia, El Salvador, and Nicaragua (Figure 5.9). The highest density of tag locations (25% level) can be found off Costa Rica and Panama. The 50% level densities are found in Costa Rica, Panama, Colombia, and two small regions in the El Salvadorian EEZ. Of the countries included, Nicaragua and El Salvador have the lowest density of satellite migration data points similar to the results presented for sailfish, again possibly attributed to the regional presence of the CRD. Blue marlin tags in this analysis included tag tracks ranging from 38-200 days providing sufficient time to disperse from the tagging locations. In total, the blue marlin 95% dispersal range of satellite tagging data points shown in Figure 5.9 spans five international borders.

Similar to sailfish, all blue marlin tags were deployed within the Costa Rican EEZ. All but one blue marlin remained local to Costa Rica a majority (>53.49%) of the time (Table 5.2) meaning all but one tagged blue marlin resided in the Costa Rica EEZ more than 53.49% of their satellite tag track. Of the total 10 blue marlin tags reporting data, an average of 70.89% of days were within the Costa Rica EEZ, 0.65% in

Nicaragua's EEZ, 2.83% in El Salvador's EEZ, 13.87% in Panama's EEZ, 11.55% in Colombia's EEZ and no time was spent in the open ocean. Unlike sailfish, a majority of tagged blue marlin stayed near the tagging location and migrated south and east to Panama and Colombia with only one blue marlin travelling north and west to Nicaragua and El Salvador. Only one blue marlin visited more than 3 EEZs with a migratory track including Costa Rica followed by a residence in Panama then a migration travelling from Panama to El Salvador covering four EEZs. Five blue marlin spend a vast majority within the Costa Rica EEZ spending over 80.00% of their residence within this region revealing a propensity to remain in the ecosystem where they were feeding (caught with live bait) during the time of deployment. Only one blue marlin left the Costa Rica EEZ soon after deployment and this fish spent 44.76 and 48.95% of its residence within Panama and Colombia, respectively. This blue marlin appears to have been in a different behavioral mode compared to those fish that remained near the tagging location. Compared to the size of the EEZ, Costa Rica clearly contains the highest proportion of the local EPO dispersal range of blue marlin. The geographical region where all blue marlin were tagged lies in an area known as the Coco's Island Ridge where seamounts are numerous and may play a role in the behavior, habitat use due most likely to feeding dynamics of tagged blue marlin. Such assertion coincides with similar behavior of other large top predators the inhabit in this area (Litvinov 2008)

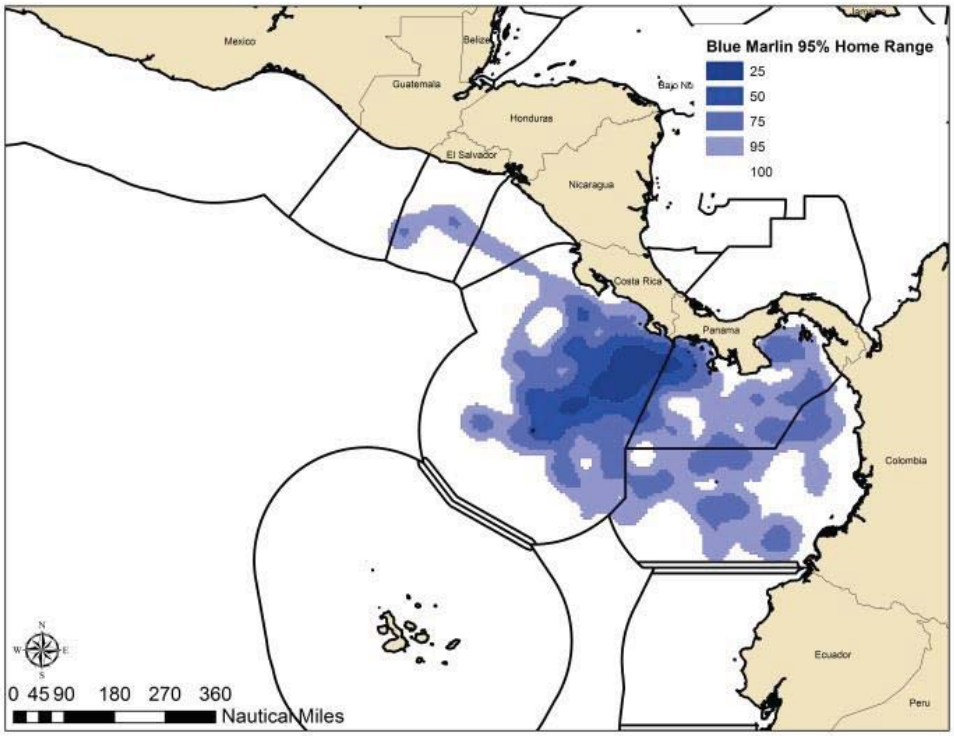

Figure 5.9 Map showing the extent of the estimated blue marlin dispersal range from satellite tagging locations. The shades of blue range from 25% to 100% darkest to lightest. The darkest blue indicates the highest density of satellite tag locations corresponding to the 25% dispersal range where 75% of tagging locations fall. The next darkest shade of blue indicates the 50% dispersal range referring to 50% of tagging locations etc.

Table 5.2 Table indicating the percent (%) residency of 10 tagged blue marlin in the Exclusive Economic Zones of countries where tag tracks occurred.

Blue marlin Tag ID	Days At Liberty	Mexico	Guatemala	El Salvador	Nicaragua	Costa Rica	Panama	Colombia	Ecuador
134240	58	0.00	0.00	0.00	0.00	96.55	3.45	0.00	0.00
134244	45	0.00	0.00	0.00	0.00	80.00	0.00	20.00	0.00
134248	38	0.00	0.00	0.00	0.00	63.16	36.84	0.00	0.00
134251	46	0.00	0.00	28.26	6.52	58.70	4.35	0.00	0.00
134254	68	0.00	0.00	0.00	0.00	91.18	8.82	0.00	0.00
134255	43	0.00	0.00	0.00	0.00	53.49	0.00	46.51	0.00
134277	200	0.00	0.00	0.00	0.00	6.29	44.76	48.95	0.00
134283	95	0.00	0.00	0.00	0.00	69.51	30.49	0.00	0.00
134245	66	0.00	0.00	0.00	0.00	100.00	0.00	0.00	0.00
134284	60	0.00	0.00	0.00	0.00	90.00	10.00	0.00	0.00
Average	71.9	0.00	0.00	2.83	0.65	70.89	13.87	11.55	0.00

Kernel Density Overlap of Sailfish and YFT

YFT purse seine fishing operations off Central America appear to interact with billfish resources as shown by the spatial relationship found between YFT and sailfish catches (Figure 10) where the degree of correlation between sailfish and YFT is mapped to determine the regions of highest overlap of sailfish and YFT habitat. However, the level and extent of such spatial overlap varies considerably showing the highest degree of association within the EEZs of Costa Rica, Guatemala, and Panama as well as in an open ocean region offshore of the Guatemala and El Salvador EEZs (Figure 5.10). Lesser overlap is observed off Nicaragua and El Salvador. There is a low level of overlap in catches in the easternmost region of the Mexican EEZ and a very small region of the northwest Colombian EEZ. Generally, it is observed that YFT catches occur over most of the sailfish habitat range, and consequently, any fishery management regulation implemented on the YFT fishery in this area will necessarily affect the sailfish population with which it appears to interact.

Considering the closed areas designed and adopted in Costa Rica to protect juvenile tunas from purse seining, provide access to the tuna resources by local fleets and prevent interactions with the recreational fisheries (Figure 3), it is observed that the more coastal Zone A&B contains a large area of sailfish and YFT catch overlap representing the area of the highest correlation of catch within the entire EPO (Figure 10). Zone C contains relatively no overlap in the western portion of the zone and low correlation in the eastern portion of such area. Zone D has no purse seine overlap between sailfish and YFT and juvenile size frequencies were not publically available for YFT to corroborate reasoning for protecting this zone as juvenile tuna habitat. The remaining EEZ not

included in the Costa Rica zonal management regime contained the second highest correlation of sailfish and YFT overlap in the EPO.

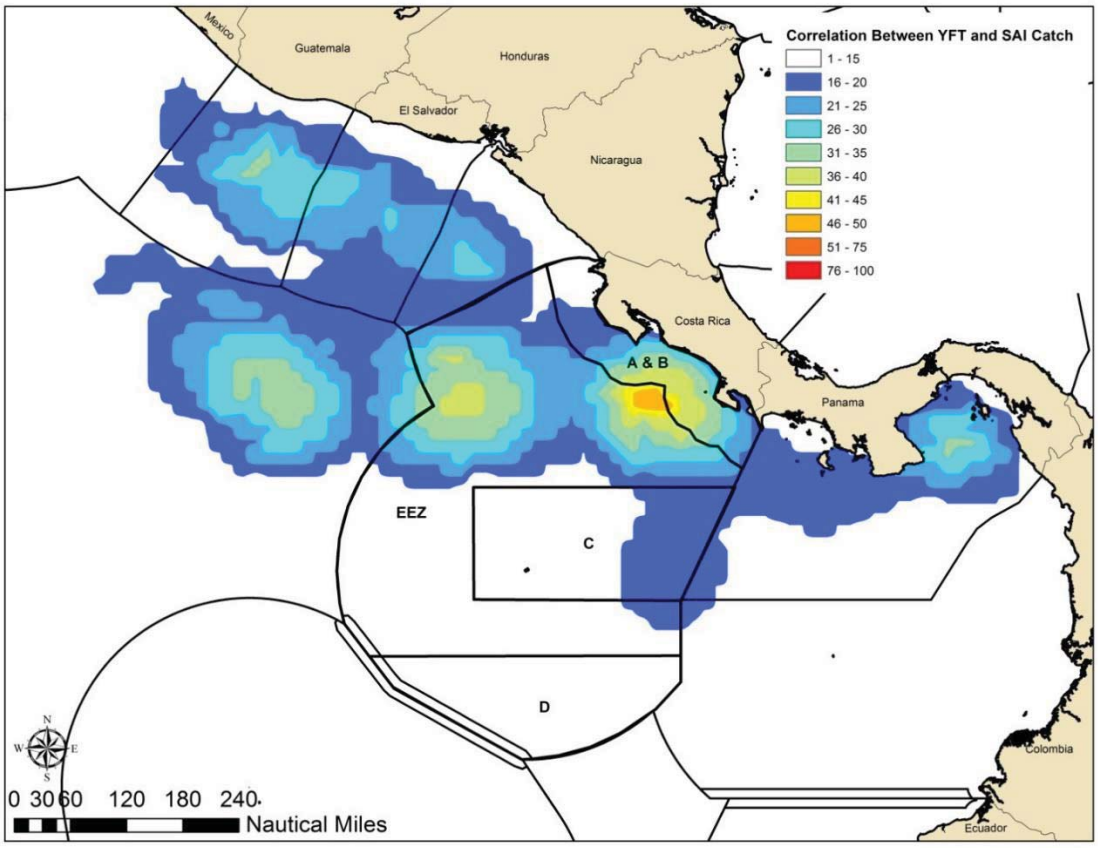

Figure 5.10 Sailfish and YFT purse seine catch overlap between 2000 and 2012 where higher values of correlation indicated higher numbers of sailfish caught with YFT in purse seine sets.

Costa Rica Closed Area Residence

The kernel density of sailfish tagging locations when compared with the YFT purse seine management areas in Costa Rica reveals that the highest relative densities of tagging locations, therefore of more concentrated habitat use by the species, occur within the Costa Rica EEZ as well as within Zones A&B and Zone C but not Zone D (Figure 5.11). It is important to note that the two areas of highest habitat use found within Zone A&B are corresponding to the two tag deployment locations where all tags were placed

representing the two major recreational fishing regions along Costa Rica's Pacific coast. These results identified by tag deployment location may appear to have bias due to spatial sampling; however, these two locations are well represented in the catch of sailfish both commercially (purse seine) and recreationally (two locations are fishing grounds for highest density of recreational fishing lodges in Costa Rica). This is further emphasized by the sailfish's ability to migrate out of this high density area within one day revealing these points to be valid indicators of sailfish presence within the area. For this purpose these two density locations represent small scale hotspots of sailfish presence in Costa Rica. Zone D has low levels of sailfish tag density only in the northern portion of this zone; however, the lowest habitat use level indicated by light green in figure 9, occurs over all the peripheral regions of main habitat use. Within the Costa Rica EEZ, sailfish spent an average of 16.97% of the time at large in Zone A&B, 13.59% in Zone C, 2.39% in Zone D, and 67.06% in the remaining non-zoned portion of the EEZ (Table 5.3).

The blue marlin kernel density map (Figure 5.12) shows that within the up to 200 days of tag dispersal, the highest habitat use of the tagged fish in the EPO occurs within the Costa Rica EEZ, with Zone C engulfing a significant fraction of the time spent in that area with lesser habitat use in the easternmost portion of Zone A&B, and just outside the Costa Rica EEZ in the nearshore of Panama's EEZ. Zone D shows some blue marlin habitat use in the eastern portion but such densities are relatively low compared to those found in Zone C. The western portion of Costa Rica's EEZ has the lowest densities as most blue marlin remained near the tagging location or traveled east and south. Within the Costa Rica EEZ, blue marlin spent 12.69% within Zone A&B, 44.87% within Zone C, 2.44% in Zone D, and 40.00% within the remaining portion of the EEZ (Table 5.4).

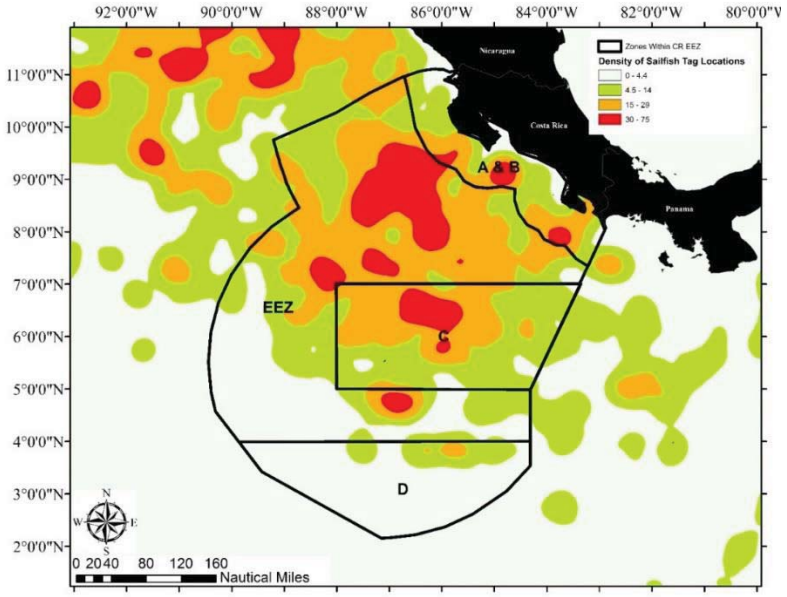

Figure 5.11 Map of the kernel density of sailfish satellite tagging locations within the Costa Rica Exclusive Economic Zone that was split into fishing zones in 2014.

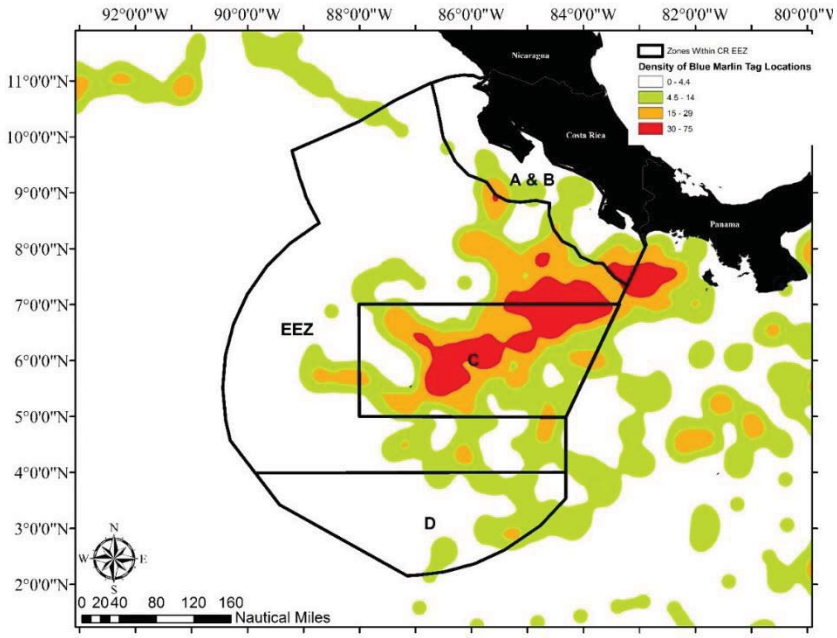

Figure 5.12 Map of the kernel density of blue marlin satellite tagging locations within the Costa Rica Exclusive Economic Zone that was split into fishing zones in 2014.

Table 5.3 Residence (% time) of satellite tagged sailfish within Costa Rica's Exclusive Economic Zone

Sailfish	A&B	C	D	No Zone
134241	15.56	17.78	0.00	66.67
134252	30.00	0.00	0.00	70.00
134258	14.04	15.79	0.00	70.18
134260	25.00	0.00	0.00	75.00
134263	2.13	40.43	0.00	57.45
134266	33.33	0.00	0.00	66.67
134267	100.00	0.00	0.00	0.00
134268	22.73	72.73	0.00	4.55
134272	2.94	32.35	0.00	64.71
134273	11.11	0.00	0.00	88.89
134275	5.88	0.00	0.00	94.12
134276	9.09	0.00	0.00	90.91
134280	2.56	20.51	20.51	56.41
134285	11.76	0.00	0.00	88.24
134288	15.15	0.00	0.00	84.85
134242	2.44	41.46	0.00	56.10
134250	26.09	0.00	0.00	73.91
134257	12.50	0.00	0.00	87.50
134270	6.45	25.81	0.00	67.74
134279	3.85	0.00	0.00	96.15
134281	3.70	18.52	29.63	48.15
Average	16.97	13.59	2.39	67.06

Table 5.4: Residence (% time) of satellite tagged blue marlin within Costa Rica's Exclusive Economic Zone

Blue Marlin	A&B	C	D	No Zone
134240	12.50	26.79	0.00	60.71
134244	5.56	63.89	8.33	22.22
134248	33.33	0.00	0.00	66.67
134251	29.63	29.63	0.00	40.74
134254	12.90	46.77	0.00	40.32
134255	4.35	69.57	8.70	17.39
134277	11.11	55.56	0.00	33.33
134283	12.28	56.14	0.00	31.58
134245	1.52	48.48	0.00	50.00
134284	3.70	51.85	7.41	37.04
Average	12.69	44.87	2.44	40.00

YFT Purse Seine Catch Relative to Area Closure

Considering the need to analyze the impact of the October 2014 presidential decree on purse seine exclusion zone definitions, purse seine YFT catch levels were analyzed within a time scope from 2009 to 2015, thus incorporating years before and after such presidential decree (Figure 5.2). Total yearly catch within the bounds of this analysis found 2009, 2010, and 2015 to contain the highest catch levels with 2015's catch being the highest (Table 5.5). Following 2010, a trend of decreased YFT catch was observed with 2011 to 2014 having the lowest catches, 25,552mt and 30,334mt respectively, leading up to the high catch seen in 2015 at 49,919mt. Catch per unit effort was greatest in 2009 followed by a decline until 2014 when the lowest CPUE of the seven years was witnessed. In 2015, CPUE increased again to near pre-2011 levels. The number of purse seine sets varied over the seven years with 2015 having the highest number of total sets and 2011 having the lowest. Between 2014 and 2015 when the presidential decree on purse seine area closure within the Costa Rica EEZ took place on October 2014, the number of total sets increased from 4124 to 4819, consequently the total catch increased from 30,343 mt to 49,919 mt, and the CPUE increased from 7.36 to 10.36 tons per set. Abundance here is not the target of examination as this is affected by recruitment which is not accounted for in this analysis; however the distribution (Figures 5.13 and 5.14) reveals important spatial changes caused by the redistribution of purse seine fishing effort.

Table 5.5 Catch of Yellowfin tuna between the geographical boundaries of 80-93W and 1-12N for years 2009-2015 including effort in number of sets, total catch and catch per unit effort

Year	Total Sets	Total YFT Catch (mt)	Yearly Regional CPUE
2009	3445	41863	12.2
2010	4261	42467	10.0
2011	2636	25552	9.7
2012	3567	35158	9.9
2013	4634	37350	8.1
2014	4124	30344	7.4
2015	4819	49919	10.4

On a per exclusion area scale, in 2014 the distribution of YFT catch shows a large portion of catch within the analysis area to be within Zone C, west of Zone C but still within the Costa Rica EEZ, and east and southeast of Zone C in the Panama and Colombia EEZs (Figure 5.13). Zone A&B has no purse seine effort and values are only given if part of the grid lies outside of this zone's border. The distribution of YFT catches between 2014 and 2015 was expected to be quite different due to restricted fishing zones closed to purse seine effort in those years, which was found to be true especially within Zone C (Figure 5.13)

It is noted that starting in 2015, after the purse seine exclusion presidential decree was enacted, the spatial catch distribution moved significantly away from Zone C both east and west. In that year Zone C had little to no YFT catch in the IATTC purse seine fishery; however, more fish were caught in the surrounding Zone C than in years past especially to the immediate north and west of the zone within Costa Rica's EEZ (Figure 5.14). This clearly is an effect of moving fishing intensity outside of the regulatory area and coupling it to more intense fishing to areas that are not under regulatory measures.

Catches in Zone D were similar in both years and again in 2015 indicating that this area is of no potential exploitation interest by the purse seine fleets. No YFT were caught in the purse seine within Zone A&B, which is indicative that the objective of keeping purse seine effort outside of the areas of recreational fishing activity may not, after all, be affected by the very low billfish bycatch reported by observers aboard the tuna purse seiners. The most evident difference is in the region bounded by latitudes 6-10^{O} and longitudes 85-93^{O} (Figure 5.14) where catches drastically increased following the closure of Zone C. Generally, more YFT were caught in the year following the implementation of the regulation and a higher CPUE was witnessed following this presidential decree. However, area C profited from less tuna fishing exploitation.

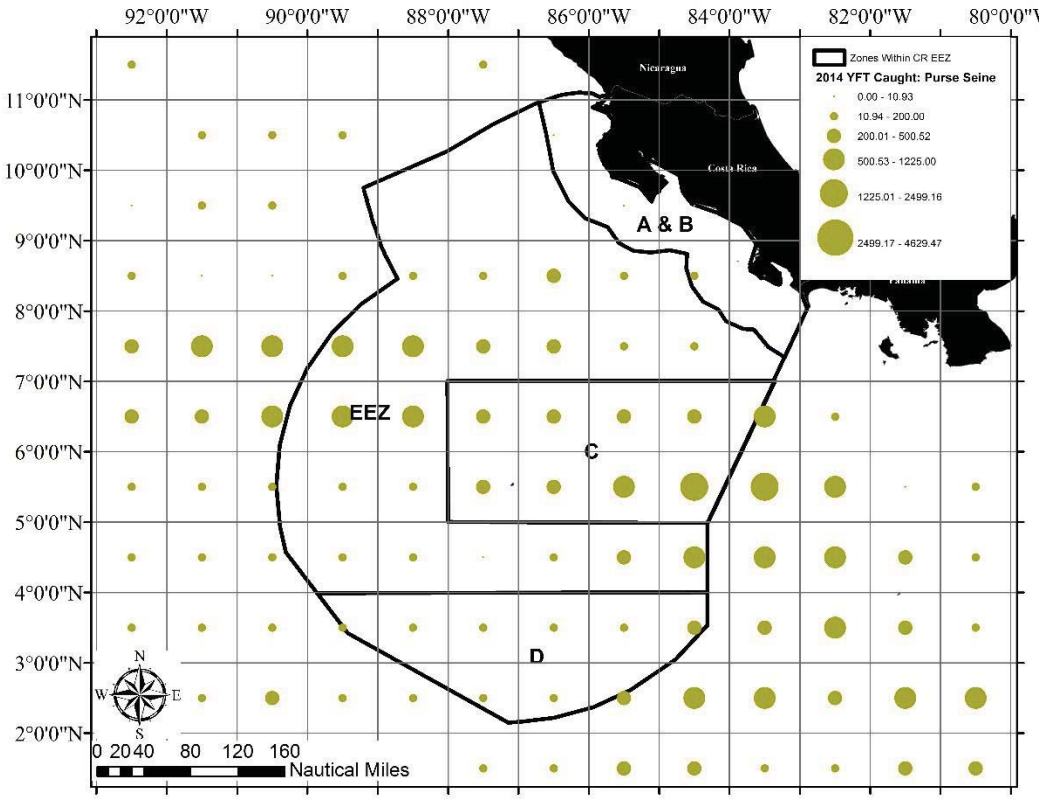

Figure 5.13 Map showing the distribution of purse seine YFT catch in the region off Costa Rica from 2014 prior to the implementation of the Presidential decree taking place at the end of that year splitting the Costa Rica EEZ into fishing zones. Purse

seine fgishing was allowed in zones C and D in this year and represented a large potion of purse seine YFT catch within the Costa Rican EEZ.

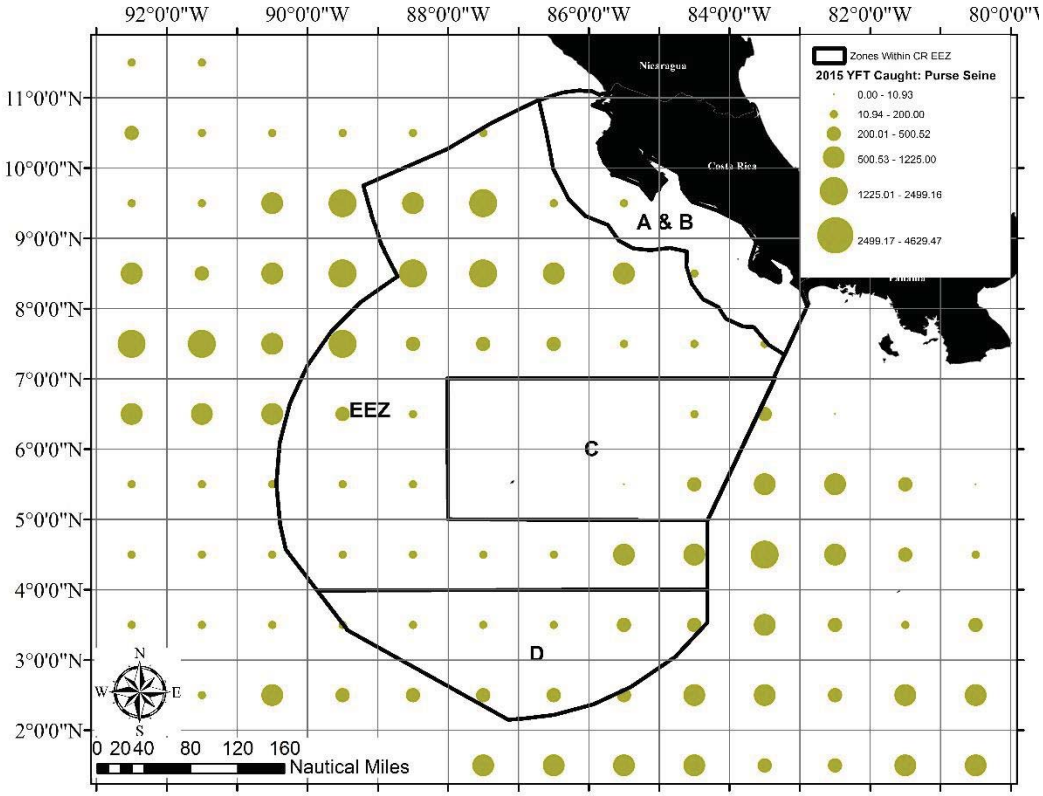

Figure 5.14 Map showing the distribution of purse seine YFT catch in the region off Costa Rica from 2015 following the implementation of the Presidential decree splitting the Costa Rica EEZ into fishing zones. Purse seine fgishing was not allowed in zones C and D in this year and this is made evident by the redistribution of YFT catch following the decree.

Discussion

Distributional Population Mean Centers

The comparisons of mean population distribution centers between the billfish catches in the tuna purse seine fishery and the billfish habitat use estimated with satellite tagging data provided a unique perspective of the relative habitat population coverage relative to the potential bycatch exploitation. This is possible because the data is originated from the spatial distribution of tuna purse seine fishing effort, which covers the

entire potential habitat range of the sailfish that is caught non-selectively in purse seines. Also, sailfish is the only billfish species to show significant schooling behavior, thus the species is more likely to be part of the catches of schooling tuna. Tagged sailfish trajectories expanded significantly over the EPO, which coincided well with the mean center of gravity for catch distributions. This finding validated the use of satellite tagging densities to express habitat use, and the resulting mean center to be used in dispersal range analysis for sailfish. The full extent of fishing effort by the purse seine as well as the kernel density, defined by the probability density function of the spatial locations of sailfish, were matching. It was found that in both datasets, sailfish were predominantly coastal billfish species which coincides with previous studies examining the population distribution of sailfish using other data sources (Ehrhardt and Fitchett 2006, Fitchett 2015, Hinton and Maunder 2011, Prince et al. 2006). This was not the case with blue marlin due to more spatially restricted but persistent migrations of the tagged individuals in a smaller area relative to catches in the EPO.

This generated a lack of blue marlin tagging locations west of the longitude occupied by the Galapagos. Contrarily, catches of blue marlin in the EPO tuna purse seine fishery stretch far west from the coastal areas where sailfish catch was restricted to mainly nearshore pelagic environments.

The lack of blue marlin satellite tagging location coverage in those areas is likely due to two potential causes: the deployment duration not lasting the full extent of the year (<200 days) to include a complete cycle of seasonal migrations or the presence of seasonally localized blue marlin stocks that are not reflected on the compounded catch data. Recent year blue marlin purse seine CPUE (Total Catch/Total Number of Sets) from

2000-2015 reveals the region occupied by the satellite tagged blue marlin to coincide with an area of higher CPUE for blue marlin off Costa Rica and Panama (Figure 5.15). Perhaps more importantly is the relatively low CPUE off Mexico, Guatemala, El Salvador, and Nicaragua where satellite tagged blue marlin did not reside. This region off Costa Rica and Panama where recreational catches are some of the highest worldwide may be a specific hotspot for the EPO blue marlin stock. Another example may be in Hawaii where blue marlin are commonly caught both commercially and recreationally which may represent a separate hotspot much like the hypothesized region off Costa Rica. It may be possible these hotspots are interconnected through migration not witnessed by satellite tagging or that the migratory interconnectedness is rare. Further genetic analysis could reveal the extent of this relationship between blue marlin hotspots. Furthermore, the homogenous character of the blue marlin catch distribution in the purse seine in the open ocean may be an indication that the population of blue marlin is distributed over a larger area than the more local EPO stock that was sampled for satellite tagging in this study. For this purpose, the dispersal range analysis performed on blue marlin should be considered, at this time, a local blue marlin stock range in the EPO.

The population distribution mean centers for the tagged and catch of YFT, catch account for the large scale of YFT fishing across the Pacific especially in the western most region of the EPO fishing area. Of the species included in this analysis, YFT had the furthest west mean centers due to the catch across the equator and towards western longitudes of the species distribution declared by the IATTC. This is very much opposite of sailfish that were mainly coastal in the eastern most section of the EPO.

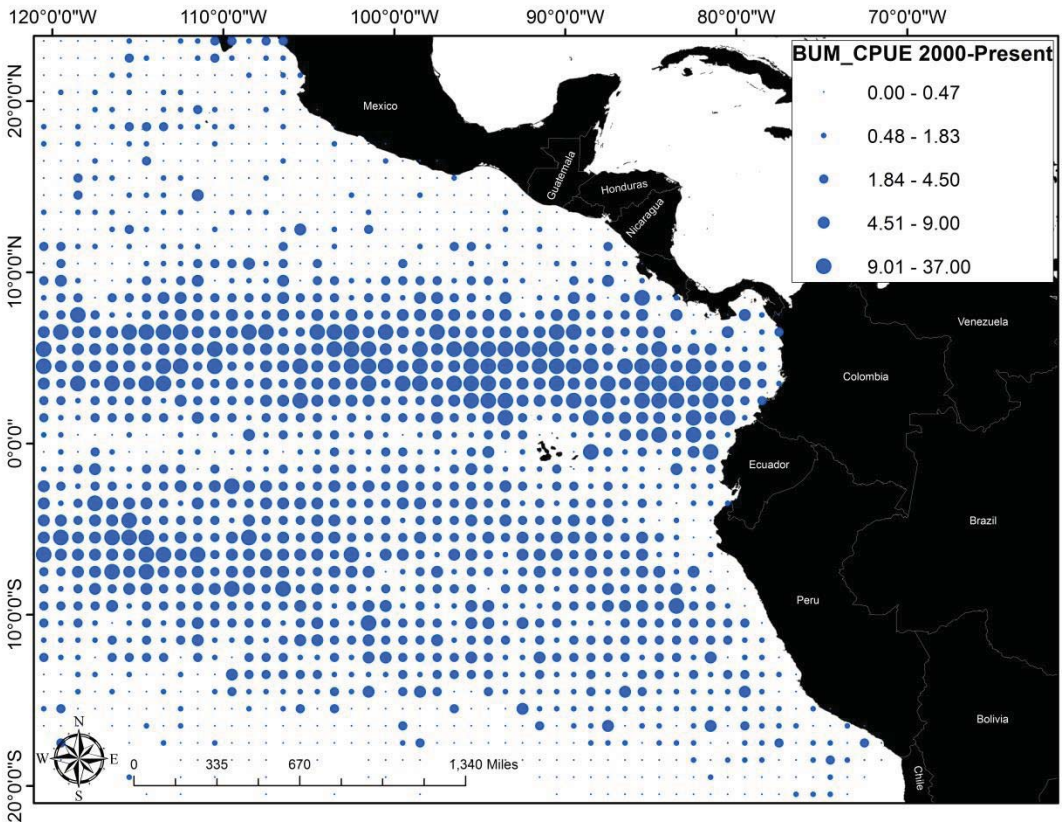

Figure 5.15 Blue marlin catch per unit effort by 1 degree (latxlon) squares for years 2000-2015.

Based solely on this mean center analysis it can be confirmed that sailfish have a much different population dynamic distribution than both blue marlin and YFT, at least as expressed by the relative spatial distribution of the YFT purse seine fishery data. One possible explanation could be related to the propensity of sailfish to form small schools compared to blue marlin which are more solitary (Personal Communications, Multiple Captains Worldwide). The shape and extent of local dispersal ranges in the EPO for sailfish and blue marlin indicate they share the same habitat which overlaps where YFT are caught but this is not indicated by mean center analysis. The likely reason for this mismatch is the fact that the purse seine fishing is non-selective, catching everything

within the active fishing area of the net, and overall fishing effort covers an extremely large area (Figure 5.16). The spatial extent of fishing outside of the EPO coastal environment could convolute comparisons of open ocean inhabiting species compared to sailfish that are caught in a relatively small portion of the fishing area.

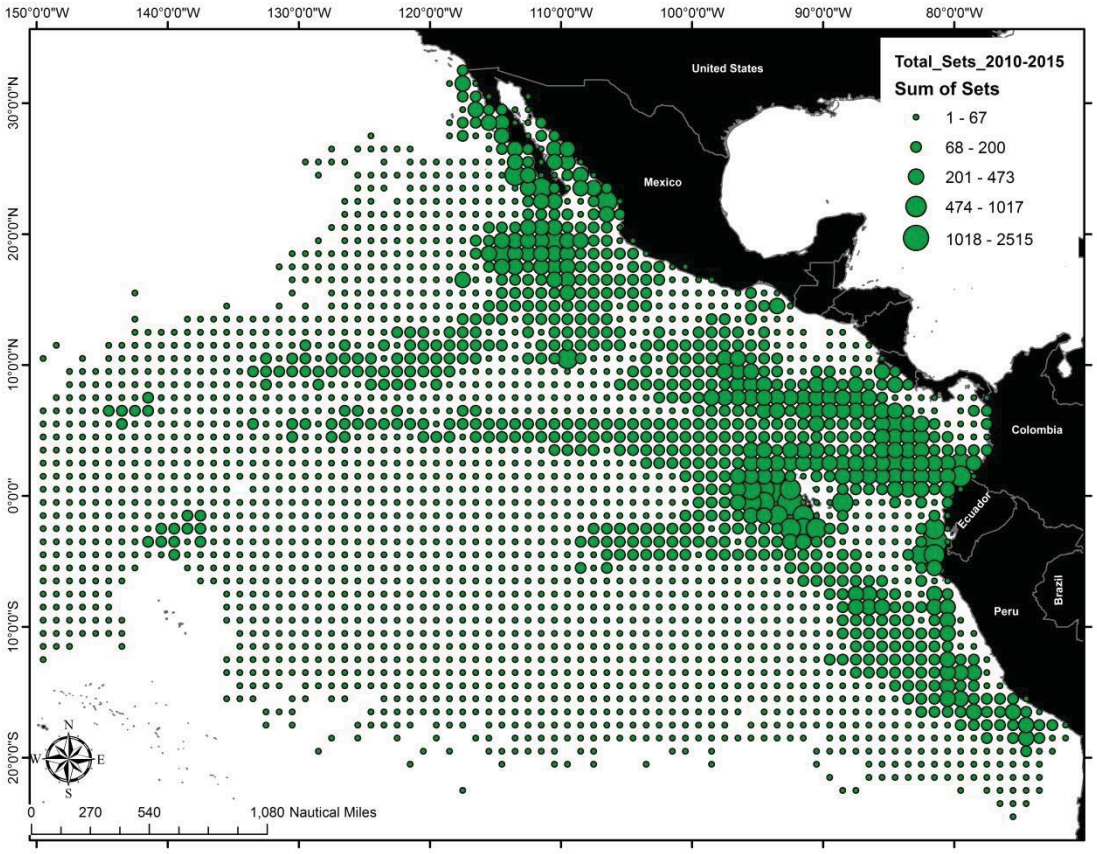

Figure 5.16 Figure showing spatial distribution of purse seine sets from 2010 to 2015.

Dispersal Range Analysis

A dispersal range represents the physical culmination of an animal's resource and habitat optimization through evolutionary adaptation of fundamental mechanisms such as feeding and reproduction. These characteristics are based on ecosystem interactions under varying environmental conditions that should result in maximizing bioenergetic

efficiency of resource use, thus optimizing biological fitness (e.g. Powell and Mitchell 2012). In terrestrial species this knowledge and understanding of habitat that improves fitness is called an animal's cognitive map (Borger et al. 2008, Powell 2000, Spencer 2012). The concept of a cognitive map has not been applied to highly migratory pelagic fish species. The amount of information that would be required to develop and define a cognitive map of the EPO pertaining preferred habitat by highly migratory species such as sailfish and blue marlin, may prove impossible. Ebersol (1980) indicates that it is possible for a more sedentary animal to be territorial over a small area, such as a reef fish; however, on larger scales this concept breaks down due to many ecosystem driving variables. For sailfish or blue marlin, it is more likely that environmental features of specific and transient habitat features may trigger a response based on natural selection where the animal innately recognizes multiple preferences or factors, or lack thereof, for said habitats.

The spatial coincidence or correlation of distributions, of catch and satellite tagging locations allows, in part, for a legitimate, validated estimation of a generic dispersal range from the 21 tagged sailfish and a local EPO dispersal range from the 10 tagged blue marlin. The major centers of the dispersal range population or stock distribution (25% level) for sailfish match well with the major recreational fishing areas off Costa Rica, El Salvador, and Guatemala (Figure 6) where some of the world's highest billfish catch rates are persistently found (Ehrhardt and Fitchett 2006). For blue marlin, the region off Costa Rica known as the Coco Island Ridge represents the majority of the dispersal range as these tagged fish, which did not migrate far from their tag deployment location compared to sailfish (Figure 7). This has important implications for billfish

spatial management considerations in those countries that rely on tourism as a major economic driver especially if this dispersal range were to change with exploitation or environmental factors.

An important ecological result of these analyses is the lack of sailfish residence within the Nicaraguan EEZ which lies in between major centers of the sailfish distribution (i.e Guatemala and Costa Rica). Sailfish need to travel through this area from the tag deployment location in Costa Rica to El Salvador and Guatemala yet spend less time than in either of those EEZs. In fact, sailfish released in Costa Rica spent more time proportionally in Mexico which was the furthest EEZ away from the deployment location. This lack of residence can be attributed to the oceanographic features of the Costa Rica Dome (CRD), which was discussed in Chapter 1 of this Dissertation. The CRD is an area of intense upwelling caused by the intercontinental Papagayo wind jet and interactions with local currents (Willett et al. 2006). Tagged sailfish travelled either around the CRD or through it; however, observed migratory routes taken across the CRD tended to be more direct and at a faster rate (Figure 5.17) compared to typical more discontinuous movements such as those observed under search patterns, suggesting some level of environmental avoidance. Also sailfish showed an affinity for the edges of the CRD likely due to the convergent and divergent oceanographic features caused by sheer forces at the edge of the CRD's features. This concept is a proof of the widely proposed hypothesis, but arguably untested, that predators are attracted to regions of convergence (Bakun 2006).

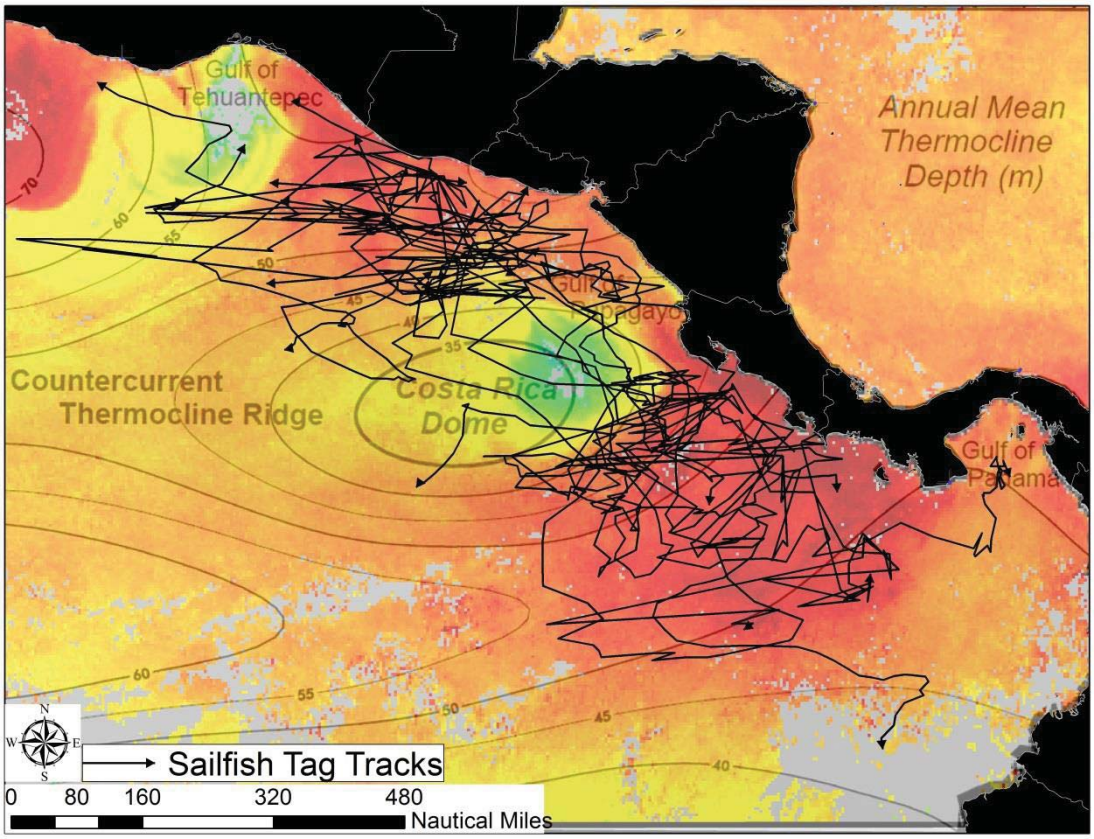

Figure 5.17 Thermocline depth isolines captured from Fiedler 2002 overlaid on winter SST from February 2013 and sailfish satellite tag tracks

Sailfish predominantly migrated away from the tagging location in Costa Rica with many traveling north and west toward Mexico where blue marlin did exactly the opposite. Almost all the tagged blue marlin remained within Costa Rican EEZ and those that migrated away travelled south and east toward Panama and Colombia with only one fish moving north and reaching El Salvador. Knowing blue marlin are highly migratory and capable of long range open ocean movements in the Pacific (Carlisle et al. 2016, IATTC Status Report 2016), it is particularly important to find such a great affinity for the region off Costa Rica known as the Coco Islands Ridge corridor under relatively persistent tag trial durations.

The Coco Island Ridge area is characterized by a large number of seamounts creating abundant relief and opportunities for oceanographically beneficial locations such as convergent boundaries, upwelling, and potential increased abundance of organisms living within the deep scattering layer (Holland and Grubbs 2007). The Coco Island Ridge region is well known among recreational anglers in Costa Rica as a rich feeding ground for billfish species, especially blue marlin where anglers take offshore multi-day charters fishing trips seeking high blue marlin catch rates. The seamount region and Coco's Island area are also known for large seasonal aggregations of schooling sharks as well as for the presence of pelagic sharks year-round (Bessudo et al. 2001, Litvinov 2008, White et al. 2015). These seamounts could potentially be aggregating other pelagic species that share prey items such as marlin species and affecting their local migratory patterns as the ecosystem provides feeding opportunities during the time period of tag deployments.

A distributional difference between sailfish and blue marlin found in these analyses may be attributed to differing sub-regional associations of prey between the two species. With blue marlin growing to a larger size and higher up on the trophic spectrum (Olson and Watters 2003) than sailfish it is likely their bioenergetics needs require different prey sources. The more coastal sailfish seeks out small pelagic species, some of them with schooling habits forcing the sailfish to feeding strategies that are different to larger isolated swimmers as the blue marlin. Blue marlin on the other hand are more associated with offshore locales such as the Coco Island Ridge where larger juvenile tunas and tuna-like species are likely the main diet option. Although this concept is somewhat speculative in the tropical EPO where diet studies are not available,

recreational fishermen in this area have developed and implemented fishing and bait techniques to target and retain small tuna species (bonita, skipjack, small YFT) to be used as live bait specifically for blue marlin recreational fishing on the Coco Island Ridge seamounts. This same technique is not employed by the recreational fishermen when targeting sailfish due to the large size of the bait relative to sailfish. Sailfish recreational fishing techniques in the region focus on ballyhoo and smaller dead bait trolling and rarely travel as far out as the Coco's Island Ridge blue marlin fishing grounds. This concept is supported by diet studies done in other parts of the world where small tuna species make up the majority of blue marlin diet and smaller non-tuna species comprising sailfish diet (Abitia-Cardenas et al. 1999, Evans and Wares 1972, Nakamura 1985, Shimose et al. 2006)

Exclusive Economic Zone Billfish Residence

The analysis of migratory range compared to EEZs has two-fold benefits: knowledge of access for each country to the migratory resources for extraction and recreational use, and secondly, the knowledge on the range of a species relative to management and protection required for resource conservation. It is impossible to protect highly migratory species such as sailfish or blue marlin within any one given country's political boundaries if knowledge on the overlapping of migratory ranges and geopolitical boundaries are not clearly defined. In fact, arguments could potentially be made in Costa Rica that regional Cocos Island Ridge seamount management zone could be defined given they have such a high proportion of blue marlin residence and recreational catch rates within the country's boundaries (Unpublished Costa Rica tournament data). With

sailfish travelling the entire length of the Central American coast as well as further north to Mexico and south to Ecuador, any conservation practice or management regime aimed to protect the species would require international agreements based on well supported scientific arguments among all the governments involved. The conditions leading to implementation of spatial management require, in addition to political will, regional institutional and political integration which is difficult to achieve given strong nationalistic positions regarding open access of fishery resources as well as user allocation issues that are economically and politically contrasting. This is not to say that individual country actions addressing conservation are not effective, but less sailfish or blue marlin killed in one country could result in improved catches in the neighboring country instead of the overall intended purpose of reducing fishing mortality.

The association of YFT and sailfish catch in the EPO tuna directed purse seine fishery (Figure 10) provides a unique piece of evidence that the location of highest association between the species is off the Costa Rican coast within travel distance of many of Costa Rica's commercial and recreational fishing ports. Such association also exists between spotted dolphin and YFT which has been responsible for historic large tuna fishing developments targeting dolphin schools in the EPO. The vulnerability of sailfish off Costa Rica is of major concern considering the lack of ability to manage the fishery based on the health of a stock that is undergoing fishing mortality from multinational fishing fleets.

There exists in international lack of science based management in many of the countries involved in industrial and artisanal tuna and tuna-associated fisheries with only 7% of all coastal countries having some sort of scientific based management regime, only

1.4% with the ability to turn science into policy, and 0.95% having the ability to enforce regulations (Mora et al. 2009). For species that cover such a broad distribution and especially those caught as bycatch in several non-billfish directed fisheries, no one management strategy or regime will suffice. A marine protected area covering the range of sailfish or blue marlin distribution would be impossible to enforce on such a large scale and would do little to curb bycatch based on the massive scale of sailfish and blue marlin habitat and extent of commercial fishing effort. Eliminating commercial fishing altogether is not feasible either due to the reliance of economically and socially important tuna industrial and artisanal fisheries.

Purse Seine Catch Relative to Area Closure

The presidential decree set forth in October 2014 to exclude tuna purse seining in Costa Rica sought to make migratory YFT available for Costa Rican fishermen as well as protect recreational fishing within a coastal buffer zone by limiting the industrial purse seine fleet and to protect juvenile tuna in the more offshore areas of the EEZ. Zone A&B is a coastal buffer specifically designed to keep purse seining away from shore and allow local fishermen, both commercial and recreational, to exploit the most coastal populations of fish. As mentioned previously, the local commercial fishermen are typically longliners which catch significantly more billfish per unit effort than the purse seine in the EPO. As shown in Figure 10, the A&B zone historically contains some of the highest instances of overlap between YFT and sailfish resources. This poses a potential ecological problem for this presidential decree where increased fishing activities targeting

tuna by local longliners, which catch proportionally much more billfish, should result in increased fishing mortality of bycatch species, such as billfish.

Both the sailfish and blue marlin dispersal ranges fell partially within Zone A&B thus both species could have higher fishing mortality than what would be expected (Figures 9 and 10); however, blue marlin are less coastal than sailfish and would be less vulnerable to fishing operations within this zone. On the other end of the spectrum, the lack of competition for resources within this area likely provides improved fishing and revenue for local fishermen both commercially and recreationally, assuming overfishing is not occurring at the YFT stock level. An important distinction to make here is that the IATTC purse seine fleet did not fish in the A&B zone after 2014 but had a history of fishing this region since the inception of the YFT purse seine fishery in the early 1950's.

The most offshore Zone D was specifically included in the purse seine exclusion regulation as an area to promote protection of YFT recruitment and juvenile habitat. These analyses cannot evaluate the efficacy of this strategy due to lack of public access of the information available on YFT size distributions spatially stratified. However, there was little to no change in purse seine catch in Zone D in the transition from 2014 to 2015 following the decree. Furthermore, neither sailfish nor blue marlin resided in significant amounts within this zone given that only 2.44% of the time satellite tagged fish within the Costa Rica EEZ inhabited in Zone D. Therefore, any changes associated with Zone D management are unlikely to affect billfish on a scale similar to impacts on Zone A&B and Zone C.

Zone C is a more oceanic protected zone designed to limit industrial purse seine fishing to allow more YFT resources for the large scale Costa Rican longline commercial

vessels. Once again, these vessels catch billfish bycatch in higher proportion than the purse seine; therefore, a noticeable source of concern regarding future conservation of the billfish resources in the area. The purse seine exclusion zone was successful in removing the IATTC purse seine effort (Figures 13 and 14) with a major spatial reorganization of YFT catches between 2014 and 2015. This however, did not affect the total amount of YFT caught as more effort and catch were witnessed in 2015 compared to 2014 as well as an improvement in CPUE after the management regulation was implemented. This also likely had a negative impact on billfish mortality with increased local longline fishing, which so far has not been reported. The industrial purse seine moved their fishing effort northwest of Zone C to a different section within Costa Rica's EEZ that allows purse seine fishing and towards the open ocean in international waters, which seems to have resulted in improved tuna fishing efficiency compared to previous years (Table 5).

Dispersal range comparisons in Zone C reveal also a strong affinity for that zone by satellite tagged blue marlin, spending almost 45% of their Costa Rica EEZ residence within this area. This affinity again points to the Coco Island Ridge region and the oceanographically important seamounts that exist there as one of strategic biological importance for the species. Based on these findings, Zone C and the Coco Island Ridge should be considered an ecological hotspot for blue marlin habitat and further investigation and research should be directed at the fishing mortality incurred on blue marlin due to the promotion of increased longlining in this area. Sailfish are more spread out within the Costa Rican EEZ and the same conclusion can not be assigned to sailfish due to a vast majority of the species' locations occurring outside of the Costa Rican management zones.

Concluding Remarks on Sailfish and Blue Marlin Habitat Range

The lack of available catch data in the EPO coastal longline fisheries is a major issue restricting assessment and conservation of billfish such as sailfish and blue marlin (Hinton and Maunder 2011). The analyses performed in this Chapter of the Dissertation seek to develop methods of analyzing billfish habitat range using satellite tags and to utilize correlation analyses to define the degree of overlap with billfish catch found in tuna commercial fisheries in the EPO. Although data is not available publicly, the EPO longline bycatch is well documented and was discussed in the overview of this chapter. As mentioned previously, the longline, both industrial and coastal/artisanal represents the majority of billfish catch in commercial fisheries thus represent the greatest risk for overexploitation of billfish species (Figure 5.2).

A quantitative examination of the overlap of sailfish satellite tag tracks with fishing effort or catch from coastal longliners was not possible due to confidentiality of the data; however, digitizing a fishing intensity map from the only published source, published by IATTC on an experimental observer program for coastal longline fishing effort map (Compean 2014) and taking a kernel density of the points was performed for qualitative examination. Although catch and the number of overlapping points were not available, the extent of longline effort was examined (Figure 5.18). The most evident point when examining the map is the amount of longline effort in the major recreational fishing destinations in Central America, which focus on billfish and also represent the areas of highest density of sailfish defined by satellite tagging locations. It is important to reiterate that the longline is targeting tuna, mahi, and sharks but is catching billfish more

than any other bycatch species (Compean 2014). The increased longline effort off Guatemala, Nicaragua, Costa Rica, and Panama all coincide with the most densely fished areas recreationally as well as the dispersal range hotspots for sailfish and blue marlin found in this Chapter. This provides the realization that the longline is, in fact, selectively fishing in the areas where billfish are most valuable in catch and release fisheries, more vulnerable, and spend the highest percentage of their residency. Logically, this is counterintuitive for Central American and Panamanian economies where a dead sailfish caught commercially is worth significantly less than a live billfish caught and released in the recreational fisheries (Ehrhardt and Fitchett 2008).

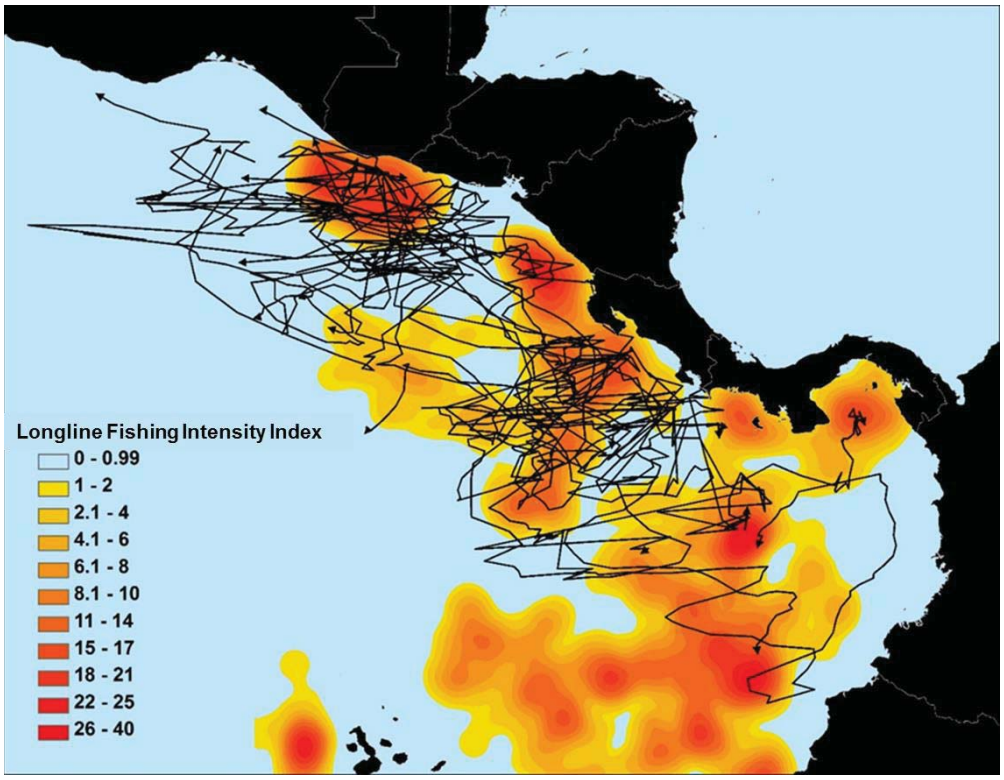

Figure 5.18 An index of longline fishing intensity (number of sets/time) is indicated in yellow to red scale with red referring to highest fishing intensity. Satellite tag tracks from sailfish are overlaid on the longline intensity indicating regions of possible vulnerability of sailfish to longline fishing practices especially off Guatemala and Costa Rica.

Although management and conservation of resources such as billfish, that occupy such vast spatial areas, may be difficult given the lack of data to determine the health of the stocks, within country management has the potential to be beneficial. Such a proposition requires knowledge and communication with all management regimes involved in the resource use. The purse seine exclusion areas promulgated in 2014 and implemented at the start of 2015 in Costa Rica successfully rearranged the distribution of catches outside of specific areas. However, such arrangement did not result in reducing the amount of fish resources removed by the fisheries effectively disqualifying the management technique as a means to reduce fishing mortality on YFT which, importantly, was never the intention of the decree. It was successful in removing the purse seine fishing effort in a zone that is now available for entry of local fisherman. These complicated issues can be problematic on the long range conservation spectrum because, although it may provide more local tuna to the local markets and money to the Costa Rican fishermen, the fishing practices are more likely to negatively affect the ecosystem due to the large bycatch generated by the longline fishing industry, especially billfish. When it is all said and done, the purse seine exclusion zones were a success for Costa Rica but may not be for the ecosystem or the economically and socially important recreational fisheries targeting sailfish and blue marlin.

Chapter 6: Conclusion

Consideration of ecosystem-based fishery management of billfish species necessitates understanding of behavioral aspects that affect their catchability as bycatch in tuna and mahi fisheries and the importance of oceanographic features that may regulate their behavior. This dissertation sought to explore behavior and habitat use of sailfish and blue marlin in the Eastern Pacific Ocean (EPO) off Central America where unique environmental forcing through wind induced upwelling, eddy formation, and low dissolved oxygen at depth impact the marine ecosystem. The resulting forced habitat limits the vertical distribution of both sailfish and blue marlin and parcels the available habitat for both predator and prey. The dissertation progresses from intra-daily behavioral characteristics relative to billfish physiology in Chapter 2 before moving to longer term migratory analysis using the behavioral change point methodology in Chapter 3. Chapter 4 uses these behavioral parameters to examine behavior relative to environmental characteristics and the tuna purse seine fishery where billfish are caught as bycatch. And finally, Chapter 5 examines the migratory behavior of sailfish and blue marlin relative to management boundaries and fishery management regimes.

Research aimed to answer the following major scientific questions: 1) how do sailfish and blue marlin use their sensory strategies to optimize efficiency of migratory pathways, 2) how do these billfish species adapt their migratory path relative to their local environment and 3) how does billfish behavior and habitat use may effect management and conservation strategies. Results in this dissertation reveal that sailfish and blue marlin have unique visual abilities to optimize feeding in ideal light conditions and that sailfish are found to show a photokinetic response to light levels. The EPO is

revealed distinct sub-ecosystems that have effects on both the vertical and horizontal distribution of sailfish and blue marlin; however, statistical testing of limited environmental variables shows that no single environmental variable can account for behavioral shifts in modelled migratory data. It is the belief of this author that the true variable most effecting distribution and behavior of billfish, not related to spawning, is the availability of prey. This importance of prey availability is clarified by blue marlin preference for Coco's Island Ridge region where fish aggregating devices have concentrated large assemblages of blue marlin prey species. Future work should attempt to quantify spatial abundance of billfish prey species in the EPO as this is likely to be the more contributing factor to behavioral shifts.

The significant population dynamic differences found between sailfish and blue marlin are attributed to very different migratory trajectories and localized behavioral characteristics. Sailfish were found to undertake more extensive spatial migratory paths throughout the EPO when compared with blue marlin, which remained within the Coco's Island Ridge a majority of their migratory path. These blue marlin also showed significantly slower migratory movement within this concentrated region indicating a preference for this habitat characterizes by seamounts and human introduced fish aggregating devices. The increased local abundance of blue marlin within this region suggests a change in catchability which has implications for the local blue marlin stock, potentially increasing vulnerability to surface fishing and changing the dynamics of seasonality of animal movement.

The large range of sailfish migratory trajectories throughout the EPO suggests regional fisheries management for the purpose of conservation should seek to consider

the convolution of international economic zones and that conservation strategies must incorporate larger spatial scales than traditional country-wide regimes. Sailfish and blue marlin residency within individual economic zones and in relation to area closures suggests there is potential for protection of these billfish stocks but that purse seine regulation should not be the target fishery to limit bycatch but rather the coastal industrial and artisanal longlines that catch billfish in much higher proportion of catch. It was determined that billfish data generated in the tuna purse seine fishery is not sufficient to examine distribution or relative abundance of sailfish and blue marlin given the bycatch nature of billfish in this fishery and the low numbers caught over space and time. This likely contributes to the difficulties encountered in performing stock assessment on sailfish or blue marlin due to lack of appropriate catch data. it is imperative that data on coastal longline fisheries, is collected and made available to better estimate abundance and distribution of billfish in the EPO where they are highly vulnerable to surface longlines.

The research presented in this dissertation utilized advanced technologies and, in many cases, newly developed data collection techniques and analysis algorithms. The use of PSATs represents the only means of assessing sailfish and blue marlin behavior and habitat use in the wild, but their use is not without drawbacks. The benefits of improved accuracy and precision in geolocation using the SeaTag compared to traditional light-based geolocation PSATs allowed for the analysis of oceanographic comparisons and preference for habitats. As technology continues to improve, the benefits of increased location accuracy will allow for the furthering of this research to highly specific locales as opposed to the more region-wide analyses presented in this dissertation. Overall, this

dissertation successfully applied technologies and methodologies never before used in billfish PSAT research and was able to use these results to better understand the driving factors of billfish migration. Understanding behavior and habitat use on an hourly time scale provides insight into physiological modalities for feeding which provides the basis for understanding how this hourly behavior transitions to daily and monthly migratory behavior. Finally, these behaviors and migrations are reviewed relative to human drawn boundaries which critically ties this ecological research to real-world applications of conservation and management.

WORKS CITED

Abitia-Cardenas, L. A., Galvan-Magaña, F., Gutierrez-Sanchez, F. J., Rodriguez-Romero, J., Aguilar-Palomino, B., & Moehl-Hitz, A. (1999). Diet of blue marlin Makaira mazara off the coast of Cabo San Lucas, Baja California Sur, Mexico. *Fisheries Research, 44*(1), 95-100. doi:http://dx.doi.org/10.1016/S0165-7836(99)00053-3

Andrade, H. (2009). Using delta-gamma generalized linear models to standardize catch rates of yellowfin tuna caught by Brazilian bait boats. In H. A. Andrade (Ed.), (Vol. 64, pp. 1171-1181).

Bakun, A. (2006). Fronts and eddies as key structures in the habitat of marine fish larvae: opportunity, adaptive response and competitive advantage. *Scientia Marina, 70*(S2), 105-122.

Beyer, H.L. (2017) "Geospatial Modelling Environment (Version 0. 7.2. 0)," (software), http://www.spatialecology.com/gme/

Bigelow, K. A., Boggs, C. H., & He, X. (1999). Environmental effects on swordfish and blue shark catch rates in the US North Pacific longline fishery. *Fisheries Oceanography, 8*(3), 178-198.

Bigelow, K. A., Hampton, J., & Miyabe, N. (2002). Application of a habitat-based model to estimate effective longline fishing effort and relative abundance of Pacific bigeye tuna (Thunnus obesus. *Fisheries Oceanography, 11*(3), 143-155. doi:10.1046/j.1365-2419.2002.00196.x

Bigelow, K. A., & Maunder, M. N. (2007). Does habitat or depth influence catch rates of pelagic species? *Canadian Journal of Fisheries and Aquatic Sciences, 64*(11), 1581-1594. doi:10.1139/f07-115

Block, B. A. (1986). Structure of the brain and eye heater tissue in marlins, sailfish, and spearfishes. *Journal of Morphology, 190*(2), 169-189. doi:10.1002/jmor.1051900203

Block, B. A., Booth, D. T., & Carey, F. G. (1992). Depth and temperature of the blue marlin, <i>Makaira nigricans , observed by acoustic telemetry. *Marine Biology, 114*(2), 175-183. doi:10.1007/bf00349517

Bone, Q., & Moore, R. (2008). *Biology of fishes* (Third ed.): Taylor & Francis.

Bonjean F. and G.S.E. Lagerloef,(2002) ,"Diagnostic model and analysis of the surface currents in the tropical Pacific ocean", J. Phys. Oceanogr., 32, 2,938-2,954

Börger, L., Dalziel, B. D., & Fryxell, J. M. (2008). Are there general mechanisms of animal home range behaviour? A review and prospects for future research. *Ecology Letters, 11*(6), 637-650.

Brandt, P., Bange, H. W., Banyte, D., Dengler, M., Didwischus, S. H., Fischer, T., . . . Visbeck, M. (2015). On the role of circulation and mixing in the ventilation of oxygen minimum zones with a focus on the eastern tropical North Atlantic. *Biogeosciences, 12*(2), 489-512. doi:10.5194/bg-12-489-2015

Braun, C. D., Kaplan, M. B., Horodysky, A. Z., & Llopiz, J. K. (2015). Satellite telemetry reveals physical processes driving billfish behavior. *Animal Biotelemetry, 3*, 2.

Brill, R. W., Holts, D. B., Chang, R. K. C., Sullivan, S., Dewar, H., & Carey, F. G. (1993). Vertical and horizontal movements of striped marlin (Tetrapturus audax) near the Hawaiian Islands, determined by ultrasonic telemetry, with simultaneous measurement of oceanic currents. *Marine Biology, 117*(4), 567-574. doi:10.1007/bf00349767

Brill, R. W., & Lutcavage, M. E. (2001). Understanding environmental influences on movements and depth distributions of tunas and billfishes can significantly improve population assessments. *Island in the Stream: Oceanography and Fisheries of the Charleston Bump, 25*, 179-198.

Burt, W. H. (1943). Territoriality and home range concepts as applied to mammals. *Journal of Mammalogy, 24*(3), 346-352.

Carlisle, A. B., Kochevar, R. E., Arostegui, M. C., Ganong, J. E., Castleton, M., Schratwieser, J., & Block, B. A. (2017). Influence of temperature and oxygen on the distribution of blue marlin (Makaira nigricans) in the Central Pacific. *Fisheries Oceanography, 26*(1), 34-48.

Chiang, W.-C., Musyl, M. K., Sun, C.-L., Chen, S.-Y., Chen, W.-Y., Liu, D.-C., . . . Huang, T.-L. (2011). Vertical and horizontal movements of sailfish (Istiophorus platypterus) near Taiwan determined using pop-up satellite tags. *Journal of Experimental Marine Biology and Ecology, 397*(2), 129-135. doi:10.1016/j.jembe.2010.11.018

Compean, G. (2014) Compliance and Regional Cooperation in the EPO. Cuarto Taller Global De Capacitacion Para El Control Y Vigilancia Pesquera, San Jose C.R.. February

De Metrio, G., Oray, I., Arnold, G., Lutcavage, M., Deflorio, M., Cort, J., . . . Ultanur, M. (2004). Joint Turkish-Italian research in the eastern Mediterranean: Bluefin tuna tagging with pop-up satellite tags. *Collect. Vol. Sci. Pap. ICCAT, 56*(3), 1163-1167.

Desert Star Systems. (2012) SeaTag-MOD Operator's Manual Version 1.01.

Domeier, M. (2006). *An analysis of Pacific striped marlin (Tetrapturus audax) horizontal movement patterns using pop-up satellite archival tags* (Vol. 79).

Domeier, M. L., Dewar, H., & Nasby-Lucas, N. (2003). Mortality rate of striped marlin (Tetrapturus audax) caught with recreational tackle. *Marine and Freshwater Research, 54*(4), 435-445. doi:http://dx.doi.org/10.1071/MF01270

Ehrhardt, N. M., Fitchett, M.D. (2008). Evaluación de las tendencias de los rendimientos de la pesca deportiva de picudos en Costa Rica como consencuencia de la marcada sobre explotación de los recursos en los cuales se basa la importante industria de pesca. . *Unpublished Letter to Government of Costa Rica*, 31pgs.

Ehrhardt, N. M., & Fitchett, M. D. (2006). On the seasonal dynamic characteristics of the sailfish, Istiophorus platypterus, in the eastern Pacific off Central America. *Bulletin of Marine Science, 79*(3), 589-606.

Erisman, B. E., Allen, L. G., Claisse, J. T., Pondella, D. J., Miller, E. F., & Murray, J. H. (2011). The illusion of plenty: hyperstability masks collapses in two recreational fisheries that target fish spawning aggregations. *Canadian Journal of Fisheries and Aquatic Sciences, 68*(10), 1705-1716. doi:10.1139/f2011-090

Evans, D. H., & Wares, P. G. (1972). *Food habits of striped marlin and sailfish off Mexico and southern California* (76). Retrieved from http://pubs.er.usgs.gov/publication/rr76

Fernández-Álamo, M. A., & Färber-Lorda, J. (2006). Zooplankton and the oceanography of the eastern tropical Pacific: A review. *Progress in Oceanography, 69*(2–4), 318-359. doi:http://dx.doi.org/10.1016/j.pocean.2006.03.003

Fieberg, J. (2007). Kernel density estimators of home range: smoothing and the autocorrelation red herring. *Ecology, 88*(4), 1059-1066.

Fiedler, P. C. (2002). The annual cycle and biological effects of the Costa Rica Dome. *Deep Sea Research Part I: Oceanographic Research Papers, 49*(2), 321-338. doi:http://dx.doi.org/10.1016/S0967-0637(01)00057-7

Fitchett, M. D. (2015). Growth, Mortality, and Availability of Eastern Pacific Sailfish. University of Miami Dissertation

Freon, P., & Misund, O. A. (1999). *Dynamics of pelagic fish distribution and behaviour*. Cambridge: University Press.

Friederichs, S. J. (2009). The influence of seasonal upwelling on the spatial and vertical distribution of sailfish (Istiophorus platypterus) in the Eastern Pacific Ocean. *Purdue University M.S. Dissertation*.

Fritsches, K., & Warrant, E. (2004). Do tuna and billfish see colours. *Pelagic Fish Res Program Newslett, 9*, 1-3.

Fritsches, K. A., Litherland, L., Thomas, N., & Shand, J. (2003). Cone visual pigments and retinal mosaics in the striped marlin. *Journal of Fish Biology, 63*(5), 1347-1351. doi:10.1046/j.1095-8649.2003.00246.x

Fritsches, K. A., Marshall, N. J., & Warrant, E. J. (2003). Retinal specializations in the blue marlin: eyes designed for sensitivity to low light levels. *Marine and Freshwater Research, 54*(4), 333-341. doi:http://dx.doi.org/10.1071/MF02126

Fritsches, K. A., Partridge, J. C., Pettigrew, J. D., & Marshall, N. J. (2000). Colour vision in billfish. *Philosophical Transactions of the Royal Society B: Biological Sciences, 355*(1401), 1253-1256.

Fritsches, K. A., & Warrant, E. J. (2001). New Discoveries in the visual performace of pelagic fishes. *University of Hawaii, Pelagic Fisheries Research Program, 6*(3), 3.

Gavaris, S. (1980). Use of a multiplicative model to estimate catch rate and effort from commercial data. *Canadian Journal of Fisheries and Aquatic Sciences, 37*(12), 2272-2275.

Godin, J. G. (1981). Circadian rhythm of swimming activity in juvenile pink salmon (Oncorhynchus gorbuscha). *Marine Biology, 64*(3), 341-349. doi:10.1007/bf00393635

Goodyear, C. P., Luo, J., Prince, E. D., Hoolihan, J. P., Snodgrass, D., Orbesen, E. S., & Serafy, J. E. (2008). Vertical habitat use of Atlantic blue marlin Makaira nigricans: interaction with pelagic longline gear. *Marine Ecology Progress Series, 365*, 233-245.

Graves, J. E., Luckhurst, B. E., & Prince, E. D. (2002). An evaluation of pop-up satellite tags for estimating postrelease survival of blue marlin (Makaira nigricans) from a recreational fishery *. *Fishery Bulletin, 100*(1), 134+.

Gunn, J. S., Patterson, T. A., & Pepperell, J. G. (2003). Short-term movement and behaviour of black marlin Makaira indica in the Coral Sea as determined through a pop-up satellite archival tagging experiment. *Marine and Freshwater Research, 54*(4), 515-525. doi:http://dx.doi.org/10.1071/MF03022

Gurarie, E. (2008). *Models and analysis of animal movements: From individual tracks to mass dispersal.* University of Washington.

Gurarie, E., Andrews, R. D., & Laidre, K. L. (2009). A novel method for identifying behavioural changes in animal movement data. *Ecology Letters, 12*(5), 395-408. doi:10.1111/j.1461-0248.2009.01293.x

Gurarie, E. (2014). bcpa: Behavioral change point analysis of animal movement. R package version 1.1. https://CRAN.R-project.org/package=bcpa

Hamilton, R. J., Almany, G. R., Stevens, D., Bode, M., Pita, J., Peterson, N. A., & Choat, J. H. (2016). Hyperstability masks declines in bumphead parrotfish (Bolbometopon muricatum) populations. *Coral Reefs, 35*(3), 751-763. doi:10.1007/s00338-016-1441-0

Harley, S. J., Myers, R. A., & Dunn, A. (2001). Is catch-per-unit-effort proportional to abundance? *Canadian Journal of Fisheries and Aquatic Sciences, 58*(9), 1760-1772. doi:10.1139/f01-112

Hastie, T., & Hastie, M. T. (2018). Package 'gam'. *GAM Package CRAN, cran. r-project. org/web/packages/gam/gam. pdf*.

Hastie, T. a. T., R. . (1986). Generalized additive models (with discussion). *Statist. Sci.*(1), 297–318.

Hastie, T. a. T., R. . (1990). *Generalized Additive Models*. London: Chapman and Hall.

Hays, G. C., Bradshaw, C. J. A., James, M. C., Lovell, P., & Sims, D. W. (2007). Why do Argos satellite tags deployed on marine animals stop transmitting? *Journal of Experimental Marine Biology and Ecology, 349*(1), 52-60. doi:https://doi.org/10.1016/j.jembe.2007.04.016

Hilborn, R., & Walters, C. J. (2013). *Quantitative fisheries stock assessment: choice, dynamics and uncertainty*: Springer Science & Business Media.

Hinke, J., Kaplan, I., Aydin, K., Watters, G., Olson, R., & Kitchell, J. F. (2004). Visualizing the food-web effects of fishing for tunas in the Pacific Ocean. *Ecology and Society, 9*(1).

Hinton, M., & Nakano, H. (1996). Standardizing catch and effort statistics using physiological, ecological, or behavioral constraints and environmental data, with an application to blue marlin (Makaira nigricans) catch and effort data from Japanese longline fisheries in the Pacific (Vol. 21): Bull. I-ATTC

Hinton, M. G., Maunder, M., Vogel, N., Olson, R., Lennert, C., Aires-da-Silva, A., & Hall, M. (2014). Document Sac-05-11c Stock Status Indicators For Fisheries Of The Eastern Pacific Ocean.

Hinton, M. G., & Maunder, M. N. (2011). Status of swordfish in the Eastern Pacific Ocean in 2010 and outlook for the future. *Inter-American Tropical Tuna Commission Report*, 1-33.

Hinton, M. G., and Maunder, M. N. 2013. Status of sailfish in the Eastern Pacific Ocean in 2011 and outlook for the future. In Inter-American Tropical Tuna Commission Scientific Advisory Committee 4th meeting La Jolla, CA. SAC-04-07c.

Holland, K., Brill, R., & Chang, R. K. C. (1990). Horizontal and Vertical Movements of Pacific Blue Marlin Captured and Released Using Sportfishing Gear. *Fishery Bulletin, 88*(2), 397-402.

Holland, K. N., & Grubbs, R. D. (2007). Fish visitors to seamounts: tunas and bill fish at seamounts. *Seamounts: Ecology, Fisheries & Conservation*, 189-201.

Holts, D., Bedford, D. (1990). *Activity patterns of striped marlin in the southern California Bight. In." Planning the Future of Billfishes, Research and Management in the 90s and Beyound.* Paper presented at the Proceedings of the Second International Billfish Symposium, Kailua-Kona, Hawaii, August 1-5, 1988. Part 2.

Hoolihan, J. P. (2005). Horizontal and vertical movements of sailfish (<i>Istiophorus platypterus) in the Arabian Gulf, determined by ultrasonic and pop-up satellite tagging. *Marine Biology, 146*(5), 1015-1029. doi:10.1007/s00227-004-1488-2

Hoolihan, J. P., Luo, J., Abascal, F. J., Campana, S. E., De Metrio, G., Dewar, H., . . . Musyl, M. K. (2011). Evaluating post-release behaviour modification in large pelagic fish deployed with pop-up satellite archival tags. *Ices Journal of Marine Science, 68*(5), 880-889.

Hu, C., Lee Z., and Franz, B.A. (2012). Chlorophyll-a algorithms for oligotrophic oceans: A novel approach based on three-band reflectance difference, J. Geophys. Res., 117, C01011, doi:10.1029/2011JC007395

IATTC Document (2016) Fishery Status Report, Tunas, Billfishes, and Other Pelagic Species in the EPO in 2015. Report #14

Jellyman, D., & Tsukamoto, K. (2002). *First use of archival transmitters to track migrating freshwater eels Anguilla dieffenbachii at sea* (Vol. 233).

Karstensen, J., Stramma, L., & Visbeck, M. (2008). Oxygen minimum zones in the eastern tropical Atlantic and Pacific oceans. *Progress in Oceanography, 77*(4), 331-350. doi:http://dx.doi.org/10.1016/j.pocean.2007.05.009

Kawamura, G., Nishimura, W., Ueda, S., & Nishi, T. (1981). Color Vision and Spectral Sensitivity in Tunas and Marlins. *Nippon Suisan Gakkaishi, 47*(4), 481-485. doi:10.2331/suisan.47.481

Kernohan, B. J., Gitzen, R. A., & Millspaugh, J. J. (2001). Chapter 5 - Analysis of Animal Space Use and Movements *Radio Tracking and Animal Populations* (pp. 125-166). San Diego: Academic Press.

Kernohan, B. J., Millspaugh, J. J., Jenks, J. A., & Naugle, D. E. (1998). Use of an adaptive kernel home-range estimator in a GIS environment to calculate habitat use. *Journal of Environmental Management, 53*(1), 83-89. doi:http://dx.doi.org/10.1006/jema.1998.0198

Kerstetter, D. W., Luckhurst, B. E., Prince, E. D., & Graves, J. E. (2003). Use of pop-up satellite archival tags to demonstrate survival of blue marlin (Makaira nigricans) released from pelagic longline gear. *Fishery Bulletin, 101*(4), 939-948.

Kessler, W. S. (2006). The circulation of the eastern tropical Pacific: A review. *Progress in Oceanography, 69*(2–4), 181-217. doi:http://dx.doi.org/10.1016/j.pocean.2006.03.009

Kimura, D. K. (1981). Standardized measures of relative abundance based on modelling log (cpue), and their application to Pacific ocean perch (Sebastes alutus). *Ices Journal of Marine Science, 39*(3), 211-218.

Klimley, A. P., Flagg, M., Hammerschlag, N., & Hearn, A. (2017). The value of using measurements of geomagnetic field in addition to irradiance and sea surface temperature to estimate geolocations of tagged aquatic animals. *Animal Biotelemetry, 5*(1), 19.

Kraus, R. T., & Rooker, J. R. (2007). Patterns of Vertical Habitat Use by Atlantic Blue Marlin (Makaira nigricans) in the Gulf of Mexico. *Gulf and Caribbean Research, 19*. doi:10.18785/gcr.1902.11

Kröger, R. H. H., Fritsches, K. A., & Warrant, E. J. (2009). Lens optical properties in the eyes of large marine predatory teleosts. *Journal of Comparative Physiology A, 195*(2), 175-182. doi:10.1007/s00359-008-0396-1

Laver, P. N., & Kelly, M. J. (2008). A critical review of home range studies. *Journal of Wildlife Management, 72*(1), 290-298.

Lisney, T., & Collin, S. (2006). Brain morphology in large pelagic fishes: a comparison between sharks and teleosts. *Journal of Fish Biology, 68*(2), 532-554.

Litvinov, F. (2008). Fish Visitors to Seamounts: Aggregations of Large Pelagic Sharks Above Seamounts *Seamounts: Ecology, Fisheries & Conservation* (pp. 202-206): Blackwell Publishing Ltd.

Lythgoe, J. N. (1979). *The ecology of vision*: Oxford : Clarendon Press New York : Oxford University Press.

Martínez-Rincón, R. O., Ortega-García, S., & Vaca-Rodríguez, J. G. (2012). Comparative performance of generalized additive models and boosted regression trees for statistical modeling of incidental catch of wahoo (Acanthocybium solandri) in the Mexican tuna purse-seine fishery. *Ecological Modelling, 233*, 20-25. doi:https://doi.org/10.1016/j.ecolmodel.2012.03.006

Maunder, M. N., & Punt, A. E. (2004). Standardizing catch and effort data: a review of recent approaches. *Fisheries Research, 70*(2-3), 141-159.

Maunder, M. N., & Punt, A. E. (2013). A review of integrated analysis in fisheries stock assessment. *Fisheries Research, 142*, 61-74.

Maunder, M. N., & Watters, G. M. (2003). A general framework for integrating environmental time series into stock assessment models: model description, simulation testing, and example. *Fishery Bulletin, 101*(1), 89-99.

McFarland, W. N., & Munz, F. W. (1975). Part III: The evolution of photopic visual pigments in fishes. *Vision Research, 15*, 1071.

Milner-Gulland, E., Fryxell, J. M., & Sinclair, A. R. E. (2011). *Animal migration: a synthesis*: Oxford University Press Oxford.

Mitchel, A. (2005). The ESRI Guide to GIS analysis, Volume 2: Spartial measurements and statistics. *ESRI Guide to GIS analysis*.

Mitchell, M. S. (1997). *Optimal home ranges: models and applications to black bears. .* (Doctoral Dissertation), NC State, Raleigh, NC.

Mora, C., Myers, R. A., Coll, M., Libralato, S., Pitcher, T. J., Sumaila, R. U., . . . Worm, B. (2009). Management Effectiveness of the World's Marine Fisheries. *PLOS Biology, 7*(6), e1000131. doi:10.1371/journal.pbio.1000131

Mourato, B. L., Carvalho, F., Musyl, M., Amorim, A., Pacheco, J. C., Hazin, H., & Hazin, F. (2014). Short-term movements and habitat preferences of sailfish, Istiophorus platypterus (Istiophoridae), along the southeast coast of Brazil. *Neotropical Ichthyology, 12*, 861-870.

Musyl, M. K., Domeier, M. L., Nasby-Lucas, N., Brill, R. W., McNaughton, L. M., Swimmer, J. Y., . . . Liddle, J. B. (2011). Performance of pop-up satellite archival tags. *Marine Ecology-Progress Series, 433*, 1-U58. doi:Doi 10.3354/Meps09202

Myers, R. A., & Worm, B. (2003). Rapid worldwide depletion of predatory fish communities. *Nature, 423*(6937), 280-283. doi:http://www.nature.com/nature/journal/v423/n6937/suppinfo/nature01610_S1.html

Nakamura, I. (1985). *FAO species catalogue. v. 5: Billfishes of the world. An annotated and illustrated catalogue of marlins, sailfishes, spearfishes and swordfishes known to date*: FAO.

Olson, R. J., Duffy, L. M., Kuhnert, P. M., Galván-Magaña, F., Bocanegra-Castillo, N., & Alatorre-Ramírez, V. (2014). Decadal diet shift in yellowfin tuna Thunnus albacares suggests broad-scale food web changes in the eastern tropical Pacific Ocean. *Mar. Ecol. Prog. Ser, 497*, 157-178.

Olson, R. J., & Watters, G. M. (2003). A model of the pelagic ecossystem in the eastern tropical Pacific Ocean. *Inter-American Tropical Tuna Commission Bulletin, 22*(3), 135-218.

Pepperell, J. G., & Davis, T. L. O. (1999). Post-release behaviour of black marlin, Makaira indica, caught off the Great Barrier Reef with sportfishing gear. *Marine Biology, 135*(2), 369-380. doi:10.1007/s002270050636

Perryman, H. A. (2017). Parameterization of an Ecosystem Model and Application for Assessing the Utility of Gulf of Mexico Pelagic Longline Spatial Closures. University of Miami Dissertation

Pierce, D. (2015). ncdf4: Interface to Unidata netCDF (Version 4 or Earlier) Format Data Files. R package version 1.15. https://CRAN.R-project.org/package=ncdf4

Pohlot, B. G., & Ehrhardt, N. (2017). An analysis of sailfish daily activity in the Eastern Pacific Ocean using satellite tagging and recreational fisheries data. *Ices Journal of Marine Science*, fsx082-fsx082. doi:10.1093/icesjms/fsx082

Polovina, J., Uchida, I., Balazs, G., Howell, E. A., Parker, D., & Dutton, P. (2006). The Kuroshio Extension Bifurcation Region: A pelagic hotspot for juvenile loggerhead sea turtles. *Deep Sea Research Part II: Topical Studies in Oceanography, 53*(3–4), 326-339. doi:http://dx.doi.org/10.1016/j.dsr2.2006.01.006

Powell, R. A. (2000). Animal home ranges and territories and home range estimators. *Research techniques in animal ecology: controversies and consequences, 1*, 476.

Powell, R. A., & Mitchell, M. S. (2012). What is a home range? *Journal of Mammalogy, 93*(4), 948-958. doi:10.1644/11-mamm-s-177.1

Prince, E. D., & Goodyear, C. P. (2006). Hypoxia-based habitat compression of tropical pelagic fishes. *Fisheries Oceanography, 15*(6), 451-464. doi: 10.1111/j.1365-2419.2005.00393.x

Prince, E. D., Holts, D. B., Snodgrass, D., Orbesen, E. S., Luo, J., Domeier, M. L., & Serafy, J. E. (2006). Transboundary movement of sailfish, Istiophorus platypterus, off the Pacific coast of Central America. *Bulletin of Marine Science, 79*(3), 827-838.

Prince, E. D., Luo, J., Phillip Goodyear, C., Hoolihan, J. P., Snodgrass, D., Orbesen, E. S., .Schirripa, M. J. (2010). Ocean scale hypoxia-based habitat compression of Atlantic istiophorid billfishes. *Fisheries Oceanography, 19*(6), 448-462. doi:10.1111/j.1365-2419.2010.00556.x

Prince, E. D., Ortiz, M., & Venizelos, A. (2002). *A comparison of circle hook and" J" hook performance in recreational catch-and-release fisheries for billfish.* Paper presented at the American Fisheries Society Symposium.

Prince, E. D., Ortiz, M., Venizelos, A., & Rosenthal, D. S. (2002). In-water conventional tagging techniques developed by the cooperative tagging center for large, highly migratory species. *Catch and Release in Marine Recreational Fisheries, 30*, 155-171.

Punt, A. E., Pribac, F., Walker, T. I., & Taylor, B. L. (2001). Population modelling and harvest strategy evaluation for school and gummy shark. *Report of FRDC Project*(99/102).

R Core Team (2016). R: A language and environment for statistical computing. R Foundation for Statistical Computing, Vienna, Austria. URL https://www.R-project.org/

Reynolds, R.W., N.A. Rayner, T.M.Smith, D.C. Stokes, and W. Wang, 2002: An Improved In Situ and Satellite SST Analysis for Climate, J. Climate platform: Model source: NCEP Climate Modeling Branch institution: National Centers for Environmental Prediction. References: http://www.esrl.noaa.gov/psd/data/gridded/data.noaa.oisst.v2.html

Rodríguez-Marín, E., Arrizabalaga, H., Ortiz, M., Rodríguez-Cabello, C., Moreno, G., & Kell, L. (2003). Standardization of bluefin tuna, Thunnus thynnus, catch per unit effort in the baitboat fishery of the Bay of Biscay (Eastern Atlantic). *Ices Journal of Marine Science, 60*(6), 1216-1231.

Sarkar, Deepayan (2008) Lattice: Multivariate Data Visualization with R. Springer, New York. ISBN 978-0-387-75968-5

Sasso, C. R., Epperly, S. P. (2007). Survival of Pelagic Juvenile Loggerhead Turtles in the Open Ocean. *The Journal of Wildlife Management, 71*(6), 1830-1835. doi:10.2193/2006-448

Schick, R. S., Loarie, S. R., Colchero, F., Best, B. D., Boustany, A., Conde, D. A., . . . Clark, J. S. (2008). Understanding movement data and movement processes: current and emerging directions. *Ecology Letters, 11*(12), 1338-1350. doi:10.1111/j.1461-0248.2008.01249.x

Schlenker, L. S., Latour, R. J., Brill, R. W., & Graves, J. E. (2016). Physiological stress and post-release mortality of white marlin (Kajikia albida) caught in the United States recreational fishery. *Conservation Physiology, 4*(1). doi:10.1093/conphys/cov066

Scott, L. M., & Janikas, M. V. (2010). Spatial Statistics in ArcGIS. In M. M. Fischer & A. Getis (Eds.), *Handbook of Applied Spatial Analysis: Software Tools, Methods and Applications* (pp. 27-41). Berlin, Heidelberg: Springer Berlin Heidelberg.

Scott, M. D., & Cattanach, K. L. (1998). Diel patterns in aggregations of pelagic dolphins and tunas in the eastern pacific. *Marine Mammal Science, 14*(3), 401-428. doi:10.1111/j.1748-7692.1998.tb00735.x

Scott, M. D., Chivers, S. J., Olson, R. J., Fiedler, P. C., & Holland, K. (2012). Pelagic predator associations: tuna and dolphins in the eastern tropical Pacific Ocean. *Marine Ecology Progress Series, 458*, 283-302.

Seaman, D. E., Millspaugh, J. J., Kernohan, B. J., Brundige, G. C., Raedeke, K. J., & Gitzen, R. A. (1999). Effects of sample size on kernel home range estimates. *The Journal of Wildlife Management*, 739-747.

Seaman, D. E., & Powell, R. A. (1996). An evaluation of the accuracy of kernel density estimators for home range analysis. *Ecology, 77*(7), 2075-2085.

Shimose, T., Shono, H., Yokawa, K., Saito, H., & Tachihara, K. (2006). Food and feeding habits of blue marlin, Makaira nigricans, around Yonaguni Island, southwestern Japan. *Bulletin of Marine Science, 79*(3), 761-775.

Silverman, B. W. (1986). *Density estimation for statistics and data analysis* (Vol. 26): CRC Press.

Sippel, T. J., Davie, P. S., Holdsworth, J. C., & Block, B. A. (2007). Striped marlin (Tetrapturus audax) movements and habitat utilization during a summer and autumn in the Southwest Pacific Ocean. *Fisheries Oceanography, 16*(5), 459-472. doi:10.1111/j.1365-2419.2007.00446.x

Skomal, G. B. (2007). Evaluating the physiological and physical consequences of capture on post-release survivorship in large pelagic fishes. *Fisheries Management and Ecology, 14*(2), 81-89. doi:10.1111/j.1365-2400.2007.00528.x

Southwood, A., Fritsches, K., Brill, R., & Swimmer, Y. (2008). Sound, chemical, and light detection in sea turtles and pelagic fishes: sensory-based approaches to bycatch reduction in longline fisheries. *Endangered Species Research, 5*(2-3), 225-238.

Spencer, W. D. (2012). Home ranges and the value of spatial information. *Journal of Mammalogy, 93*(4), 929-947. doi:10.1644/12-mamm-s-061.1

Stramma, L., Johnson, G. C., Firing, E., & Schmidtko, S. (2010). Eastern Pacific oxygen minimum zones: Supply paths and multidecadal changes. *Journal of Geophysical Research: Oceans, 115*(C9), C09011. doi:10.1029/2009jc005976

Tamura, T., & Wisby, W. J. (1963). The Visual Sense of Pelagic Fishes Especially the Visual Axis and Accommodation. *Bulletin of Marine Science, 13*(3), 433-448.

Turchin, P. (1998). *Quantitative analysis of movement: measuring and modeling population redistribution in animals and plants* (Vol. 1): Sinauer Associates Sunderland.

United States Navy. 2016. US Naval Observatory Astronomical Applications Department Sun and Moon Data Services. Retrieved from aa.usno.navy.mil/data/ (retrieved August 2016).

Vokoun, J. C. (2003). Kernel density estimates of linear home ranges for stream fishes: advantages and data requirements. *North American Journal of Fisheries Management, 23*(3), 1020-1029. doi:10.1577/m02-141

Walters, C. J., & Martell, S. J. (2004). *Fisheries ecology and management*: Princeton University Press.

White, G. C., & Garrott, R. A. (2012). *Analysis of wildlife radio-tracking data*: Elsevier.

Willett, C. S., Leben, R. R., & Lavín, M. F. (2006). Eddies and Tropical Instability Waves in the eastern tropical Pacific: A review. *Progress in Oceanography, 69*(2-4), 218-238. doi:10.1016/j.pocean.2006.03.010

Wilson, S., Lutcavage, M., Brill, R., Genovese, M., Cooper, A., & Everly, A. (2005). Movements of bluefin tuna (Thunnus thynnus) in the northwestern Atlantic Ocean recorded by pop-up satellite archival tags. *Marine Biology, 146*(2), 409-423.

Wilson, S., Polovina, J., Stewart, B., & Meekan, M. (2006). Movements of whale sharks (Rhincodon typus) tagged at Ningaloo Reef, Western Australia. *Marine Biology, 148*(5), 1157-1166.

Wood, S. (Generalized Additive Models: An Introduction with R). *2006*. Boca Raton, FL: Chapman and Hall/CRC.

Wood, S., & Wood, M. (2016). Package mgcv. R package version 1.7.

World Ocean Atlas. Garcia, H. E., Locarnini, R. A., Boyer, T. P., Antonov, J. I., Baranova, O. K., Zweng, M. M., Reagan, J. R. and Johnson, D. R., 2014. World Ocean Atlas 2013, Volume 3: Dissolved Oxygen, Apparent Oxygen Utilization, and Oxygen Saturation. Ed. by S. Levitus. NOAA Atlas NESDIS 75, Silver Spring, MD, 27 pp.

Worton, B. (1987). A review of models of home range for animal movement. *Ecological Modelling, 38*(3-4), 277-298.

Worton, B. J. (1989). kernel methods for estimating the utilization distribution in home-range studies. *Ecology, 70*(1), 164-168. doi:10.2307/1938423

Worton, B. J. (1995). Using Monte Carlo simulation to evaluate kernel-based home range estimators. *The Journal of Wildlife Management*, 794-800.

Zhang, Z., Wang, W., & Qiu, B. (2014). Oceanic mass transport by mesoscale eddies. *Science, 345*(6194), 322-324. doi:10.1126/science.1252418